UNIVERSITÀ DEGLI STUDI DI MILANO

Scuola di Dottorato in Scienze e Tecnologie Chimiche

Dipartimento di Chimica

PhD Course in Industrial Chemistry - XXIX Cycle

Stereoselective catalytic reactions under continuous flow conditions

Tutor: Prof. Maurizio Benaglia

Co-tutor: Dott. Alessandra Puglisi

Riccardo Porta

R10404

2014-2016

Dedicato a mia Mamma,

alla mia Famiglia e a Sara.

Con un ringraziamento speciale a tutte le persone

che mi hanno accompagnato durante il mio percorso

senza le quali non avrei potuto raggiungere questo traguardo.

SUMMARY

ABSTRACT

This PhD Thesis deals with the application of different catalytic methodologies under continuous flow conditions. In particular, the combination of flow chemistry with different enabling technologies is explored.

In *Chapter 1* the combination of continuous flow processes with the use of different solid supported chiral organocatalysts is described. The fabrication of chiral, packed-bed and monolithic, organocatalytic reactors and their use in stereoselective transformations are reported. The possibility to recycle the immobilized chiral catalysts is also discussed.

- In *section 1.2* the use of polystyrene- and silica-supported chiral imidazolidinones to perform continuous flow stereoselective Diels-Alder cycloadditions and stereoselective aldehydes alkylation is studied.
- In *section 1.3* the immobilization onto different materials of primary amines derived from Cinchona alkaloids and the application under flow conditions are explored.
- In *section 1.4* chiral picolinamides for the continuous stereoselective reduction of imines with trichlorosilane are studied.

Chapter 2 describes the application of different synthetic strategies using flow micro(meso)-reactors, aimed to the synthesis of chiral active pharmaceutical ingredients or immediate advanced precursors of compounds of industrial interest. In particular,

- in *section 2.2* the organocatalytic, stereoselective synthesis of (*S*)-Pregabalin and (*S*)-Warfarin within microreactors is investigated.
- *Section 2.3* presents the continuous flow synthesis of primary amines through a metal-free reduction of nitro compounds with trichlorosilane.
- In *section 2.4* a catalytic strategy for a multistep synthesis of chiral, biological active 1,2-amino alcohols using 3D-printed flow reactors is highlighted.

Chapter 3 covers the research work carried out during my research period in Aachen, Germany which was focused on the development of a new synthetic methodology using photoredox catalysis. In particular, the photocatalytic reductive coupling of imine with olefins for the preparation of γ-amino esters and its application under continuous flow conditions are discussed.

INTRODUCTION TO FLOW CHEMISTRY

Traditionallly, organic synthesis has always relied on batch reactions. Substrates, solvents and catalysts are added into a flask and then stirred at a given temperature for a precise reaction time after which the crude mixture is analyzed and the product is isolated. The production of fine chemicals (*i.e.* drugs, food additives, agrochemicals or flavors) has always been based on sequential batch processes constituted by multiple unit operations.

A conceptually different approach to chemical synthesis is represented by flow processes (Figure 1) where the reagents are continuously pumped into a reactor which can be heated, cooled or irradiated (with microwaves or light) and can contain immobilized reagents, catalysts or scavengers in order to eliminate side-products or trace metals.

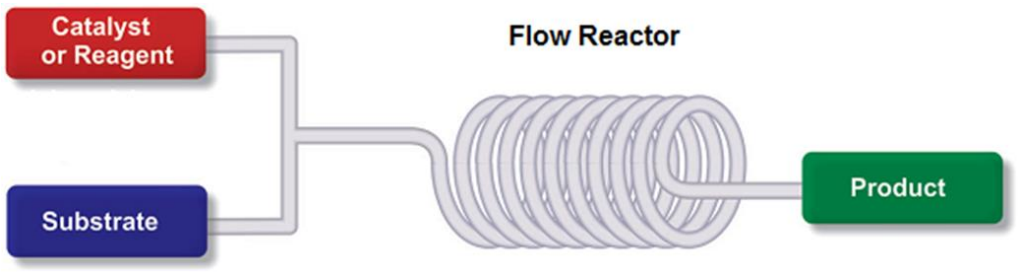

Figure 1. General representation of a continuous flow reaction.

Continuous flow reactors are generally constituted by coiled tubing or chip-based devices having high surface area-to-volume ratio. This results in several advantages over classical batch reactors, in particular in improved heat and mass transfers. All reaction parameters can be precisely monitored thus making the process more reliable and reproducible. In this way the reaction time is reduced, the efficiency is increased and the mixing of substrates is significantly improved. Additionally, the formation of undesired side-products due to hot-spots is considerably reduced.

The closed environment where a continuous flow reaction takes place ensures other benefits, mainly concerning safety issues: hazardous and highly toxic chemicals or reaction intermediates can be generated *in-situ* and converted into more elaborated molecules by combining different reagent streams. This minimizes risks for the operator because no handling or isolation of dangerous species is required.

Furthermore, thanks to a relatively short residence time into the flow reactor and to sequential operations, reactions that involve the formation of unstable intermediates which cannot be stored or isolated in batch mode become feasible.

Flow processes are suitable for automation and offer the opportunity to run multistep reactions without isolation of intermediates, and allowing real time analysis for optimal reaction conditions and minimization of waste. [1]

The choice of the specific reactor is fundamental and it is determined by the characteristics of the synthetic process being performed. Principal aspects are the physical state of the reagents employed (liquids, solids, gases), the reaction thermodynamic (exo- or endo-thermic), reaction kinetics, mixing, heat and mass transfer and residence time. A lot of commercially available systems to perform continuous flow reactions are available on the market, offering solutions to different problems. Tube based laboratory reactors are typically coiled and they are usually made of stainless steel hastelloy, copper, polyether ether ketone (PEEK) or perfluorinated polymers. The choice of the material depends on the reaction conditions and on the stability toward the chemicals employed. The volumes range from 1 μL to liters with channel diameters spanning from 100 μm to 16 mm, depending on the specific requirements of the system.
Scaling up a given reaction represents one of the main challenges in synthetic chemistry. When moving the production from laboratory to production scale several parameters must be taken into account in order to avoid undesired complications (*e.g.* runaway reactions, inefficient mixing or by-product formation). This process usually requires long times resulting in an increase of the overall costs. Scaling up a continuous flow reaction from bench scale to production quantities requires minimal re-optimization and no need for changes in the synthetic pathway. A possible strategy to achieve scale up involves running the reaction in many parallel flow reactors (*numbering-up* approach). Alternatively the reactor size can be increased (*scale-up* approach).
Even though flow reactors offers many benefits over batch procedures, some limitations still need to be overcome. The main issue is related to the precipitation of solid species which can cause the clogging of the reactor. The precipitation of inorganic salts or insoluble materials during a reaction is a very common situation in synthetic chemistry. It is easy to understand that this represents a big problem in the case a flow system. Recently new technologies for the handling of solids in flow have been developed, however technical advances are still required to avoid undesirable situations.
The use of solid catalysts also represents a possible restriction in flow: indeed due to the generally low turnover number of heterogeneous catalysts a frequent replacement of the catalytic species within the rector is required.
When operating with multiphase systems an extremely accurate control of reaction parameters is required, since otherwise non efficient mixing into the reactor may occur. Recently some technologies to overcome this issue have been developed (*e.g.* tube-in-tube reactor for gas-liquid biphasic systems)[2] but some improvement for large scale application is still required.

The implementation of continuous flow processes in pharmaceutical and fine chemical industries is still relatively limited. Until recently, a continuous manufacturing approach was a prerogative of petrochemical and bulk chemical companies where large volumes of relatively simple compounds were produced. The challenge for the application of continuous manufacturing in the fine chemical sector has always been the complexity and diversity of the products, and the associated

complex process conditions. Usually, molecules produced by pharma and agrochemical companies require 6 to 10 synthetic steps (convergent or sequential) and might involve chemo- regio- and stereo-selective transformations which necessitate quenching, work-up, separation and purification operations. These products are generally produced in relatively small volumes and they possess a short-life time. For these reasons, batch procedures involving the use of multipurpose plants still dominate the production of fine chemicals: a small number of temperature- and pressure-controlled vessels can be used for virtually all the reactions, separations and purification steps associated to a long and complex synthetic route.
However thanks to the recent development of commercially available modular devices to perform continuous flow synthesis and to the growing interest of the scientific community (at the academic and industrial level) toward flow chemistry, the continuous manufacturing of pharmaceutical is rapidly expanding becoming an enabling tool for medicinal chemists.

Given all these advantages, it is not surprising that continuous processing is emerging as one of the techniques that can significantly impact the synthesis of APIs (or APIs intermediates).
An interesting example of industrial importance that demonstrates the interest of pharmaceutical companies towards flow processes has appeared in 2013 and concerns the development of a continuous end-to-end manufacturing plant for the preparation of Aliskiren hemifumarate by the Novartis-MIT Center for Continuous Manufacturing Figure 2).[3] In this work, continuous flow technologies have not been limited to the synthesis of organic molecules, but all synthetic steps, phase separations, crystallizations, drying, and formulation to the final pharmaceutical product were implemented in one integrated, fully continuous process. The process starts from a chemical intermediate and involves reactions and the required ancillary operations (quench, work up, isolation and purification) *in continuo*. That means that not only chemical transformations and separations, but also crystallizations, drying and formulation are all integrated in one automated continuous process. Notably, the pilot plant produces 100 g/hour of Aliskiren, featuring two synthetic steps, API salt formation and crystallization, and delivering as the final products of this process the tablets containing 112 mg of free Aliskiren. The continuous reactor used in the work has a volume of 0.7 L and would allow the preparation of 0.8 tons of API/year.

Figure 2. Flow system employed at MIT for the preparation of Aliskiren.

More recently Adamo and co-workers at MIT have developed a continuous flow manufacturing platform that can produce thousands of formulated, ready-to-use, liquid drug doses per day.[4] This work represent a tremendous advancement in the continuous flow synthesis of pharmaceuticals and addresses challenges in reconfiguration for multiple synthesis of diverse compounds, tight integration of process streams for reduced footprints, innovation in chemical synthesis and purifications equipment, and compact systems for crystallization and liquid formulation.

The fully integrated machine has the dimensions of a refrigerator (*h*: 1.8 m, *l*: 0.7 m, *w*: 1.0 m; 100 kg; it is 1/40 the size of the plant for the production of Aliskiren) and is composed by individual synthesis, purification and formulation modules. The system is capable of complex multistep synthesis, multiple in line purifications, reaction workup, semi-batch crystallization, real-time process analysis and formulation of high purity drug products. The synthesis of 4 active pharmaceutical ingredients (*i.e.* diphenhydramine hydrochloride, lidocaine hydrochloride, diazepam and fluoxetine) that meets US Pharmacopeia standards has been demonstrated. As illustrated in Figure 3, the system is composed by 2 units: the upstream unit contains reaction-based equipment for the manufacture of APIs (feeds, pumps, flow reactors, separators, back-pressure regulators, in-line analytical instruments); the downstream unit is dedicated to the purification and formulation of the final drug product. Despite having many complex operations, the entire platform can be managed easily by a single operator.

Figure 3. Reconfigurable flow platform for the synthesis of drugs.

This reconfigurable platform enables the on demand synthesis and formulation of many drug products (Figure 3). In principle, after regulatory approvals, this system could be employed for the production of pharmaceuticals “on demand” (for example for small patient populations or to meet humanitarian needs). The reproduction of this platform would be simpler cheaper and faster to operate than a full batch plant. The possibility to produce drugs on-site could be particularly advantageous for products with a short shelf life. Additionally the manufacture of the active ingredient on demand could minimize formulation complexity relative to tablets which need yearlong stability.

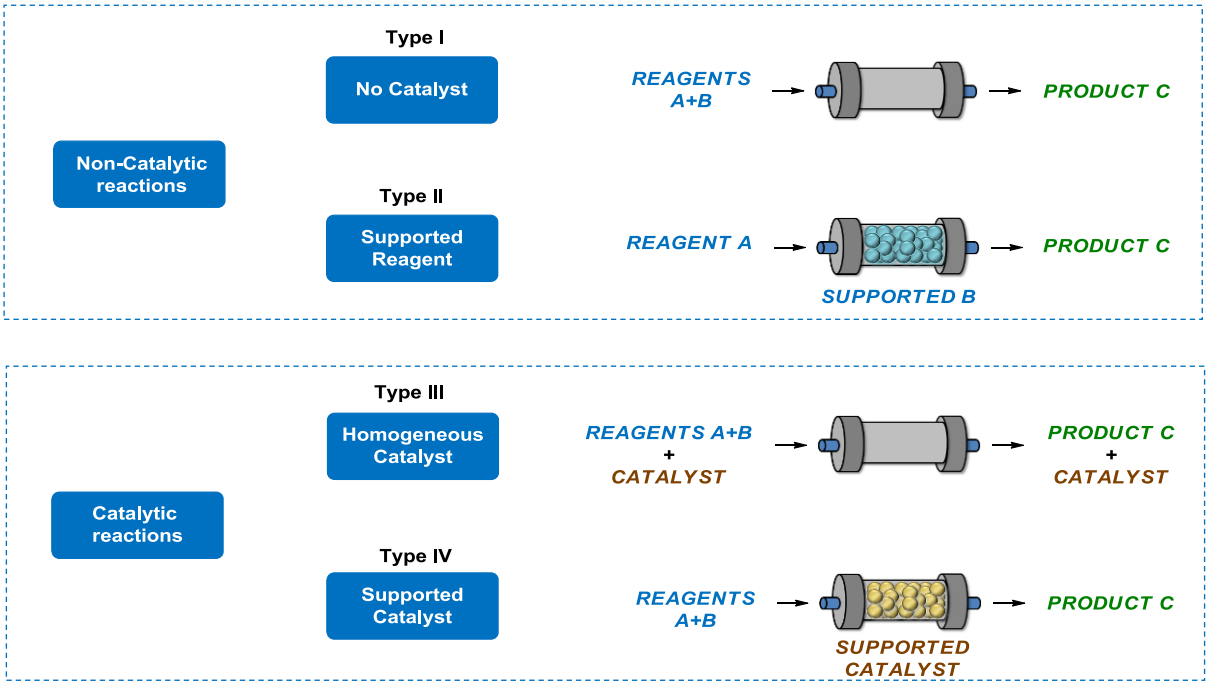

Figure 4. Different types of continuous flow reactions.

As depicted in Figure 4, continuous flow systems can be generally divided into four different types. In type I, the reagents (A and B) are directed to the reactor and at the end of the process, the outcome containing the product (C) is collected. In type II, one of the reagents (B) is supported onto a non-soluble material and confined into the reactor; the substrate (A) is passed through the reactor and the exiting reaction mixture will contain only the desired product (C)(if the reaction goes to completion). Both types I and II do not involve the use of any catalytic species during the reaction. In type III, a homogeneous catalyst is used: the catalyst flows through the reactor together with the reagents and at the end product (C) is collected along with the catalyst (a purification step to isolate C is required). In type IV, the catalyst is confined into the reactor while the reagents passed by; of course, an immobilization step of the catalyst onto a solid support is necessary, but no separation step to isolate the product from the catalyst is required; type IV reactors enables catalysts recycle. The latter type (IV) is commonly considered the most convenient system to perform a reaction in flow, since catalytic methodologies are nowadays essential for the development of sustainable and efficient processes.[5] The continuous flow

reactors described in this thesis work belong to Types 1 (chapter 2.3), 3 (chapters 2.2, 2.4 and 3.2) and 4 (chapter 1).

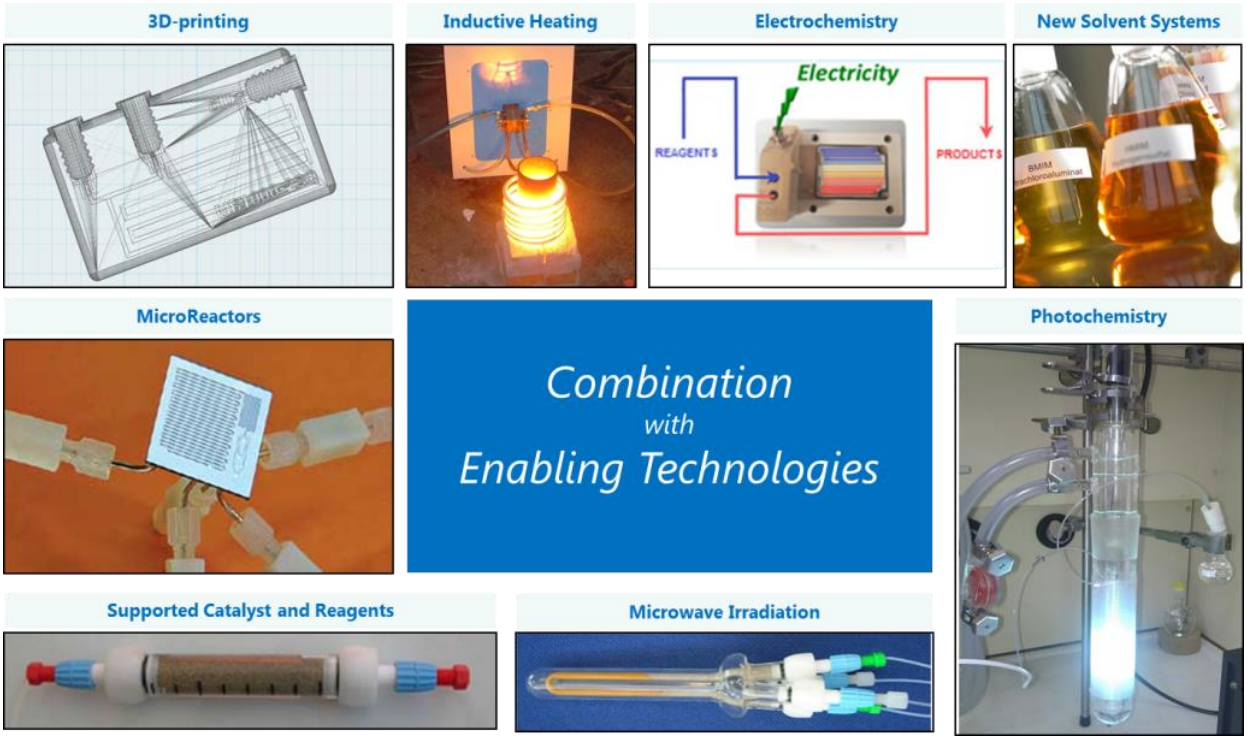

Figure 5. Enabling technologies generally combined to flow processes.

Flow methodologies can be easily combined to many enabling technologies in order to increase process efficiency.[6] Representative enabling technologies combined to continuous processes are supported reagents or catalysts, microreactor technology, 3D printing, photochemistry, microwave irradiation, inductive heating, electrochemistry or new solvent systems (Figure 5). This combination allows the development of fully automated process with an increased throughput.

In chapter 1 the combination of continuous flow processes with the use of different solid supported chiral organocatalysts will be described.

In chapter 2 the application of synthetic methodologies to flow micro(meso)-reactors will be discussed.

Chapter 3 will cover the research work carried out during my research period in Aachen, Germany. In particular the development of a new synthetic methodology using photoredox catalysis and its application under continuous flow conditions will be presented.

CHAPTER 1 SUPPORTED ORGANOCATALYSTS

1.1 Introduction

Catalysis is one of the key principles of green chemistry and therefore is largely employed in synthetic chemistry in order to develop sustainable and efficient processes.[7]
By definition, the use of a catalytic methodology is *green* because it increases energy efficiency and reduces waste compared to the use of stoichiometric reagents. Since catalysts often allow to run a reaction under relatively mild conditions, this approach offers significant advantages from the energetic and economic point of view.
A general tendency in catalysis is to develop more and more efficient catalytic species which possess high Turn Over Numbers (and therefore can be employed in low loadings) in order to reduces costs generally associated to the use of precious catalysts.
The use of solid-supported catalysts is a widely studied field of research which can, in principle, ensure many advantages over the use of homogeneous species: indeed the use of a heterogeneous catalysts favors an easy separation of the product at the end of a reaction (*e.g.* by filtration or precipitation of the catalyst); additionally the catalytic species can be recovered and reused in another reaction cycle, provided that the catalyst is not deactivated.[8]

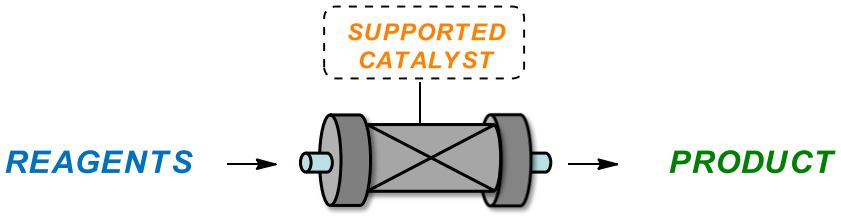

Figure 6. General representation of a catalytic reactor for continuous flow processes.

Thanks to the recent advent of continuous flow methodologies in synthetic organic chemistry, the combination of supported catalysts and flow reactors has gained much attention. Catalytic reactors (*i.e.* flow reactors containing solid catalysts) can convert the entering reagents into the desired products with no need for additional unit operations such as catalysts separation and product isolation (Figure 6). The catalyst resides into the reactor and can be reused with obvious advantages from an economical point of view.

According to the mode of inclusion of the catalyst into the flow apparatus, catalytic reactors can be divided into three classes as depicted in Figure 7.[9]

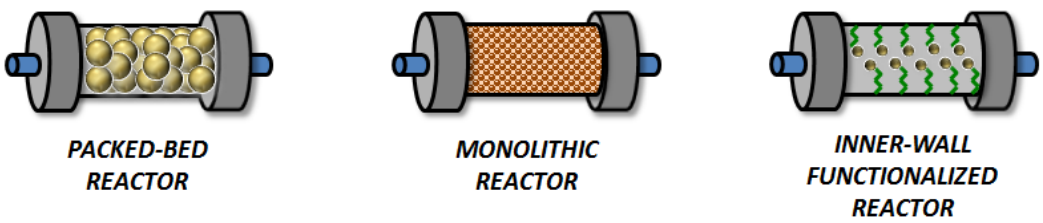

Figure 7. Different types of catalytic reactors.

In the *packed-bed* reactor the catalyst is immobilized onto an insoluble support and is randomly charged into the reactor.
In a *monolithic reactor* the catalyst is prepared in the form of a structured material, the "monolith", consisting of a regular or irregular network of channels. In general the monolith is built by the copolymerization of different monomers (one bearing the catalyst) carried out in the presence of a porogens, inside the reactor. The main advantage of monolithic reactors compared to packed-bed ones is that the packing is more homogeneous and a more controlled fluid dynamics is generally achieved. Monoliths can support high flow rates at very modest pressure and have a large surface area.
In *an inner wall-functionalized reactor* the catalyst is covalently attached onto the interior wall of the reactor. The wall-coated microreactors substantially minimize the mass transfer resistance and ensure a smooth flow of reagents without leading to any adverse pressure drop or blockage of the channels; however, their use is still very limited due to the complexity of the synthesis.

Stereoselective synthesis represents an effective strategy for the preparation of chiral molecules. Compared to chiral resolution of racemic mixture, where half of the products is discarded or must be recycled, the use of stereoselective catalysis for asymmetric synthesis is more convenient in order to develop a sustainable process. However the application of stereoselective catalysis under continuous flow conditions is still underdeveloped.[10]
Very recently, Kobayashi and co-workers have reported the stereoselective synthesis of the antidepressant drug (S)-Rolipram through a multistep continuous flow processes involving the using of solid supported catalysts and reagents (Figure 8).[11] In particular, this work features a stereoselective Michael addition promoted by a polystyrene supported $CaCl_2$-(*S*)-Pybox adduct as a chiral organometallic complex. This is the first time that a *in continuo* highly stereoselective catalytic reaction between achiral substrates is integrated into a multistep synthesis of a drug. First reaction step involved the synthesis of nitroalkene **b** starting from aldehyde **a** and nitromethane. A toluene solution of the 2 reagents was flushed through a reactor containing silica-supported amine (SiO_2-NH_2) as a base and anhydrous $CaCl_2$ as a dehydrating agent. The system was found to be stable at 75 °C for at least one week, giving the products in 90% yield. Once nitroalkenes **b** was formed it was combined with malonate **c** and trimethylamine and transferred to a catalytic reactor containing Polymer Supported (PS) (*S*)-pybox-calcium chloride maintained at 0 °C. The stereoselective Michael addition afforded compound **d** in 84% yield and 93% ee. The following nitro-group reduction was performed at ambient pressure and 100 °C employing a catalytic reactor containing a polysilane-supported palladium/carbon (Pd/DMPSi-C, where DMPSi is dimethylpolysilane) catalyst. γ-Lactam **e** was obtained in 74% yield and 94% ee (no epimerization occurred). The final stage of multistep synthesis of **f** involved ester hydrolysis and decarboxylation of compound **e**. The reaction was found to proceed at 120 °C into a continuous flow reactor containing silica-supported carboxylic acid (SiO_2-COOH). Enantiomerically pure (*S*)-Rolipram **f** could be isolated upon crystallization from H_2O/MeOH of the crude mixture with a 50% overall yield of (from aldehyde **a**). The flow system was stable for at least one week producing (*S*)-Rolipram **f** (>99%) with an output of 1 g/d. All chemical steps were performed without the

isolation of any intermediates and without the separation of any catalysts, by-products or excess reagents.

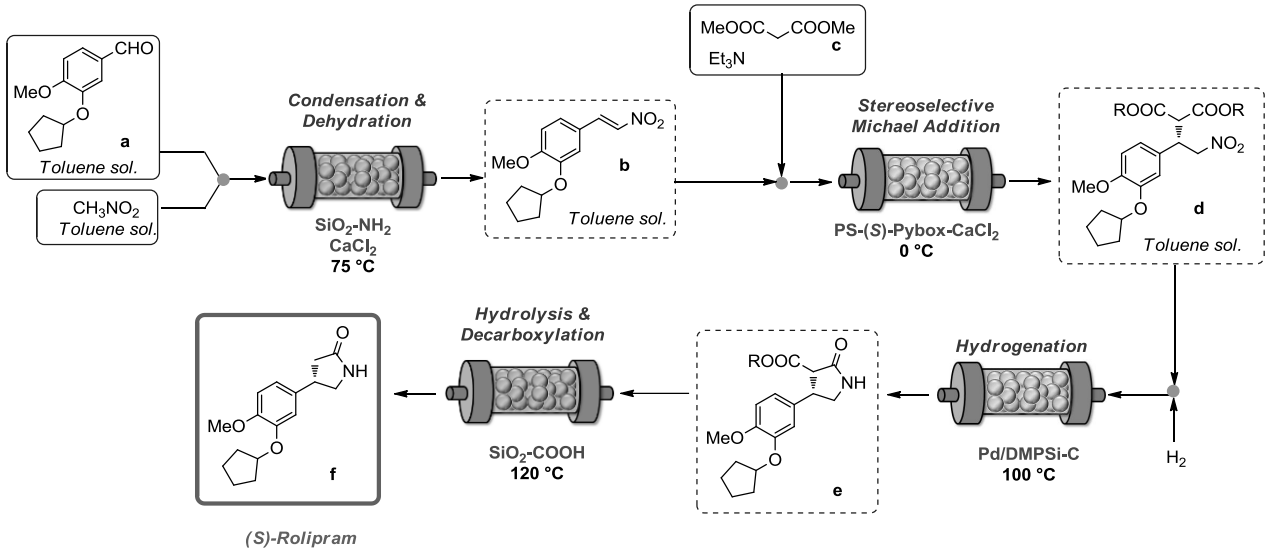

Figure 8. Continuous flow synthesis of Rolipram using catalytic reactors.

Nowadays chiral organocatalysis can be successfully used as alternative methodology to enzymatic or organometallic catalysis to perform stereoselective reactions.[12] However, the main concern associated to the use of organic molecules as catalysts are the very low TONs (loadings of 10-20 mol% are typically required) when compared to the other systems. The immobilization of the catalysts onto a solid support can partially overcome this drawback favoring an easy recovery and recycle of the catalytic species. Even more convenient is the incorporation into catalytic flow reactors where no additional isolation steps are needed.[13] Additionally, due to the absence of coordinated metal species, solid supported organocatalysts are particularly suitable for the application in catalytic reactors, since the risk of metal leaching is intrinsically avoided.[14]

This chapter will cover the synthesis of different solid supported chiral organocatalysts (*i.e.* imidazolidinones, primary amines derived from cinchona alkaloids and picolinamides) and their application in catalytic reactors for continuous flow reactions. At first the comparison between the heterogeneous catalysts with their homogeneous counterparts will be examined. Issues of catalysts loadings and recyclability will be addressed in order to assess the practical applicability of these systems. Finally the possibility to employ these systems for the continuous flow stereoselective synthesis of chiral molecules will be demonstrated.

1.2 Chiral Imidazolidinones

1.2.1 Stereoselective cycloadditions

In 2000, the MacMillan research group reported the use of a chiral imidazolidinone derived from natural amino acid *L*-phenylalanine as organocatalysts to promote Diels-Alder cycloadditions. The catalyst was developed in the context of a general strategy for stereoselective organocatalytic reactions promoted by chiral amines alternatives to Lewis acid catalyzed ones. The reversible formation of iminium ions from α,β-unsaturated aldehydes and amines emulates the equilibrium dynamics and π-orbital electronics that are inherent to Lewis acid catalysis resulting in a LUMO-lowering activation (Figure 9). The iminium ion formation is enhanced by the presence of acid additives so the catalyst operates in its protonated form.

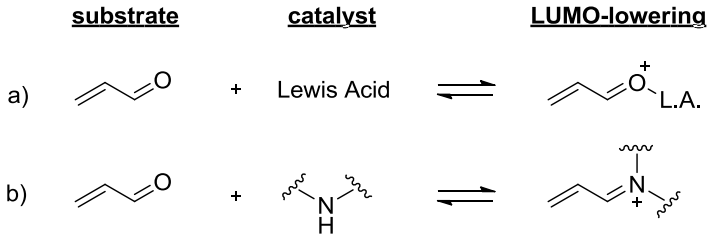

Figure 9. Modes of activation of α,β-unsaturated aldehydes.

The catalytic cycle for the stereoselective Diels-Alder reaction promoted by MacMillan catalyst is outlined in Figure 10: the condensation of the α,β-unsaturated aldehyde with the enantiopure secondary amine leads to the formation of an iminium ion that is sufficiently activated to engage a diene reaction partner. Accordingly, Diels-Alder cycloaddition would lead to an adduct which upon hydrolysis provides the enantioenriched product, while releasing the chiral amine catalyst.

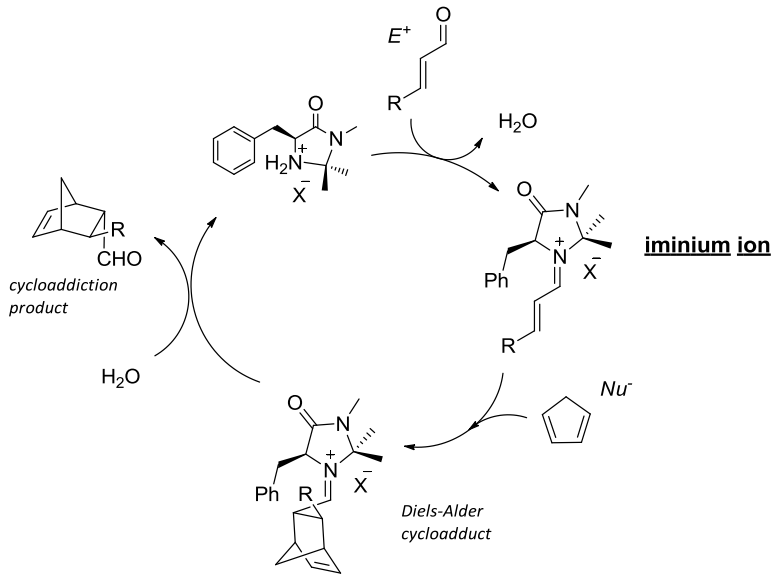

Figure 10. Reaction mechanism for stereoselective cycloaddition promoted by chiral imidazolidinone.

Given its popularity, due to wide applicability and easy availability, it is not surprisingly that the catalyst has been covalently anchored onto different supports.[15] Despite the great number of proposed solutions, the development of a supported chiral imidazolidinone for the application in catalytic flow reactor has not been explored yet.

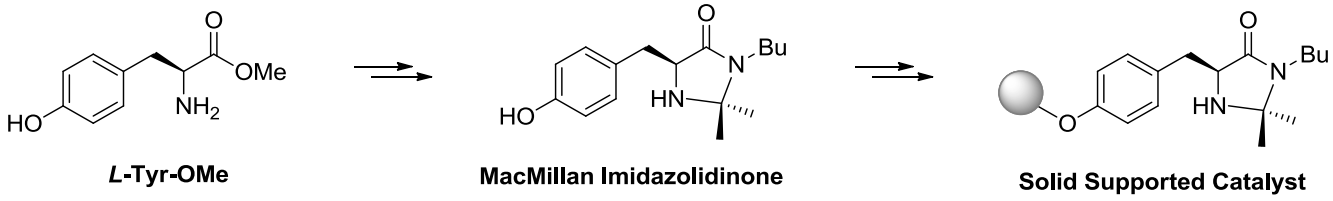

For this purpose, we decided to investigate the use of two supporting materials with different properties to anchor the organic catalyst: inorganic silica and organic polystyrene.

Silica supported imidazolidinone

In our research group we have previously reported the use of chiral imidazolidinones supported on mesoporous silica nanoparticles. We employed the same synthetic strategy to prepare heterogeneous imidazolidinones supported on commercially available silica nanoparticles (Scheme 1).

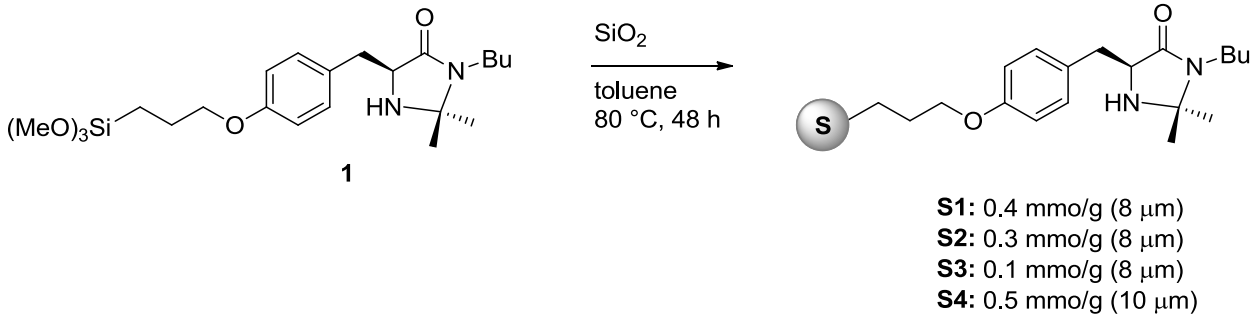

Scheme 1. Synthesis of silica supported catalysts **S1-S4**.

The synthesis involved the grafting of intermediate **1** onto silica in toluene at 80 °C for 48 hours. In order to study the influence of the morphological properties on the catalytic activity, two different types of commercially available silica were used as supports: with Apex Prepsil Silica Media 8 μm (Grace Davison - Discovery Sciences, asymmetry 0.9, pore diameter 120 Å, mean particle size 8.4 μm and surface area 162 m_2/g) three supported catalysts with different loadings were prepared (**S1** load 0.4 mmol/g, **S2** load 0.3 mmol/g and **S3** load 0.1 mmol/g). With Luna Silica 10 μm (pore diameter 101 Å, mean particle size 8.57 μm, and surface area 380 m_2/g) catalyst **S4** with a loading of 0.5 mmol/g was prepared. The loading of the chiral imidazolidinone supported onto silica was determined by weight difference.

In order to evaluate the influence of the linker on catalyst performances, we also explored a different anchoring strategy: according to Scheme 2, a click reaction between azido-functionalized silica and imidazolidinone **2** was performed in the presence of CuI as catalysts and Hunig's base in chloroform as solvent. Catalyst **S5** was obtained with a loading of 0.4 mmol/g.

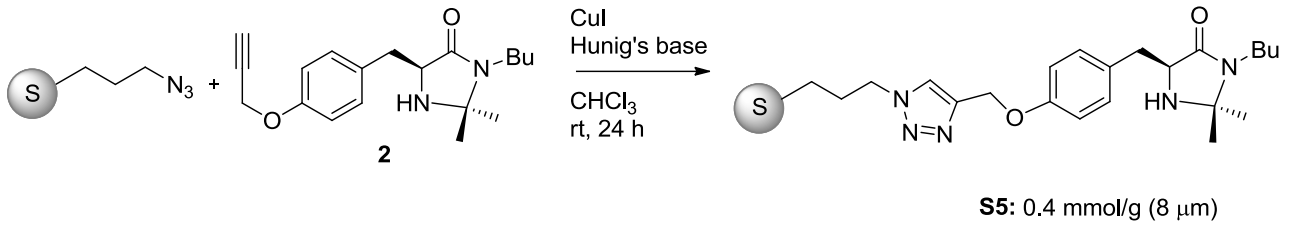

Scheme 2. Synthesis of silica supported catalysts **S5**.

In order to test catalysts performance, we chose as model the cycloaddition reaction between cyclopentadiene and cinnamaldehyde in the presence of the supported catalysts, an acid co-catalyst (HX) in acetonitrile/water (Table 1).

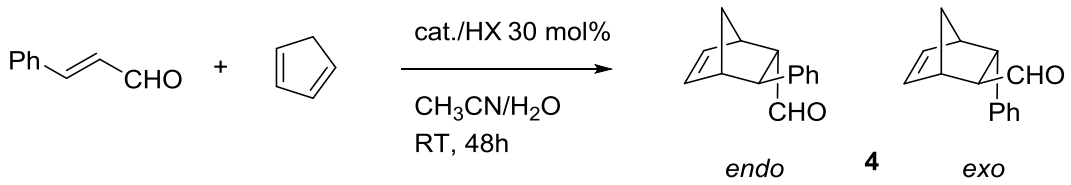

Table 1. Stereoselective cycloadditions in batch promoted by **S1-S5**.

entry	catalyst	HX	yield (%)[a]	*endo:exo*[b]	*ee % (endo,exo)*[c]
1	**S1**	HBF_4	75	55:45	75, 76
2	**S1**	TFA	69	50:50	80, 82
3	**S2**	HBF_4	42	50:50	46, 53
4	**S3**	HBF_4	34	50:50	47, 49
5	**S4**	HBF_4	78	55:45	78, 77
6	**S4**	TFA	66	55:45	83, 86
7	**S5**	HBF_4	91	55:45	93, 91
8	**S5**	TFA	52	55:45	87, 97

[a]isolated yield after chromatographic purification; [b]evaluated by ^{1}H-NMR on the crude reaction mixture; [c]evaluated by HPLC or GC on chiral stationary phase .

Catalyst **S1** and **S4** promoted the reaction in good yields and ee up to 82% (entries 1, 2, 5 and 6). The use of **S2** and **S3**, which have a lower loading of imidazolidinone resulted in poor yields and low ee (entries 3 and 4). **S5**, which features a triazole linker on its structure, promoted the reaction in good yields and very good ee, up to 93% (entries 7 and 8). This suggests that a longer linker between the solid support and the catalytically active site positively influences the enantioselectivity of the process.

The solid supported catalysts could be easily recovered after reaction time by simple filtration of the crude mixture. However, attempts to recycle the catalysts were unsuccessful. In the second reaction cycle, under the same experimental conditions, all the catalysts tested (**S1**, **S4** and **S5**) promoted the reaction in poor yields (lower than 30%) and very low ee (around 25%). This indicates that the organic catalyst supported onto silica is deactivated under reaction conditions

(probably the presence of the acid co-catalyst accelerates the degradation of the imidazolidinone ring).

With the aim of extending catalysts activity we explored the use of packed-bed flow reactors where the contact time between reagents and catalyst could be reduced. As catalytic reactors, three empty HPLC column (*l*: 12.5 cm, *id*: 0.4 cm, V: 1.57 mL) containing 1 gram of **S1**, **S4** and **S5** were employed. The void volume was determined experimentally for each reactor and it was necessary to calculate the residence time.

The model cycloaddition between cyclopentadiene and cinnamaldehyde was studied. The reagents were pumped in the reactor by a syringe pump and the products were collected at the way out of the reactor.

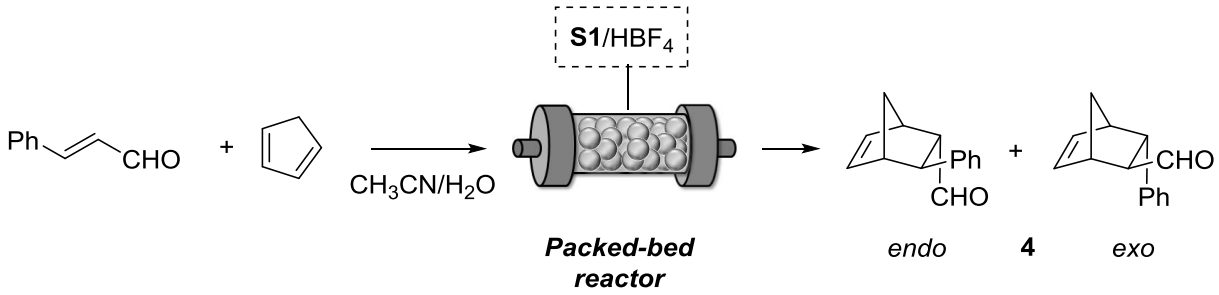

Table 2. Continuous flow cycloaddition promoted by **S1**.

entry	Running time (h)	flow rate (µL/min)	residence time (h)	HX	yield (%)[a]	*endo:exo*[b]	*ee %* *(endo,exo)*[c]
1	10-30	5	10	HBF_4	55	46:54	40, 60
2	30-50	3	16,5	HBF_4	91	47:53	71, 73
3	50-96	3	16,5	HBF_4	92	42:58	85, 81
4	96-150	2	25	HBF_4	95	44:56	83, 80
5	10-20	5	10	TFA	94	48:52	85, 85
6	20-96	5	10	TFA	84	47:53	85, 83
7	96-120	5	10	TFA	78	48:52	73, 71
8	120-150	5	10	TFA	77	49:51	77, 73
9	150-170	5	10	TFA	60	49:51	75, 74

[a]isolated yield after chromatographic purification; [b]evaluated by ^{1}H-NMR on the crude reaction mixture; [c]evaluated by HPLC or GC on chiral stationary phase .

The catalytic reactor containing **S1** showed a good activity in terms of chemical yields and enantioselectivity (up to 85%). By using both TFA and HBF_4 as co-catalysts the flow system produced cycloadducts **4** for more than 150 hours. Trifluoroacetate salt of the supported imidazolidinones promoted a faster reaction than its tetrafluoroborate counterpart (Table 2, entries 1-4 *vs*. entries 5-9).

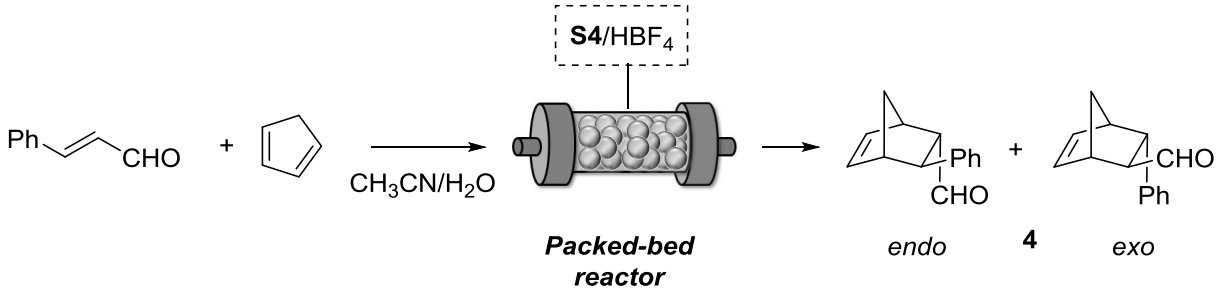

Table 3. Continuous flow cycloaddition promoted by **S4**.

entry	Running time (h)	flow rate (µL/min)	residence time (h)	HX	yield (%)[a]	*endo:exo*[b]	*ee %* *(endo,exo)*[c]
1	10-24	5	10	HBF_4	54	n.d	n. d.
2	24-48	5	10	HBF_4	76	52:48	71, 68
3	48-72	5	10	HBF_4	76	51:49	69, 66
4	72-96	5	10	HBF_4	60	51:49	68, 58
5	10-24	5	10	TFA	60	62:37	n. d.
6	24-48	5	10	TFA	50	53:47	67, 70
7	48-72	5	10	TFA	32	52:48	68, 70
8	72-96	5	10	TFA	25	53:47	63, 63

[a]isolated yield after chromatographic purification; [b]evaluated by ^{1}H-NMR on the crude reaction mixture; [c]evaluated by HPLC or GC on chiral stationary phase .

The packed-bed reactor containing **S4** proved to be less active than the previous one, indicating that the supporting material influences catalytic performance (Table 3). Using a residence time of 10 hours, products **4** were obtained in moderate yields and modest ee (around 70%). After 100 hours of continuous production the catalytic reactor became inactive.

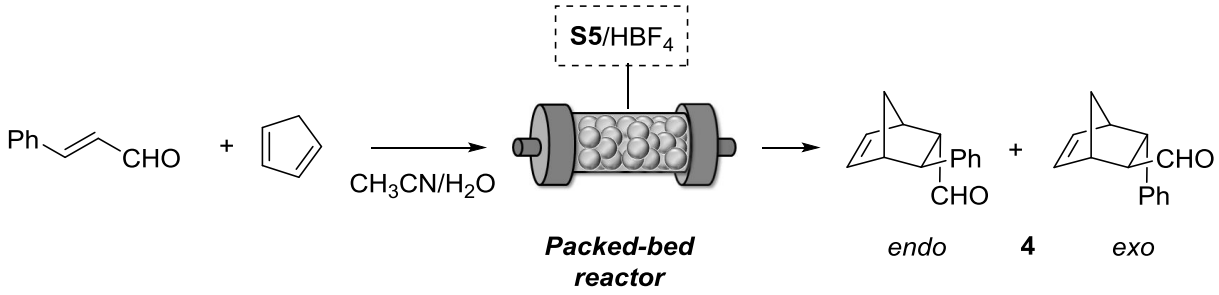

Table 4. Continuous flow cycloaddition promoted by **S5**.

entry	Running time (h)	flow rate (µL/min)	residence time (h)	HX	yield (%)[a]	*endo:exo*[b]	*ee %* *(endo,exo)*[c]
1	10-30	5	10	HBF_4	60	50:50	74, 91
2	30-50	5	10	HBF_4	50	47:53	80, 94
3	50-72	5	10	HBF_4	35	49:51	82, 87

[a]isolated yield after chromatographic purification; [b]evaluated by ^{1}H-NMR on the crude reaction mixture; [c]evaluated by HPLC or GC on chiral stationary phase .

The packed bed reactor prepared using **S5**, despite showing higher enantioselectivities (up to 94%) compared to the previous ones, promoted the model cycloaddition in modest yields and just after 72 hours the catalysts was completely inactive (Table 4).

The flow system with of **S1** proved to be the most active. The supported catalysts promoted the model cycloaddition for more than 150 hours, demonstrating that the flow process could extend catalyst lifetime and reduce the imidazolidinone deactivation observed in batch.

Polymer supported imidazolidinone

The synthesis of polymer supported catalysts is depicted in Scheme 2 and involved a click reaction between imidazolidinone **2** and 1-(azidomethyl)-4-vinylbenzene in the presence of CuI and Hunig's base. Resulting intermediate **3** was subjected to radical copolymerization with divinylbenzene as co-monomer in the presence of toluene and 1-dodecanol as porogens and AIBN as initiator. **P1** was obtained with a loading of 0.57 mmol/g that was determined by the stoichiometry of the polymerization reaction.

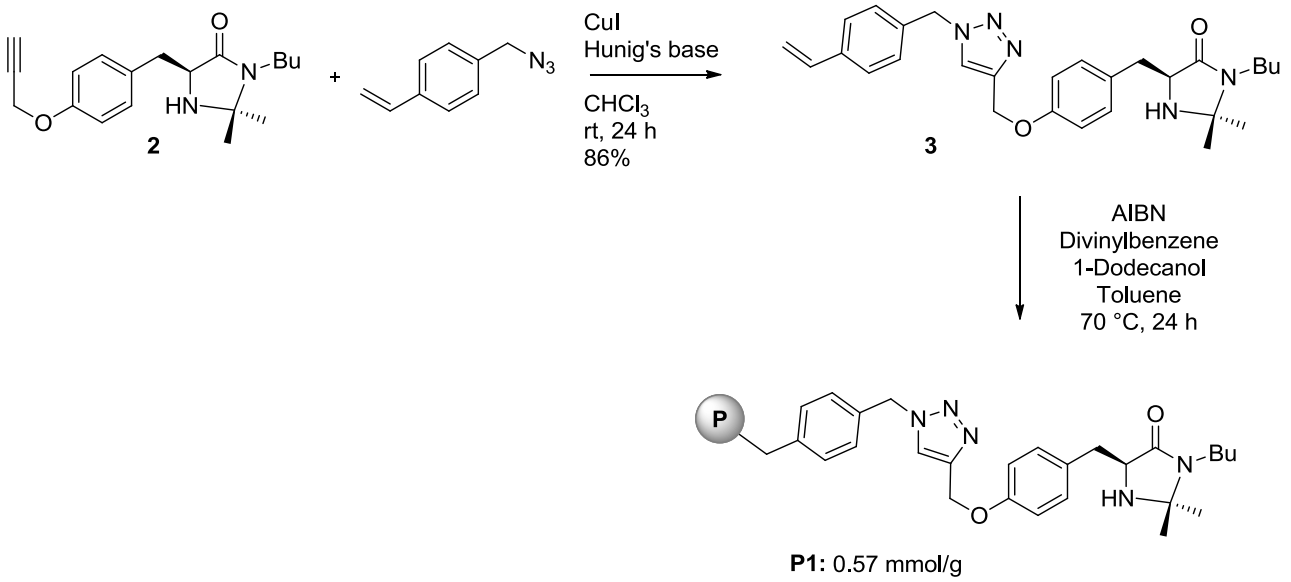

Scheme 3. Synthesis of polymer supported catalyst **P1**.

P1 was tested in the benchmark cycloaddition under the same experimental conditions employed for **S1-S5**. The catalyst afforded cycloadducts **4** in very good yields and excellent ee, up to 90% (Table 5, entries 1 and 3). Notably, when the catalyst was recycled, it maintained a good level of chemical activity and a very good enantioselectivity (entry 4).

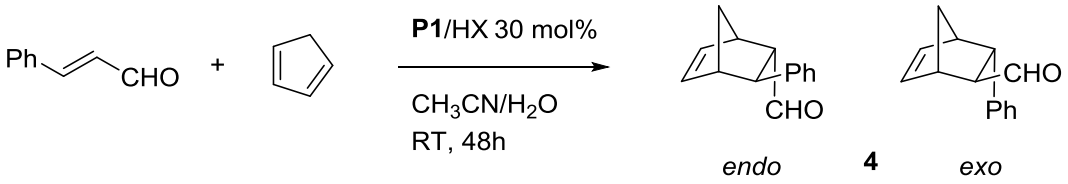

Table 5. Stereoselective cycloadditions in batch promoted by **P1**.

Entry	HX	T (h)	Yield (%)[a]	*endo:exo*[b]	*ee % (endo,exo)*[c]
1	TFA	48	85	44/56	90 (89)
2[d]	TFA	48	25	42/58	71 (75)
3	HBF_4	48	97	43/57	90 (88)
4[d]	HBF_4	72	70	44/56	85 (83)

[a]isolated yield after chromatographic purification; [b]evaluated by ^{1}H-NMR on the crude reaction mixture; [c]evaluated by HPLC or GC on chiral stationary phase; [d] catalyst recycled.

These preliminary results indicate that polystyrene as supporting material is better than silica. This is probably due to the apolar nature of the organic polymer compared to silica which presents Si-OH groups on his surface that can interfere with the activity of the supported catalyst

We next focused our attention on the preparation of a packed bed reactor containing **P1**. As flow reactor an HPLC column (*l*: 6 cm, *id*: 0.4 cm, V: 0.75 mL) filled with 0.3 grams of **P1** was employed. The void volume was determined experimentally and it was necessary to calculate the residence time. The system was used for the enantioselective cycloadditions of cyclopentadiene and three different aldehydes. For the first 24 hours product **4** was formed in 75% yield and 91% and 92% ee for *endo* and *exo* isomers, respectively (Table 6, entry 1). The reactor was then washed with solvent mixture and then subjected to a second cycloaddition to afford product **5** in good yield and ee (entries 3 and 4). The same procedure was repeated twice and products **6** and **4** were obtained in very good yields and ee (entries 6, 7 and 9). The catalytic reactor operated for 150 hours with no appreciable loss in chemical or stereochemical activity.

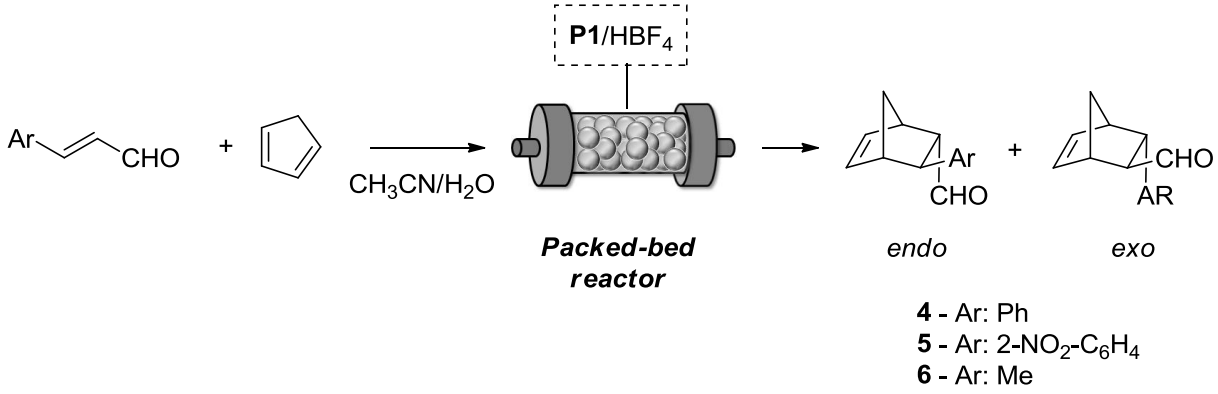

Table 6. Continuous flow cycloadditions promoted by **P1**.

entry[a]	Running time (h)	Product	yield (%)[b]	*endo:exo*[c]	*ee % (endo,exo)*[d]
1	0-24	**4**	75	47/53	92 (91)
2[e]	24-32	-	-	-	-
3	32-48	**5**	88	49/51	90 (91)
4	48-60	**5**	95	47/53	91 (90)
5[e]	60-72	-	-	-	-
6	72-86	**6**	94	52/48	83 (75)
7	86-108	**6**	97	49/51	85 (75)
8[e]	108-120	-	-	-	-
9	120-150	**4**	73	47/53	94 (89)

[a] Flow rate = 2μL/min, Res. time = 12 h; [b]isolated yield after chromatographic purification; [c]evaluated by ^{1}H-NMR on the crude reaction mixture; [d]evaluated by HPLC or GC on chiral stationary phase; [e] column wash.

Although the flow system proved to be stable for a long period of time, a major limitation was related to the low flow rate employed (2 μL/min). When we tried to increase the flow rate of the

process, thus reducing the residence time into the reactor, a decrease in the catalytic activity was observed (Table 7). For example, with a residence time of 1.2 hours, only 21% of product was obtained (entry 5).

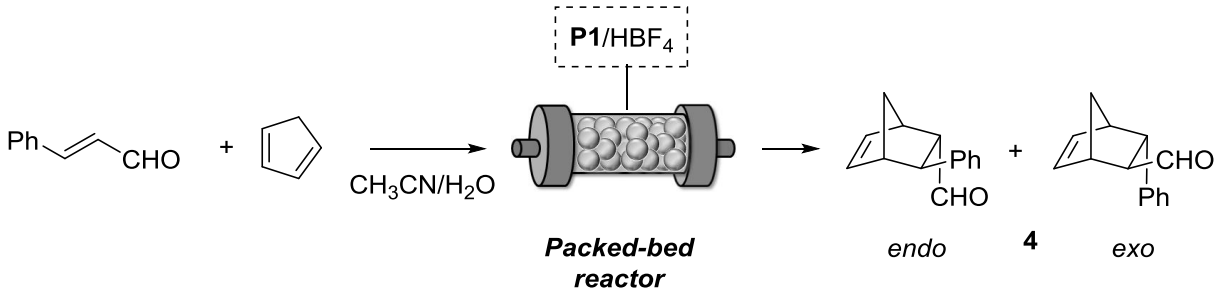

Table 7. Continuous flow cycloaddition promoted by **P1**.

entry	Running time (h)	flow rate (μL/min)	residence time (h)	yield (%)[a]	*endo:exo*[b]	*ee %* *(endo,exo)*[c]
1	0-24	2	12	80	48/52	85 (80)
2	24-44	7.7	3	65	48/52	86 (87)
3	44-50	7.7	3	52	47/53	89 (86)
4	55-70	18.8	1.2	21	48/52	87 (85)

[a]isolated yield after chromatographic purification; [b]evaluated by ^{1}H-NMR on the crude reaction mixture; [c]evaluated by HPLC or GC on chiral stationary phase .

The flow reactor was not suitable for operation at high flow rates, as these prevented the supported catalyst to have sufficient contact time with the reagents.

To overcome this problem we explored the use of monolithic reactors. As already reported above, these reactors feature a large surface area and can be employed at high flow rates. Monolithic reactor **M1** was prepared inside a HPLC column (*l*: 6 cm, *id*: 0.4 cm, V: 0.75 mL) by radical copolymerization of monomer **3** with divinylbenzene as co-monomer, in the presence of toluene and 1-dodecanol as porogens and AIBN as initiator (Scheme 3). The reactor was sealed and heatedat 70 °C for 24 hours. The reactor was then washed with THF pump in order to remove excess of porogens. The void volume was determined experimentally and it was necessary to calculate the residence time.

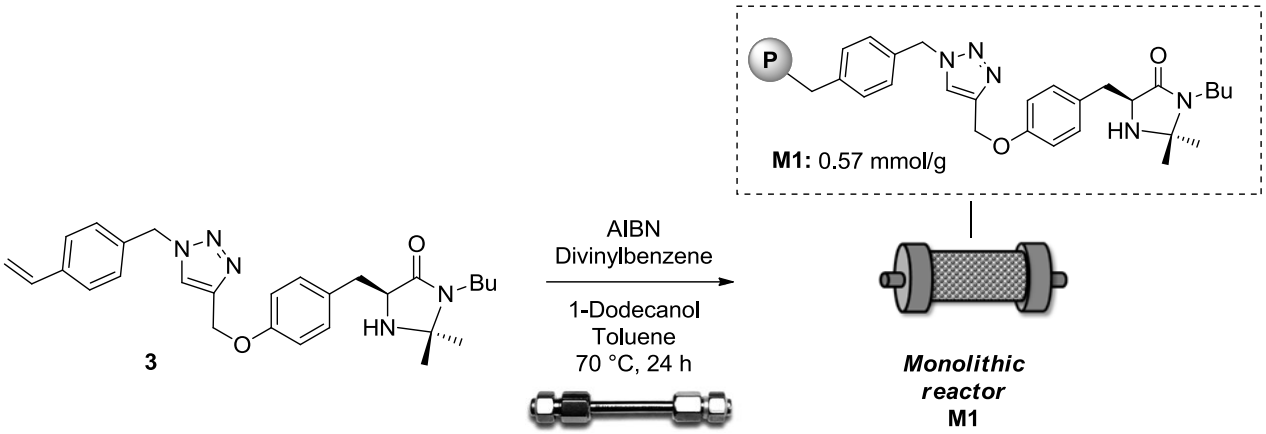

Scheme 4. Synthesis of monolithic reactor **M1**.

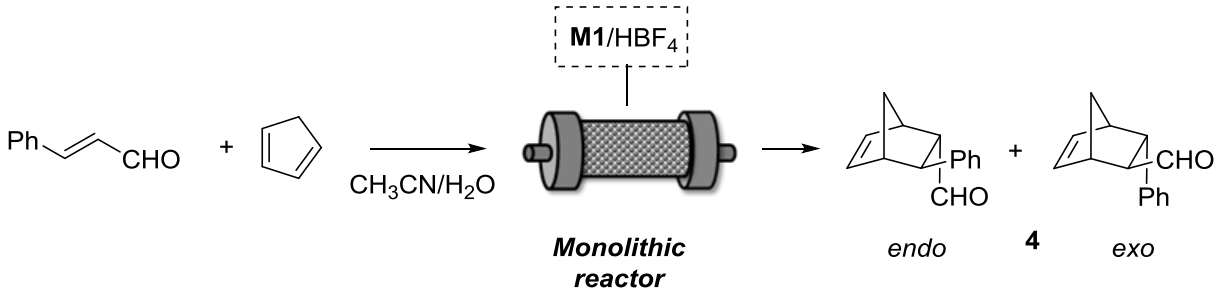

Table 8. Continuous flow cycloaddition promoted by **M1**.

entry	Running time (h)	flow rate (μL/min)	residence time (h)	yield (%)[a]	*endo:exo*[b]	*ee % (endo,exo)*[c]
1	0-4	2	12	n.d.	-	-
2	4-24	2	12	75	47/53	92 (91)
3	24-44	7.7	3	67	48/52	90 (90)
4	44-55	18.8	1.2	68	47/53	90 (86)
5	55-70	18.8	1.2	73	45/55	90 (88)

[a]isolated yield after chromatographic purification; [b]evaluated by ^{1}H-NMR on the crude reaction mixture; [c]evaluated by HPLC or GC on chiral stationary phase .

Monolithic reactor **M1** was tested in the model cycloaddition between cyclopentadiene and cinnamaldehyde in the presence of HBF_4 as co-catalyst. Differently from packed bed reactors, the monolithic reactor could work at high flow rates with no appreciable loss in chemical or stereochemical activity (Table 8). After 70 hours of continuous operation the desired cycloadducts were produced in 73% yield and 88% ee with a residence time of just 1.2 hours (entry 5).

To further demonstrate the advantages related to the use of monolithic reactors with respect to packed bed-ones we made a comparison of Turn Over Numbers (TON) and productivities (calculated as 1000* mmol product*mmol catalyst^{-1} * time^{-1}) obtained with three different flow systems. Results are reported in Figure 11.

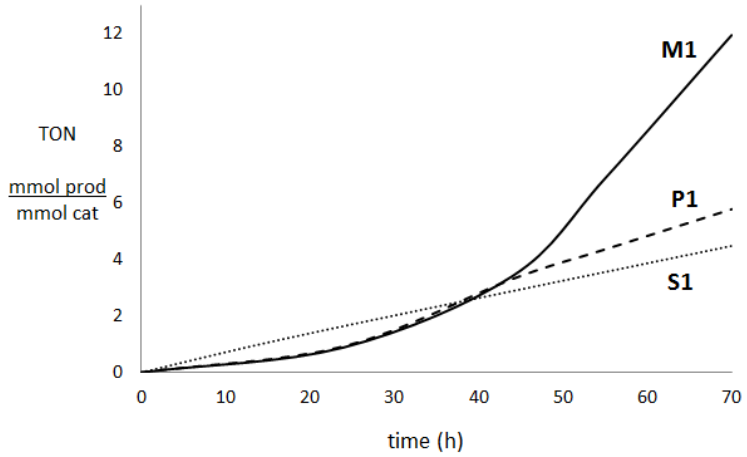

PRODUCTIVITY:

$$\frac{1000 \times \text{mmol PRODUCT}}{(\text{mmol CATALYST} \times \text{time})}$$

MONOLITHIC	**M1**:	339 h^{-1}
PACKED-BED	**P1**:	120 h^{-1}
PACKED-BED	**S1**:	64 h^{-1}

Figure 11. Comparison of TONs and productivity of flow systems using **S1**, **P1** and **M1**.

Monolithic reactor **M1** is much more efficient in terms of TONs and productivity than packed bed **P1** and **S1**. The greater performances are ensured by the possibility to work at higher flow rates with no erosion in the chemical or stereochemical activity. Thus in the same unit of time, larger quantities of product can be obtained.

In conclusion, different chiral imidazolidinones supported onto silica and polystyrene were prepared. Polystyrene supported catalyst **P1** proved to be more efficient than silica supported ones, and its activity was comparable to the one of non-supported imidazolidinone. The recyclability of the supported catalysts was studied but a quite rapid decrease in the activity was observed. The use of packed bed reactors for continuous flow cycloadditions favored a longer catalyst lifetime compared to batch procedure. The use of a monolithic reactor enabled the use of higher flow rates compared to packed bed reactors: this increased the productivity of the flow process and the overall TON of the supported catalyst.

To the best of our knowledge this is the first study that addressed a comparison of differently supported catalysts in a stereoselective synthesis carried out under flow conditions.

1.2.2 Stereoselective alkylation of aldehydes

Enantiomerically pure α-alkyl-substituted aldehydes are remarkably important key substrates for the synthesis of more complex molecules.[16] Consequently there has been substantial interest in the development of a methodology to access these valuable compounds in enantiomerically pure form.

Recently, novel synthetic α-alkylation methodologies have been developed by S_N1-type reactions, in which carbocations of sufficient stability generated in situ from alcohols, or stable carbenium ions are employed to perform enantioselective α-alkylation of aldehydes (Scheme 5) catalyzed by MacMillan-type catalysts, according to the mechanism reported in Figure 12.[17]

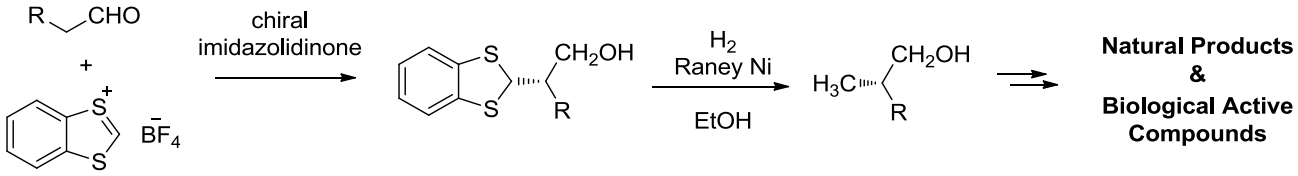

Scheme 5. Stereoselective alkylation of aldehydes.

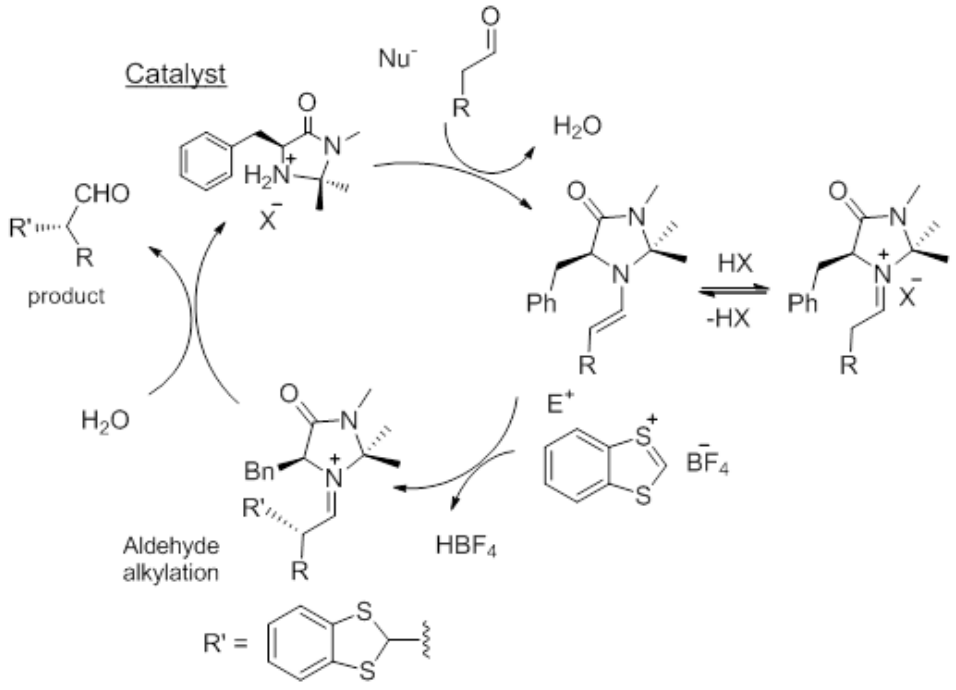

Figure 12. Reaction mechanism for the stereoselective alkylation of aldehydes promoted by chiral imidazolidinone

In order to develop a continuous flow process with the catalytic reactors previously described, we made some preliminary batch experiments using supported catalysts **S1** and **P1** (Table 9). We chose as model reaction the alkylation of propanal with 3 different cationic electrophiles (**7**, **8** and

9) in the presence of 30 mol% of supported catalysts, HBF_4 as co-catalysts, NaH_2PO_4 as scavenger (of HBF_4 released from the electrophile) and CH_3CN/H_2O mixture as solvent.

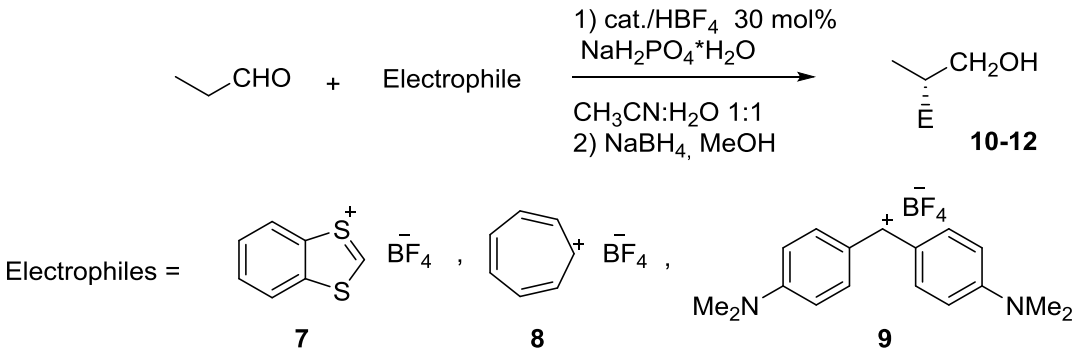

Table 9. Stereoselective alkylations in batch promoted by **S1** and **P1**.

Entry	Cat	Electrophile	Product	Yield (%)[(a)]	ee (%)[(b)]
1	**S1**	**7**	**10**	75	90
2	**P1**	**7**	**10**	67	86
3	**S1**	**8**	**11**	81	79
4	**P1**	**8**	**11**	72	90
5	**S1**	**9**	**12**	84	67
6	**P1**	**9**	**12**	64	95

(a) Isolated yield after chromatography. (b) Enantiomeric excess was determined by HPLC on chiral stationary phase.

Products **10-12** were obtained in good yields and fair to very good enantioselectivity. Interestingly, polymer supported imidazolidinone **P1** promoted the reaction with higher enantioselectivity compared to silica supported **S1** affording the products with ee up to 95% (entries 1, 3 and 5 *vs*. entries 2, 4 and 6).

Once the compatibility of supported catalysts in the batch reaction was demonstrated we explored the use of packed-bed reactors for the continuous flow alkylation of aldehydes. Two stainless-steel HPLC columns (*l*: 6 cm, *id*: 0.4 cm, V: 0.75 mL) were filled with **P1** (0.3 g) and **S1** (0.3 g), respectively. The void volume was determined experimentally for each reactor and it was necessary to calculate the residence time.

Initially we studied the alkylation of propanal with **7**: the packed bed reactor containing **S1** afforded the product in 65% yield and 80% ee (Table 10. entry 1). When the flow rate was increased from 0.1 mL/h to 5.4 mL/h the ee was not altered and the productivity of the flow system raised to 1030 h^{-1} (albeit a lower yield was obtained, entry 2). Packed-bed reactor containing **P1** promoted the reaction in moderate yield and very good ee (up to 95%, entries 3-7). Also in this case when the flow rate was raised to 10.8 mL/h the yield diminished to 11% (the productivity of the system is comparable to the one obtained with **S1**)(entry 7).

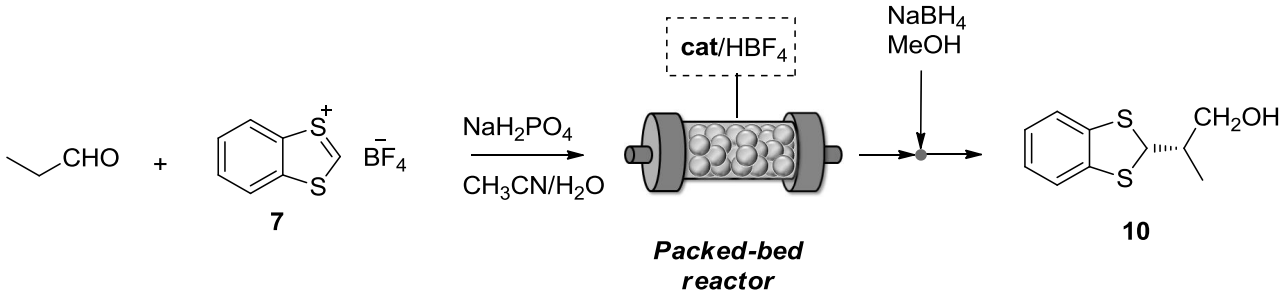

Table 10. Continuous flow stereoselective alkylation of propanal with **7** to pure product **10**.

Entry	Cat.[(a)]	Flow rate (mL/h)	Res. time (min)	Yield (%)[(a)]	ee (%)[(b)]	Prod. (h^{-1})[(c)]
1	**S1**	0.1	276	65	80	70
2	**S1**	5.4	5	19	82	1030
3	**P1**	0.1	354	60	80	40
4	**P1**	0.7	53	41	94	270
5	**P1**	1.3	28	25	93	310
6	**P1**	2.0	18	18	95	230
7	**P1**	10.8	4	11	87	1190

(a) Isolated yield. (b) ee was determined by HPLC on chiral stationary phase (c) Productivity determined as: mmol product * mmol catalyst^{-1} * time^{-1} * 1000.

We then investigated the alkylation of propanal with electrophile **8**. The flow system showed a behavior similar to the one obtained in the previous reaction. Product **11** was obtained in very good ee with both catalysts **S1** and **P1** (Table 11). Notably, using a residence time of 4 minutes only, **11** was obtained in 94% ee and with a productivity of 3830 h^{-1} (entry 4).

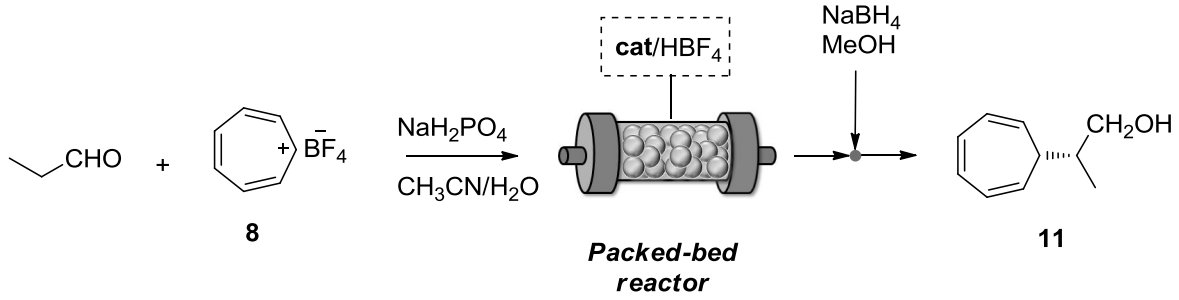

Table 11. Continuous flow stereoselective alkylation of propanal with **8** to pure product **11**.

Entry	Catalyst	Flow rate (mL/h)	Res. time (min)	Yield (%)[(a)]	ee (%)[(b)]	Prod. (h^{-1})[(c)]
1	**S1**	4.8	6	18	86	1150
2	**P1**	0.7	53	65	94	590
3	**P1**	1.5	24	52	93	1060
4	**P1**	10.8	4	26	94	3830

(a) Isolated yield. (b) ee was determined by HPLC on chiral stationary phase (c) Productivity determined as: mmol product * mmol catalyst^{-1} * time^{-1} * 1000.

Having identified **P1** as the catalytic system that promoted the reaction in higher enantioselectivity, we used it to further investigate the scope of the reaction under continuous flow conditions. The packed bed reactor containing **P1** was employed for the alkylation of octanal (Table 12) and phenylacetaldehyde (Table 13) with electrophile **7**. In both cases, the desired products, **12** and **13**, were obtained in very good ee but quite low yields.

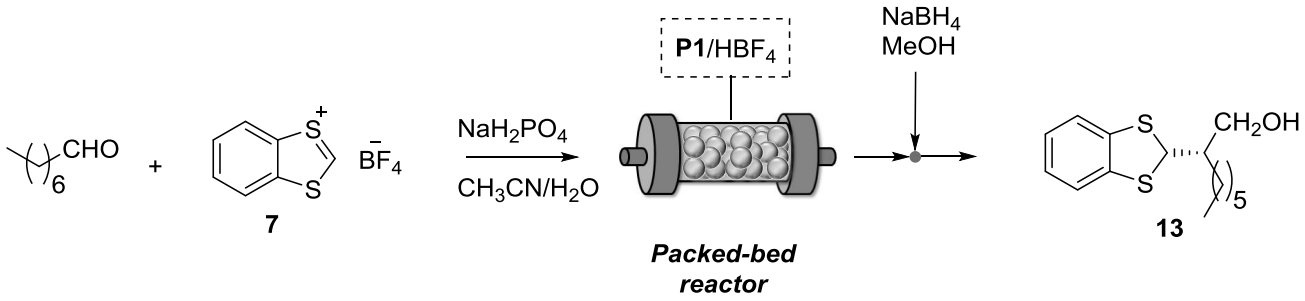

Table 12. Continuous flow stereoselective alkylation of octaanal with **7**.

Entry	Flow rate (mL/h)	Res. time (min)	Yield (%)[(a)]	ee (%)[(b)]	Productivity (h^{-1})[(c)]
1	1.5[(a)]	24	31	94	470
2	5.4[(a)]	7	9	90	600

(a) Isolated yield. (b) ee was determined by HPLC on chiral stationary phase (c) Productivity determined as: mmol product * mmol catalyst^{-1} * time^{-1} * 1000.

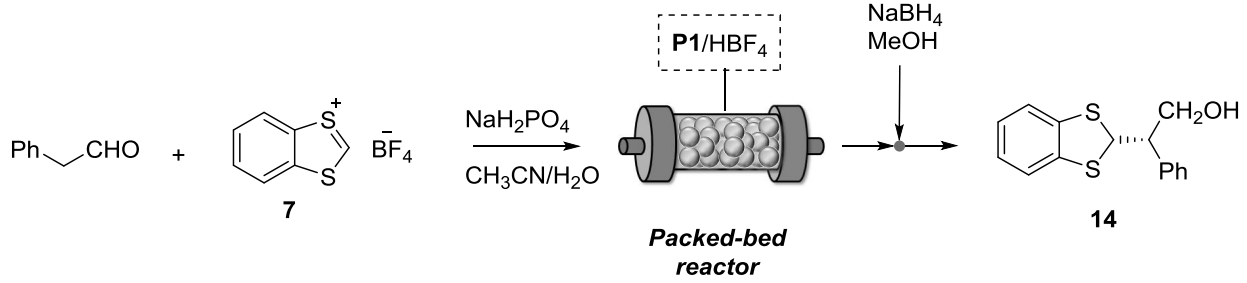

Table 13. Continuous flow stereoselective alkylation of phenylacetaldehyde with **7**.

Entry	Flow rate (mL/h)	Res. time (min)	Yield (%)[(a)]	ee (%)[(b)]	Productivity (h^{-1})[(c)]
1	1.5[(a)]	24	29	90	440
2	5.4[(a)]	7	18	90	970

(a) Isolated yield. (b) ee was determined by HPLC on chiral stationary phase (c) Productivity determined as: mmol product * mmol catalyst^{-1} * time^{-1} * 1000.

The flow systems prepared showed a good activity in the stereoselectivie alkylation of aldehydes, affording the desired products in very good ee (up to 95%) and higher productivities compared to the batch procedure. However when high flow rates were employed quite low yields were

obtained. In order to overcome this drawback a procedure to recover and recycle unreacted electrophile **7** should be implemented in our flow reactor systems. However, despite some attempts, an efficient methodology has not been developed yet.

Even if some improvements are still required, this procedure represent the first continuous flow stereoselective alkylation of aldehydes using solid supported imidazolidinones.[18]

1.3 Chiral Primary amines derived from cinchona alkaloids

Among chiral primary amines employed as organocatalysts, Cinchona alkaloids derivatives play a crucial role. Cinchona alkaloids are commercially available compounds, easily extracted from natural products. Most employed cinchona alkaloids are quinine, cinchonidine, quinidine and cinchonine. Their primary amines derivatives readily obtained by literature procedures are depicted in Figure 13.[19]

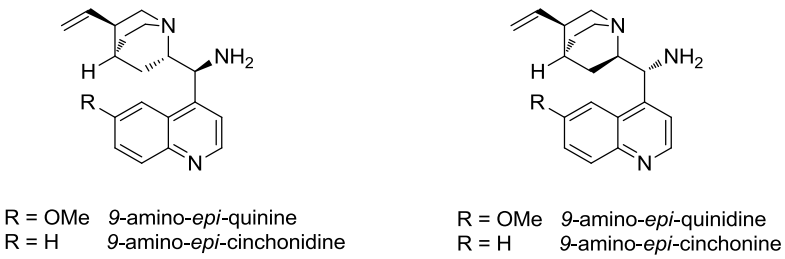

R = OMe *9*-amino-*epi*-quinine
R = H *9*-amino-*epi*-cinchonidine

R = OMe *9*-amino-*epi*-quinidine
R = H *9*-amino-*epi*-cinchonine

Figure 13. Chiral primary amines derived from cinchona alkaloids.

These molecules represent a well-established class of stereoselective organocatalysts capable of promoting a great number of chemical transformations with excellent levels of enantioselectivity.[20] Cinchona-derived primary amines are general and effective catalysts for a wide variety of asymmetric α, β and γ functionalization of carbonyl compounds.[21] It has also been demonstrated that they are able to combine orthogonal aminocatalytic modes (iminium and enamine activations) into one mechanism, thus promoting cascade reactions with α,β-unsaturated ketones and even with the challenging α,β-disubstituted enals.[22]

Despite of the wide application of chiral primary amines derived from Cinchona alkaloids as homogeneous catalysts, the development of their supported versions and their application in continuous flow processes are almost unexplored.[23]

Initially we decided to focus our attention on the preparation of supported chiral primary amine using solid materials with different properties and characteristics. In particular we employed an organic insoluble polymer (highly cross-linked polystyrene), an organic soluble polymer (polyethylenglycol PEG) and an inorganic insoluble material (silica). With such different materials we could determine the influence that each solid matrix can have on the reaction outcome and possibly identify the best support.

Polymer supported primary amines

We selected the double bond on quinuclidine ring of Cinchona alkaloids as anchoring site. We started from alkyne **15**, prepared according to a well-known procedure,[24] and we introduced a linker through click reaction in order to obtain compound **16**. The hydroxy group was then converted into the corresponding primary amine through a stereospecific 3-step sequence. Resulting monomer **17** was then subjected to radical copolymerization with divinylbenzene as co-

monomer, in the presence of toluene and 1-dodecanol as porogens and AIBN as initiator (Scheme 6).

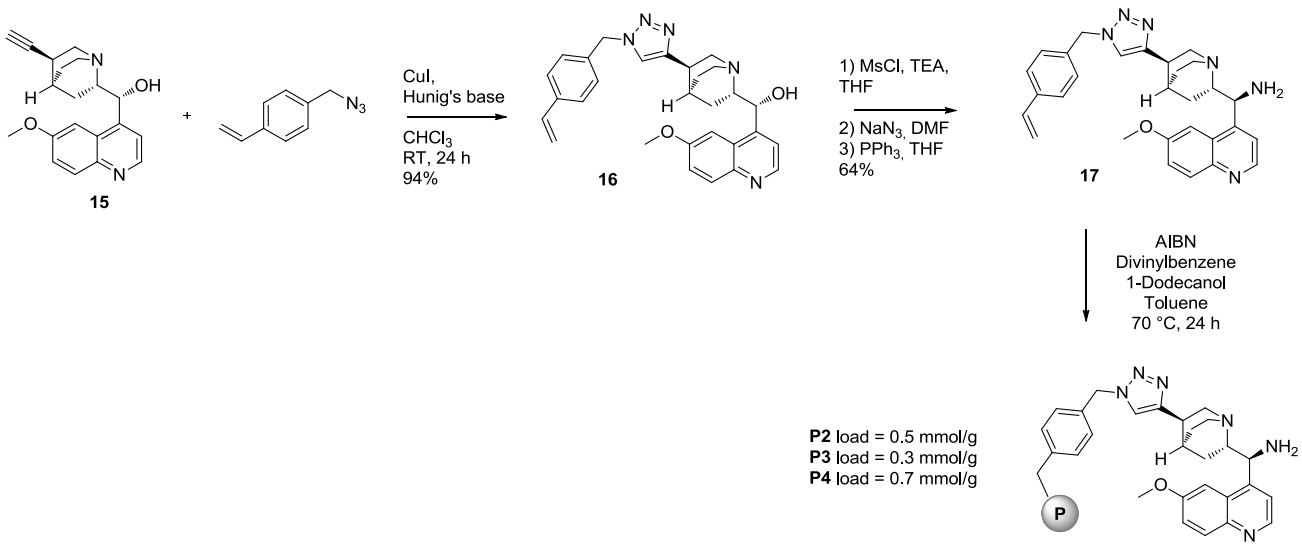

Scheme 6. Synthesis of polystyrene supported catalysts **P2-P4**.

Changing the stoichiometry of polymerization reaction we prepared three polystyrene supported catalysts (**P2**, **P3** and **P4**) with different loadings.

We also prepared a supported catalyst without any spacer between the chiral primary amine and the solid support in order to observe a possible variation in the catalytic activity. Catalyst **P5** was prepared directly from 9-amino-*epi*-quinine **18** by radical copolymerization under the usual conditions (Scheme 7). The loading of **P5** was determined by the stoichiometry of the polymerization reaction.

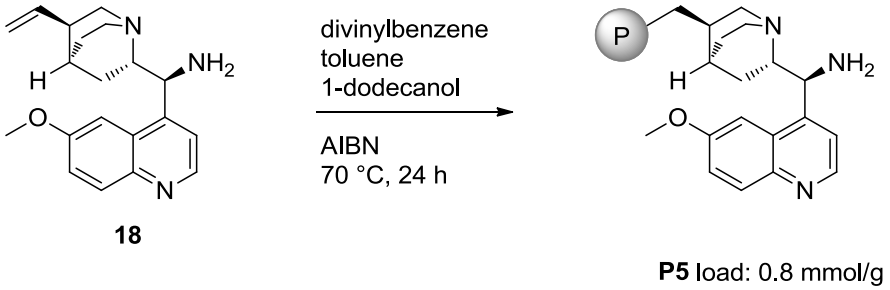

Scheme 7. Synthesis of polystyrene supported catalyst **P5**.

PEG supported primary amines

PEG is a well-known material that has already been employed in our laboratories as solid support for various organic catalysts or reagents.[25] Due to its solubility properties, PEG feature a unique behavior: it can be used in homogeneous reactions since it is soluble in water and certain organic solvents (CH_2Cl_2, MeOH, toluene); then it can be recovered as heterogeneous system by precipitation in solvents as ethers where it is insoluble. In order to prepare a PEG supported chiral

amine **G1**, we started from easily available PEG **19** which was subjected to a nucleophilic substitution with primary amine **20** in the presence of Cs_2CO_3 as base.

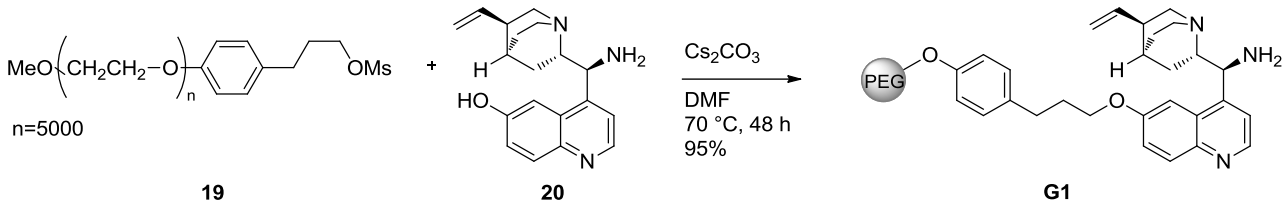

Scheme 8. Synthesis of PEG supported catalyst **G1**

G1 was obtained in 95% yield by simple precipitation in Et_2O/MTBE mixture.

Silica supported primary amines

The synthetic strategy for the preparation of silica supported primary amine involved an initial protection of primary amine **18** as trifluoroacetamide **21**. This was subjected to Pt-catalyzed hydrosilylation with trimethoxy silane (otherwise inhibited by primary amine functional group) which was then grafted onto commercially available silica nanoparticles. Once **S6** was obtained, the primary amine functionality was restored by treatment with methylamine in ethanol at 40 °C. Catalyst **S7** was obtained with a loading of 0.5 mmol/g as, determined by weight difference. Deprotection of **S6** to **S7** was monitored by solid state NMR (see experimental section for further details).

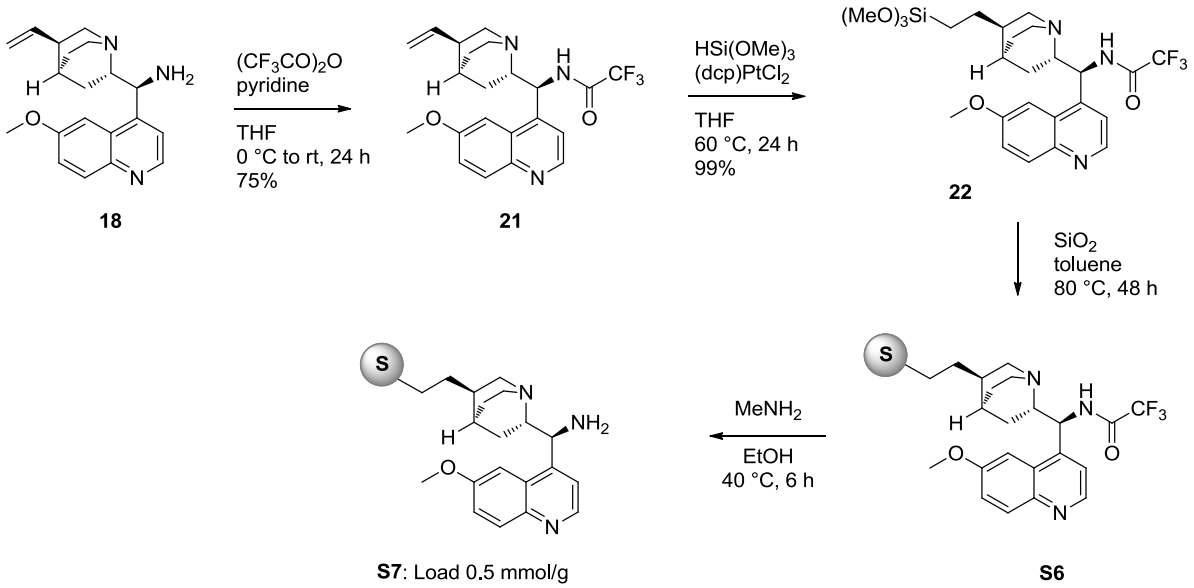

Scheme 9. Synthesis of silica supported catalyst **S7.**

In order to avoid the protection/deprotection sequence of primary amine as trifluoroacetamide we also explored a different procedure to prepare a silica supported primary amine. Exploiting radical thiol-ene coupling reaction, thiol-functionalized silica **S8** and primary amine **18** were reacted in the presence of AIBN as radical initiator in chloroform/toluene mixture as solvent at 80 °C for 24 h. Silica supported catalyst **S9** was obtained with a loading of 0.5 mmol/g, determined by weight difference.

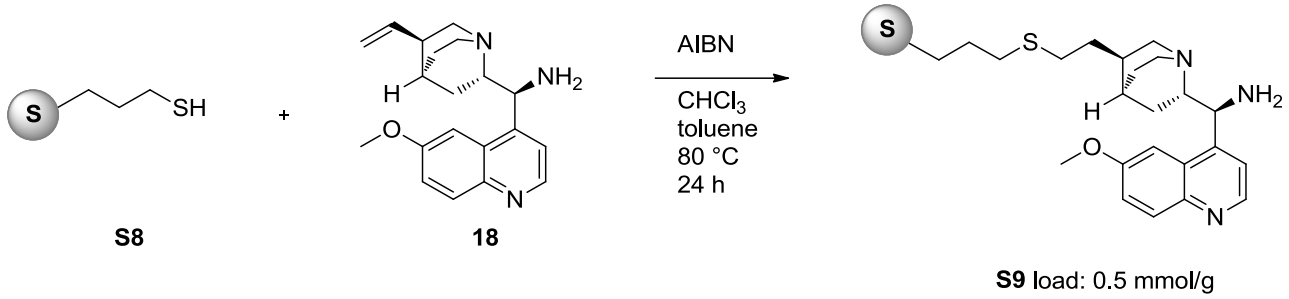

Scheme 10. Synthesis of silica supported catalyst **S9**.

Stereoselective reactions in batch

In order to study the catalytic activity of the obtained solid supported primary amines we chose as model the reaction between *i*-butyraldehyde and *trans*-β-nitrostyrene in the presence of benzoic acid as co-catalyst. The reaction involved an activation of the a-branched aldehyde through the formation of an enamine intermediate which attacks the electrophilic nitroalkene in a conjugate addition. This transformation has been reported by Connon *et al.* in 2007 and It is known to proceed in the presence of 9-amino-*epi*-dihydroquinidine in very good yield (93%) and ee (88%).[26]

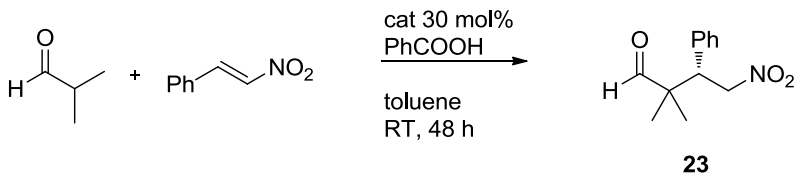

Table 14. Stereoselective Michael reaction in batch to afford product **23**.

Entry	Catalyst	Yield (%)[a]	ee (%)[b]
1	**P2**	81	94
2	**P3**	59	90
3	**P4**	99	95
4[c]	**P4**	98	95
5	**P5**	67	95
6	**G1**	87	94
7	**S7**	81	78
8	**S9**	77	73

(a) Isolated yield after chromatography. (b) Enantiomeric excess was determined by HPLC on chiral stationary phase; (c) 20 mol% of cat was used.

We performed the same reaction in the presence of our solid supported catalysts using toluene as solvent at room temperature (Table 14). Polystyrene supported catalysts **P2**-**P5** promoted the reaction in very good yields and ee up to 95% (Table 14, entries 1-5). The use of catalyst **P5** which did not feature any spacer in its structure resulted in a lower chemical activity (yield 67%). PEG supported catalyst **G1** afforded product **23** in 87% yield and 94% ee, a result totally comparable to the one obtained with the non-supported catalyst (entry 6). Both silica supported catalysts **S7** and **S9** showed a good chemical activity but a lower enantioselectivity (entries 7 and 8) indicating that silica as supporting material slightly reduced the stereoselectivity of the supported chiral primary amine.

From the results reported in Table 14 **P4** and **G1** proved to be most effective catalysts in terms of both chemical and stereochemical activities. Therefor these two supported systems were selected to explore recycling experiments. At the end of each reaction cycle the catalysts was isolated by filtration (**P4**) or precipitation (**G1**) and reused in another reaction cycle. Results are summarized in Table 15. Polystyrene supported catalyst **P4** could be used for 3 reaction cycle without appreciable loss in chemical and stereochemical activity. Form the 4th to the 6th cycle the chemical yield significantly decreased while the enantioselectivity remained very high. PEG supported catalyst G1 showed a similar behavior: for 3 reaction cycles **23** was obtained in very good yield and ee and then the chemical performances diminished until the 6th cycle.

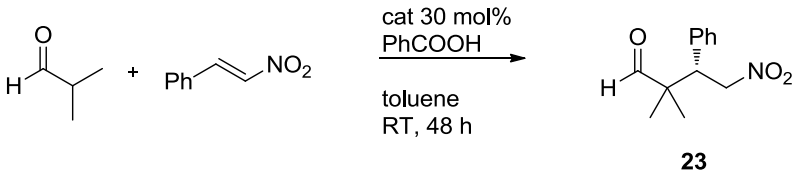

23

Table 15. Recycling experiments of supported catalysts **P4** and **G1**.

Cycle	P4		G1	
	Yield (%)[a]	ee (%)[b]	Yield (%)[a]	ee (%)[b]
1st	99	95	87	94
2nd	99	94	95	97
3rd	88	96	95	98
4th	53	96	60	86
5th	37	97	60	86
6th	28	95	37	85

In order to demonstrate if supported catalysts **P4** and **G1** could ensure some advantages compared to the non-supported catalyst we also made some recycling experiments with 9-amino-*epi*-quinine **18**, under the same reaction conditions. After each reaction cycle the catalysts was recovered after column chromatography and reused in another reaction cycle (Table 16). After the 1st reaction cycle the catalysts was recovered in 94% yield while after the 2nd cycle only 32% of **18** was recovered (decomposition of the catalyst was observed). In the 3rd cycle the desired product **23** was obtained only in 15% yield and no more catalyst **18** could be recovered from reaction

mixture. This experiment demonstrated that supporting chiral primary amines derived from cinchona alkaloids reduced deactivation observed under homogeneous conditions. Solid supported catalysts **P4** and **G1** could be employed for 6 reaction cycles while non supported catalysts **18** after just three reaction cycles completely lost his acivity.

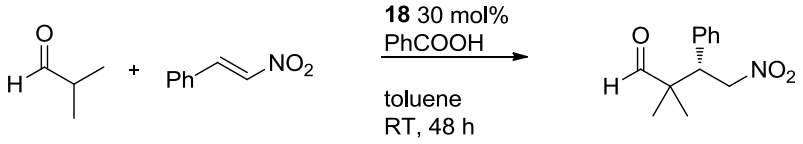

Table 16. Recycling experiments of non-supported catalyst **18**.

Cycle	Yield (%)[a]	ee (%)[b]	catalyst 18 recovered (%)[c]
1st	85	90	94
2nd	84	90	32
3rd	15	85	0

After having identified the best catalytic systems the scope of the reaction was investigated (Scheme 11). **P4** promoted in very good yields and ee the reaction of differently substituted aromatic and aliphatic nitroalkenes while **G1** was not active with aliphatic substrates. Products **27** and **28**, deriving from differently substituted aldehydes were obtained in good yields and ee with both catalysts. Ketones were less reactive than aldehydes and products **29** and **30** were obtained in moderate yields albeit in very high ee.

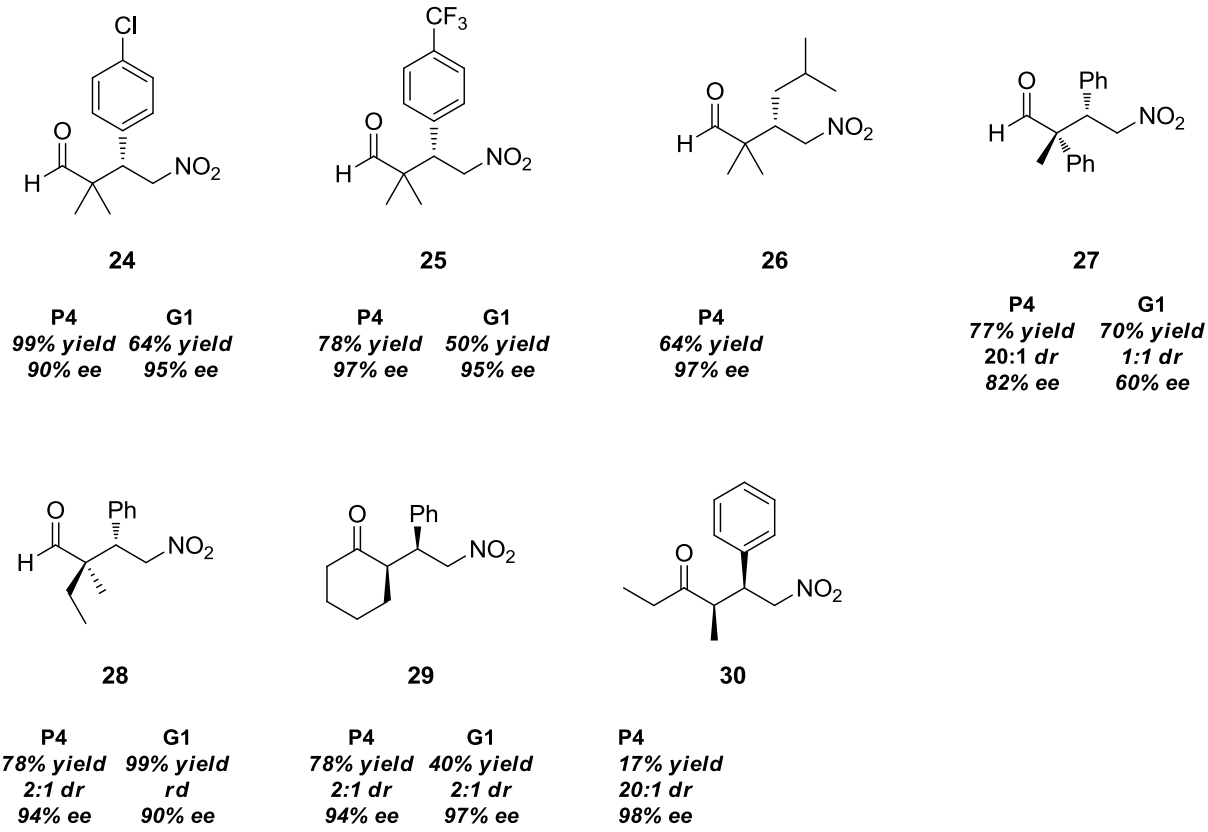

Scheme 11. Scope of the reaction.

With the same supported catalysts we also explored the possibility of performing reactions involving a different mechanism of activation in order to demonstrate the general applicability of our systems. The enantioselective conjugate addition of nitroalkanes to enones catalyzed by Cinchona-alkaloid-derived primary amine, which is known to proceed through iminium ion activation, was reported in 2013 by Wang and co-workers (Table 17, entry 1).[27] The model reaction between benzalacetone and nitromethane in the presence of polystyrene supported catalyst **P4** was carried out in chloroform at 60 °C and afforded the desired product in 65% yield and 90% ee (entry 2), slightly lower those obtained with the non-supported counterpart. When PEG supported catalysts was used **31** was obtained in 65% yield and 57% ee (entry 3).

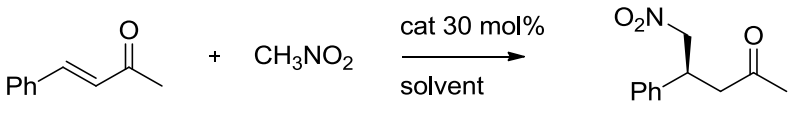

31

Table 17. Stereoselective conjugate addition of nitroalkanes to enones in batch.

Entry	Catalyst	Yield (%)[a]	ee (%)[b]
1[c]	**18**	67	99
2[d]	**P4**	65	90
3[e]	**G1**	65	57

c lit; d chcl3 60 grad 72h e neat mw 60g

Next we investigated the activation of α,β-unsaturated carbonyl compounds through activation via dienamine. The addition of (E)-3-nitroacrylates to α,β-unsaturated ketones promoted by aminocinchona alkaloid derivatives in the presence of acidic additives was recently developed in our laboratories.[28] The reaction allowed us to obtain highly functionalized cyclohexanones bearing three contiguous stereogenic centers in excellent diastereo- and enantioselectivity. As a model reaction, the addition of (E)-ethyl 3-methyl-3-nitroacrylate to benzalacetone in toluene was performed in the presence of 30 mol% of supported catalyst and 40 mol% of salicylic acid as an additive. The reaction in the presence of supported catalysts **P4** or **G1** gave products **32** in low yield and moderate ee (Table 18, entries 2 and 3).

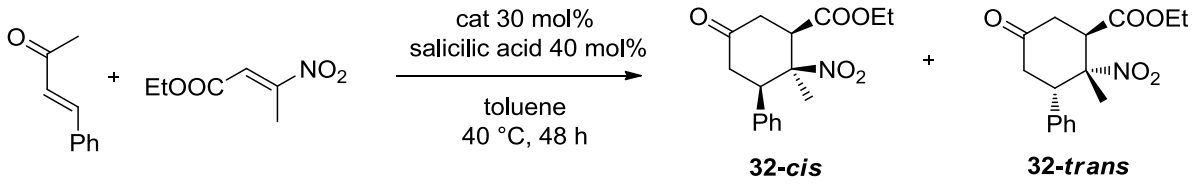

Table 18. Stereoselective synthesis of cyclohexanones in batch.

Entry	Catalyst	Yield (%)[a]	*dr*[b]	ee (%)[c]
1[d]	**18**	75	8:2	97
2	**P4**	35	3:1	77
3	**G1**	28	3:1	79

We finally focused the attention on a synthetic application of our methodology to the preparation of (*S*)-Warfarin **33** which is an anticoagulant drug.[29] Non-supported catalyst **18** promoted the reaction between 4-hydroxy-coumarin and benzalacetone in the presence of TFA in dioxane as solvent in 95% yield and 93% ee (Table 19, enrty1). **P4** afforded **33** in slightly lower yield and the same ee of the non-supported catalyst (entry 2). Catalyst **G1** was less active and gave *S*-Warfarin in 60% yield and 83% ee only(entry 3).

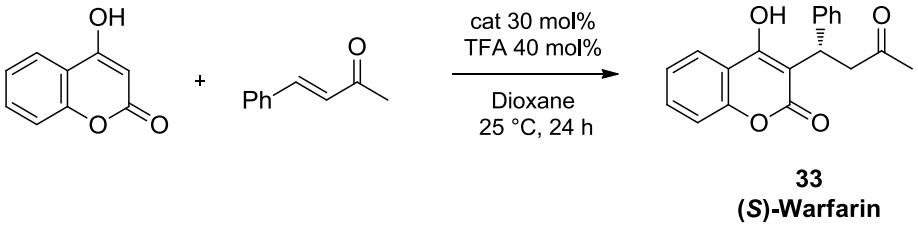

Table 19. Stereoselective synthesis of (S)-Warfarin in batch.

Entry	Catalyst	Yield (%)[a]	ee (%)[b]
1[c]	**18**	95	93
2	**P4**	83	93
3	**G1**	60	83

Stereoselective reactions under continuous flow conditions

Once the activity of the supported catalysts in batch was demonstrated, we turned our attention to their application in continuous flow processes. Since **P4** showed the best chemical and stereochemical behavior, it was selected to prepare a packed bed reactor, that was tested in the model reaction between *i*-butyraldehyde and *trans*-β-nitrostyrene in the presence of benzoic acid as co-catalyst. Supported catalyst **P4** (0.3 g) was placed into a stainless-steel HPLC column (*l*: 6 cm, *id*: 0.4 cm, V: 0.75 mL) and the reagents were pumped into the reactor through a syringe pump at 0.1 mL/h (res time: 4 hours). The outcome of the reactor was collected every 20 hours and the crude was analyzed in order to determine reaction yield and ee. Results of the continuous flow experiments are reported in Table 20.

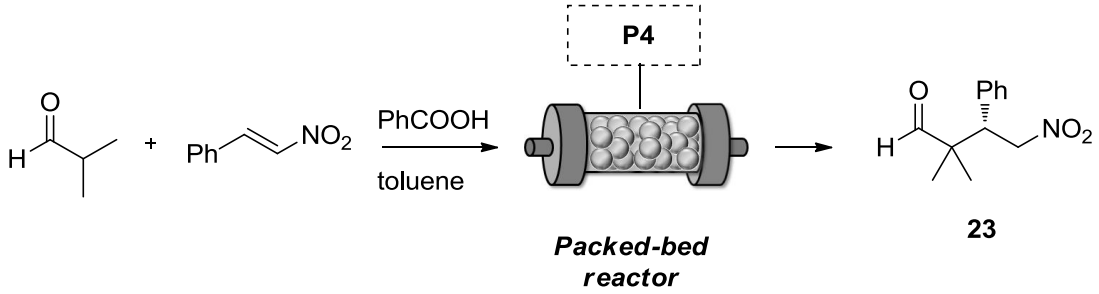

Table 20. Stereoselective continuous flow Michael reaction.

Entry[a]	Operation time (h)	yield (%)[b]	ee (%)[c]
1[d]	0-20	99	85
2	20-40	99	88
3	40-60	95	90
4	60-80	86	91
5	80-157	77	93
	157-160 [d]		
6	160-178	81	90
	180-182 [d]		
7	182-200	70	85

(a) flow rate = 0.1 mL/h, res. time = 4h; (b) Isolated yield after chromatography. (c) Enantiomeric excess was determined by HPLC on chiral stationary phase; (d) A solution of PhCOOH was flushed through the reactor at 0.5 mL/h before run 1, 6 and run 7.

Compound **23** was continuously produced in very good yield and high ee for 160 hours (Table 21, entries 1-5). After this time it was necessary to flush a solution of PhCOOH co-catalyst in order to "re-activate" the catalyst. The continuous flow system was active for up to 200 hours affording product **23** in good yield and ee up to 90% (entries 6 and 7).

We then employed another packed bed reactor containing catalyst **P4** (0.3 g) for the preparation of (*S*)-Warfarin **33**. A mixture of 4-hydroxy-coumarin and benzalacetone in the presence of TFA in dioxane was flushed through a syringe pump at 0.1 mL/h (res. time 4 h). Product **33** was obtained in 90% yield and 87% ee (Scheme 12).

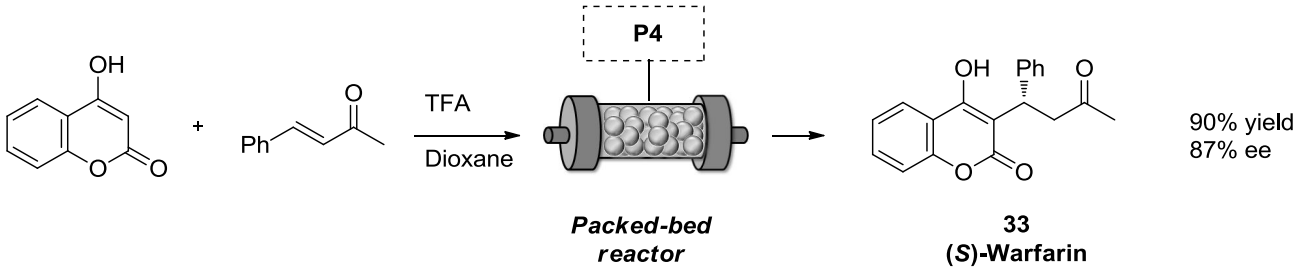

Scheme 12. Stereoselective continuous flow synthesis of (*S*)-Warfarin.

In conclusion, chiral primary amines derived from cinchona alkaloids have been supported onto three materials with different properties. These catalysts were tested in the functionalization of different carbonyl compounds and the results obtained were comparable to the ones obtained with the non-supported catalyst. Polystyrene supported catalyst **P4** proved to be the most effective and it was more stable in recycling experiments than the homogeneous catalyst. The immobilization of the catalyst on a solid support reduced the deactivation of the catalytic species observed in homogeneous conditions. The general applicability of the catalyst was demonstrated and the possibility to develop continuous flow processes for the synthesis of chiral molecules was studied. Finally **P4** was employed for the continuous flow synthesis of anticoagulant (*S*)-Warfarin.

1.4 Chiral Picolinamides

Chiral amines are very important pharmacophore that can be found in several pharmaceuticals and agrochemical compounds (Figure 14).[30]

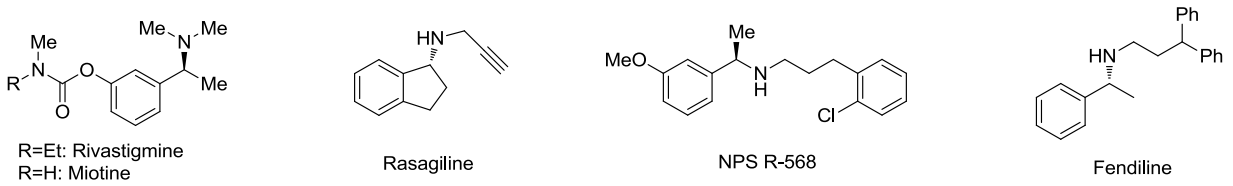

Figure 14. Examples of paharmaceutical or agrochemical compounds contaiing chiral amines moiety.

Among several available methodologies, the stereoselective reduction of imines with trichlorosilane ($HSiCl_3$) catalyzed by chiral lewis bases has been investigated by numerous academic research groups including ours and has proved to be very efficient.[31]

Trichlorosilane is a colorless volatile liquid, supplied by the silicon industry at the cost of most organic solvents. In this purified form, it is the principal precursor to ultrapure silicon in the semiconductor industry and the basic component of purified polysilicons, frequently used also in the synthesis of silicon containing organic compounds.

Trichlorosilane is a weak Lewis acid that, once coordinated by a Lewis base through an n-σ* interaction involving nonbonding electron pairs of the donor and antibonding orbitals of the acceptor, expands its coordination sphere and acquires a "hypervalent state". Silicon atom is not deactivated by the base lone pair donation; on the contrary, its Lewis acidity is increased, due to the electron density redistribution occurring after the base coordination, this results in an increased positive charge on silicon and negative charge on its ligands which can be delivered onto an electrophilic substrate, which can or cannot on his turn coordinated by silicon atom. In fact, by virtue of the silicon increased Lewis acidity, a compound featuring a lone pair can be coordinated and activated towards nucleophilic attack, where the nucleophile can be an external species or just one of the silicon substituents. If this is the case, the reaction proceeds through a cyclic transition state. Thus, employing an enantiomerically pure Lewis base to activate the silicon-based reactant, it is possible to control the stereochemical outcome of the promoted nucleophilic reaction in a rather efficient way. Moreover, using the chiral Lewis base in substochiometric quantities, it is possible to develop stereoselective catalytic strategies (Figure 15):

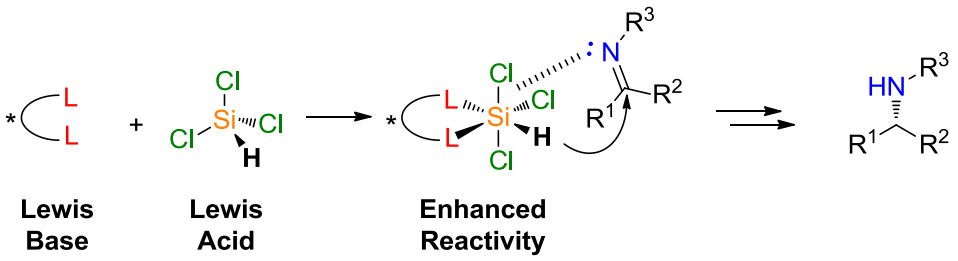

Figure 15. Activation of $HSiCl_3$ by a Lewis base.

Our research group developed different chiral Lewis bases to be used in combination with $HSiCl_3$ for the enantioselective reduction of C=N double bonds.[32] In particular we developed different catalysts with a picolinamide moiety as Lewis base employing different chiral scaffolds. Examples of chiral picolinamides developed in our laboratories are reported in Figure 16.

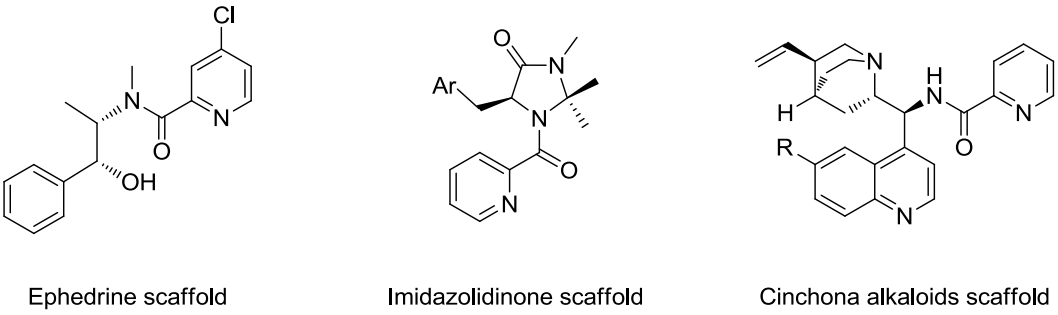

Ephedrine scaffold | Imidazolidinone scaffold | Cinchona alkaloids scaffold

Figure 16. Chiral picolinamides developed in our research group.

Our idea was to develop new solid supported chiral Lewis bases in order to implement a continuous flow process for the stereoselective synthesis of chiral amines using $HSiCl_3$. In this chapter we report the synthesis and application of chiral Lewis bases featuring chiral imidazolidinone (section 1.4.1) and cinchona alkaloids (section 1.4.2) as scaffold. Silica and polystyrene were employed as supporting material.

1.4.1 Chiral Imidazolidinone as Scaffold

The stereoselective reduction of imines with $HSiCl_3$ using picolinamides with a chiral imidazolidinone as scaffold has been previously investigated in our laboratories.[33] Chiral picolinamide **45l** derived from (*L*)-phenylalanine promoted the synthesis of chiral amine **48** in 88% yield and 88% ee (-10 °C, catalyst loading of 10 mol%).

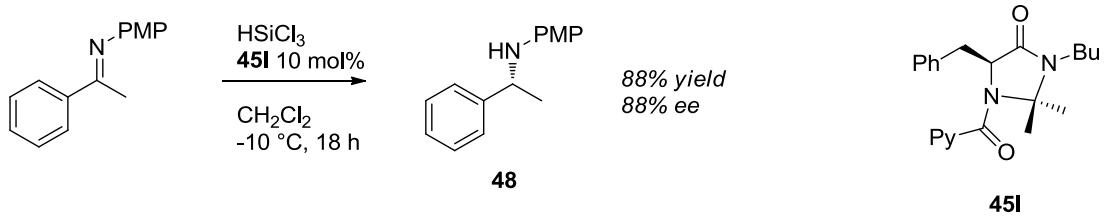

Scheme 13.

We decided to employ (*L*)-Tyrosine to obtain a chiral picolinamide catalyst and exploit the phenolic residue as an handle to anchor the catalyst onto a solid support (Scheme 14).

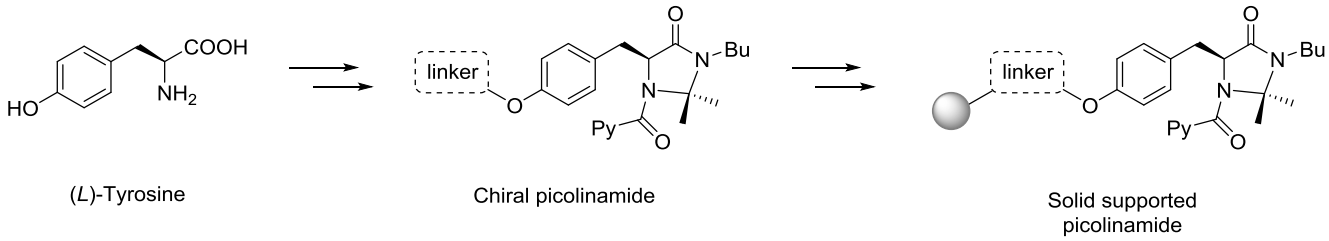

Scheme 14.

Silica supported picolinamides

The synthesis of silica supported picolinamide **S10** involved the preparation of picolinamide **35** starting from the known compound **34**.[34] The double bond of **34** was then converted into the corresponding trimethoxysilyl derivative **36** that was grafted onto commercially available SiO_2 (Apex Prepsil Silica Media 8 µm) to afford **S10** (load 0.25 mmol/g). The loading was determined by weight difference.

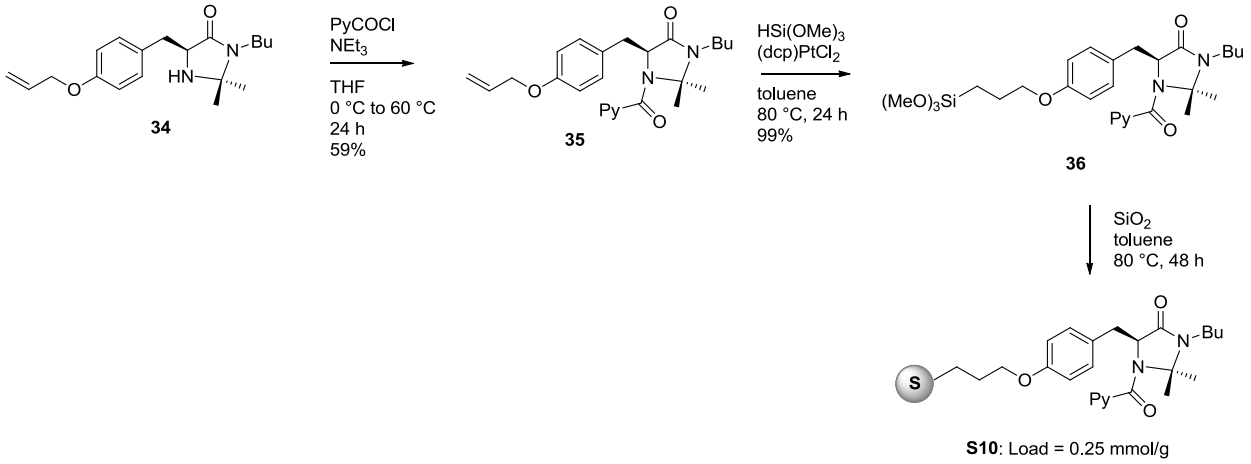

Scheme 15. Synthesis of silica supported catalyst **S10**.

We also prepared another silica supported picolinamide which features a linker longer than that of **S10** between the active site and the solid support. Starting from imidazolidinone **2**, a click reaction with 1-(allyloxy)-4-(azidomethyl)benzene gave compound **37** that was then converted into the corresponding picolinamide **38**. Platinum catalyzed hydrosilylation with $HSi(OMe)_3$ followed by grafting onto commercially available SiO_2(Apex Prepsil Silica Media 8 µm) afforded **S11** (load = 0.3 mmol/g).

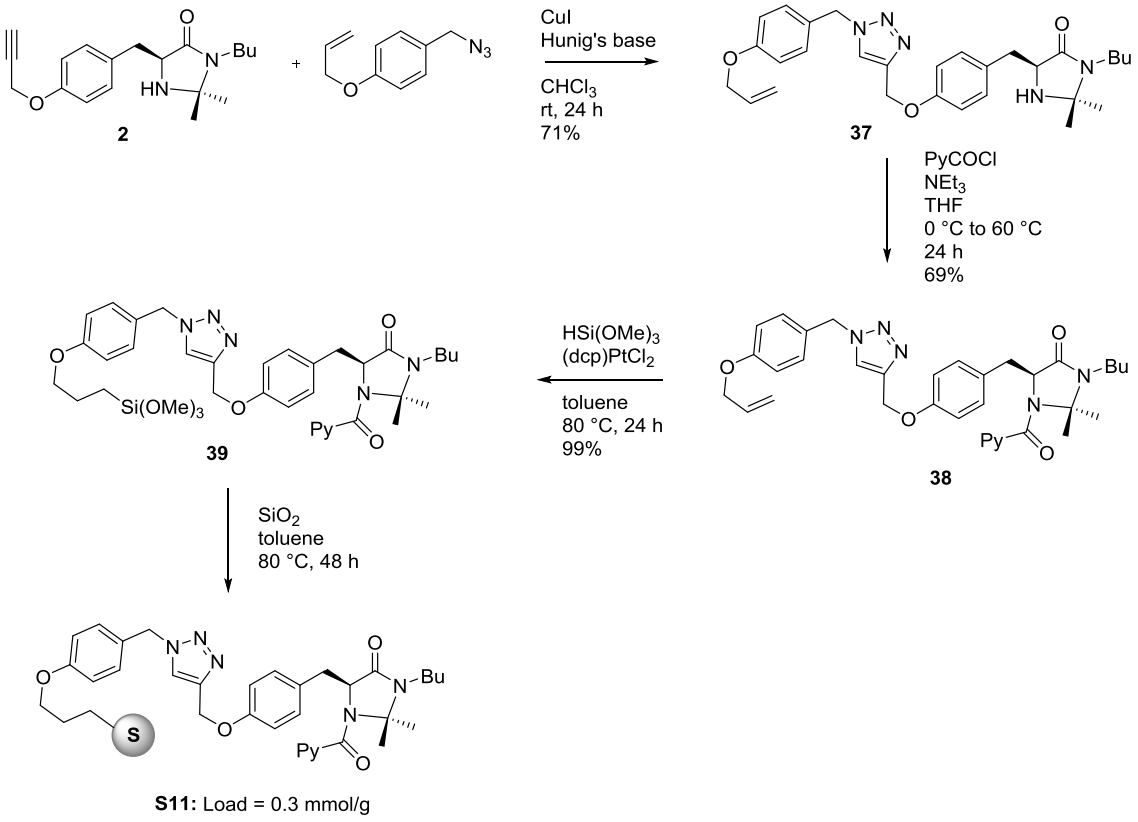

Scheme 16. Synthesis of silica supported catalyst **S11**.

Polystyrene supported picolinamides

The synthetic strategy for the preparation of polymer supported picolinamide started from imidazolidinone **3** that was converted into the corresponding picolinamide by reaction with picolinic acid and ethylchloroformate in the presence of *N*-methyl-morpholine as base. Monomer **45** was then polymerized by radical copolymerization with divinylbenzene as co-monomer, in the presence of toluene and 1-dodecanol as porogens and AIBN as initiator (Scheme 15). The loading of **P6** was determined by the stoichiometry of the polymerization reaction.

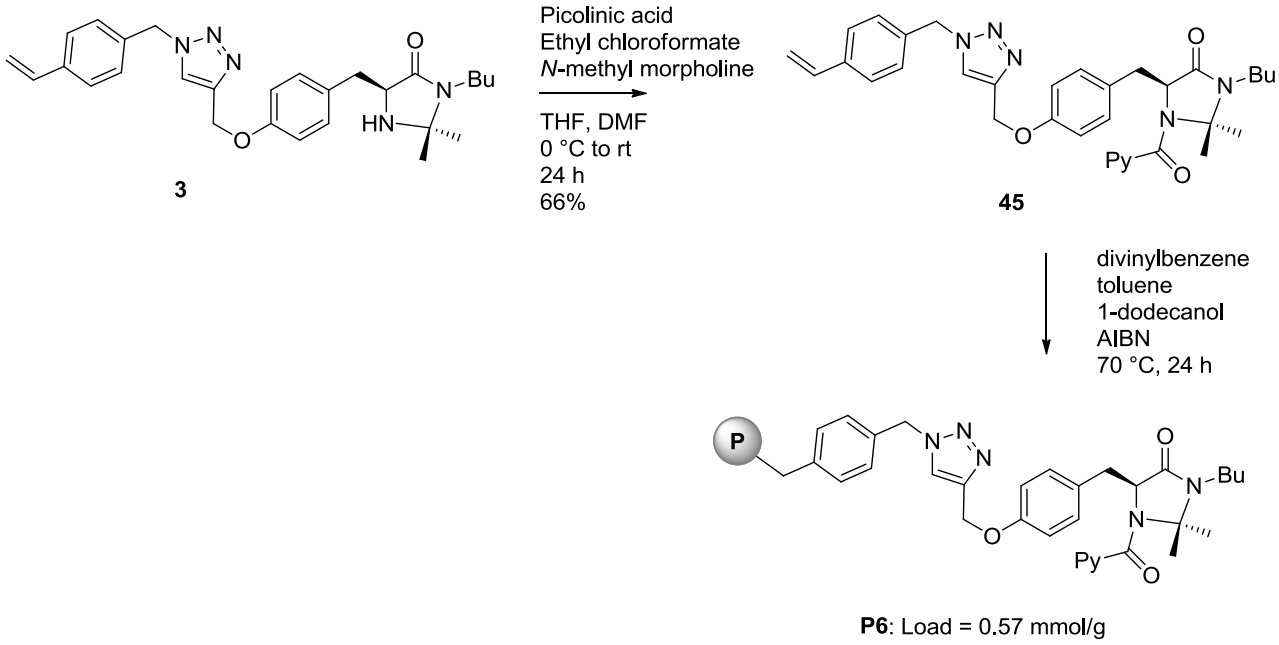

Scheme 17. Synthesis of polymer supported catalyst **P6**.

Stereoselective reactions in batch

The reduction of imines derived from acetophenone with trichlorosilane was chosen as model reaction to test the solid supported picolinamides (Table 21). **S10** promoted the reaction in excellent yield and very good ee (entries 1 and 2). The presence of a longer linker in the structure of catalyst **S11** did not improve neither the yield nor the stereoselectivity of the process (entries 3 and 4). Polystyrene supported picolinamide **P6** proved to be the best catalytic system affording the desired products in very good yields and excellent ee (97%, entries 5 and 6)

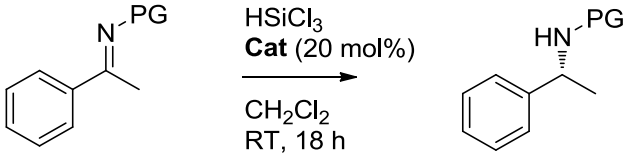

Table 21. Catalyst screening

Entry	Catalyst	PG	Yield (%)[a]	ee (%)[b]
1	**S10**	Ph	97	82
2	**S10**	PMP	98	86
3	**S11**	Ph	70	21
4	**S11**	PMP	95	75
5	**P6**	Ph	94	97
6	**P6**	PMP	92	97

(a) Isolated yield after chromatography. (b) Enantiomeric excess was determined by HPLC on chiral stationary phase.

On the basis of these preliminary results, **P6** was employed for further experiments. As reported in Table 22 the amount of the supported catalyst could be reduced to 1 mol% without any loss in the chemical or stereochemical activity (Table 22, entry 1). When the reaction time was reduced to 4 hours, a loading of 5 mol% of **P6** gave chiral amine **48** in 82% yield and 94% ee.

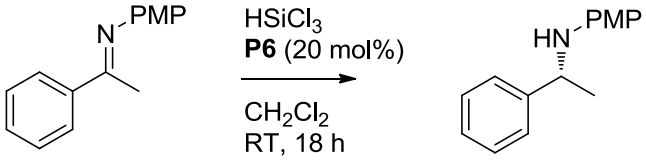

48i **48**

Table 22. Catalyst loading screening

Entry	P6 (mol%)	Yield (%)[a]	ee (%)[b]
1	20	94	97
2	10	94	96
3	5	92	95
4	5[c]	82	94
5	1	96	94
6	1[c]	46	91

(a) Isolated yield after chromatography. (b) Enantiomeric excess was determined by HPLC on chiral stationary phase; (c) reaction time: 4h.

We then studied the scope of the reaction. Different aryl substituted imines were reduced with $HSiCl_3$ in the presence of **P6** (Scheme 16). Imines carrying both electron withdrawing (**51**-**55**) and electron donating groups (**49**, **50**, **56**) were reduced in very good yields and excellent ee. Notably, amine **57**, which is the precursor of Rivastigamine, was obtained in 80% yield and 95% ee. Unfortunately, amine **58**,precursor of Rasagiline, was obtained only in 62% yield and 55% ee.

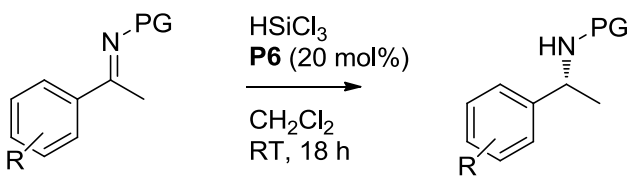

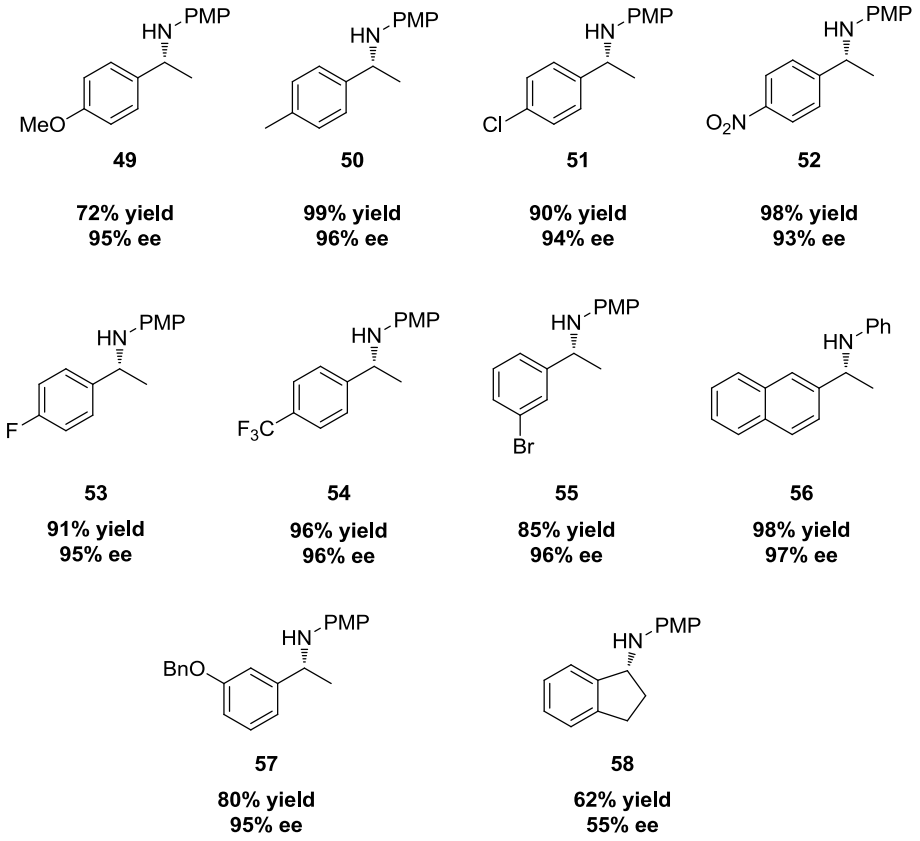

Scheme 18. Scope of the reaction.

As already observed with the homogeneous catalyst **45n**, the synthesis of fluorinated imines, which are important pharmaceutical building blocks, was not successful as adducts **59** and **60** were obtained in very good yields but poor ee (Scheme 17).

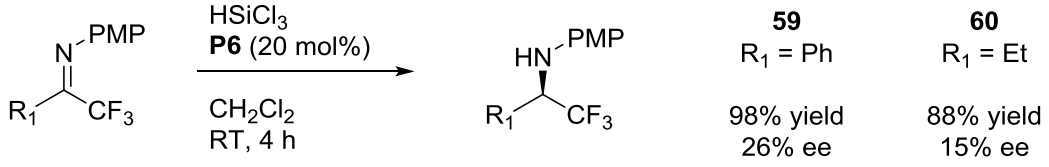

Scheme 19. Reduction of fluorinated ketoimines

α-Amino ester **61** was obtained in very good yield and moderate enantioselectivity (Scheme 18).

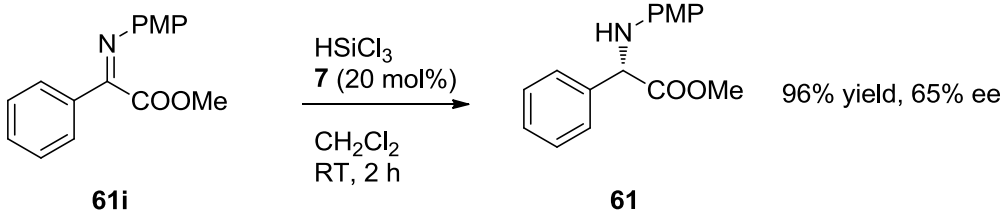

Scheme 20. **Reduction of α-amino ester.**

β-Amino esters **62**-**64**, which are precursors of β-lactams, were obtained in very good yields and good ee (Table 23).

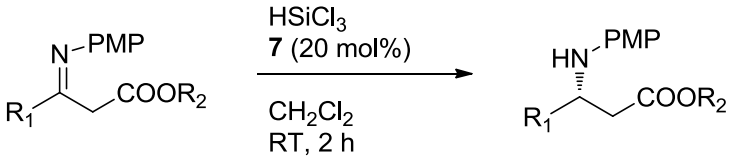

62-64

Table 23. Reduction of β-amino esters.

Entry	R_1	R_2	Yield (%)[a]	ee (%)[b]
1	C_6H_5-	COOMe	98	84
2	4-CF_3-C_6H_4-	COOMe	98	78
3	4-NO_2-C_6H_4-	COOEt	87	84

(a) Isolated yield after chromatography. (b) Enantiomeric excess was determined by HPLC on chiral stationary phase.

In order to demonstrate the practical applicability of supported catalyst **P6**, we explored the possibility to recycle the catalysts. When recycling experiment were conducted for 18 hours for each cycle, amine **48** was obtained as racemic mixture already at the 2nd run. It was necessary to reduce reaction time to 2 hours to maintain a high level of stereoselectivity (Table 24). Under these conditions it was possible to run four reaction cycles without any loss in the chemical or stereochemical activity of the process (ee up to 95 %). In the 5th cycle, **48** was obtained in very low yield and reduced ee. At the 6th cycle the catalysts was completely deactivated.

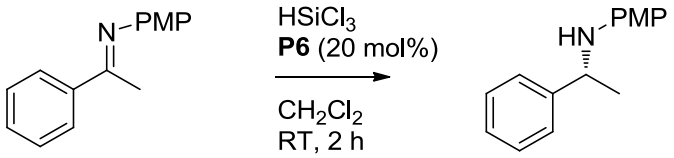

48i **48**

Table 24. Recycling experiments.

Cycle	Yield (%)[a]	ee (%)[b]
1st	84	94
2nd	82	95
3rd	85	95
4th	90	95
5th	27	81
6th	0	-

(a) Isolated yield after chromatography. (b) Enantiomeric excess was determined by HPLC on chiral stationary phase.

When amine **57** was selected as target for recycling experiments better resuts were obtained. **P6** promoted the reduction with $HSiCl_3$ of **57i** in good yields and very good ee for seven reaction cycles (Table 25).

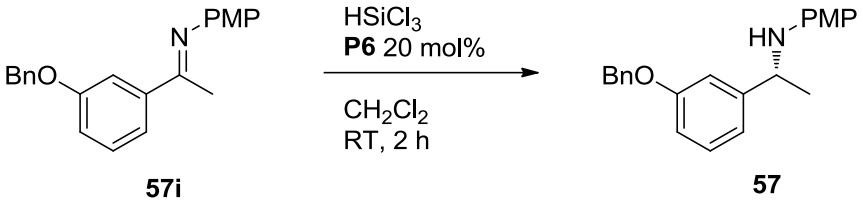

57i **57**

Table 25. Recycling experiments.

Cycle	Yield (%)[a]	ee (%)[b]
1st	80	94
2nd	81	94
3rd	80	94
4th	79	93
5th	87	93
6th	84	90
7th	76	87

(a) Isolated yield after chromatography. (b) Enantiomeric excess was determined by HPLC on chiral stationary phase.

Stereoselective reactions under continuous flow conditions

Polystyrene supported catalyst **P6** was then employed for the preparation of packed bed reactors for the continuous flow reduction of imines with $HSiCl_3$. **P6** (0.3 g) was placed into a stainless-steel HPLC column (*l*: 6 cm, *id*: 0.4 cm, V: 0.75 mL). The void volume was determined experimentally, the residence time calculated. A 0.05 M solution of imine and $HSiCl_3$ in CH_2Cl_2 was pumped into the reactor through a syringe pump at 0.4 mL/h (res time: 1 hour) at room temperature. The outcome of the reactor was collected into a flask containing NaOH 10% solution. After phase separation and concentration the product was isolated. Every hour the product was collected and analyzed in order to determine the conversion and the ee as a function of time.

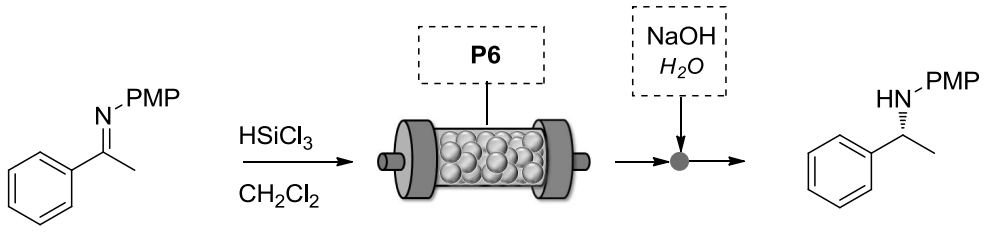

48i ***Packed-bed reactor*** **48**

Table 26. **Flow synthesis of amine** 48.

Entry[a]	Running time (h)	Yield (%)[b]	ee (%)[c]
1	0-2	92	85
2	2-3	94	83
3	3-4	93	81
4	4-5	94	77
5	5-6	94	75
6	6-7	94	73

(a) Flow rate: 0.4 mL/h, Residence time: 1 h; (b) Determined by NMR. (c) Enantiomeric excess was determined by HPLC on chiral stationary phase.

As reported in Table the flow system was stable for seven hours, producing chiral amine **48** in excellent yield and good ee. The stereoselectivity of the process slightly decreased with time, probably because of a partial decomposition of the catalyst. For this reason a second continuous flow reactor was prepared and the continuous flow process was run at a residence time of 30 min. As reported in Table 27 an increase in the stereoselectivity of the process was observed, albeit the chemical yield was lower because of the shorter reaction time.

Table 27. Flow synthesis of amine **48.**

Entry[a]	Running time (min)	Yield (%)[b]	ee (%)[c]
1	0-60	61	87
2	60-90	62	86
3	90-120	62	83
4	120-150	65	81
5	150-180	63	79

(a) Flow rate: 0.8 mL/h, Residence time: 0.5 h; (b) Determined by NMR. (c) Enantiomeric excess was determined by HPLC on chiral stationary phase.

Finally we employed **P6** for the continuous flow synthesis of chiral amine **57**, precursor of Rivastigamine (Table 28). The continuous flow process, afforded the desired product in 82% yield and 83% ee for the first 2.5 hours. Then **58** was continuously produced for other 3 hours in 79% yield and 74% ee.

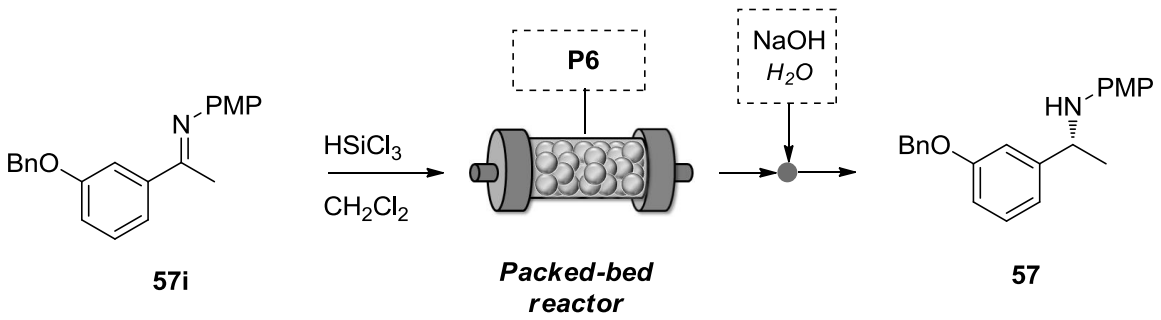

Table 28. Flow synthesis of amine **57.**

Entry[a]	Running time (min)	Yield (%)[b]	ee (%)[c]
1	0-150	82	83
2	150-330	79	74

(a) Flow rate: 0.8 mL/h, Residence time: 0.5 h; (b) Isolated yield after chromatography. (c) Enantiomeric excess was determined by HPLC on chiral stationary phase.

In conclusion a new class of solid supported chiral Lewis bases for the catalyticreduction of imines with trichlorosilane was studied. Polystyrene proved to be a support more effective than silica, allowing enantioselectivities up to 97%. Polymer supported catalyst **P6** showed a broad scope and a very good recyclability, even with a loading of 1 mol% only. **P6** was used to prepare packed bed reactors for the continuous flow synthesis of chiral amines under continuous flow conditions. The flow system was employed for the stereoselective synthesis of amine **57**, precursor of Rivastigamine.

1.4.2 Cinchona alkaloids as Scaffold

In 2014 a new class of chiral lewis bases for the reduction of imines with trichlorosilane has been developed in collaboration with the group of Professor Burke in Evora. These catalysts are based on a chiral scaffold derived from Cinchona alkaloids and feature a picolinamide moiety as catalytic active site for the coordination to $HSiCl_3$. As reported in scheme 21 catalyst **46** promoted the reduction of imine **48i** in 98% yield and 81% ee at 0°C.

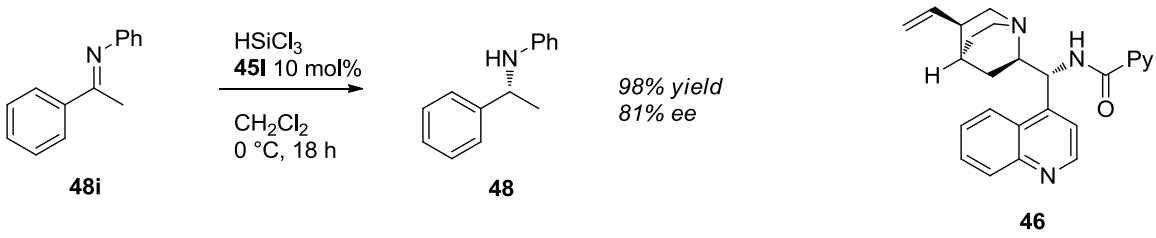

48i **48** **46**

Scheme 21. Stereoselective reduction of imine **48i** with picolinamide **46.**

Our strategy to develop a solid supported version of this class of catalysts was based on the functionalization of the double bond of the quinuclidine moiety in order to introduce a linker necessary to anchor the organic molecule onto a solid support (Scheme 22).

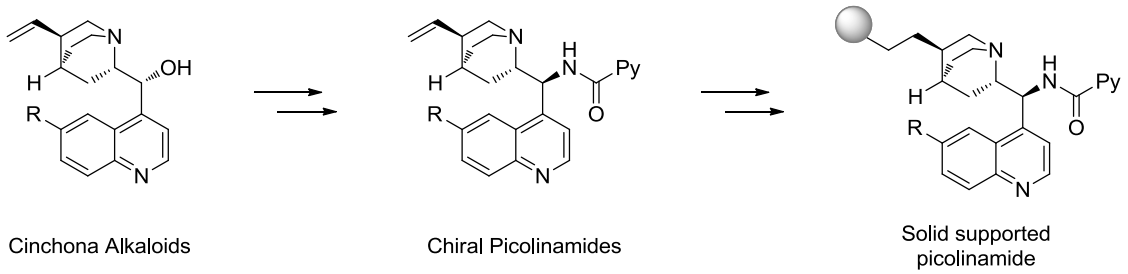

Cinchona Alkaloids Chiral Picolinamides Solid supported picolinamide

Scheme 22. General strategy for the preparation solid supported Picolinamides.

Silica supported picolinamides

The synthetic strategy to prepare silica supported picolinamides involved the functionalization of the double bond of the quinuclidine ring with a trimethoxysilyl derivative, essential to graft onto commercially available silica nanoparticles. The synthesis of catalysts **S12** and **S13** is depicted in Scheme 23. Primary amine derived from cinchona alkaloids (**18** or **42**) were converted into the corresponding picolinamides by reaction with picolinic acid and isobutyl chloroformate in the presence of TEA in THF. The double bond of compound **40** and **43** was then quantitatively converted into trimethoxysilyl derivatives **41** and **44** by reaction with trimethoxysilane $HSi(OMe_3)$ using $dcpPtCl_2$ as catalyst for the hydrosilylation reaction. Final grafting was performed in the presence of commercially available SiO_2 nanoparticles (Apex Prepsil Silica Media 8 µm) in toluene at 80 °C for 24 hours. Catalyst loadings were determined by weight difference.

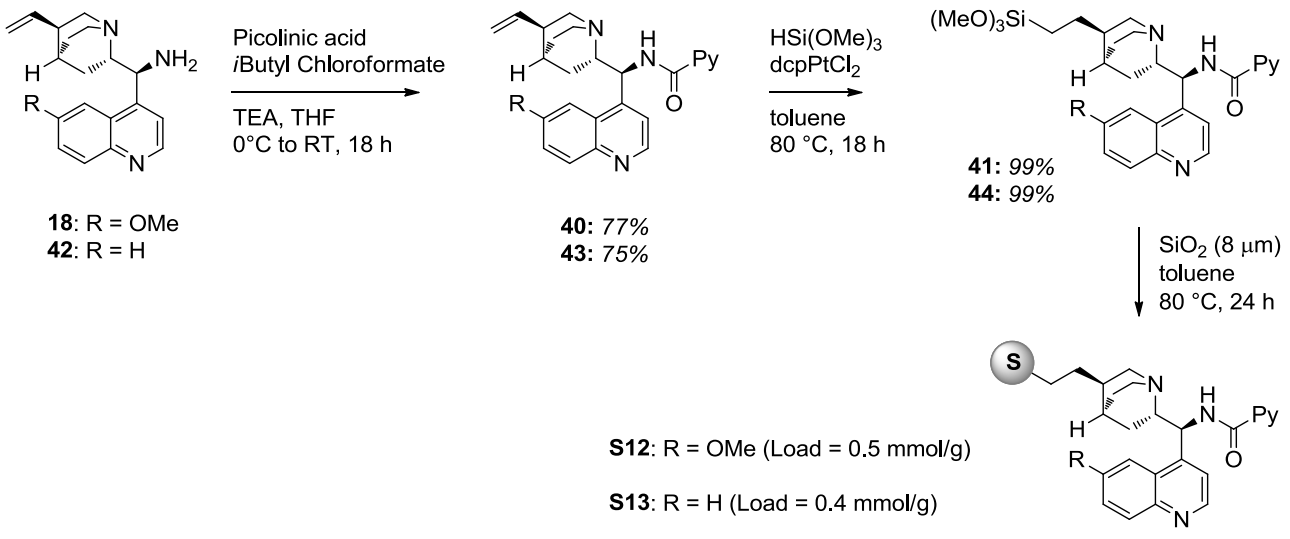

Scheme 23. Synthesis of silica supported catalysts **S12** and **S13**.

Polystyrene supported picolinamide

For the preparation of the polystyrene supported catalyst **P8** an alternative strategy was employed (Scheme 24): chiral picolinamide **46** derived from 9-amino-*epi*-cinchonine was subjected to thiol-ene coupling (initiated by AIBN) with polymer **P7**, a polysterene bearing a thiol functionality.[35] The loading of **P8** (0.3 mmol/g) was determined by weight difference.

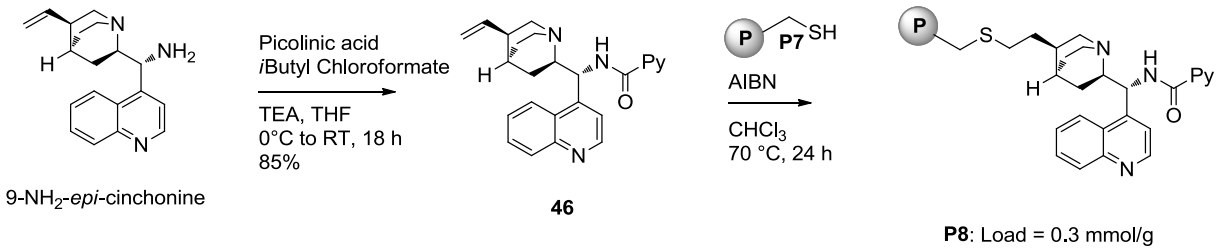

Scheme 24. Synthesis of polymer supported catalyst **P8**.

Catalyst **P9** (loading = 0.2 mmol/g) was prepared starting from picolinamide **43** following the same strategy used for the preparation of **P8** (Scheme 25).

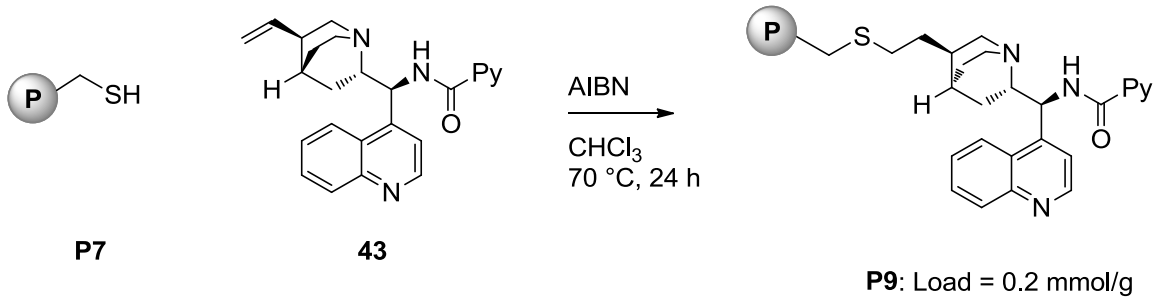

Scheme 25. Synthesis of polymer supported catalyst **P9**.

Stereoselective reactions in batch

Solid supported picolinamide **S12**, **S13**, **P8** and **P9** were tested in the reduction of imine **48i** with $HSiCl_3$ in CH_2Cl_2 at room temperature for 18 hours. Silica supported catalyst **S12** gave the corresponding amine **48** in moderate yield and low ee (Table 29, entry 1). The use of **S13** resulted in a complete conversion of the starting material and the enantioselectivity improved up to 62% (entry 2). Gratifingly, upon using polystyrene supported catalyst **P8**, the reaction proceeded in quantitative yield and 90% ee (entry 3), a result comparable to the one obtained with the homogeneous catalyst. Lowering the catalyst loading to 10 mol% did not alter the reaction outcome (entry 4), while using 5 mol% of **P8** resulted in slightly lower ee (entry 5). Using the pseudo-enantiomeric catalyst **P9**, amine **48** was obtained in 98% yield and a lower ee (63%, entry 6).

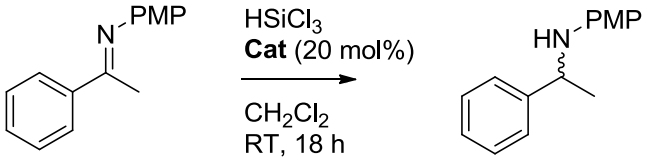

48i **48**

Table 29. Catalyst screening.

Entry	Catalyst	Yield (%)[a]	ee (%)[b]
1	**S12**	64	30 (*S*)
2	**S13**	95	62 (*S*)
3	**P8**	98	90 (*R*)
4[c]	**P8**	95	91 (*R*)
5[d]	**P8**	95	79 (*R*)
6	**P9**	95	63 (*S*)

(a) Isolated yield after chromatography. (b) Enantiomeric excess was determined by HPLC on chiral stationary phase. (c) 10 mol% of **P8** was used; (d) 5 mol% of **P8** was used.

Once the best reaction conditions have been established, we tested catalyst **P8** in the reduction of different substituted imines with $HSiCl_3$ (Table 30). Electron poor imine **52i** was converted into the corresponding chiral amine **52** with 93% yield and 85% ee (entry1). 4-Fluoro-substituted imine and 4-trifluoromethyl-substituted imine afforded the coresponding products **53** and **54** in quantitative yield and 87% and 84% ee, respectively (entries 2 and 3). The reactions with electron rich imine **56i** afforded amine **56** in 96% yield and 85% ee (entry 4).

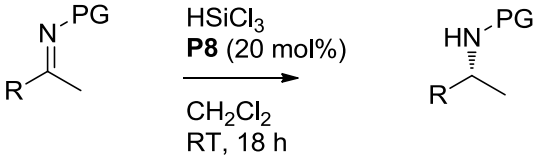

Table 30. Substrate scope.

Entry	R	PG	Yield (%)[a]	ee (%)[b]
1	**52:** 4-NO_2-C_6H_4-	PMP	93	85
2	**53:** 4-F-C_6H_4-	PMP	98	87
3	**54:** 4-CF_3-C_6H_4-	PMP	97	84
4	**56:** naphtyl	PMP	96	85

(a) Isolated yield after chromatography. (b) Enantiomeric excess was determined by HPLC on chiral stationary phase.

Stereoselective reactions under continuous flow conditions

We next decided to focus our attention on the preparation of catalytic reactors in order to perform the stereoselective reduction of imines with trichlorosilane under continuous flow conditions. A Omnifit glass column (*i.d.* = 1 cm, *l* = 10 cm) was filled with catalyst **P8** (170 mg, 0.05 mmol) and was equipped with one fixed-length endpiece and one adjustable-length endpiece (bed length = 1 cm, internal volume = 0.78 mL). A 0.05 M solution of imine **52i** and trichlorosilane (5 equiv.) in dry dichloromethane was injected to the reactor through a syringe pump with a flow rate of 0.02 mL/min (residence time 25 minutes, determined experimentally) at room temperature. The outcome of the reactor was collected into a flask containing NaOH 10% solution. After phase separation and concentration the product was isolated with no need for further purifications. Each 25 minutes the product was collected and analyzed in order to determine the conversion and the ee. Results of the continuous flow experiments are reported in Table 31.

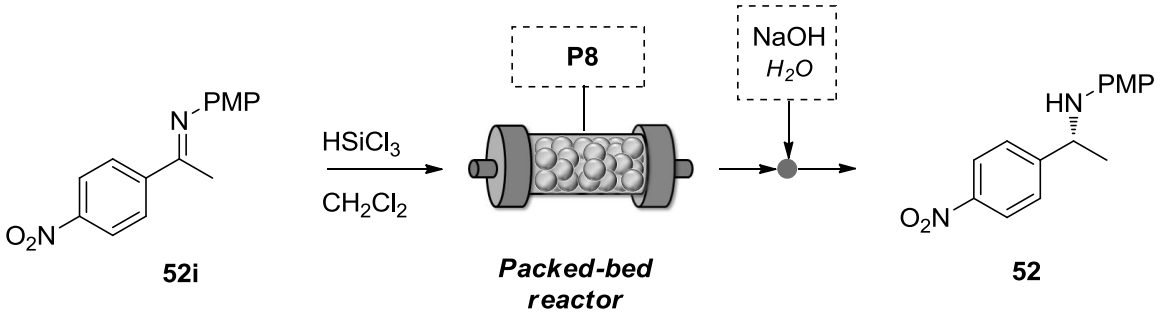

Table 31. Flow synthesis of **52**.

Entry[a]	Running time (min)	Yield (%)[b]	ee (%)[c]
1	0-50	98	47
2	50-75	98	44
3	75-100	93	30
4	100-125	93	25
5	125-150	87	22
6	150-175	86	20

(a) Flow rate: 1.2 mL/h, Residence time: 25 min h; (b) Determined by NMR. (c) Enantiomeric excess was determined by HPLC on chiral stationary phase.

As reported in Table 31 the continuous flow process was run for 3 hours and chiral amine **52** was continuously obtained in very high yield. However the enantioselectivity of the process was quite low and it dropped from 47% (Table 31, entry 1) to 20% (entry 7). These results demonstrates how the use of a catalytic reactor can be advantageous in terms of products isolation and unit operations, but requires further studies in order to increase the stereoselectivity of the process.

In conclusion the synthesis of solid supported chiral picolinamides derived from cinchona alkaloids was studied. Polystyrene supported catalysts were more effective than silica supported ones in terms of enantioselectivity. However they showed a poor recyclability and the application under continuous flow conditions resulted in very low enantioselectivity.

CHAPTER 2 MICROREACTOR TECHNOLOGY

2.1 Introduction

By definition, flow microreactors are reactors that operate with fluids geometrically constrained within a reactor volume which has the characteristic dimension (typically diameter) smaller than 0.5 mm.[36] The intrinsic advantages associate to the use of flow microreactors are determined by the scale-dependent processes of heat and mass transfer.[37]

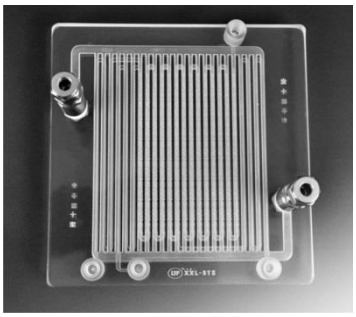

Figure 17. Representation of a glass microreactor.

The fluid movement into microfluidic devices with small volumes is characterized by low Reynolds numbers *Re* (generally below 250) which determine a strictly laminar flow regime (a flow regime is considered laminar until Re < 2500) (Figure 18). Generally viscous forces dominate over inertial ones and the absence of turbulence and back-mixing makes mass transfer dependent only by the diffusion between fluids.

Re = (inertial forces) / (viscous forces) = $\rho\, d\, \nu / \mu$.

The Reynolds number is a dimensionless number used to quantify the relative importance of inertial and viscous forces into a fluid. *Re* accounts for characteristics of both the fluid (ρ density; μ dynamic viscosity) and the environment where the fluid flow (ν fluid velocity; *d* characteristic dimension).

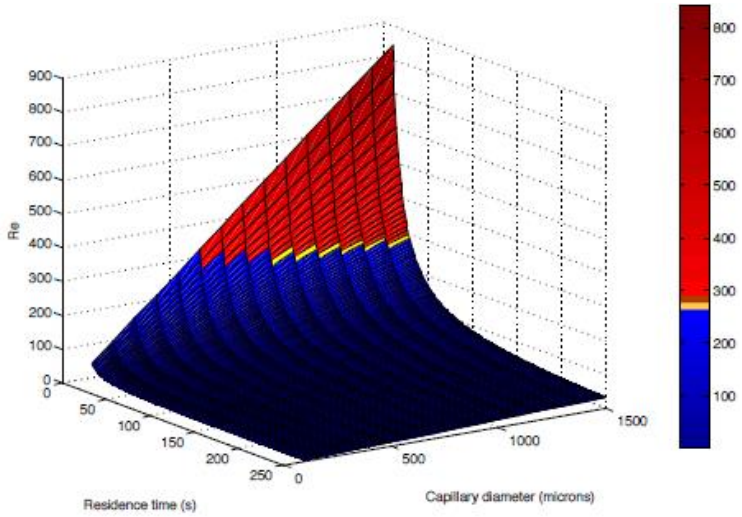

Figure 18. 3D plot showing the variation of Reynolds number with the characteristic dimension of the device and the residence time (flow rate) of the reaction within the device. The microfluidic regime is characterized by Reynolds numbers below 250 (blue), the transitional regime is shown in yellow and situations where it is not possible to operate within a microfluidic regime are show in red.

The small dimension of reactor channels and the high ratio surface area/volume ensure a rapid heat transfer from the outer within the fluid. This behavior is determined by dimensionless Peclet number *Pe* which describes the ratio between heat transport due to bulk fluid motion and to diffusion. Typically microfluidic devices have low *Pe* (generally below 1000) due to the relative importance of diffusion as diameter channel diminishes (Figure 19).

Pe = (advective transport) / (diffusive transport) = $\rho\ d\ \nu\ C_p / k$.

ρ: density of the fluid; *d:* channel diameter; ν: fluid velocity; C_p: fluid specific heat capacity; k: thermal conductivity.

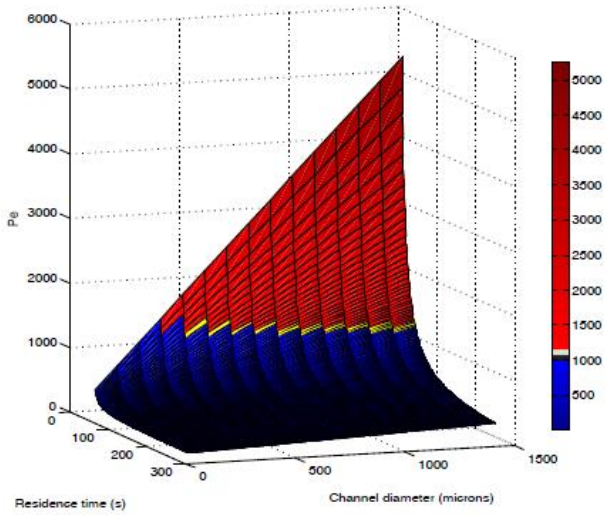

Figure 19. 3D plot showing the variation of the Péclet number with the characteristic dimension of the device and the residence time (flow rate) of the reaction within the device. The microfluidic regime is characterized by Péclet numbers below 1000 (blue), the transitional regime is shown in yellow and situations where it is not possible to operate within microfluidic parameters are show in red.

The properties described above give access to many advantages which have made microreactor technology extremely attractive for both academia and industry.
The fast heat and mass transfer giver rise to faster reaction compared to batch mode. Additionally, the confined environment of a flow microreactor enables the possibility of working above the boiling point of the solvent and at high pressure. This increases reaction rate and the overall efficiency of the process.
The control of reaction conditions can be made with high precision leading to an increase of the selectivity of the process (*e.g.* kinetic versus thermodynamic control of the reaction pathway).

The use of small reagents volumes reduces waste and costs and renders the process more sustainable. In particular when a microreactor is used just for informatics rather than for product synthesis, it is possible to obtain the same chemical information (and in some cases even more) of a batch process, but with a reduced amount of precious reagents.

Safety is the major advantage related to the use of microfluidic devices: thanks to the small volumes of reagents the handling of potentially hazardous or toxic materials is limited, and thus the process is safer for the operator. Moreover, due to the short residence time in the microreactor it is possible to perform reactions that involve unstable and highly reactive intermediates that could not be otherwise handled or stored in traditional batch mode. Furthermore, the high surface-area-to-volume ratios within the channel allow the rapid transport of heat during exothermic reactions, avoiding dangerous runaway events.

Microreactors are usually employed for small-scale synthesis of molecules and in analytic and diagnostic applications. However micro channels suffer from restricted flow capacity with a high tendency to pressure drops.
Mesofluidic devices generally have internal diameters ranging from 0.5 mm up to a few mm and are more suitable for large scale synthesis (preparation of multigram to multikilogram quantities).[38] Mesoreactors possess improved flow capacities and suffer from lower pressure drops compared to microreactors. Additionally these systems can be integrated into multistep processes and combined with packed-bed reactors (containing solid supported catalysts or reagents) thanks to their ability to tolerate higher flow rates.
On the contrary, the increase of reactor diameter results in a reduction of heat and mass transfer capabilities.

In this chapter we deal with micro- and meso-reactors of type III and IV (Figure 4). In section 2.2 the continuous flow stereoselective synthesis of APIs intermediates within micro and mesoreactors will be described. In section 2.3 the reduction of nitro compounds with trichlorosilane in flow mesoreactors will be presented. In section 2.4 the use of 3D-printed mesoreactors for the stereoselective synthesis of chiral 1,2-amino alcohols will be discussed. Our purpose was not to study fluid dynamics within micro- and meso-reactor channels or investigate flow processes from an engineering point of view. We wanted to demonstrated the feasibility of new continuous flow synthetic processes that have not been reported so far.

2.2 Stereoselective Flow Synthesis of APIs Intermediates

Recently, the safe manufacturing of organic intermediates and APIs under continuous flow conditions has been deeply examined in a review by Kappe and co-workers.[39]

The use of organocatalysis to promote continuous flow stereoselective transformations has recently been explored by different research groups.[40]

In 2014 our group reported for the first time the use of chiral thiourea **66(*R,R*)** for the stereoselective nucleophilic addition of acetyl acetone and diethyl malonate to β-nitrostyrene derivatives under continuous flow conditions (Scheme 26).[41] For the screening of the reaction conditions a commercially available Chemtrix Labtrix® Start Standard platform was used. The system was equipped with two syringe pumps (Chemix Fusion 100) to deliver the reagents through two syringes into a glass microreactor (Chemtrix SOR 3223).

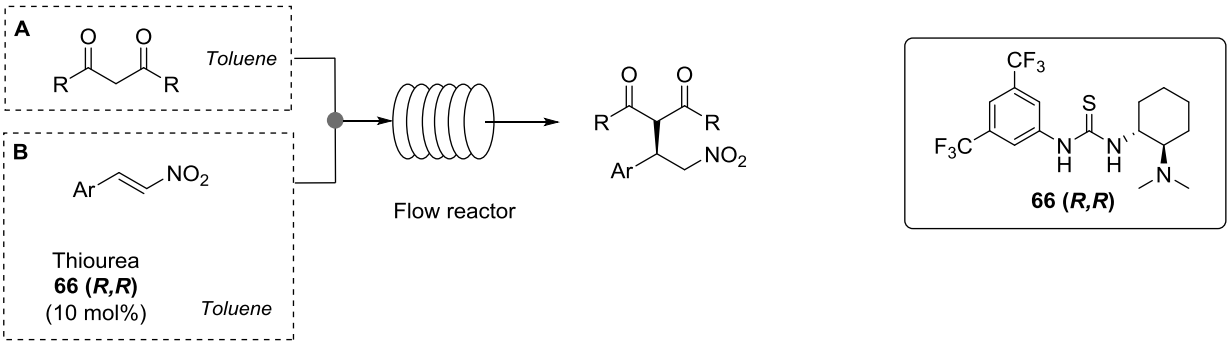

Scheme 26. Stereoselective Michael addition in flow.

The addition of acetylacetone to β-nitrostyrene was selected as a model reaction for the initial optimization study. It was found that good results were obtained using a short residence time (5 min) and a temperature of 70 °C (91% yield, 80% ee). This methodology was also carried out replacing commercially available Chemtrix glass microreactors with less expensive PEEK tubings generally employed as HPLC connections. Under the same experimental conditions no loss in chemical activity or stereoselectivity was observed.

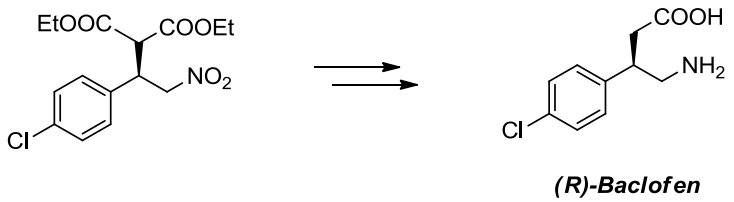

Figure 20. Synthesis of (R)-Baclofen.

The methodology was then extended to the use of diethyl malonate as the nucleophile, and applied to the synthesis of a product of pharmaceutical interest, the $GABA_B$ receptor agonist Baclofen (Figure 20). Under the best conditions the addition of malonate to 4-chloronitrostyrene was promoted in 98% yield and 85% ee. This synthetic application was realized using a PTFE tubing with a total volume of 0.5 mL as flow reactor.

Figure 21. Different types flow reactors employed.

On the basis of these results we decided to extend the continuous flow methodology to the use of aliphatic nitroalkenes for the preparation of a precursor of (*S*)-Pregabalin (Section 2.2.1). We also explored the use of a different organocatalyst such as 9-amino-*epi*-quinine for the continuous flow synthesis of the anticoagulant (*S*)-Warfarin (Section 2.2.2).

2.2.1 (S)-Pregabalin

(*S*)-Pregabalin, marketed under the trade name Lyrica, is a wide-administered anticonvulsant and antiepileptic drug. As reported in the literature, the stereoselective nucleophilic addition of diethylmalonate to nitroalkene **67** promoted by chiral Takemoto's thiourea **66(S,S)** could be considered a suitable strategy for the preparation of chiral intermediate **68.**[42,43] Reduction of the nitro moiety followed by hydrolysis and decarboxylation, affords (*S*)-Pregabalin (Scheme 27).

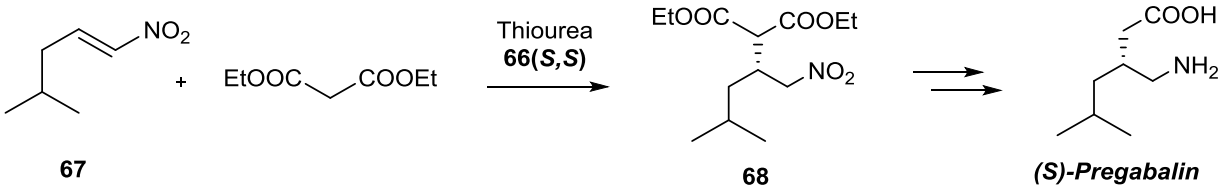

Scheme 27. General strategy for the preparation of chiral intermediate **68**.

In our initial experiments we employed a PEEK microreactor with a total volume of 10 μL (*id*: 0.127 mm, *l*: 79 cm) in order to demonstrate the compatibility of the organocatalytic methodology with continuous flow processes. A syringe pump equipped with two syringes was used to feed the microreactor with the reagents through a T-junction. In one syringe the aliphatic nitroalkene **67** was charged, while in a second syringe diethylmalonate and Takemoto's thiourea **66** were loaded (Scheme 28). The microreactor was coiled in a bundle and immersed in a preheated oil bath. After a screening of reagent concentrations and temperatures (Table 32) it was found that product **68** was formed in 36% yield and 79% enantiomeric excess using a residence time of 5 min and a temperature of 60 °C (Table 32, entry 3). By increasing reaction temperature or diethyl malonate equivalents no improvements in the conversion were observed. This was attributed to the lower reactivity of aliphatic nitroalkene compared to aromatic ones.

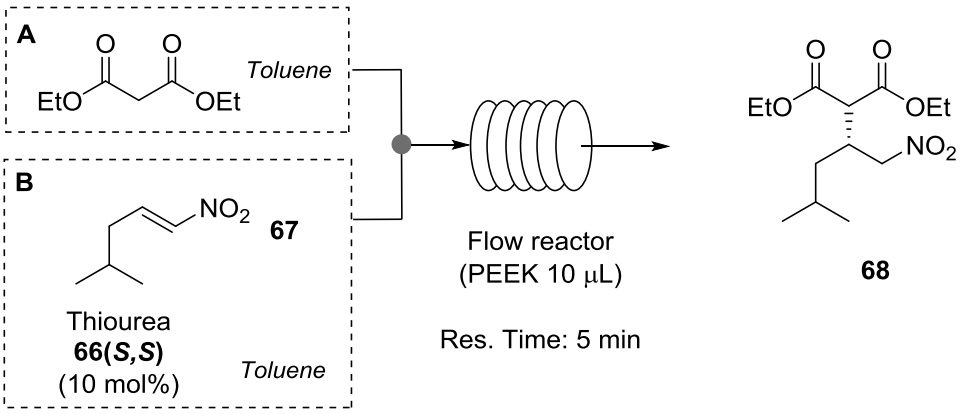

Scheme 28. Flow synthesis of (*S*)-Pregabalin intermediate **68**.

Table 32. Screening of reaction conditions.

Entry	T (°C)	Yield (%)[a]	ee (%)[b]
1[c]	25	0	-
2[c]	60	35	77
3[c]	100	28	71
4[d]	**60**	**36**	**79**
5[d]	80	30	76
6[e]	60	25	77
7[e]	85	24	73

(a) Determined by H-NMR using phenantrene as internal standard. (b) Enantiomeric excess was determined by HPLC on chiral stationary phase. (c) 2 equiv. of diethyl malonate were used. (d) 3 equiv. of diethyl malonate were used. (e) diethyl malonate was used neat.

After initial experiments into a 10 μL microreactor, we scaled up the process by using a 500 μL reactor made of PTFE tubing (*id*: 0.58 mm, *l*: 189 cm). Using the same experimental set up as before, the reagents were pumped to the reactor (Scheme 29) at different flow rates (Table 33). Best results were obtained with a residence time of 2 min, as product **68** was produced in 37% yield and 80% ee.

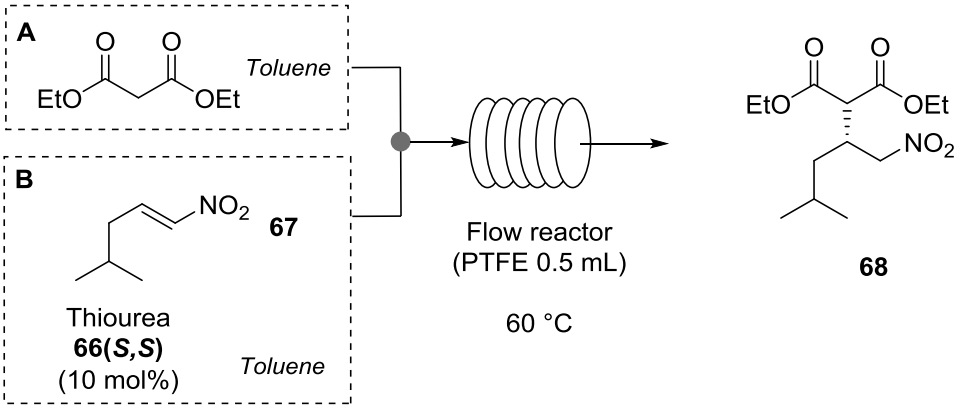

Scheme 29. . Flow synthesis of (*S*)-Pregabalin intermediate **68**.

Table 33. Screening of reaction conditions.

Entry	Flow Rate (μL/min)	Res. Time (min)	Yield (%)[b]	ee (%)[c]
1	2	30	55	76
2	4	15	56	76
3	6	10	40	79
4	12	5	37	79
5	30	2	37	80

(a) Determined by H-NMR using phenantrene as internal standard. (b) Enantiomeric excess was determined by HPLC on chiral stationary phase

Working on a 10 mmol scale it was possible to continuously produce 1 g/h of **68** in 80% ee. The main limitation of this methodology is represented by the low chemical conversion. However this issue can be easily overcome by distillation of the crude mixture which allows a recycle of unreacted reagents.

2.2.2 (S)-Warfarin

(*S*)-Warfarin, known with the brand name Coumadin or Jantoves, is an oral blood anticoagulant. Since it can be prepared through different organocatalytic strategies,[44,45] we identified the nucleophilic addition of 4-hydroxy-coumarin to benzalacetone catalyzed by cinchona-derived primary amine **18**[46] as the most straightforward methodology compatible with flow microreactors.

In our initial experiments we employed a PEEK microreactor with a total volume of 10 μL (*id*: 0.127 mm, *l*: 79 cm) in order to demonstrate the compatibility of the organocatalytic methodology with continuous flow processes. A syringe pump equipped with two syringes was used to feed the microreactor with the reagents through a T-junction. In one syringe 4-hydroxy-coumarin was charged, while in a second syringe benzalacetone and amine **18** were loaded (Scheme 30). The microreactor was coiled in a bundle and immersed in a preheated oil bath. After a screening of reagent concentrations and temperatures (Table 34) it was found that product **33** was formed in 61% yield and 93% enantiomeric excess using a residence time of 10 min and a temperature of 75 °C (Table 34, entry 5).

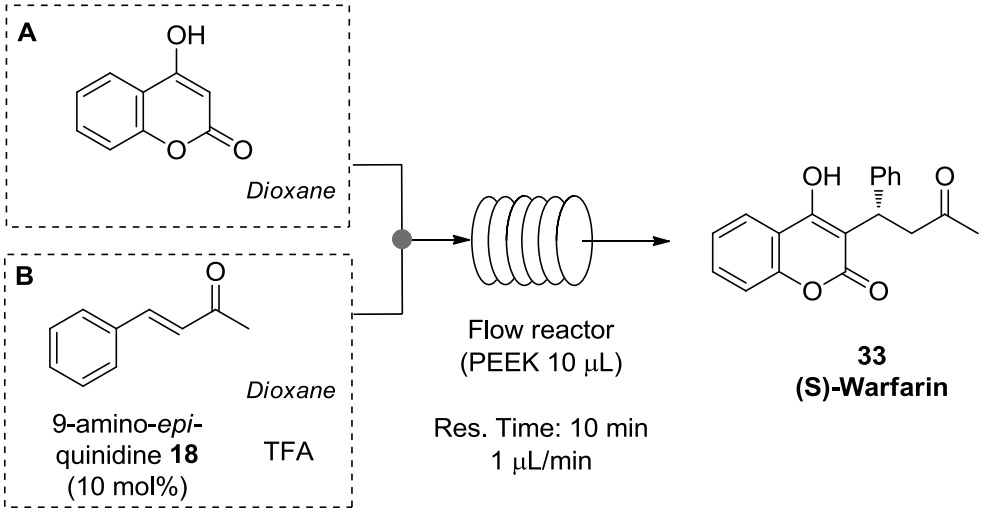

Scheme 30. Flow synthesis of (*S*)-Warfarin **33**.

Table 34. Screening of reaction conditions.

Entry	T (°C)	Yield (%)[a]	ee (%)[b]
1	40	38	95
2	50	51	95
3	60	55	95
4	75	61	93
5	90	65	90

(a) Determined by H-NMR. (b) Determined by HPLC on chiral stationary phase.

After preliminary screening of reaction conditions we explored the possibility to scale up the reaction by using a 500 μL microreactor (*id*: 0.58 mm, *l*: 189 cm), made of PTFE (Scheme 31).

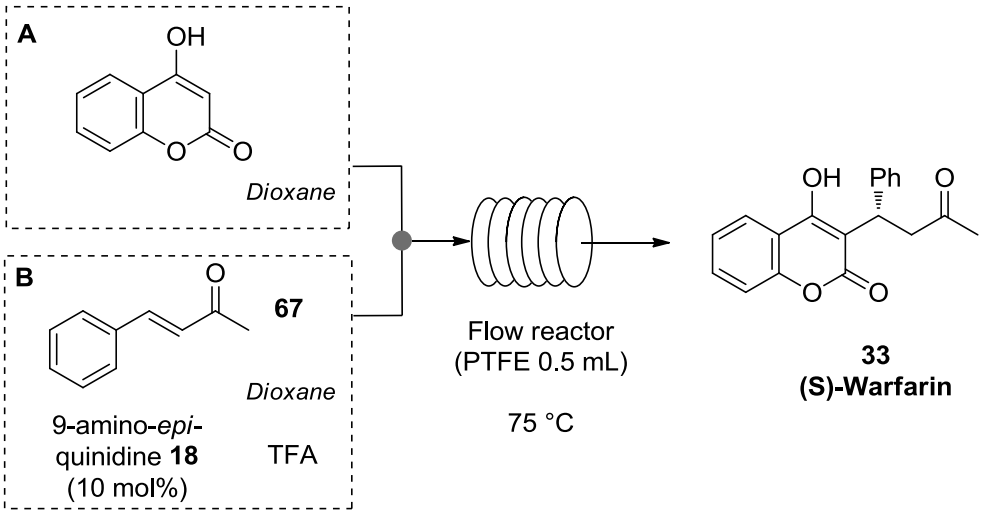

Scheme 31. Flow synthesis of (*S*)-Warfarin **33**.

However when a residence time of 10 minutes and a temperature of 75 °C were used, product **33** was obtained in only 29% yield (Table 35, entry 1). Attempts to increase the residence time resulted in lower yields and ee (entries 2 and 3). These results can be attributed to a worse mixing and heat transfer within PTFE microreactor (500 μL, *id* 0.58 mm) compared to PEEK microreactor (10 μL, *id* 0.13 mm) caused by different reactor diameters.

Table 35. Screening of reaction conditions.

Entry	Flow Rate (μL/min)	Res. Time (min)	Yield (%)[a]	ee (%)[b]
1	50	10	29	95
2	17	30	20	86
3	8	60	20	81

(a) Determined by H-NMR. (b) Determined by HPLC on chiral stationary phase.

In order to overcome these drawbacks we explored a numbering up approach: 4 PEEK microreactors of 10 μL (*id*: 0.127 mm, *l*: 79 cm) were connected in parallel and placed into an oil bath heated at 75 °C. The reagents were pumped through a syringe pump and were directed to a valve (2 inlets and 4 outlets) that split the stream into the 4 reactors. Reaction outcome was collected into a flask and analyzed in order to determine yield and ee (Scheme 32). Running the flow reaction with a residence time of 10 minutes, product **33** was obtained in 36% yield and 91% ee.

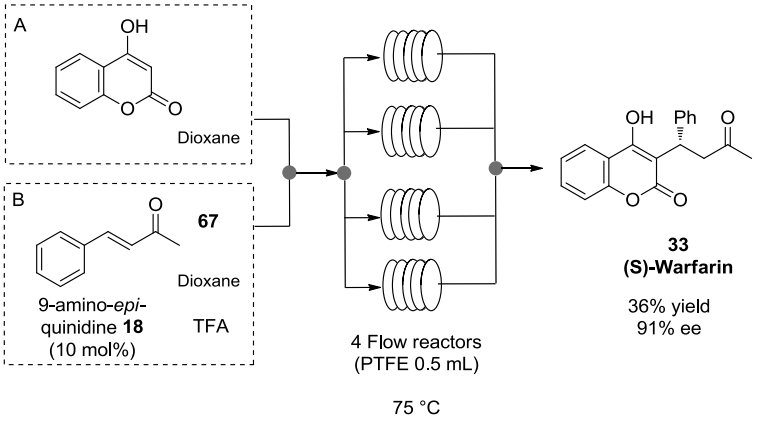

Scheme 32. Flow synthesis of (*S*)-Warfarin **33** using numbering up approach.

In conclusion we demonstrated the possibility to prepare (*S*)-Warfarin under continuous flow conditions through a stereoselective organocatalytic methodology. However this system suffers from scarce reproducibility. In addition when scale-up or numbering up approaches were explored poor results in terms of chemical yields were obtained.

2.3 Continuous Flow Reduction of Nitro Compounds

The reduction of nitro compounds to amines is a fundamental transformation in organic synthesis. Among the different available methodologies for the reduction of nitro compounds,[47] our research group has recently reported a very convenient, mild, metal-free and inexpensive procedure, of wide applicability.[48] The simple combination of trichlorosilane ($HSiCl_3$) and a tertiary amine generates in situ a dichlorosilylene species which is the actual reducing agent (Figure 22).[49]

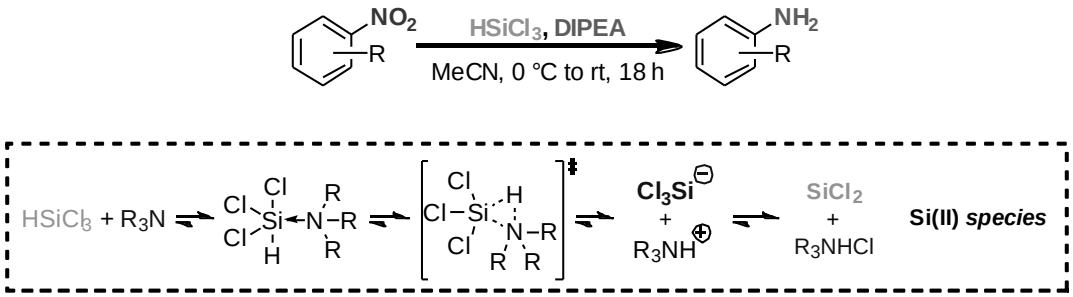

Figure 22. Reduction of nitro compounds with $HSiCl_3$.

Even though nitro derivatives are fundamental building blocks in organic synthesis, their application on a large scale is still quite limited because they are dangerous and potentially explosive chemicals. Flow chemistry has recently emerged as a powerful technology in synthetic chemistry that can reduce risks associated to the use of hazardous chemicals and favors reaction scale up. The possibility to efficiently perform nitro reduction *in continuo* would make the transformation safer and more appealing in view of an industrial application and a possible scale up of the process.

For these reasons we decided to explore the metal-free reduction of both aromatic and aliphatic nitro derivatives to amines with $HSiCl_3$ under continuous flow conditions.

Typically, the transformation of nitro compounds to amines under continuous flow conditions is performed through the metal-catalyzed hydrogenation[50] with ThalesNano H-Cube®, which exploit H_2 generated in-situ by water electrolysis.[51] The procedure involves relatively mild reaction conditions, but the presence of noble metal catalysts, packed into disposable cartridges, suffers from functional group compatibility and catalyst poisoning during time.

In 2012 the Kappe research group reported the microwave-assisted continuous flow synthesis of anilines from nitroarenes using hydrazine as reducing agent and Iron oxide nanocrystals as catalyst.[52] This methodology ensured fast transformations (2 to 8 minutes) for a wide number of substrates and was extended to large scale preparation of pharmaceutically relevant anilines.[53] However this procedure required harsh reaction conditions (T = 150 °C), was limited to aromatic substrates and could not be applied to compounds bearing ketones or aldehydes as functional groups.

With our methodology we provide an alternative continuous flow metal-free methodology for the synthesis of both aliphatic and aromatic amines, which requires inexpensive reagents, mild and fast reaction conditions (25 °C, 5 minutes), and a very simple and user friendly reaction setup.

A nitro derivative is reacted with commercially available $HSiCl_3$ in the presence of a tertiary base (typically Hunig's base) in an organic solvent. The continuous flow reduction of 4-

nitrobenzophenone **69a** was chosen as model reaction. A syringe pump equipped with two gas-tight 2.5 mL syringes was used to feed the reagents into a 0.5 mL PTFE reactor (*id:* 0.58 mm, *l*: 189 cm) through a T-junction (Syringe A: 0.8 M $HSiCl_3$ solution in CH_2Cl_2; Syringe B: 0.2 M **69a** solution in CH_2Cl_2, Hunig's base 6 equiv.).(Scheme 33).

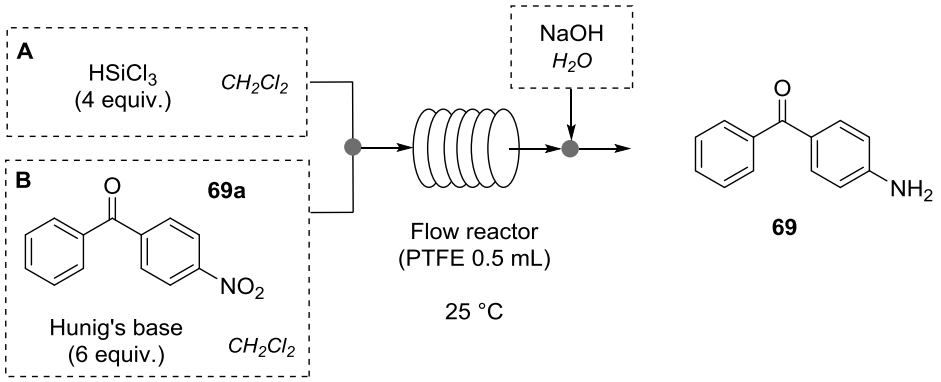

Scheme 33. Continuous flow reduction of 4-nitrobenzophenone using a 0.5 mL PTFE flow reactor.

The outcome of the reactor was collected into a flask containing 10% NaOH solution in order to quench the reaction; after phase separation the crude reaction mixture was analyzed by ^{1}H-NMR to determine the conversion. When the reaction reached a full conversion (>98%) no further purification step was required and the aniline was recovered as a clean product after simple concentration of the organic phase and extraction with ethyl acetate. A screening of flow rates was initially performed and the results are reported in Table 36. The data show that the reaction is very fast and a complete conversion to aniline **69** was achieved for very short residence times (10, 5 and 2.5 min, entries 1-3). With a 1.2 minutes residence time, 91% conversion was reached.

Having demonstrated that the flow transformation is very fast we next explored reaction scale up employing a larger flow reactor (5 mL PTFE reactor, *id:* 2.54 mm, *l*: 100 cm), in order to increase the productivity of the process.

Using the same reaction set-up illustrated in Scheme 34, a residence time of 50 minutes was necessary to reach a full conversion of the starting material (entry 5). This is mainly due to the wider internal diameter of the reactor (2.54 mm vs 0.58 mm) which affects the mixing of the reagents.[54] Lowering the residence time resulted in minor yields (entry 7, 25 min residence time, 82% yield). TEA, a cheaper base than Hunig's base, could also effectively promote the reduction with only marginally lower conversion (entry 6 vs entry 5).

Table 36. Screening of reaction conditions.

Entry[a]	Flow rate (mL/min)	Res.time (min)	Conversion (%)[b]
1	0.05	10	98 (96)
2	0.1	5	98 (96)
3	0.2	2.5	98 (93)
4	0.4	1.2	91 (85)
5[c]	0.1	50	97
6[c,d]	0.1	50	87
7[c]	0.2	25	82

(a) Reaction performed using 0.2 M solution of Ar-NO_2 (0.6 mmol) in CH_2Cl_2, $HSiCl_3$ (4 equiv.), Hunig's base (6 equiv.) at room temperature; (b) reaction conversion determined by NMR of the crude; isolated yields in brackets; (c) reaction performed into 5 mL PTFE reactor; (d) reaction performed using EtN_3 as a base.

We next focused on expanding the scope of the reaction and prove its general applicability. Using both 0.5 mL and 5 mL reactors, under the best reaction conditions, the continuous flow reduction of different nitroarenes was studied (Scheme 35).

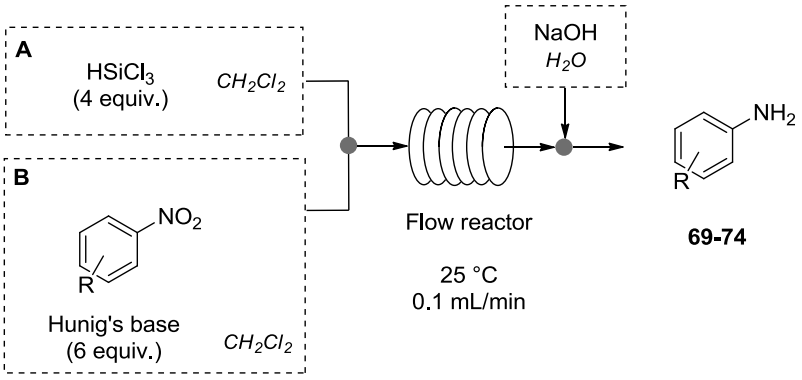

Scheme 34. Continuous flow reduction of aromatic nitrocompounds.

Table 37. Scope of the reaction.

Entry[a]	R	0.5 mL Reactor[b] Yield (%)[c]	5 mL Reactor[d] Yield (%)[e]
1	4-NO_2-benzophen. **69**	98 (96)	97
2	4-Me **70**	98 (96)	98
3	4-Br **71**	98 (92)	98
4	2,4-Cl_2 **72**	98 (92)	92
5	4-F **73**	98 (90)	91
6	COOMe **74**	98 (95)	98

(a) Reaction performed using 0.2 M solution of Ar-NO_2 in CH_2Cl_2, $HSiCl_3$ (4 equiv.), Hunig's base (6 equiv.) at room temperature; (b) Residence time=5 min; (c) Reaction conversion determined by NMR of the crude; isolated yield in brackets; (d) Residence time=50 min; (e) Determined by NMR of the crude.

As already demonstrated for the batch procedure, the reaction in continuo tolerates a large a variety of functional groups: aromatic nitro groups are selectively reduced in quantitative yields in the presence of ketones (Table 37, entry 1), halogens (entries 3-5) and esters (entry 6).

The methodology was also extended to aliphatic nitro compounds (Scheme 36). These substrates are less reactive than aromatic ones and typically require higher hydrogen pressures or reaction temperatures to be completely reduced to the corresponding aliphatic amines.

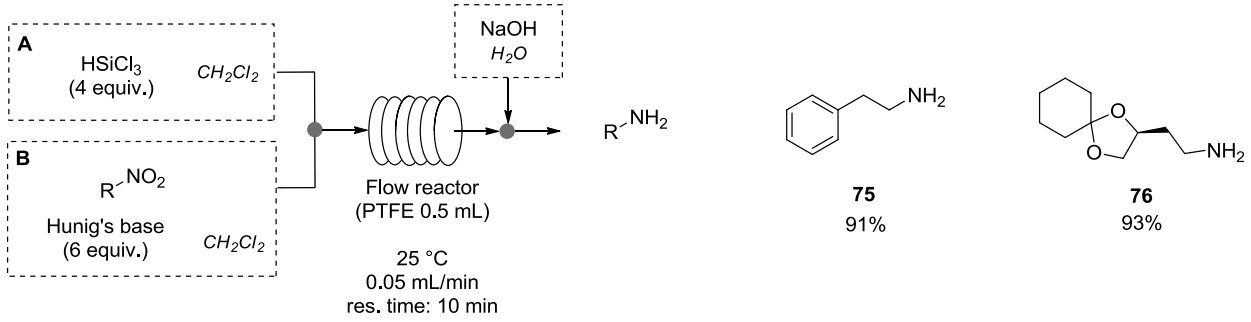

Scheme 35. Continuous flow reduction of aliphatic nitrocompounds.

By employing our metal-free methodology, at 25 °C and with a 0.5 mL reactor, full conversion was observed by using a residence time of 10 minutes only and aliphatic amines **2g** and **2h** were isolated in 91% and 93% yields, respectively.

We then applied the trichlorosilane-mediated continuous flow nitro reduction to the synthesis of advanced precursors of molecules of pharmaceutical interest. The reduction of nitro compound **77a** afforded 2-(4'-chlorophenyl)-aniline **77**, direct precursor of the fungicide Boscalid (Scheme 37). Under the best reaction conditions in 5 mL PTFE reactor (flow rate 0.1 mL/min, 50 min residence time), the desired amine **77** was recovered in quantitative yield as a clean product with no need for purification.

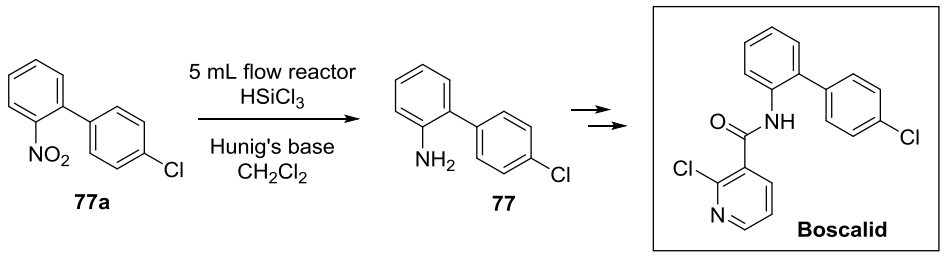

Scheme 36. Synthesis of 2-(4'-chlrophenyl)-aniline 4 with 5 mL flow reactor.

We also investigated the continuous flow reduction of nitro ester **78a**, that can be conveniently prepared in one step through the organocatalyzed addition of diethyl malonate to trans-β-nitrostyrene promoted by a chiral thiourea.[55] The corresponding amide **78** is a direct precursors of the GABA receptor agonist Baclofen (Scheme 38).

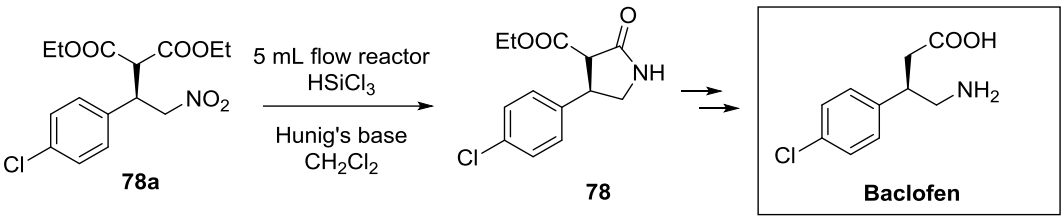

Scheme 37. Synthesis of intermediates 6 direct precursors of drug Baclofen.

Nitro compound **78a** was continuously reduced into a 5 mL reactor and, after work-up under neutral conditions, chiral lactam **78** was isolated in 55% yield.

Finally we explored the possibility of performing a reaction scale-up, followed by an in-line extraction in order to obtain a full continuous process with no need for intermediate operations. A syringe pump equipped with two 25 mL syringes was used to feed the reagents into a 5 mL PTFE reactor through a T-junction (Syringe A: 24 mmol $HSiCl_3$ in 15 mL CH_2Cl_2.; Syringe B: substrate **69a** 6 mmol, Hunig's base 36 mmol in 15 mL CH_2Cl_2) with a flow rate of 0.1 mL/min (residence time 50 min). The outcome of the reactor was collected into a separatory funnel containing NaOH 10% solution (10 mL) and CH_2Cl_2 (10 mL) (Scheme 39). The biphasic system was kept under stirring and the organic layer was continuously collected into a flask. Concentration of CH_2Cl_2 gave pure amino compound **69** in 94% yield. This system allowed to obtain almost 1 g of pure compound in about 4 hours.

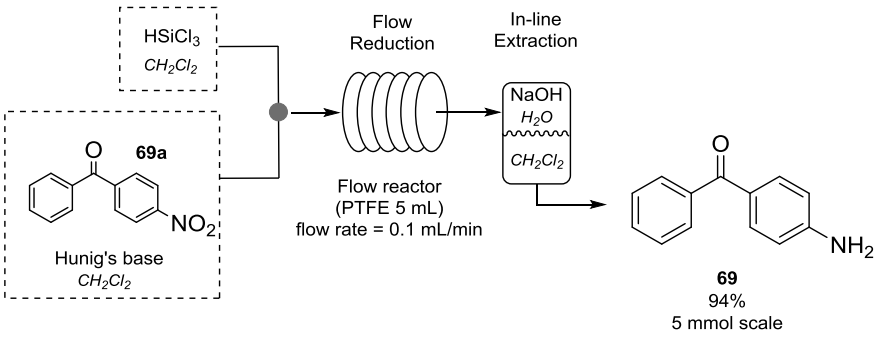

Scheme 38. Continuous flow reduction of 1a and in-line extraction.

In conclusion, a very convenient, mild, metal-free reduction of aliphatic and aromatic nitro derivatives under continuous flow conditions has been successfully developed. The general applicability to differently substituted compounds and the possibility to scale up the process have been demonstrated. The use of extremely inexpensive and not hazardous chemicals, the very high chemoselectivity and the possibility to realize a completely automated reduction/work up/isolation process are distinctive features that make the protocol suitable for the reduction of a large variety of products and attractive also for future industrial applications.

2.4 Synthesis of Chiral 1,2-Amino Alcohols using 3D-printed Reactors

Chiral 1,2-amino alcohols are very important structures in many biologically active natural products, pharmaceuticals and chiral ligands.

The aim of our project was the development of a stereoselective synthesis of chiral 1,2-amino alcohols under continuous flow conditions.[56] Four different targets displaying biological activities were identified (Figure 23). Metaraminol and Methoxamine are used in the prevention and treatment of hypotension, Norephedrine is used as a stimulant, decongestant, and anorectic agent, Levonordefrin is used as topical nasal decongestant and vasoconstrictor in dentistry.

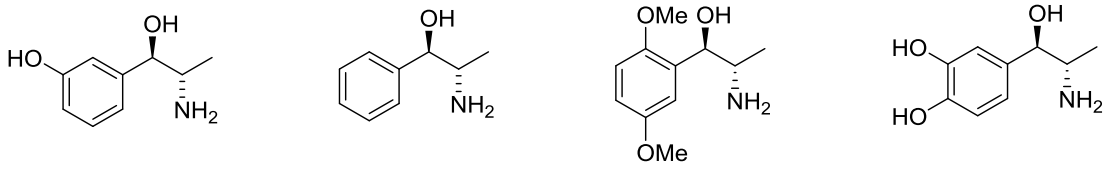

Figure 23. Chiral 1,2-amino alcohols target.

As synthetic strategy we chose a two-step sequence involving a stereoselective copper-catalyzed Henry reaction between aromatic aldehydes and nitroethane followed by a palladium catalyzed hydrogenation of nitro groups to primary amines (Scheme 40).

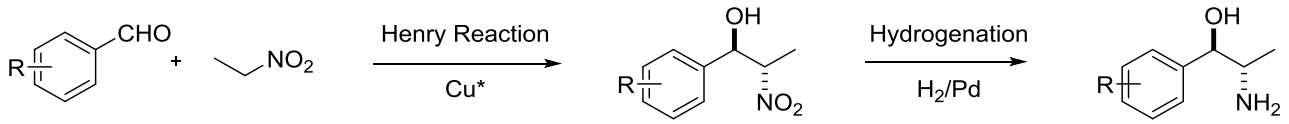

Scheme 39. Synthetic pathway chosen: Henry reaction followed by palladium-catalyzed reduction.

The stereoselective Henry reaction was performed in the presence of a copper catalyst and camphor-derived aminopyridine ligands. The continuous flow reaction was run into home-made 3D printed flow reactors obtained in various polymeric materials having different sizes and shapes (Scheme 41).

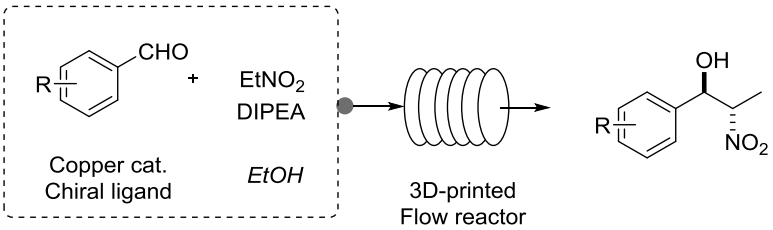

Scheme 40. Continuous flow Henry Reaction.

The continuous flow hydrogenation of resulting nitroalcohols to aminoalcohols was performed using Thalenano H-Cube Mini[57] (continuous flow hydrogenator) which generates molecular hydrogen by water electrolysis (Scheme 42). In this case the flow methodology for the reduction of

nitrocompounds with trichlorosilane was not suitable for 1,2-nitroalcohols becaused it caused the epimerization of the stereogenic centers of the substrates.

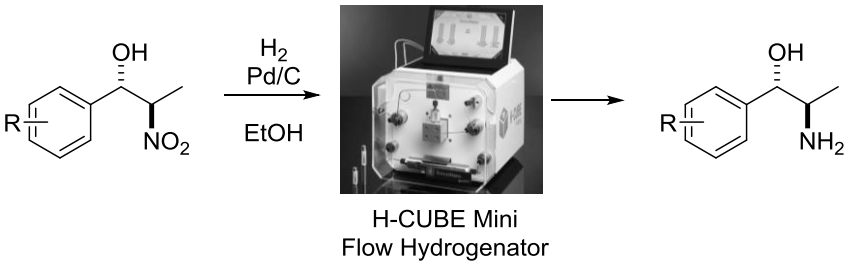

Scheme 41. General flow Pd-catalyzed reaction using H-Cube Mini.

2.4.1 3D-Printing of flow reactors

Three-dimensional (3D) printing has the capability to transform scientific ideas in bespoke and low cost devices that previously required expensive and dedicate facilities to make. By a simply additive manufacturing process, these appliances could be realized on a layer-by-layer basis through a series of cross-sectional slices. The desired object is mathematically described as a virtual design realized with a CAD (Computer Aided Design) program and stored in a virtual file with Stereo-Lithography format (generally with .STL extension) that could be interpreted as g-code by the 3D-printer through a "slicer" (Figure 24).

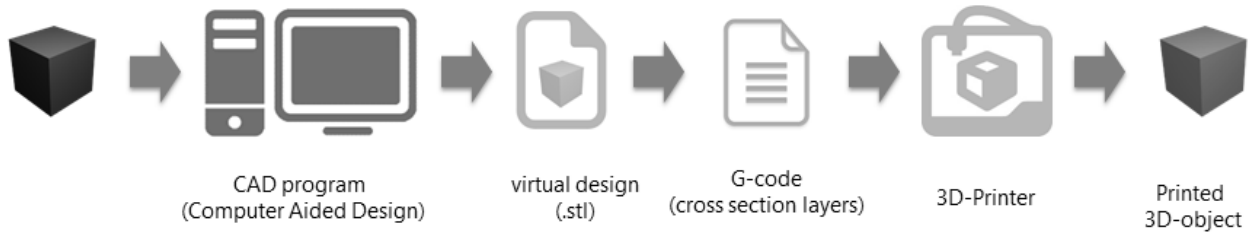

Figure 24. Steps to print an object.

The definition of the process is hard to find, since many types of 3D printers involving different technologies to realize finals objects are known. The first method involves the use of a melting material to produce the layers and it is indicated with FDM (Fused Deposition Modeling) or FFF (Fused Filament Fabrication) acronym. With this approach, a plastic filament or metal wire is unwound from a coil, heated to melt and fed in a nozzle that can be moved both in horizontal and vertical direction by a numerically controlled mechanism to realize objects according the virtual design. This technology was developed and patented by S. Scott Crump in the late 1980s[58] and remain an expensive market niche until the expiration of the patents. Since then, a large open-source development community started to develop and support new and less expensive equipment and now, 3D-printers (based on this technology) are accessible with low costs and are commonly available in many stores. Others types of 3D printers are based on stereolithography technology (SLA), hypothesized by D. Jones in 1974[59] and further developed by W. K. Swainson[60] and C. W. Hull[61].

Among all these technologies, and due to the patent expiration, only FDM is actually available at lower cost thanks also to the strong interest of the open-source development community in this field. FDM 3D-printers are now commercially available in many informatics stores, and some kits could be purchase for less than 500 euro.[62]

The development of 3D-printing devices and technologies has been associated to the new industrial revolution permitting the realization of "Real-Life Objects" faster, cheaper and more importantly, on-demand. This is a virtuous industrial revolution, in which, instead of building many machines to produce multiple copies of a single type of object, we are realizing a single machine that can create endless different objects, with high accuracy. As computers allowing to "virtualize" the physical elements surround us, 3D printing follows the opposite path, offering the opportunity to bring in the physical world virtual objects.

The design files could be shared online or as part of the publication process, so that technology can be shared between laboratories in a reproducible manner. Source of cost effectiveness includes also the absence of costly tools, molds or punches as the absence of milling or sanding procedure at the end of the printed process. Due to the high-automated manufacturing, designs could be easily shared with all the internet community. A single user could produce directly the object using a desktop 3D-printer with high level of precision and conformity to the original design, often around one-tenth of a millimeter. Furthermore due to the low cost of modifying prototypes, and the growing development of different materials that could be printed (as plastics, resins, metals, ceramic and polymers) marketers can easily replicate, modify or create many different manufactured version based on a customer feedback.

A further implementation of 3D-printers in chemical laboratory was the building of research equipment,[63] often shared on free and open repository as Thingiverse (www.thingiverse.com). There are many examples of vial racks, Buchner funnels, microtiter plates, customizable filter wheel, filter bracket, holders, lab jack and so on.[64]

However, according to the words of L. Cronin, one of a pioneer in 3D printing of inorganic cluster molecules: "I don't want chemistry reduced to plastic trinkets, I want new science to occur as a result of use of ubiquitous 3-D printing and molecular design",[65] many other application start to be reported in the last few years. 3D-printed devices has been utilized for realize portable cell lysis device for DNA extraction, printable rotor for centrifuging standard microcentrifuge tubes, miniprep column and orbital shaker. More recently, J. M. Pearce reported a new open-source 3D-printed syringe pump using an open-source Raspberry Pi computer as a wireless control device and a 3D printer, obtaining performances comparable with most of the syringe pumps commercially available but in lower price.[66] 3D-printing and liquid handling with a syringe pump could also be combined to produce user-friendly reactionware for chemical synthesis and purification,[67] continuous parallel ESI-MS analysis of metal complexes formation.[68] 3D printed flow plates have been successfully employed also for the electrolysis of water,[69] and for continuous flow organic chemistry as the imine syntheses and imine reductions processes.[70] In the latter example, Cronin and co-workers has reported the reductive amination of different anilines with benzaldehyde (Scheme 42). A two-step process has been developed: in the first 3D printed reactor R1 (made of polypropylene) the condensation between amine and benzaldehyde in methanol was performed with a residence time of 14 minutes; the formation of imine occurred in quantitative yield and was followed inline using Mettler Toledo ReactIR instrument monitoring the disappearance of the peak of aldehyde at 1705 cm-^{1}. The resulting imine intermediates were not isolated, but directed into the second 3D printed reactor R2 (made of polypropylene) which was fed with a stream of $NaBH_3CN$. Also the second strep was monitored inline through ReactIR instrument: complete disappearance of imine peak at 1630 cm^{-1} was registered after 14 minutes of residence time. At the end of the multistep flow process, benzylanilines were obtained in very good yields (78-99%).

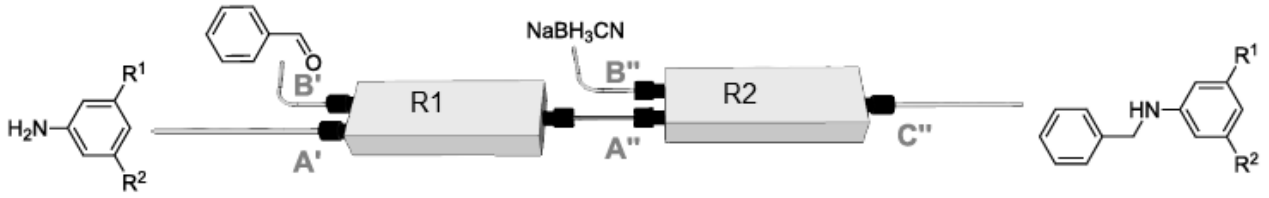

Scheme 42. Reductive amination in flow with 3D printed reactors.

Other examples involves the use of 3D printed devices as reusable electrodes for electrochemical detection.[71]

3D printed devices have been utilized for application in the biomedical fields,[72] as three-dimensional polymer composite scaffolds for biodegradable tissues,[73] using starch-based polymers[74] and for the realization of bones tissue,[75] and cell culture medium.[76]

Furthermore, the potential of 3D printing technology had a significantly impact in the field of microfluidics devices,[77] that could incorporate also membranes in order to study drug transport and effect through the cellule,[78] or could quantitatively investigate the properties of stored red blood cells for transfusion in medicine.[79] Recently, more complexes devices has been realized by Filippini where with a commercial micro-stereo lithography 3D printer realized conventional PDMS (polydimethylsiloxane) glass lab-on-a-chip devices for glucose concentration diagnostics.[80]

In this thesis work we decided to explore the preparation of 3D printed reactors made of different materials (Poly Lactic Acid, High Impact Polystyrene or Nylon) and with different dimensions, channel sized and shapes in order to perform a stereoselective continuous flow Henry reaction. The advantage of using 3D printed reactors is represented by the ease with which they can be prepared and by the fact that the reactors can be designed *ad-hoc* in accordance to the characteristics required by the synthetic process.

2.4.2 Continuous Flow Henry Reaction

The addition of nitroalkanes to aldehydes, the so-called Henry reaction, is a powerful and efficient method for the construction of carbon-carbon bond[81] and results in the formation of β-nitroalcohols. The catalytic asymmetric procedure for Henry reaction has gained particular attention due to the great importance of these compounds. The first asymmetric version of the Henry reaction was reported by Shibasaki in 1992.[82] Since then, interest in this area has been expanded and numerous reports have appeared in the literature on development of various metal[83] and non-metal[84] based catalysts.

During the Henry reaction, up to two stereogenic centers can be formed in one step. Therefore, control of the stereochemistry is an important issue. This control, however, is made difficult by the reversibility of the reaction and easy epimerization at the nitro-substituted carbon atom. Thus, many of the reported experimental procedures for this reaction yield mixtures of diastereomers and enantiomers, hence limiting their synthetic application.

Among the metal-based procedures, those using copper complexes as catalysts have held a prominent position in the development of an enantioselective Henry reaction.[85] The first example of an enantioselective copper-catalyzed Henry reaction was reported by the group of Jørgensen. They described the reaction between nitromethane and α-keto esters using copper(II) complexes with bis-oxazoline ligands in the presence of triethylamine to give the corresponding α-hydroxy-β-nitro esters with good yields and enantioselectivities. (Scheme 43).[86]

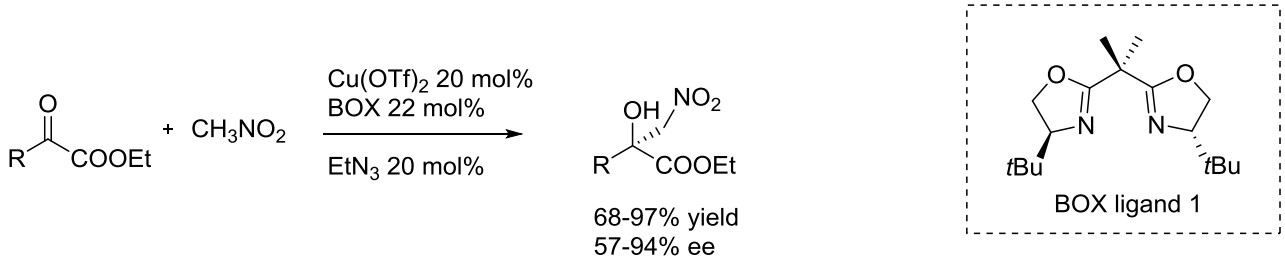

Scheme 43. Copper-catalyzed Henry reaction with bis-oxazoline ligands, reported by Jørgensen.

Later, Evans *et al.* reported the first enantioselective copper-catalyzed Henry reaction with aldehydes using BOX ligands with copper(II) acetate in EtOH. The best result was obtained with a BOX ligand derived from cis-1-aminoindan-2-ol (Scheme 44).[87] An important feature of this reaction is that the acetate ion acts as an internal base to favor the formation of the required nitronate; therefore, the use of an additional base, such as triethylamine, is not required.

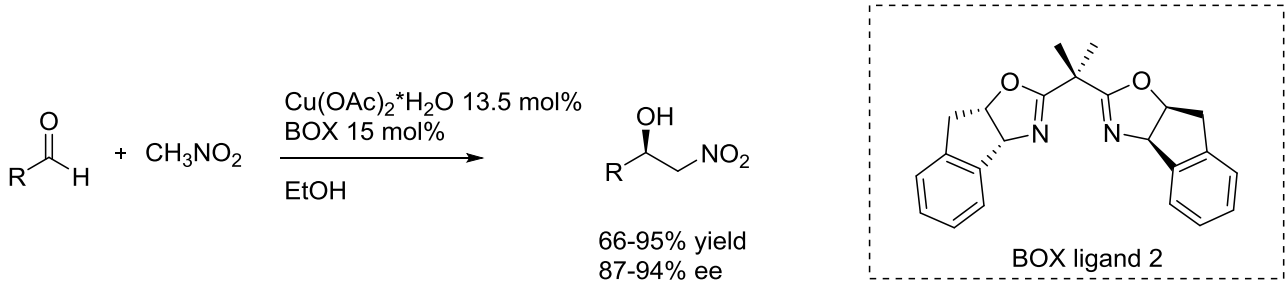

Scheme 44. First enantioselective copper-catalyzed Henry reaction with aldehydes, reported by Evans.

Comparing with the well-developed Henry reaction of aldehydes with nitromethane, the Henry reaction with other nitroalkanes is more challenging as often suffering from low reactivity and poor stereoselectivity. The simultaneous control of diastereo- and enantioselectivity of nitroalkanes has been a formidable challenge, and only a limited number of asymmetric catalysts have been identified.

In 2008 Pedro *et al.* reported a highly enantio- and diastereoselective Cu-catalyzed Henry reaction between aldehydes and nitroalkanes using a new family of aminopyridine complexes derived from camphor as chiral ligands (Scheme 45).[88]

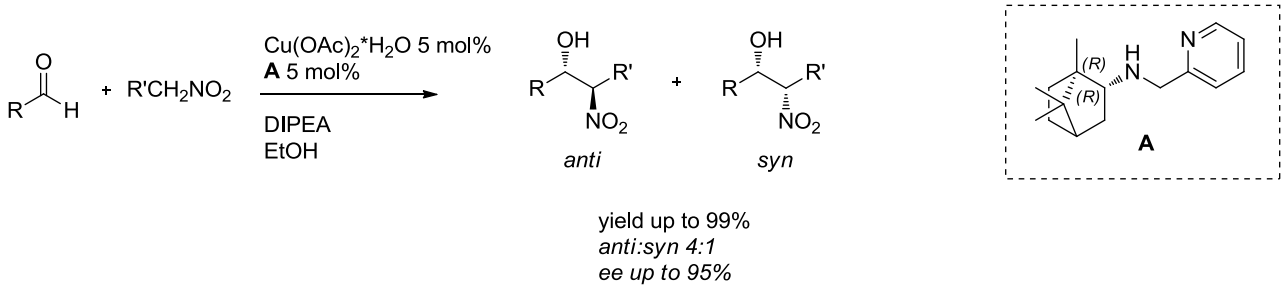

Scheme 45. Cu-catalyzed Henry reaction between aldehydes and nitroalkanes using camphor derived complexes.

The aminopyridine ligand coordinatesthe copper ion with a strongly basic amine nitrogen (sp^3) and a weakly basic pyridine nitrogen (sp^2) to form a complex in which both equatorial coordination positions of the hypothetical square planar complex would be electronically differentiated. Furthermore, the possibility of rotation around the carbon-nitrogen bond would allow better accommodation of the camphor skeleton in the metal complex compared to the one obtained with previously reported iminopyridine ligand. (Figure 25).

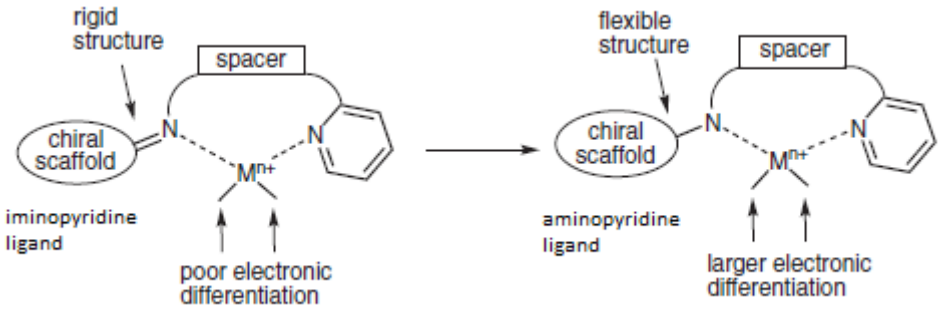

Figure 25. Different properties of amino- and imino-pyridine ligands.

On the basis of previous works in our research group, the stereoselective Henry reaction between aromatic aldehydes and nitroethane was performed in the presence of $Cu(OAc)_2$ as catalyst and aminopyridines **81** and **83** as chiral ligand. Even if chiral aminopyridines **81** and **83** do not show great selectivity in terms of *anti/syn* ratio compared to other chiral ligands they represent a good compromise in terms of availability of and ease in the chemical synthesis.

As illustrated in Scheme 46 the synthesis of **81** involved a two-step sequence starting from the natural enantiomer of camphor, according to a published procedure.[50] Using the same strategy we also prepared enantiomer **83** starting from non-natural (*L*)(-)camphor (Scheme 46).

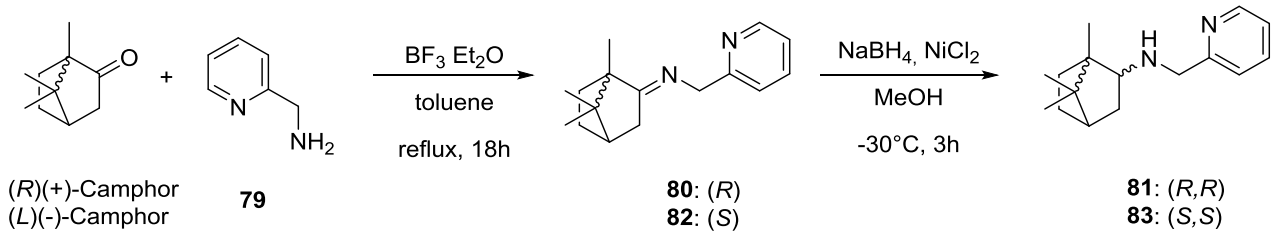

Scheme 46. Synthesis of chiral ligands **81** and **83**.

Initially a batch reaction between 3-(benzyloxy)benzaldehyde and nitroethane was performed in order to evaluate the activity of the catalytic system (Scheme 47). Product **84** represents a precursor of Metaraminol.

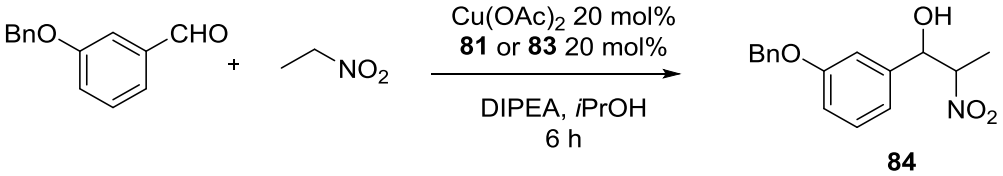

Scheme 47. Batch synthesis of **84.**

$Cu(OAc)_2$ and chiral ligand were dissolved in *i*PrOH and stirred for 10 minutes in order to form the chiral complex. Then 3-(benzyloxy)benzaldehyde was added to the reaction mixture that was stirred for other 30 minutes. The mixture was then cooled to the indicated temperature and DIPEA and nitroethane were added. The reaction was allowed to stir for 6 hours then was quenched with 10% aqueous HCl. After extraction with AcOEt the product was isolated by column chromatography on silica gel. Results of the preliminary screening in batch are reported in Table 38.

Table 38. Screening of reaction conditions.

entry	Aminopyridine	T (°C)	yield (%)	dr (*anti/syn*)[a]	ee$_{anti}$ (%)[b]
1	**81**	0	94	1/1	51 (*S,R*)
2	**83**	0	98	1/1	36 (*S,R*)
3	**81**	-45	89	7/3	84 (*R,S*)
4	**83**	-45	90	7/3	86 (*R,S*)
5[c]	**83**	-45	91	65/35	92 (*R,S*)

[a]Determined by H-NMR of the crude; [b]determined by HPLC on chiral stationary phase; [c]EtOH as solvent.

Running the reaction in the presence of aminopyridine **81** or **83** at 0 °C resulted in the formation of the corresponding product **5** in very good yield but poor diastereo- and enantioselectivity (Table 38, entries 1 and 2). Lowering the reaction temperature to -45 °C did not altered significantly the yield but significantly improved the stereoselectivity in favor of the desired *anti* isomer with good stereoselectivity: 84% ee using ligand **81** and 86% using ligand **83**.

We next moved to continuous flow experiments. In order to find best reaction conditions we chose the addition of nitroethane to 3-(benzyloxy)benzaldehyde as model reaction. As continuous

a flow reactor a 1 mL 3D printed reactor made of High Impact Poly Styrene (HIPS) (squared channel: 1.41 x 1.41 mm) was selected. On the basis of preliminary experiment in flow EtOH was identified as solvent in place of iPrOH due to solubility problems into reactor channels. The set-up of the continuous flow experiment is illustrated in Scheme 48.

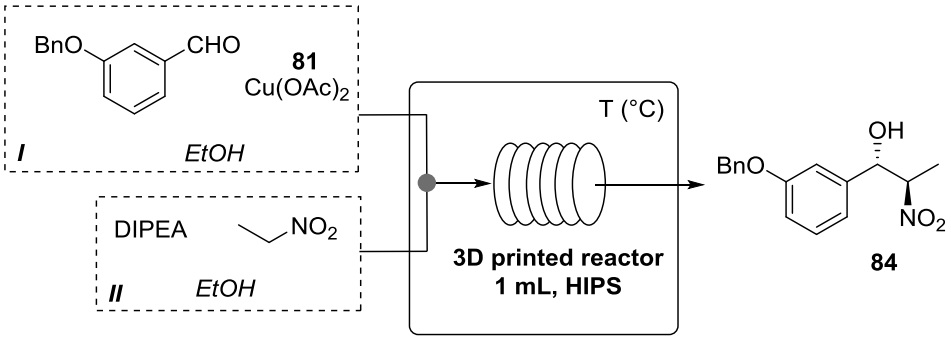

Scheme 48. Continuous flow synthesis of **84**.

Syringe ***I*** was charged with a preformed mixture of 3-(benzyloxy)benzaldehyde (0.25 mmol), **81** (0.0625 mmol) and $Cu(OAc)_2$ (0.05 mmol) in EtOH (1 mL, 0.250 M). Syringe ***II*** was charged with nitroethane (2.5 mmol), DIPEA (0.25 mmol) and EtOH (750 µL). The two syringes were connected to a syringe pump and the reagents directed to the flow reactor at the indicated flow rate and temperature. The outcome of the reactor was collected into a cooled bath (-78 °C) in order to quench the reaction. At the end of the process the crude product was treated with HCl 10%. After extraction with AcOEt the product was isolated by column chromatography on silica gel. Results of continuous flow experiments are reported in Table 39.

Table 39. Screening of reaction conditions.

entry	T (°C)	Flow rate (mL/min)	Res. time (min)	yield (%)	dr (*anti/syn*)[a]	ee$_{anti}$ (%)[b]
1	25	0.2	5	61	6/4	70
2	25	0.1	10	87	1/1	49
3	0	0.1	10	73	65/35	85
4	0	0.05	20	91	63/37	78
5	-20	0.1	10	20	75/25	81
6	-20	0.033	30	72	73/27	87
7[c]	-20	0.033	30	75	71/29	86[d]

[a] Determined by H-NMR of the crude; [b] determined by HPLC on chiral stationary phase; (S,*R*) enantiomer; [c] **83** as chiral ligand; [d] (*R,S*) enantiomer.

Running the reaction at 25 °C using a residence time of 5 minutes resulted in the formation of **84** in 61% yield, 6 to 4 mixture of isomers in favor of *anti* isomer and 70% ee (Table 39, entry 1). Increasing the residence time to 10 minutes gave the product in higher yield but poor ee (entry 2). When the reaction temperature was lowered to 0 °C an improvement in the stereoselectivity of the process was observed (entries 3 and 4). At -20 °C and 10 minutes of residence time *anti* nitroalcohol **84** was obtained in 3/1 *dr* and 81% ee (entry 5). Running the reaction at -20 °C

employing a residence time of 30 minutes gave best results: **84** was obtained in 72% yield, 73/27 *dr* and 87% ee of *anti* isomer (*R,S* configuration)(entry 6). Using chiral ligand **83** in place of **81** under the same reaction conditions afforded product **84** in comparable results: 75% yield, 71/29 *dr* and 86% ee of *anti* isomer (*S,R* configuration)(entry 7). This demonstrated that chiral ligands **81** and **83** performed similarly, affording the opposite enantiomer of product **84**. Since ligand **81** derives from the natural enantiomer of camphor the following experiments were conducted with **81** for costs reasons.

Having identified the best reaction conditions in terms of temperature (-20 °C) and residence time (30 min) we explored the use of different type of flow reactors (Scheme 49) employing the same experimental set-up described in Scheme 48.

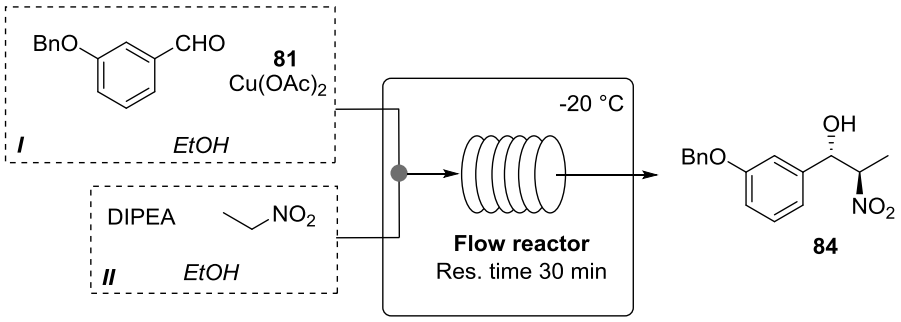

Scheme 49. Continuous flow synthesis of **84**.

Using a 1 mL 3D-printed reactor made of Poly-Lactic-Acid (PLA)(square channel: 1.41 x 1.41 mm) nitroalcohol **84** was obtained in very good yield (87%), 65/35 dr and 79% ee for the *anti* isomer (Table 40, entry 1). The use of a commercially available coiled tube made of Poly-TetraFluoroEthylene (PTFE)(circular channel: *id*: 0.58 mm) as continuous flow reactor afforded similar results in terms of chemical and stereochemical efficiency (entry 2).

Table 40. Continuous flow synthesis of **84**.

entry	Flow reactor	yield (%)	dr (*anti/syn*)[a]	ee_{anti} (%)[b]
1	3D-printed PLA **1 mL** (squared channel: 1.41 x 1.41mm)	87	65/35	79
2	PTFE coiled tube **0.5 mL** (circular channel: *id*: 0.58 mm)	90	70/30	80

[a]Determined by H-NMR of the crude; [b] determined by HPLC on chiral stationary phase.

The comparison of continuous flow experiments reported in Tables 39 and 40 highlighted that 3D-printed reactor made of HIPS gave better results in terms of stereoselectivity than the reactor made of PLA (Table 40 entry 6 *vs.* Table 3 entry 1). However HIPS as material gave some problems in terms of compatibility with organic solvents and after a few experiments the reactor started to decompose. For this reason the following experiments were conducted using 3D-printed reactors made of PLA which is more robust and less sensitive to decomposition by organic solvents. It could also be underlined that there are no big advantages in terms of chemical yield and ee using a 3D

printed reactor instead of a commercially available one (Table 40 entries 1 *vs.* 2). However 3D printed reactors are extremely cheap and can be designed *ad-hoc* by the operator.

Next we focused our attention on the preparation of intermediate **85**, precursor of norephedrine.

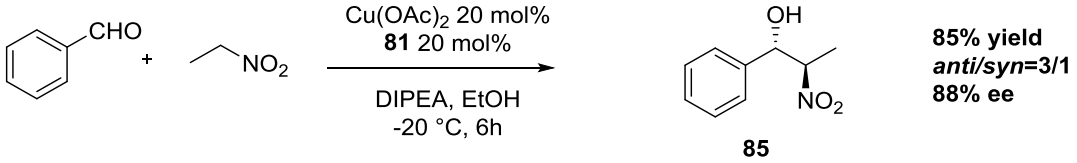

Scheme 50. Batch synthesis of 85.

The batch reaction between benzaldehyde and nitroethane in the presence of 20 mol% of $Cu(OAc)_2$ and chiral ligand **81** afforded nitroalcohol **85** in 85% yield, 3/1 *dr* and 88% ee for the major isomer (Scheme 49).

On the basis of the results obtained for the flow synthesis of nitroalcohol **84** we explored the continuous flow synthesis of intermediate **85** (Scheme 50).

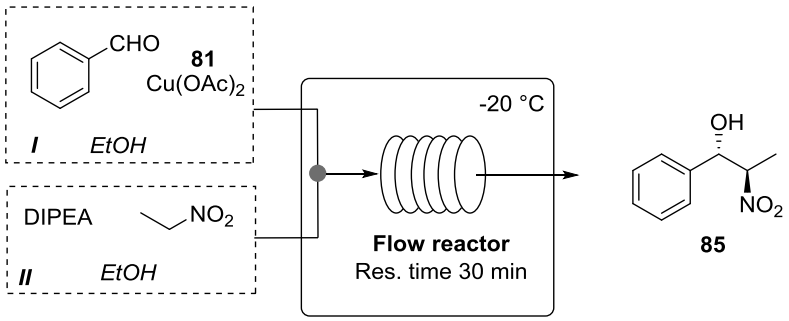

Scheme 51. Continuous flow synthesis of **85.**

Syringe ***I*** was charged with a preformed mixture of benzaldehyde (0.25 mmol, 25.4 µL), **81** (0.0625 mmol) and $Cu(OAc)_2$ (0.05 mmol) in EtOH (0.975 mL, 0.250 M). Syringe ***II*** was charged with nitroethane (2.5 mmol), DIPEA (0.25 mmol) and EtOH (0.750 mL). The two syringes were connected to a syringe pump and the reagents charged into the flow reactor at -20 °C for a residence time of 30 minutes.. The outcome of the reactor was collected into a cooled bath (-78 °C) in order to quench the reaction. At the end of the process the crude was treated with HCl 10%. After extraction with AcOEt the product was isolated by column chromatography on silica gel. Results of the continuous flow experiments are reported in Table 41.

Table 41. Screening of different flow reactors.

entry	Flow reactor	conversion (%)	dr (*anti/syn*)[a]	ee$_{anti}$ (%)[b]
1	PTFE coiled tube **0.5 mL** (circular channel: *id*: 0.58 mm)	98	67:33	81
2	3D-printed PLA **1 mL** (squared channel: 1.41 x 1.41mm)	96	67:33	79
3	3D-printed NYLON **1 mL** (squared channel: 1.41 x 1.41mm)	97	68:32	80
4	3D-printed PLA **1 mL** (circular channel: *id*: 1.59 mm)	98	67:33	84
5	3D-printed PLA **1 mL** (squared channel: 1.0 x 1.0mm)	98	67:33	80
6	3D-printed PLA **10 mL** (squared channel: 2.65 x 2.65mm)	96 (78 isolated)	74:26	89

[a]Determined by H-NMR of the crude; [b]determined by HPLC on chiral stationary phase.

Using a 0.5 mL coiled tube made of PTFE (circular channel: *id*: 0.58 mm) as continuous flow reactor gave nitroalcohol **85** with full conversion, 67/33 *dr* and 81% ee of *anti* isomer (Table 41, entry 1). Running the stereoselective Henry reaction into 1 mL 3D printed reactors made of PLA (squared channel: 1.41 x 1.41mm) or NYLON (squared channel: 1.41 x 1.41mm) did not altered the outcome of the reaction (entries 2 and 3). Even changing the size or the shape of the 3D printed reactors made of PLA caused no significant change in the outcome of the reactor: intermediate **85** was obtained in very good conversions, reasonable *dr* and good ee (entries 4 and 5). Finally we performed a reaction scale up using a 10 mL 3D-printed reactor made of PLA (squared channel: 2.65 x 2.65mm). Pleasingly, when the reaction was performed on a bigger scale **85** was obtained in very good yield, 74/26 *dr,* and 89% ee, higher than when performed into 1 mL reactors.

The third target identified was nitroalcohol **86**, precursor of Methoxamine. The batch reaction between 2,5-dimethoxy benzaldehyde and nitroethane in the presence of DIPEA, chiral aminopyridine **81** and $Cu(OAc)_2$ in EtOH at -20 °C afforded the corresponding product in 72% yield, 3/1 *dr* and 91% ee (Scheme 51).

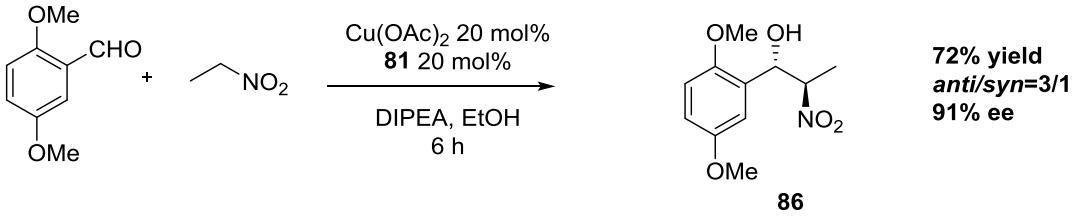

Scheme 52. Batch synthesis of **86**.

Then we explored the synthesis of intermediate **86** under continuous flow conditions using the same experimental set-up described above (Scheme 53). The experiments were conducted in accordance to the best reaction conditions (T = -20 °C, res. time 30 min).

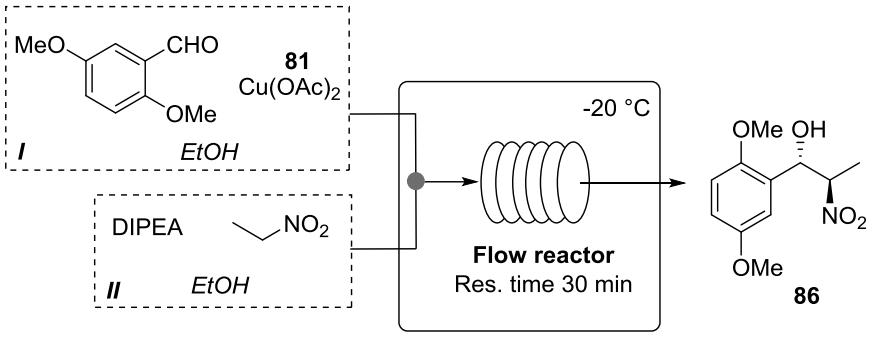

Scheme 53. Continuous flow synthesis of **86**.

The use of two different flow reactors was explored (Table 42). When a 1 mL 3D printed reactor mad of PLA(squared channel: 1.41 x 1.41mm) was used, nitroalcohol **86** was obtained in 89% yield, 73/27 *dr* and 85% ee for the *anti* isomer (Table 42, entry 1). Using a 0.5 mL PTFE coiled tube (circular channel: *id*: 0.58 mm), the product was obtained in lower yield and comparable *dr* and ee (entry 2).

Table 42. Continuous flow synthesis of **86**.

entry	Flow reactor	yield (%)	dr (*anti/syn*)[a]	ee$_{anti}$ (%)[b]
1	3D-printed PLA **1 mL** (squared channel: 1.41 x 1.41mm)	89	73/27	85
2	PTFE coiled tube **0.5 mL** (circular channel: *id*: 0.58 mm)	67	70/30	82

[a]Determined by H-NMR of the crude; [b]determined by HPLC on chiral stationary phase

The last target studied was chiral aminoalcohol **87**, precursor of Levonordefrin. The stereoselective Henry reaction between 3,4-bis(benzyloxy)benzaldehyde and nitroethane in the presence of DIPEA, chiral aminopyridine **81** and $Cu(OAc)_2$ in EtOH/THF mixture as solvent at -20 °C afforded the corresponding product in 53% yield, 65/35 *dr* and 84% ee (Scheme 54).

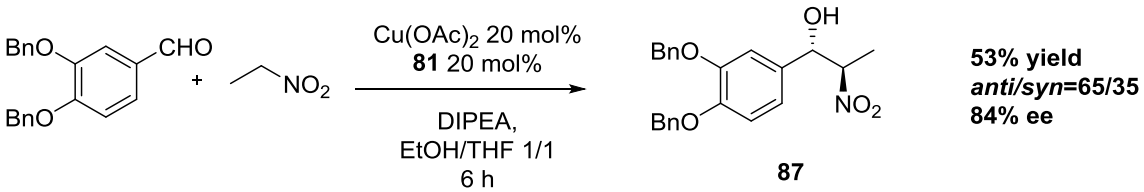

Scheme 54. Batch synthesis of **87**.

In this case the addition of THF as co-solvent was crucial because of the poor solubility of aldehyde **87** in EtOH.

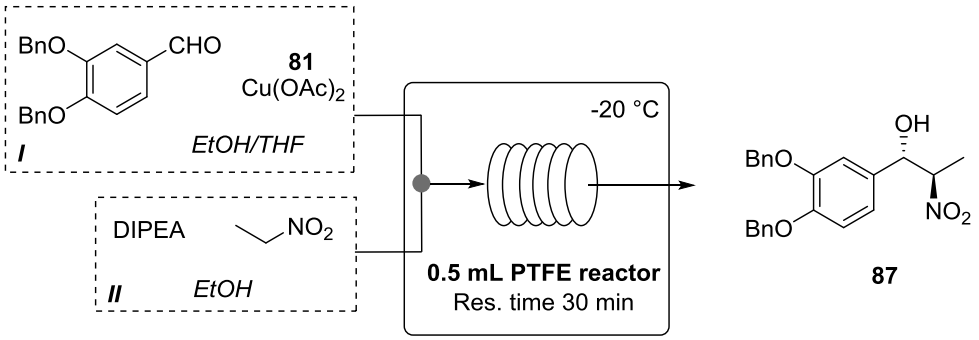

Scheme 55. Continuous flow synthesis of **87**.

Also in this case we investigated the flow processes (Scheme 55). Running the reaction using a 0.5 mL coiled tube made of PTFE (circular channel: *id*: 0.58 mm) as continuous flow reactor afforded **87** in 67% yield, 61/39 dr and 74% ee. Unfortunately these results were not reproducible due to the precipitation of the starting material into reactor channels. For this reason we couldn't explore the reaction using 3D printed reactors.

2.4.3 Continuous flow Hydrogenation

In order to obtain the desired chiral amino alcohols, the nitroaldol products **84**,**85** and **86** prepared through the stereoselective Henry reaction were subjected to a continuous flow hydrogenation with Thalenano H-Cube Mini equipped with a cartridge of Pd/C 10% *wt.* as catalyst.
A rapid screening of reaction conditions was performed using nitroalcohol **85** which is the direct precursor of Norephedrine (Scheme 56).

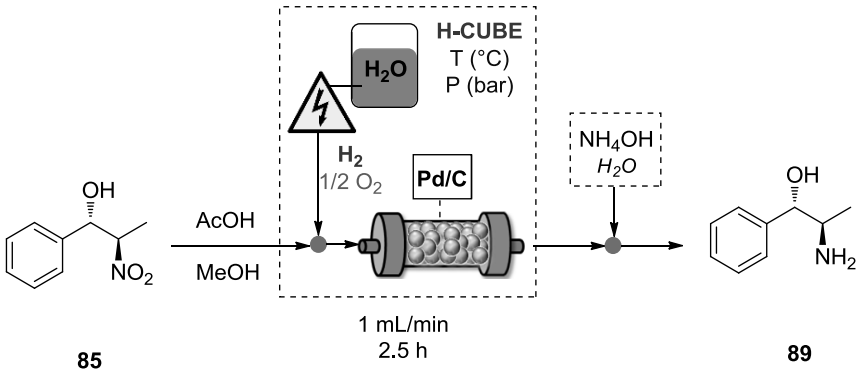

Scheme 56. Continuous flow synthesis of **89**.

A 0.1 M solution of nitroalcohol in MeOH was prepared and pumped into the H-CUBE Mini. Temperature and pressure were set at the indicated value and the continuous flow reduction was started at a flow rate of 1 mL/min. The outcome of the reactor was recirculated for a reaction time of 2.5 hours. After preliminary experiment AcOH was found to be essential to promote the reaction, otherwise only the unreacted starting material was recovered. The progress of the reaction was monitored by TLC.

Table 43. Screening of reaction conditions.

entry	Solvent [M]	T (°C)	P H_2 (bar)	conversion (%)
1	MeOH (0.1)	25	10	90
2	MeOH (0.1)	30	15	98
3	EtOH (0.1)	30	15	80
4	EtOH (0.03)	30	15	98
5	AcOEt (0.1)	30	15	10
6	AcOEt/EtOH 1/1 (0.1)	30	15	40

As first attempt the reaction was performed in MeOH at 25°C and 10 bar of H_2. The desired amino alcohol **89** (in its acetate salt form) was obtained in 90% conversion (determined by H-NMR after solvent evaporation)(Table 43, entry 1). Increasing the reaction temperature to 30 °C and the H_2 pressure to 15 bar resulted in a complete conversion of the starting material into **89** (entry 2). In view of a multistep process we also investigated the use of EtOH and AcOEt as solvents. A 0.1 M solution of **85** in EtOH was reduced with a conversion of 80% after 2.5 hours of reaction at 30°C and 15 bar (entry 3). In order to reach a full conversion a dilution to 0.03 M was necessary (entry 4). AcOEt proved to be a bad solvent for continuous flow hydrogenation with H Cube (entries 5

and 6). It also caused the precipitation of **89** into reactor channels due to its poor solubility in the solvent

In order to increase the reaction conversion from 80% to 98% it was necessary to dilute the reaction mixture from 0.1 to 0.03 M (entry 3 *vs.* entry 4). Amino alcohol **89** was obtained in its neutral form after a simple treatment with NH_4OH with no need for further purification. In all cases no erosion of the stereochemical integrity of the process was observed (ee determined after derivatization of norephedrine in its bis-acetylamide

Having identified the best reaction conditions we explored the reduction of nitroalcohol **86** for the synthesis of Methoxamine (Scheme 57). The continuous flow hydrogenation with H-CUBE Mini was performed at 30 °C and 15 bar of H_2 for 2.5 hours. A complete conversion of the starting material into amino alcohol **90**(in its acetate salt form) was observed. Also in this case no erosion of stereochemical integrity was observed (ee determined after derivatization of methoxamine onto the corresponding bis-acetylamide). Amino alcohol **90** was obtained in its neutral form after a simple treatment with NH_4OH with no need for further purification.

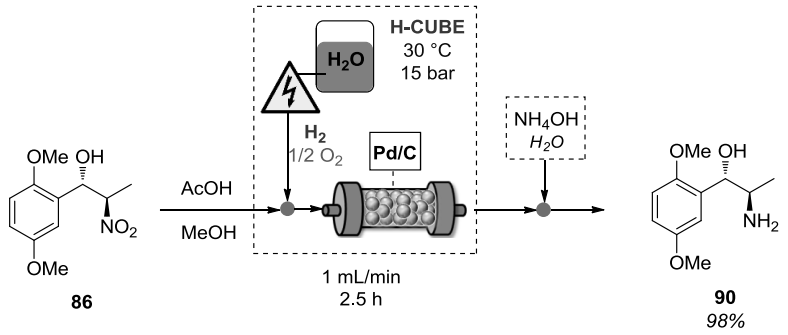

Scheme 57. Continuous flow synthesis of **89**.

In order to obtain Metaraminol, nitroalcohol **84** had to be subjected to a nitro group reduction and O-debenzylation. We identified the continuous flow hydrogenation in the presence of Pd/C as catalyst as a possible synthetic strategy to perform both reactions in one step (Scheme 58).

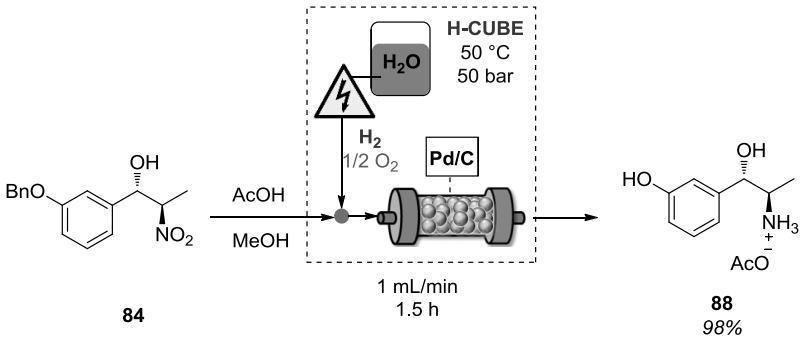

Scheme 58. Continuous flow synthesis of **88**.

A 0.1 M solution of **84** in EtOH in the presence of 30 equivalents of AcOH was loaded in the H-CUBE Mini at 1 mL/min. After 2.5 hours of recirculating process at 50 °C and 50 bar of H_2 amino alcohol **88** (in its acetate salt form) was obtained with a complete conversion. The enantiomeric excess was maintained during the reaction (ee determined by HPLC on chiral stationary phase).

2.4.4 Multistep Process

After proving the feasibility of the two-step sequence for the synthesis of chiral 1,2-amino alcohols we explored the possibility of simulating a continuous flow multistep process without the need for isolation and purification of the nitroalcohol intermediate or solvent switching (Scheme 59). This procedure would be appealing for the stereoselective synthesis of chiral 1,2-amino alcohols on a preparative scale.

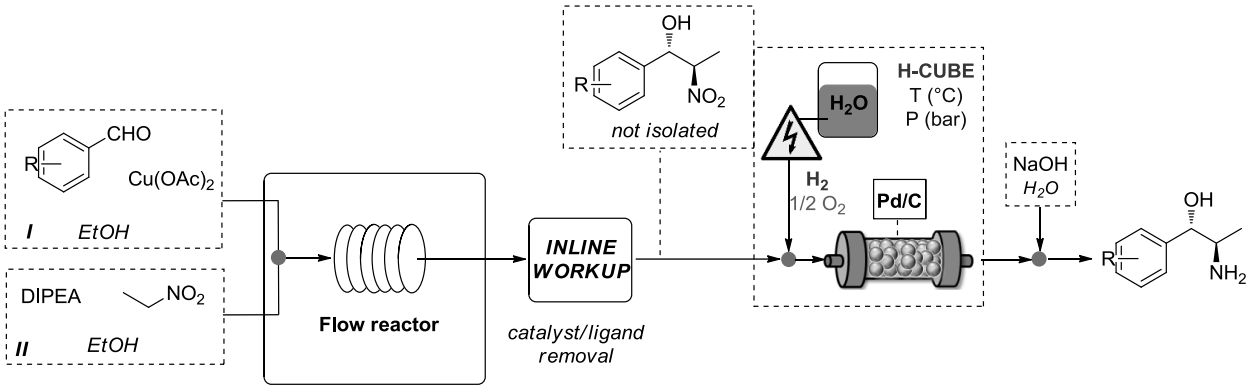

Scheme 59. Multistep synthesis of **amino alcohols.**

After the initial stereoselective Henry reaction performed into 3D printed flow reactor, the key step was the removal of Cu catalyst and chiral ligand in order to not interfere with the continuous flow hydrogenation which involved the use of Palladium as catalyst. The reaction between benzaldehyde and nitroethane was chosen as model reaction to develop a multistep flow process for the synthesis of 1,2-amino alcohol **89** (Scheme 59).

At first we tried to remove Cu/ligand complex of Henry reaction through an acidic work up using HCl 10% *wt.* followed by extraction with AcOEt. Unfortunately this strategy was not successful because large quantities of AcOEt were necessary to completely extract nitroalcohol **89**. Additionally AcOEt proved to be a non-suitable solvent for the continuous flow hydrogenation step (Table 43, entries 5 and 6).

As alternative approach to remove Cu/ligand complex of Henry from the crude reaction mixture we identified a filtration on a short pad of silica followed by elution with EtOH. In this way no solvent switching is necessary. The compatibility of EtOH as solvent for the continuous flow hydrogenation step was already proved above (Table 43, entry 4). Additionally the precious chiral ligand can be easily recycled by simple treatment of silica with an HCl solution in EtOH.

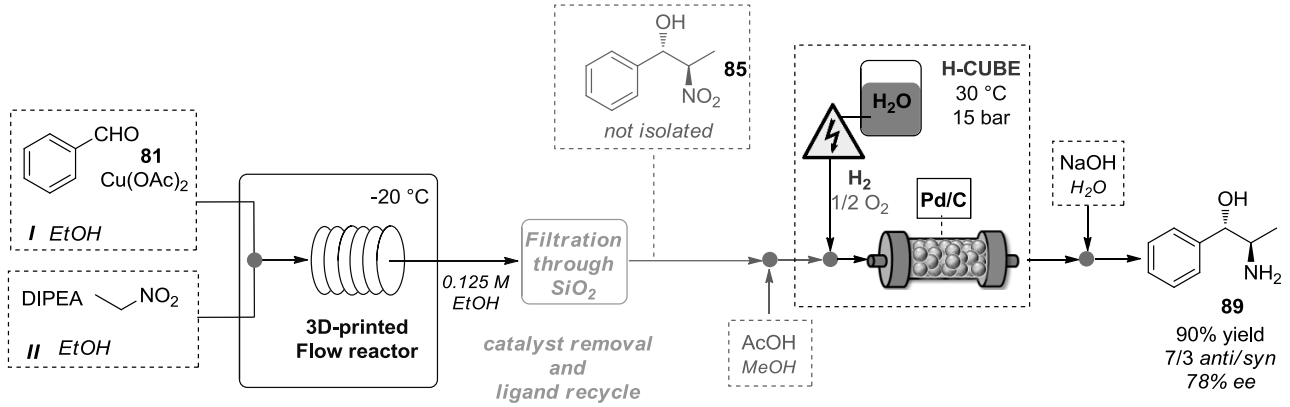

Scheme 60. Multistep synthesis of **89**.

Syringe ***I*** was charged with a preformed mixture of benzaldehyde, **81** (0.375mmol) and $Cu(OAc)_2$ (0.075 mmol) in EtOH (1.5 mL, 0.250 M). Syringe ***II*** was charged with nitroethane (0.270 mL, 3.75 mmol), DIPEA (65 µL, 0.375 mmol) and EtOH (1.26 mL). The two syringes were connected to a syringe pump and the reagents directed to the flow reactor at -20 °C for a residence time of 30 minutes. The outcome of the reactor (dark blue solution, 3 mL) was filtered over a short pad of silica (*h*: 1 cm, *d*: 2 cm) by elution with EtOH (6 mL). To the resulting mixture (light yellow) 30 equivalents of AcOH were added and the resulting mixture was subjected to continuous flow hydrogenation with H CUBE (T: 30 °C, P: 1 bar, flow rate 1 mL/min, t: 2.5 h). The solvent was then evaporated, treated with NH_4OH 33% wt. and extracted five times with AcOEt. Amino alcohol **85** was obtained in 90% yield (over 2 steps), 7/3 *dr* and 78% ee as a pure withe solid (*dr* and ee were determined after derivatization of **85** into the corresponding bis-acetylamide).

In conclusion, a new continuous flow process for the stereoselective synthesis of chiral 1,2-amino alcohols has been developed. Three targets displaying biological activities (Norephedrine, Metaraminol and Methoxamine) have been prepared through a two-step sequence:

- the first step consisted of a stereoselective Henry reaction promoted by a copper complex of a chiral aminopyridine ligand derived from camphor. The reaction was performed into 1 mL 3D-printed flow reactors made of different materials (PLA, HIPS, NYLON). The use of 3D printed reactors allowed for a rapid screening of reactors with different sizes, shapes and channel dimensions. The process afforded the desired products in very good yields, moderate diastereoselectivity and enantiomeric excesses up to 89%. The use of a 10 mL 3D printed reactor for the scale up of the process has also been demonstrated.
- the second step involved a continuous flow hydrogenation with Thalesnano H CUBE Mini in the presence of Pd/C as catalyst. This process allowed to obtain pure 1,2 amino alcohols with no need for further purification.

Finally, in view of a possible industrial application, a multistep continuous flow process for the synthesis of Norephedrine has been demonstrated: using optimal reaction conditions the final product was isolated without any reaction intermediates purification or solvent switching operation.

In principle a fully automated continuous flow process for the stereoselective synthesis of chiral 1,2 amino alcohols can be developed.

CHAPTER 3 PHOTOREDOX CATALYSIS

3.1 Introduction

The use of visible light in organic synthesis is not a new idea having been pioneered by the Italian chemist Giacomo Ciamician in 1912 when he published a visionary paper "*The future of photochemistry"*.[89] He suggested developing novel technologies that allowed the direct harvesting of energy from sunlight and converting it into chemicals or fuels. The society at that time was not ready for such ideas and it took until recently for concepts as renewable energy and sustainable use of natural resources to be more widely accepted and implemented. While the conversion of light into electrical energy by photovoltaics is already highly developed and commercialized, the methods using visible light in chemical synthesis are still quite limited. However, there are several advantages related to the use of visible light: most organic compounds are not colored and absorb light with a wavelength shorter than 400 nm. Visible light is abundant and it is the most intensive part of the sunlight spectrum, but only in some cases we will consider to do chemical synthesis in the sunlight, as irradiation is not constant and weather dependent. The development of high power light emitting diodes (LED) allows the efficient and simple generation of visible light of high intensity and in a small wavelength range. Last, but not least, visible light is safe to use. However, we also have to consider the limitations of the energy source: Visible light is not high in energy. A blue photon (440 nm) contains approximately the energy of a carbon – iodine bond. If we use only visible light for initiating chemical reactions, we must employ starting materials that are already high in energy or contain weak chemical bonds.

Photoredox catalysis, based on the exploitation of an abundant and renewable source as light, has attracted more and more attention in the last years as an emerging strategy requiring mild conditions. In this catalytic methodology, light absorbing compounds (*i.e.* photoredox catalysts) are employed in substoichiometric amounts to activate substrates through photoinduced single electron transfers (SET). Thus, activated species are formed without the need for radical initiators or stoichiometric oxidants or reductants and otherwise difficult or impossible reaction pathways are accessed. Light irradiation converts photocatalysts into their photoexcited states which are chemically more reactive because of the significantly altered electronic distribution. Photoredox catalysis rely on the general property of excited states to be both more easily reduced ("reductive pathway") as well as more easily oxidized ("oxidative pathway") than their corresponding ground state; in this way the photocatalyst can serve either as an electron donor or an electron acceptor to be regenerated in the catalytic cycle (Figure 26).

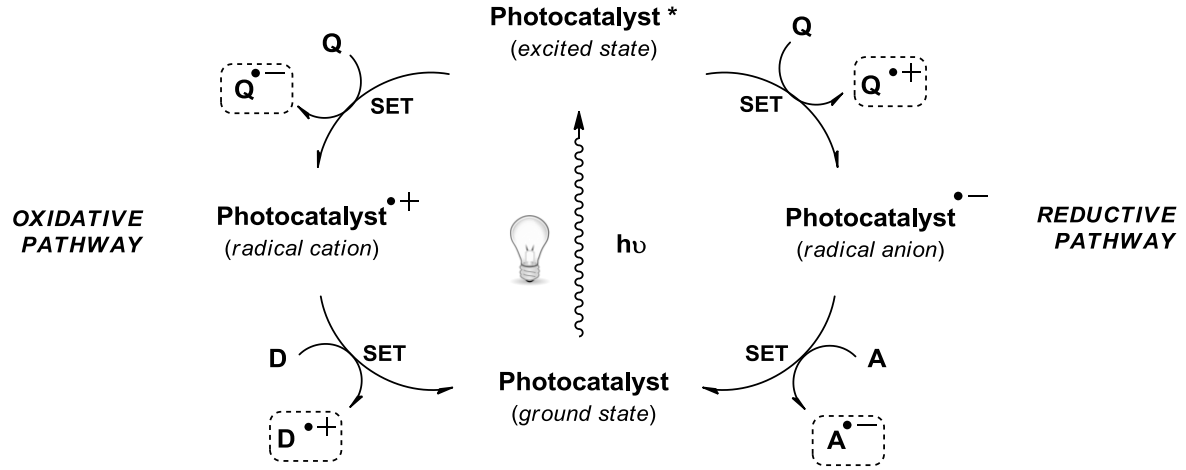

Figure 26: photoredox catalytic cycles: oxidative pathway (on the left) and reductive pathway (on the right). Q = quencher; D = donor; A = acceptor; SET = Single Electron transfer.

As depicted in Figure 26, for each pathway the photocatalyst undergoes two distinct single electron transfer steps; both the quenching and the regenerative electron transfers can be productive with respect to a desired chemical transformation. Ideally, the two electron transfer processes are connected by substrates or intermediates of the photocatalyzed reaction ($Q^{\bullet+}$ and $A^{\bullet-}$ in the reductive pathway, $Q^{\bullet-}$ $D^{\bullet+}$ in the oxidative pathway) and therefore any sacrificial electron donor or acceptor is required.
The so-formed electronically excited molecules can be considered as completely new entities in comparison with their ground state precursors; they show their own chemical behavior and give access to unconventional reaction pathways otherwise difficult or impossible to reach by thermochemical or electrochemical activation, affording complex molecular structures.[90]

Despite several advantages offered by photochemical transformations, the implementation of this energy source in large-scale production of chemicals has been largely disregarded. Indeed scale-up process of traditional batch photochemical reactions has generally found to be detrimental and poorly effective, often resulting in product decomposition due to over-irradiation. These shortcomings arise from the logarithmic decrease with path length of the transmission of light through a liquid medium ("Beer-Lambert Law"). In this way, the non-homogeneous light distribution within the entire reaction mixture prevents a uniform irradiation which results in a loss of efficiency.

$T = I/I_0 = 10 \wedge (\varepsilon * l)$
where T: light transmission; I_0: intensity of the light striking a substance; I: intensity of light transmitted through the substance; ε: the absorption coefficient of the substance; *l*: the distance that light travels through the substance.

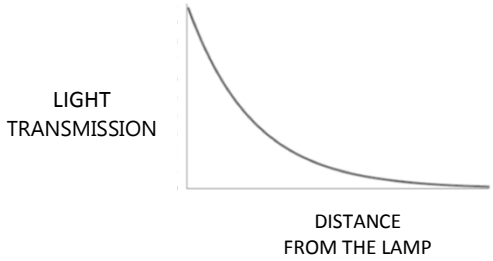

Figure 27. Beer-Lambert law.

These drawbacks associated with batch photochemical reactors could be overcome by using continuous flow microreactor technology. Performing photochemical reactions in micro- or mesoflow systems is significantly more efficient than when developed in batch: indeed the narrow width of flow reactor coils ensures an excellent and uniform distribution of light within the entire reaction mixture, resulting in higher reaction selectivity, shorter reaction times and lower catalyst loadings. The scale-up of a photocatalyzed reaction in flow would become easier as many flow photoreactors could be connected in parallel and the level of efficiency would remain high. In addition, the irradiation of smaller volumes of flammable solvents would also reduce safety concerns with respect to batch photochemical reactions.[91]

For all these reasons the development of novel continuous flow photoredox catalyzed transformations would be highly desirable from an industrial point of view.

In this chapter we will describe the development of a new visible light photoredox synthetic methodology. Its application under continuous flow conditions and a direct comparsion with the batch procedure will also be examined.

3.2 Reductive Coupling of Imines with Olefins

The development of new strategies for the umpolung of carbonyl compounds has been of great interest over the past years, as it would open new retrosynthetic opportunities for the synthesis of complex molecules. Even though the umpolung of aldehydes and ketones has been widely studied, the number of effective procedures for the umpolung of imines is still quite limited. A general strategy is the deprotonation of imines to form 2-azaallyl anions. These intermediates can be used in organocatalyzed or metal-catalyzed cross-coupling processes, yielding alkylated or arylated umpolung products.[92] A major shortcoming of this strategy is the need for strong bases and biased substrates to ensure regioselectivity in the functionalization of the 2-azaallyl anion. Another strategy is the one-electron reduction of an imine to give a free amino radical anion or a 3-membered metallacycle depending on the nature of the reductant employed.[93] However, direct electron-transfer is difficult due to the high reduction potentials of imines ($E_{1/2}$red = – 1.98 V vs SCE for N-benzylideneaniline),[94] and either *ad-hoc* designed substrates with low reduction potentials or overstoichiometric amounts of highly reducing metals salts based on titanium, zirconium or samarium are usually needed.

The umpolung of imines using visible light photoredox catalysis has recently been demonstrated by a few works that involve both intramolecular and intermolecular functionalization using different reaction partners.[95]

Rueping and co-workers recently demonstrated that visible light induced reduction of imines to α-amino radicals using photocatalysts with low ground state reduction potentials was possible by a strategic choice of the reductive quencher.[96] Tributylamine acted both as an electron-donor for the catalyst and as a hydrogen-bond donor for the substrate, enabling a proton-coupled electron transfer as key step, which would be strongly endoergonic otherwise. The resulting radical then underwent dimerization to give symmetrical aromatic diamines (Scheme 61).

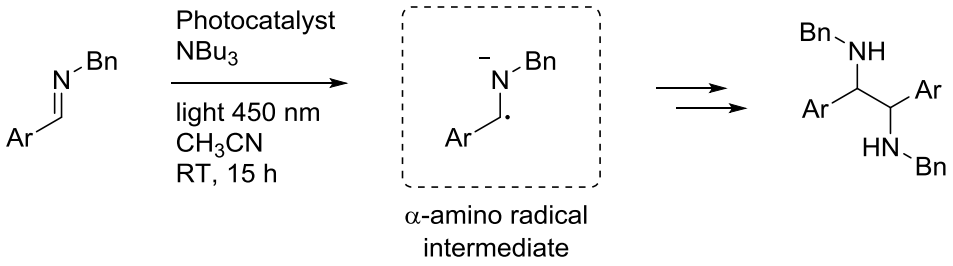

Scheme 61. Photoredox pinacol coupling of imines.

Exploiting the strategy for the formation of α-amino radical intermediate we explored the possibility to perform an unprecedented cross-coupling reaction between imines and olefins promoted by visible light photoredox catalysis.[97]

Based on previous works on the functionalization of imines we hypothesized a plausible reaction mechanism for this transformation (Scheme 62): upon excitation by visible light, the photocatalyst (PC) becomes highly oxidizing (PC^*) and is reduced by tributylamine (NBu_3) to give the

corresponding radical cation **A**, which rapidly undergoes a 1,2-hydrogen shift to form the α-ammonium radical **BH$^+$**. This intermediate activates the imine (**C**) for a subsequent proton-coupled electron transfer which regenerates the catalyst and gives the α-amino radical **D** along with **B**. Cross-coupling between these two nucleophilic radicals is disfavored in the presence of electron-deficient olefins **94**, onto which **D** readily adds in accordance with the polar effect. The resulting electrophilic radical **E** undergoes hydrogen atom transfer from **B** to give **F** and the expected saturated product **95** (the formation of **F** was detected by ^{13}C-NMR analysis of the crude reaction mixture: resonance at δ_C = 97.0 ppm). Thus, the additive plays here a triple role: reduction of the excited-state catalyst, hydrogen-bonding to render the reduction of the imine less endoergonic, and finally hydrogen-atom donation. Notably, such a reaction manifold avoids side-reactions typically observed when using trialkylamines as reductive quenchers, such as reduction of **D** by HAT from tributylamine or **B** and radical addition of **D** onto **F**.

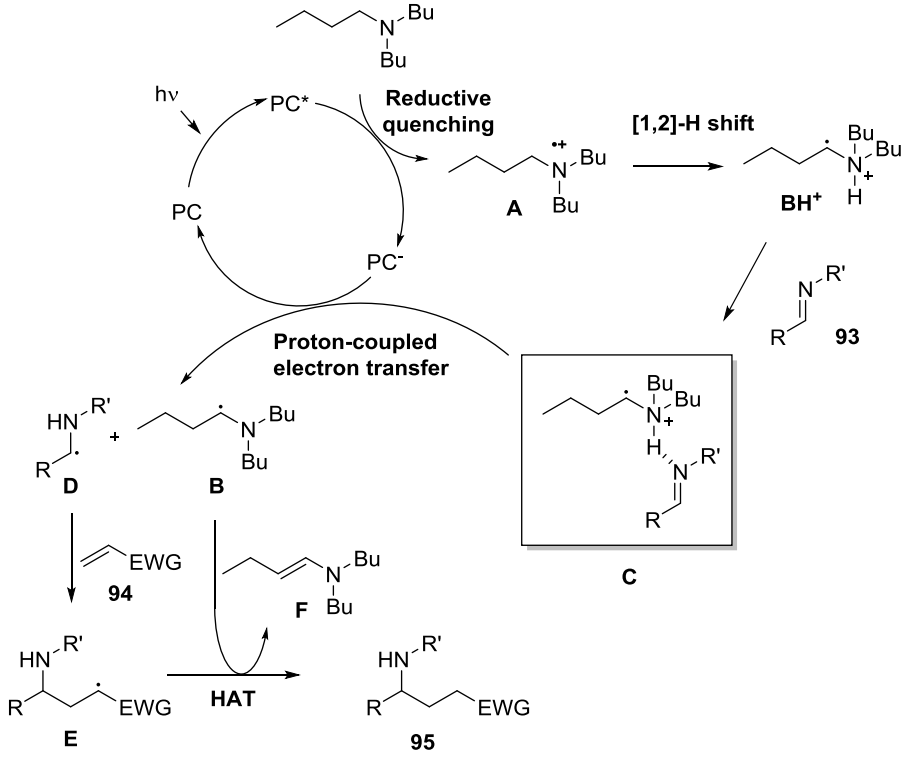

Scheme 62. Postulated reaction mechanism.

Based on previous studies of the group, we started our investigation on the photoredox-catalyzed reductive cross-coupling of imines with olefins by irradiating a mixture of imine, tributylamine and methyl acrylate in DMF, using Ir[F(CF$_3$)ppy]$_2$(bpy)PF$_6$ **IrA** or Ir(ppy)$_2$(dtbbpy)PF$_6$ **IrB** as photoredox catalyst (see Figure 1 for the structure of the catalysts). In contrast with many other *N*-protected substrates, *N*-benzylideneaniline gave little to no imino-pinacol coupling and selectively coupled with the olefin in 59% and 57% yield respectively. Further optimisation showed that no additives other than tributylamine were needed, and that the use of ethanol as a sustainable alternative to DMF greatly enhanced the yield. Under the optimal conditions, *N*-benzylideneaniline **93a** was dissolved in ethanol in the presence of 3 equivalents of methyl acrylate, 1.5 equivalents of tributylamine and 2 mol% of **IrA** and irradiated at 450 nm with blue LEDs for 24 hours to give the expected product **95aa** in 84% yield (Table 44, entry 1). Slightly higher yields could be obtained by

letting the reaction proceed for 24 additional hours. Concentrating the reaction medium was detrimental, giving the product in only 52% yield. Lower loading of **IrA** or use of commercially available catalyst **IrB** still gave the product in reasonable yields, providing alternative conditions to non-specialists (entries 4 and 5). No conversion was observed in absence of tributylamine or photocatalyst, in the dark, or under air atmosphere. Addition of catalytic amounts of bases completely inhibited the reaction, confirming a proton-coupled electron transfer as the key step (entry 10).

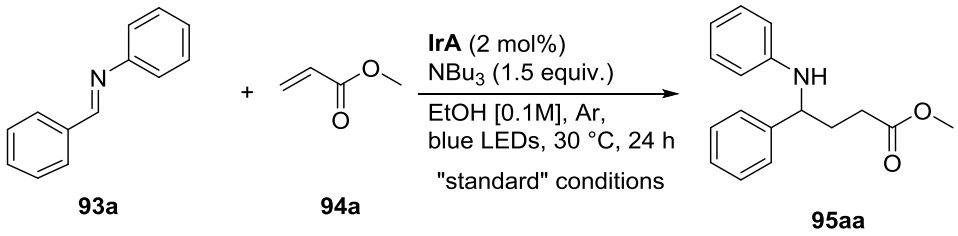

Table 44. Screening of reaction conditions.

Entry	Modification from "standard" conditions	Yield (%)[a]
1	None	84
2	48 h	89
3	[0.3 M]	52
4	1 mol% of photocatalyst **IrA**	61
5	2 mol% of photocatalyst **IrB**	59
6	Without NBu_3	0
7	In the dark	0
8	Without photocatalyst	0
9	Under air atmosphere	0
10	With 20 mol% of K2CO3 or K3PO4	0

[a] Isolated yields.

The reduction potential of **93a** is –1.98 V *vs* SCE, compared to the reduction potential of the catalyst **IrA** of –1.29 V *vs* SCE. Thus, the imine is not likely to be reduced without protonation. To add experimental evidence to our thermodynamic rationalization, we performed the reaction in presence of acidic or basic additives (Table 45): acidic additives did not influence the yield, but no product was observed and **93a** was recovered when using basic additives.

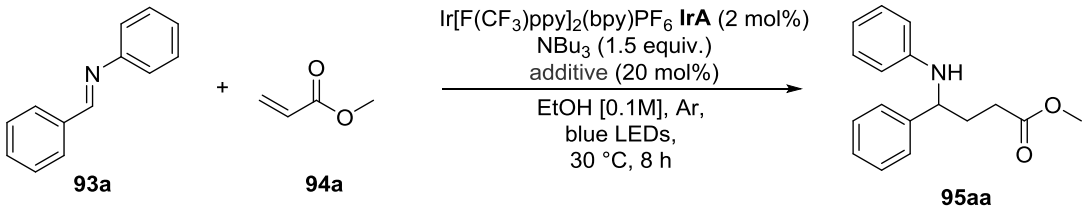

Table 45. Screening of additives.

Entry[a]	Additive	Yield(%)[b]
1	none	52
2	H_2O	54
3	CF_3COOH	52
4	Oxalic Acid	56
5	Diphenylphosphate	37
6[c]	K_2CO_3	0
7[c]	K_3PO_4	0

[a] isolated yields; [b] 24 h reaction time; [c] **93a** recovered.

In order to demonstrate that the coupling between radicals **B** and **D** is disfavored due to the polar effect, we screened the amount of olefin **3a** (Table 46) and we observed that **95aa** was obtained in very good yield when 3 (or more) equivalents of **94a** were used. The use of a stoichiometric amount of **94a** resulted in a decreased yield of 95aa and in the formation of by-products **97** and **98**. Running the reaction in the absence of **94a** favoured the formation of **97**, in accordance with our previous results on the photoredox-catalyzed imino-pinacol coupling. **99** was not detected in any of our control experiments. Thus, pinacol coupling or reduction by hydrogen-atom transfer are favored over radical cross-coupling.

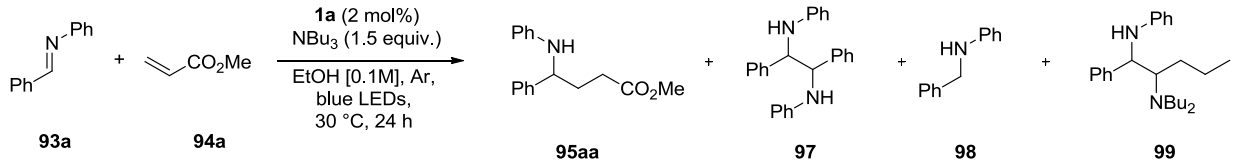

Table 46. Screening of **94a** equivalents.

Entry	94a (equiv.)	95aa(%)[a]	97(%)[a]	98(%)[a]	99
1	3	84	traces	traces	Not detected
2	1	55	18	6	Not detected
3[b,c]	0	0	60	10	Not detected

[a] isolated yields; [b] reaction performed using **IrA** as catalyst; [c] full conversion of **93a** observed.

As already stated, tributylamine plays a triple role necessary for the formation of the desired product: reductive quenching, activation by proton-coupled electron transfer (PCET) and hydrogen atom transfer (HAT).

Tributylamine is a well-established reductive quencher of ruthenium and iridum-based photocatalysts. As mentioned above, byproduct **F** was observed in the crude reaction mixture, thus strongly supporting the intermediacy of **B** and its involvement in a HAT. Additionally, we investigated the impact of reductive quenchers with different chemical properties to demonstrate how all three features are essential.

Trialkyl amines (linear, branched or cyclic) can both activate the imine by PCET and undergo HAT, and all gave **95aa** in high yields (Table 47, entries 1, 2 and 3).

Triphenylamine and tris(4-bromophenyl)amine cannot undergo a 1,2 hydrogen shift after oxidation, and thus cannot activate the imine through PCET. Using these amines as reductive quenchers, **93a** was recovered and no product was obtained (entries 4 and 5).

Tribenzylamine, similarly to trialkyl amines, can take parth both PCET and HAT events. In this case however, although imine **93a** was fully consumed, validating the PCET event- no product **95aa** was obtained (entry 6). A complex mixture of products was instead observed, as the α-amino radical of tribenzylamine has a structure similar to radical intermediate **D** and thus is able to undergo competitive cross-coupling and cross-imino-pinacol.

In contrast to the previous entry, using Hantzsch ester gave the product in good yield since it can activate the imine by PCET and donate an hydrogen atom, without the formation of reactive α-amino radicals (entry 7).

Finally, alternative reductive quenchers such as sodium dithionite and sodium ascorbate have oxidation potentials accessible by the catalyst, but cannot activate the imine through PCET. With these quenchers **93a** was recovered and no product was obtained (entries 8 and 9).

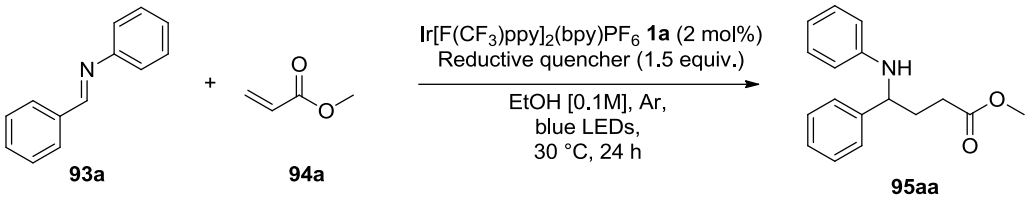

Table 47. Screening of reductive quenchers.

Entry[a]	Reductive quencher	$E_{1/2}^{ox}$ ($Q/Q^{\bullet+}$) (V vs SCE)	Yield(%)[a]	Remarks
1	NBu_3	+0.78	84	Full conversion
2	Hunig's Base	+0.68	78	Full conversion
3	N-Methyl Pyrrolidine	+0.68	75	Full conversion
4[b]	NPh_3	+0.92	0	**93a** recovered
5[b,d]	$N(p\text{-}Br\text{-}C_6H_4)_3$	+1.22	0	**93a** recovered
6[b]	NBn_3	+1.17	0	Full conversion
7[c]	Hantzsch Ester	+0.72	68	Full conversion
8[c]	$Na_2S_2O_4$	+0.77	0	**93a** recovered
9[e]	Na-ascorbate	+0.33	0	**93a** recovered

[a] isolated yields; [b] because of the higher oxidation potential the reaction was performed using the more oxidizing Iridium catalyst **1c**; [c] reaction performed using **IrB** as catalyst; [d] DMSO was used as solvent.

With the optimal conditions in hand, we explored the scope of the reaction (Scheme 63). First, we established that not only acrylates, but also other electron poor alkenes such as acrylonitrile, acrylamides as well as vinyl sulfones can be coupled with **93a** in good yields. Next, we showed that acrylates with side-chains of various size and lipophilicity gave the corresponding products in very

good yields. A free hydroxy group (**95ah**) as well as a trialkyl amine (**95ai**) were tolerated, without signs of oxidation under the reaction conditions. A bromide-containing acrylate derivative smoothly reacted to give product **95al**, even though reduction of alkyl bromides by photoredox catalysis has previously been reported.[98] Methacrylate and itaconate derivatives gave the expected products (**95aj**, **95am** respectively) in good yields and selectivities, while using methyl 2-acetamidoacrylate as acceptor gave the highly valuable γ-aminobutyric amino acid derivative **95am** in high yield and moderate selectivity. Conjugated dienes were also competent substrates, as using methyl 4-methylpentadien-2,4-oate as acceptor **95ao** was obtained as the only product in good yield.

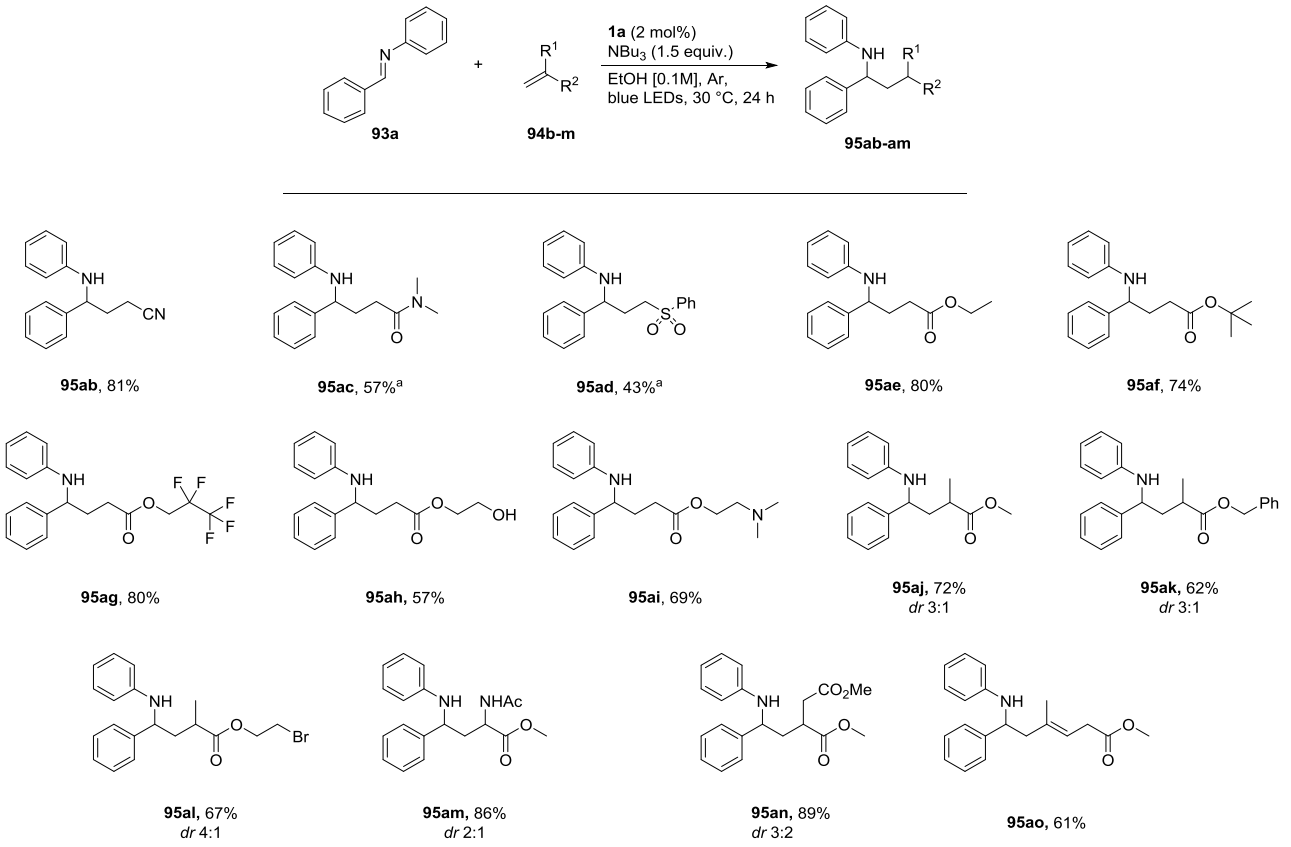

Scheme 63. Substrate scope.

Next, we decided to investigate the substrate scope regarding imines (Scheme 63). While trying to broaden the scope of the nitrogen protecting group, we found that several imines underwent decomposition, pinacol coupling, reduction, or simply did not react at all under the standard reactions conditions. *N*-arylimines however were robust and cleanly afforded the desired products in most cases. Electron-rich as well as electron deficient groups were tolerated, and once again, no dehalogenation was observed (**95ea-95ia**). The synthetically valuable products **95ja** and **95ka** were obtained in moderate yields.

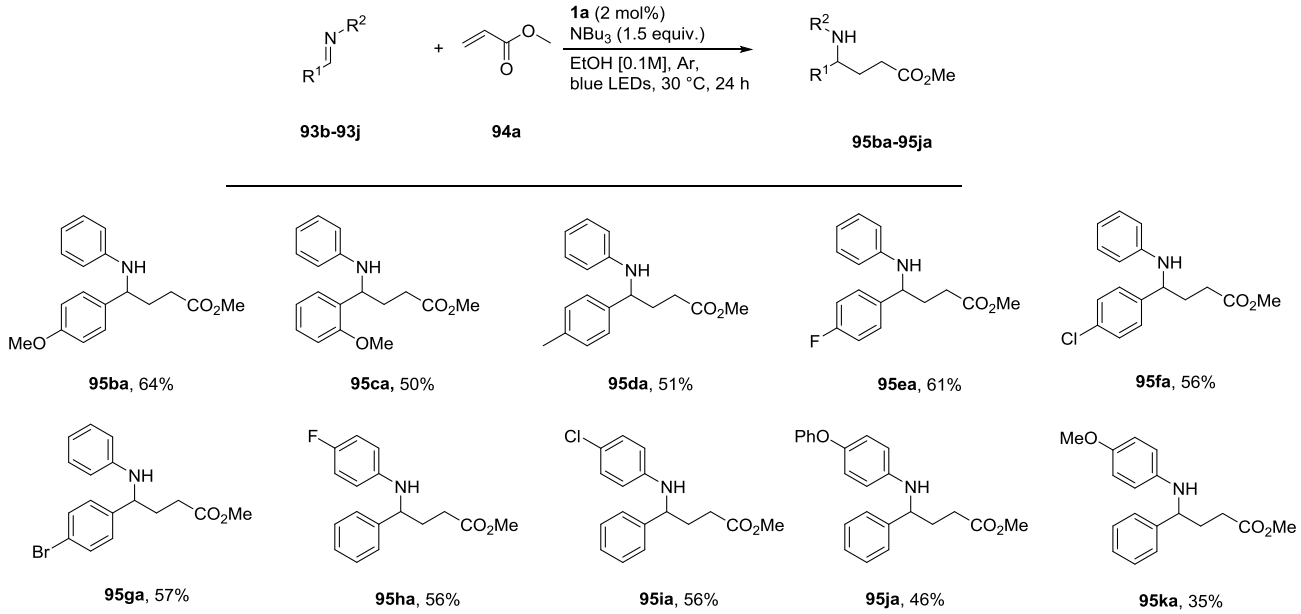

Scheme 64. Substrate scope.

As illustrated in Scheme 64, the conversion of γ-aminobutyric ester derivatives **95aa**, **95aj, 95am** and **95an** to the corresponding γ-lactams proceeded almost quantitatively by heating the starting materials in toluene in the presence of catalytic amounts of *para*-toluenesulfonic acid (Scheme 4a). Additionally, the reaction was not only limited to reductive alkylation but could also be extended to reductive allylation of imines by using appropriate allyl sulfone derivatives as coupling partners, resulting in the formation of products **95b** and **95c**.

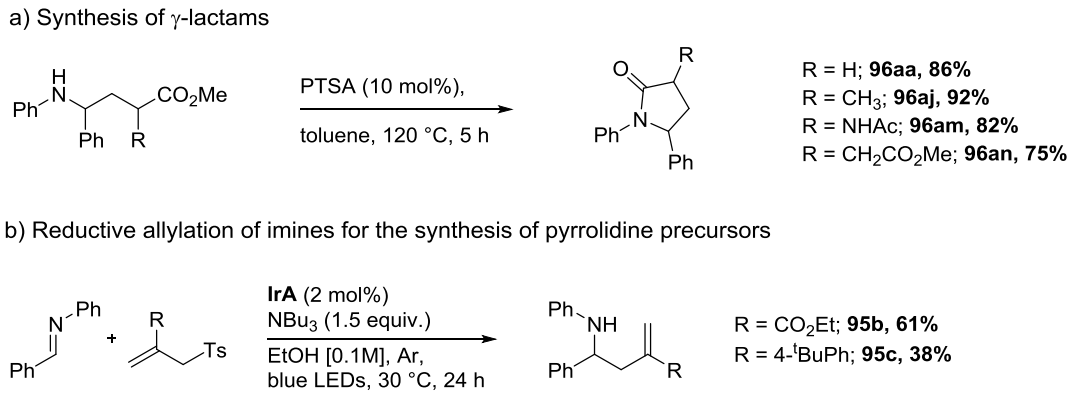

Scheme 65. Products derivatization.

Finally, we investigated the outcome of the reaction under continuous flow conditions (Scheme 66). A PTFE tubing (*id* = 0.8 mm, *l* = 10 m, V_i = 5 mL) was wrapped around a glass beaker (*id* = 9 cm, *h* = 5 cm) and placed into a dewar flask where 2 rows of 11W blue LEDs strips were previously fixed. One end of the tubing was connected to a steel needle and the other placed into a receiving flask. The reaction mixture was prepared under argon atmosphere and loaded into a 5 mL plastic syringe, pumped into the flow reactor through a syringe pump at the indicated flow rate and irradiated with blue LEDs. Afterwards the reactor was washed with 5 mL of degassed EtOH at the

same flow rate under continuous light irradiation. The output of the reactor was collected into a round bottom flask, concentrated *in vacuo*, and the residue was purified by column chromatography on silica gel.

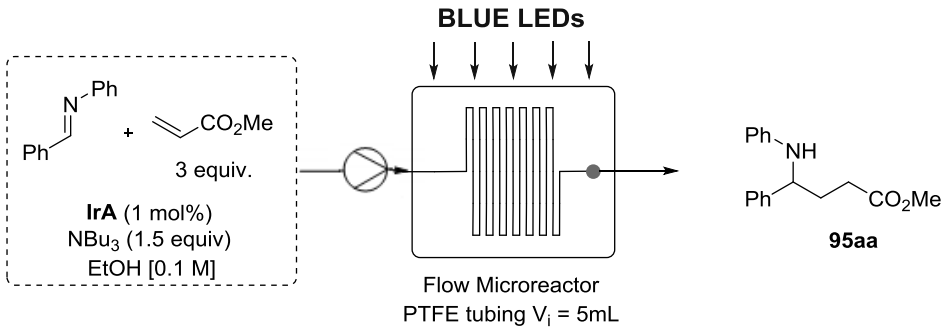

Scheme 66. Continuous flow reaction.

Table 48. Screening of reaction conditions in flow.

Entry[a]	M (mol/L)	Residence time (h)	Flow rate (mL/h)	IrA (mol%)	Yield(%)[b]
1	0.05	4	1.25	2	77
2	0.1	4	1.25	2	79
3	0.1	2	2.50	2	62
4	0.1	4	1.25	1	74
5[c]	0.1	4	1.25	1	80

[a] Reaction performed according to continuous-flow method using **93a** (0.3 mmol, 54.3 mg), **94a** (0.9 mmol, 81 μL), **IrA** (as indicated), NBu_3 (0.45 mmol, 111 μL) and degased EtOH (3.0 mL); [b] isolated yields; [c] reaction performed on 0.5 mmol scale.

From the results reported in Table 48, it is clear that the reaction under flow condition is much faster than the one in batch: using a residence time of 4 hours (instead of 24 required in batch), **95aa** was obtained in 79% yield. A further decrease in the reaction time resulted in a lower yield of 62%. Notably, under flow conditions, catalyst loading could be reduced to 1 mol%, affording the desired product in 74% yield. Finally performing the reaction on 0.5 mmol scale with 1 mol% of **IrA**, product **95aa** was obtained on 80% yield.

Once best reaction conditions were identified we evaluated the scope of the reaction under flow conditions (Scheme 67). By using 1 mol% of **IrA** and with a retention time of 4 hours the products were obtained in good yields and moderate selectivity, totally comparable to the ones obtained in batch.

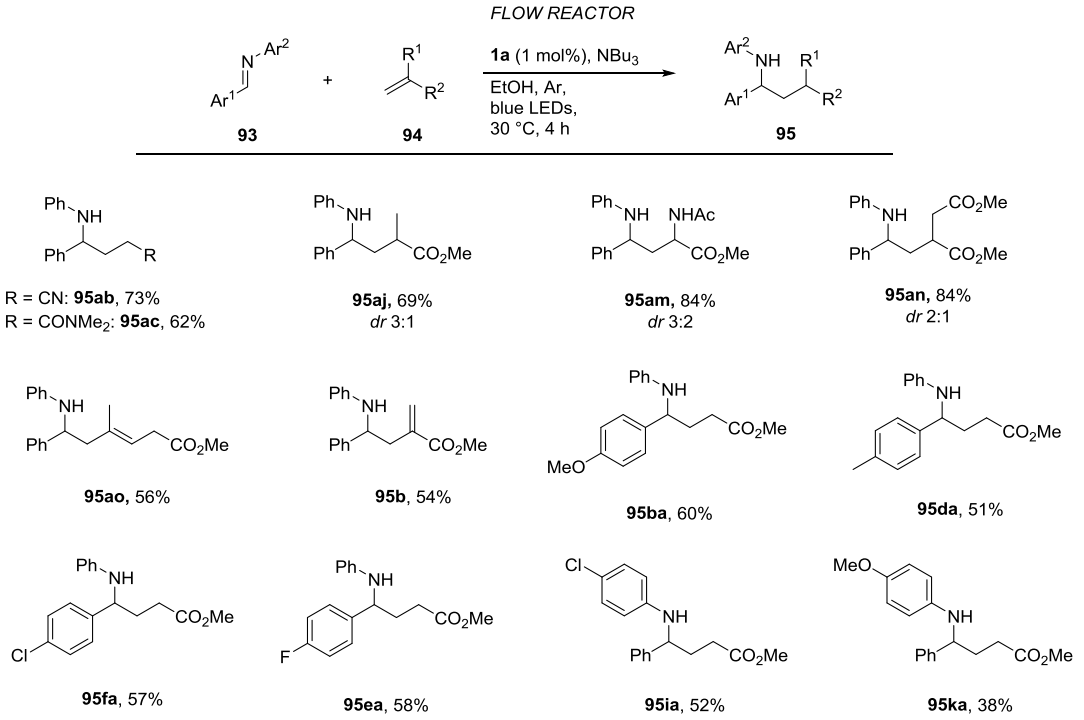

Scheme 67. Scope of the reaction in flow.

The integration of inline analytical devices into the flow stream of a synthetic methodology improves process automation and also reduces risks associated to handling and isolation of intermediates. In particular, IR flow cells have recently proved to be effective tools for reaction monitoring, mechanistic investigations as well as quantitative measurements in multistep processes and self-optimization studies.[99] In order to have a better understanding of the reaction rate we next decided to monitor the reaction profile during time using a FlowIR instrument equipped with DiComp ATR (diamond-composite attenuated total reflection) probe (Scheme 68). For inline analysis we identified signals at ν = 1633 cm^{-1} and ν = 1607 cm^{-1} corresponding to starting imine **93a** and product **95aa**, respectively. Monitoring the flow photoredox coupling of **93a** and **94a** under optimal conditions at different reaction times, substrate consumption and product formation could be readily determined (Figure 28).

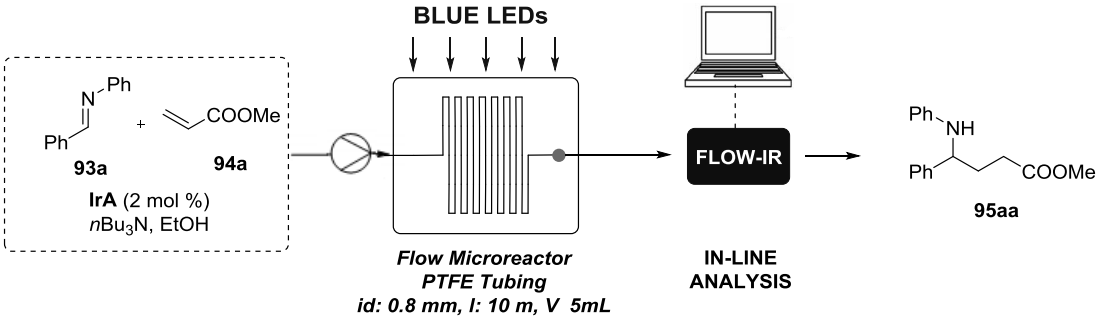

Scheme 68. Continuous flow in-line analysis.

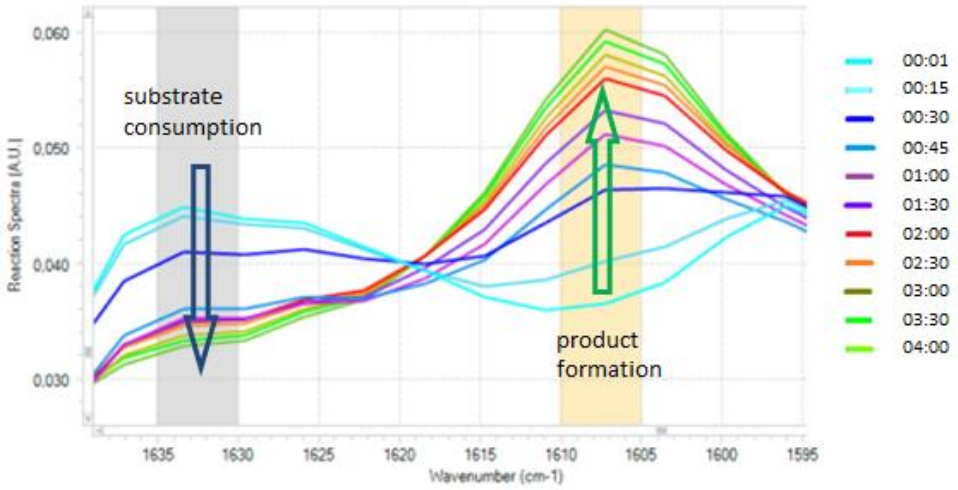

Figure 28. Reaction progress monitored by in-line IR analysis.

As depicted in Figure 29, the comparison between batch and continuous flow conditions clearly demonstrates how both processes have a similar reaction profile, but light irradiation in flow microreactor ensures a faster transformation, which reach completion after 4 hours only and a half amount of catalyst.

.

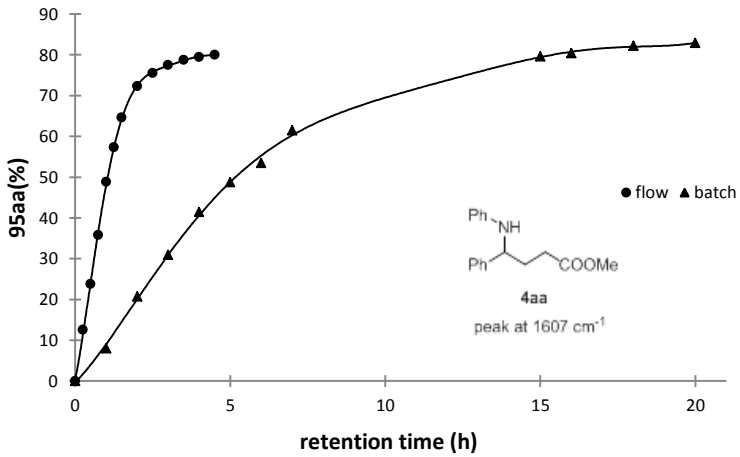

Figure 29. Reaction profile in batch and flow.

In conclusion, a new synthetic methodology based on the functionalization of imines through visible-light photoredox catalysis has been developed and its general applicability has been studied. The application under continuous flow conditions has been investigated and the advantages related to the use of photoflow reactors have been demonstrated.

CHAPTER 4 EXPERIMENTAL SECTION

4.1 Supported Organocatalysts

4.1.1 Chiral Imidazolidinones

Silica-supported imidazolidinones

*Synthesis of catalysts **S1-S4***

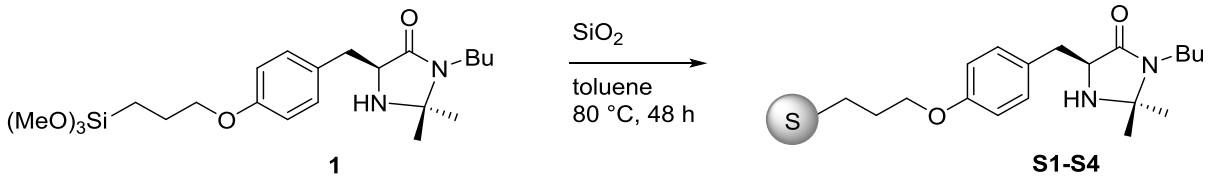

1 S1-S4

Compound **1**[i] (0.57 g, 1.3 mmol) was suspended in dry toluene (15 mL) and SiO_2 (see below for details) was added. The mixture was gently stirred at 80 °C for 48 hours under nitrogen atmosphere. After reaction time the solid was filtered, washed dichloromethane/methanol 9:1 mixture and dried under high vacuum at 40 °C for 3 hours. The loading (mmol/g) of the supported catalysts was determined by weight difference.

S1 was prepared using Apex Prepsil Silica Media 8 µm (1.00 g). Loading = 0.4 mmol/g.

S2 was prepared using Apex Prepsil Silica Media 8 µm (0.70 g). Loading = 0.3 mmol/g.

S3 was prepared using Apex Prepsil Silica Media 8 µm (0.25 g). Loading = 0.1 mmol/g.

S4 was prepared using Luna Silica 10 µm (1.00 g). Loading = 0.5 mmol/g.

*Synthesis of catalysts **S5***

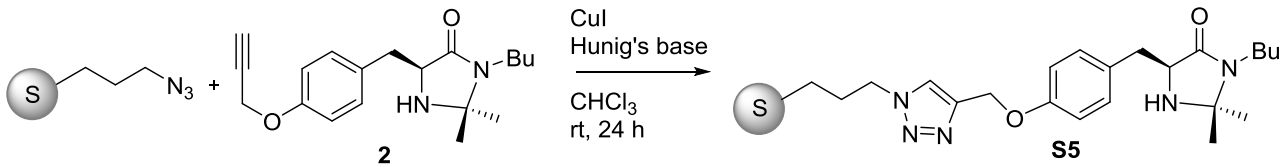

2 S5

Catalyst **S5** (loading = 0.4 mmol/g) is already known and was prepared according to a procedure previously published in our research group.[i]

[i] A. Puglisi, M. Benaglia, R. Annunziata, V. Chiroli, R. Porta, A. Gervasini, *J. Org. Chem.* **2013**, *78*, 11326.

Characterization

The supported catalysts were characterized by performing cross-polarization (CP) and direct-polarization (DP) magic angle spinning (MAS) ^{13}C and ^{29}Si NMR experiments in order to obtain evidence for the presence of the organic moieties in the siliceous materials and confirm their chemical structure.

^{13}C CPMAS NMR.

The ^{13}C spectra of the prepared catalysts demonstrated that the materials were indeed functionalized as expected and the organic residues were stably bound to the inorganic material (see the chemical shifts of C-1 and C-3 carbons). As a comparison, we report the ^{13}C resonances of catalyst **S1**, in which the imidazolidinone moiety is directly linked to the silica surface, and catalyst **S5**, bearing a triazole spacer between the imidazolidinone and the silica surface. The ^{13}C resonances reported in Table 1 are assigned based on the chemical shifts found in the solution spectra of organic precursors.

As expected based on previous experiments, ^{13}C spectrum of catalyst **S5**, synthesized by cycloaddition of imidazolidinone **2** with the supported azide, revealed about 25% of unreacted azide starting material. The ratio between the two organic moieties (the azide and the imidazolidinone) can be calculated by integrating the signal of carbon atoms C-1 (9.0 ppm) and C-10 (13.0 ppm). (The data should be considered within the limit of the analytic technique).

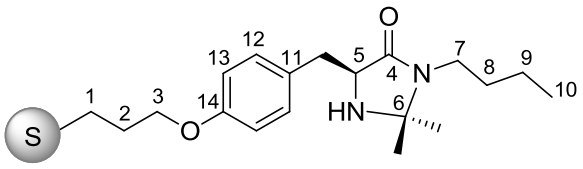

S1

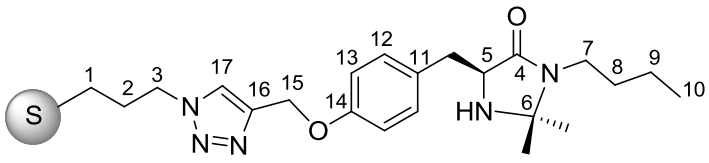

S5

Cat	C1	C2	C3	C4	C5	C5'	C6	C7	C8	C9	C10	C11	C12	C13	C14	C15	C16
S1	7.6	22.1	69	175	59	39	76	51	31	20	12	130	130	114	158		
S5	9	23	52	174	58	40	76	50	28	20	13	129	129	114	157	62	143

^{13}C NMR resonances (ppm) in the solid state spectra of catalysts **S1** and **S5.**

[29]Si DP and CPMAS NMR.

The [29]Si NMR spectra of siliceous materials are extensively used to determine the functionalization degree of the materials as well as to give insights about the substitution of the surface silicon atoms. It is well recognized that a given surface silicon atom bearing a functional group can have a variable number n of Si-O-Si bonds, leading to so-called T_1, T_2, and T_3 substructures. The bonding schemes, for these hybrid materials containing organic functionalities, lead to very different geometries on the surface, as illustrated in Figure 2. The [29]Si spectra gives also information about the bulk surface species Q_4 [$(SiO)_4$ Si] and proton-rich Q_n sites: Q_3 [$(SiO)_3$ SiOH], Q_2 [$(SiO)_2$ $Si(OH)_2$] and Q_1 [(SiO) $Si(OH)_3$]. Knowledge of the surface incorporation patterns and the conformations of functional groups for such materials is an essential step toward developing efficient functional substrates.

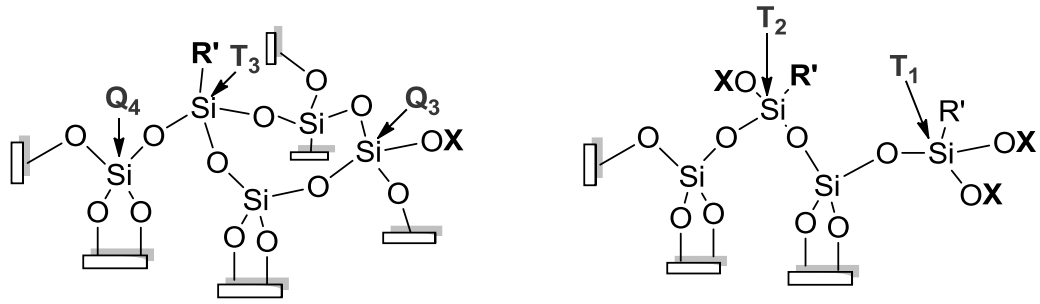

X= H or Et
R'= organic residue of catalysts 1-4

[29]Si DP/MAS experiments, carried out according to previously described methods,[ii] were performed in this study for the prepared catalysts. As expected, the [29]Si solid state spectra are dominated by resonance lines at -113, -103 and - 96 ppm representing silicon sites Q_4, Q_3 and Q_2 , respectively. On the other hand, different patterns were found in the spectra of the catalysts as concerns the functionalized T_n species, where the silicon atoms are directly bound to at least one organic moiety.

The presence of peaks assigned to T_3, T_2 and T_1 confirmed that the organic groups are indeed covalently bound to the surface. Quantitative measurements of T_n and Q_n silicon groups could be properly achieved by [29]Si DP/MAS experiments, as reported previously[iii] in order to determine T_n and Q_n relative concentrations, surface coverage and molar concentrations of organic moieties. As a comparison, in Table 2 we report the data of catalyst **S1**, in which the imidazolidinone moiety is directly linked to the silica surface, and catalyst **S5**, bearing a triazole spacer between the imidazolidinone and the silica surface.

[ii] a) S. Huh, J. W. Wiench, Y. Wi-Chul, M. Pruski, V. S.-Y. Lin, *Chem. Mater.,* **2003**, *15*, 4247. b) S. Huh, H. T. Chen, J. W. Wiench, M. Pruski, V. S.-Y. Lin, *Angew. Chem., Int. Ed.*, **2005**, *44*, 1826.

[iii] a) A. Puglisi, R. Annunziata, M. Benaglia, F. Cozzi, A. Gervasini, V. Bertacche, M. C. Sala, *Adv. Synth. Catal.,* **2009,** *351,* 219; b) A. Puglisi, M. Benaglia, R. Annunziata, V. Chiroli, R. Porta, A. Gervasini, *J. Org. Chem*., **2013**, *78*, 11326.

Cat	T_1 % -54 ppm	T_2 % -60 ppm	T_3 % -68 ppm	Q_2 % -96 ppm	Q_3 % -103 ppm	Q_4 % -113 ppm	SC (%)	MC (mmol/g)
S1	-	2.5	2.8	0	22.5	72.2	19.1	0.67
S5	-	4.1	13.0	4.4	30.5	48.0	33.0	1.43[a]

^{29}Si DP/MAS NMR Chemical Shifts, relative concentrations of T_n and Q_n silicon groups (in %), surface coverage (SC, in %) and molar concentrations of organic moieties (MC, in mmol/g) of catalysts **S1** and **S5**.
[a)] overall (catalyst + azide)

As it can be noted, catalyst **S5** has a larger surface coverage, estimated as SC = (T_1+ T_2+ T_3) / (Q_2 + Q_3 + T_1+ T_2+ T_3), due the structure of the siliceous material, in which the organic moiety can cover the interior wall of the mesopores. Catalyst **S1**, derived from grafting of a trialcoxysilane to a commercially available silica, presents smaller T_2 and T_3 values, leading to a smaller SC. In the case of **S1**, the calculated loading (MC) is in good agreement with that obtained by weight difference of a silica sample before and after functionalization (0.67 *vs* 0.53 mmol/g); the MC of **S5**, on the other hand, is overestimated (0.95 *vs* 0.40 mmol/g). Even if in the quantification of organic residues on silica matrix some discrepancies among different analytical techniques arise, MAS-NMR remains a powerful method for the characterization of functionalized siliceous materials since it can be used not only to study different surface incorporation patterns but also to determine the ratio between two different organic residues.

Morphological properties

The morphological examination of the sample particles was performed by collecting images of the surfaces by SEM analysis. The images of the surfaces of all the inorganic- organic hybrid materials compared with those of bare silica showed a variety of particle shapes and sizes densely agglomerated.

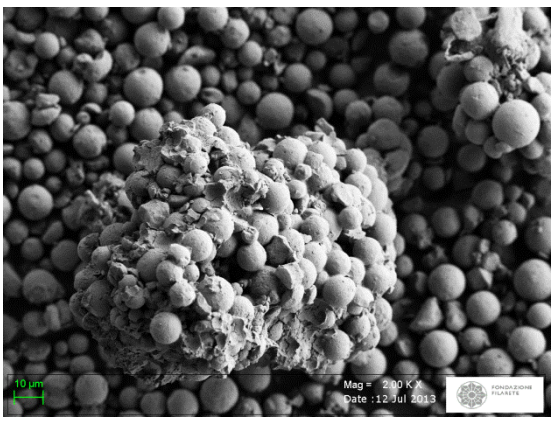

Figure 30. SEM image of a sample of catalyst **S5**

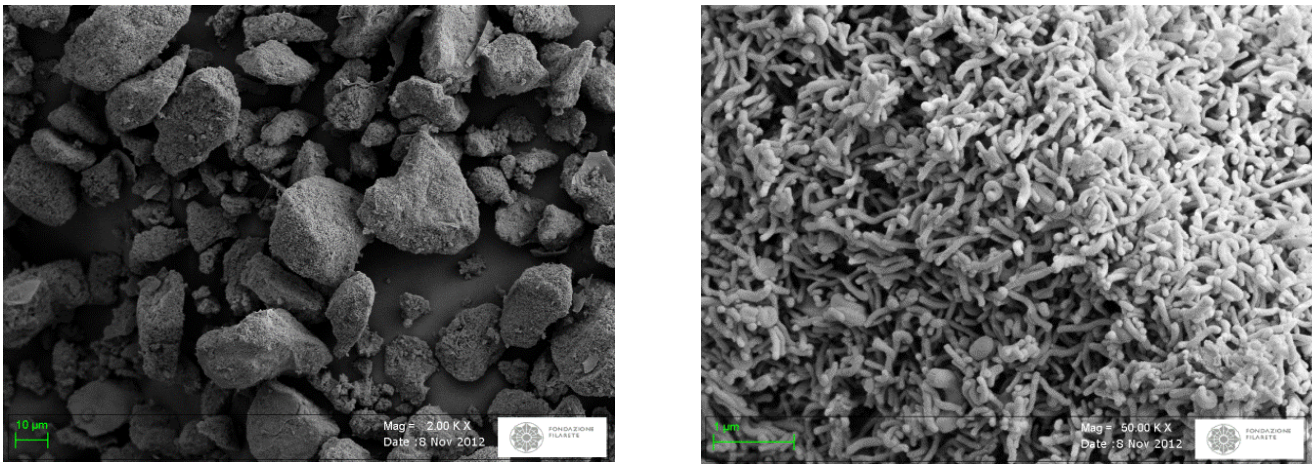

Figure 31. *SEM images of a sample of catalyst **S5** at 2000 X (left) and 50000 X (right).*

Figure 30 represents the SEM image of catalyst **S5**: the micrograph clearly shows some aggregation of the material; this particles aggregation can explain the experimental observation that, after a prolonged fluxing of the column (six volumes of column), no reagents or products, presumably retained inside the column, were detected at the exit (see below for catalytic experiments).

Figure 31 shows the micrographs of catalyst **S5** at two different magnification: as expected, rod-shaped particles of different lengths and diameters (ca. 0.4 µm in length and 500 nm in diameter), with curved hexagonal-shaped tubular morphology, completely cover irregular polyhedral-shaped grains which can be associated with the silica morphology.

SEM image of catalyst **S1** (Figure 32) shows a regular distribution of particles size and confirms that no mechanical degradation occurred after functionalization of the siliceous material.

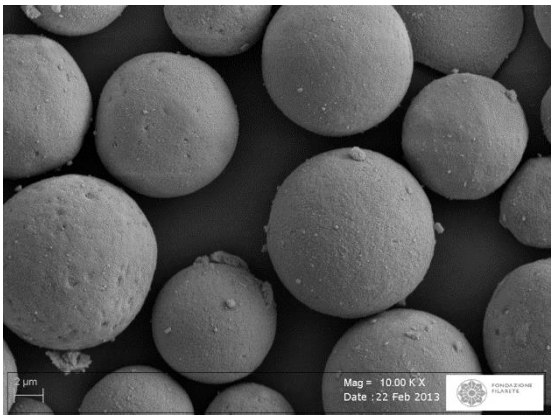

Figure 32. *SEM image of a sample of catalyst **S1.***

Polymer supported imidazolidinone

*Synthesis of monomer **3***

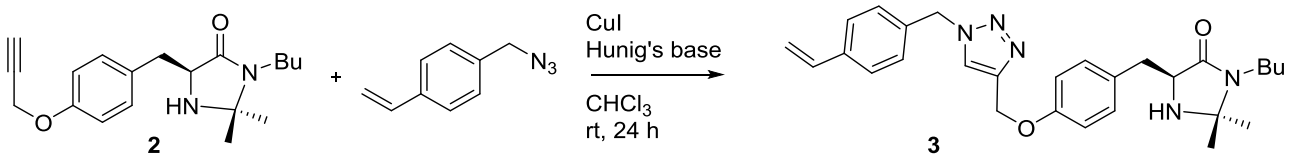

Compound **2**[i] (1.5 mmol, 0.47 g) was dissolved in dry chloroform (15 mL) under nitrogen atmosphere then CuI (0.08 mmol) and Hunig's base (4.5 mmol) were added. The mixture was stirred at rt for 15 minutes, then a solution of 4-azidomethylstyrene (1.9 mmol) in dry chloroform (3 mL) was slowly added. The mixture was stirred for 24 hours at rt then NH_4OH (5 ml, 33 wt% solution) was added. The organic layer was washed twice NH_4OH (5 ml, 33 wt% solution), once with brine (8 mL), dried with sodium sulfate and concentrated *in vacuo* yielding to a brownish oil. The residue was purified by column chromatography on silica gel eluting with ethyl acetate to afford **3** as yellowish oil (1.29 mmol, 0.61 g, 86% yield).

^{1}H NMR (600 MHz, $CDCl_3$) δ_H 7.50 (s, 1H), 7.40 (d, J = 8.0 Hz, 2H), 7.23 (d, J = 8.0 Hz, 2H), 7.12 (d, J = 8.4 Hz, 2H), 6.87 (d, J = 8.6 Hz, 2H), 6.69 (dd, J = 17.6, 10.9 Hz, 1H), 5.73-5.58 (m, 1H), 5.50 (s, 2H), 5.26-5.30 (m, 1H), 5.13 (s, 2H), 3.70 (t, J = 5.3 Hz, 1H), 3.28 (ddd, J = 14.3, 9.8, 6.0 Hz, 1H), 3.04 (dd, J = 14.3, 5.8 Hz, 1H), 2.99 (dd, J = 14.3, 4.8 Hz, 1H), 2.88 (ddd, J = 14.5, 9.8, 5.6 Hz, 1H), 1.62 (bs, 1H), 1.38-1.54 (m, 2H), 1.25-1.30 (m, 2H), 1.24 (s, 3H), 1.13 (s, 3H), 0.90 (t, J = 7.4 Hz, 3H) ppm; **^{13}C NMR** (151 MHz, $CDCl_3$) δ 173.8, 157.1, 144.5, 138.1, 135.9, 133.8, 130.7, 129.4, 128.3, 126.8, 122.6, 114.9, 114.7, 76.0, 62.0, 58.8, 53.9, 40.2, 35.9, 31.4, 28.0, 26.5, 20.3, 13.7 ppm. **HRMS** (ESI): calc. for $[C_{28}H_{36}N_5O_2]^+$ 474.2871, measured 474.2874.

*Synthesis of catalysts **P1***

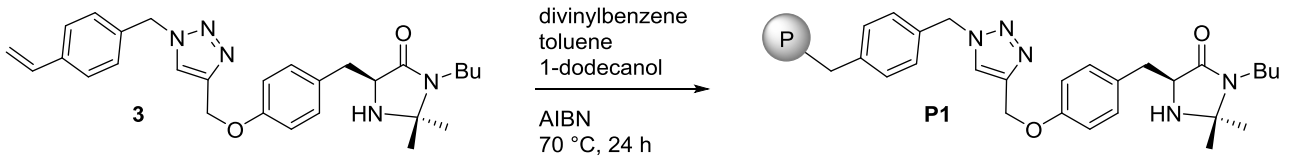

A mixture of compound **3** (0.29 g, 0.61 mmol, 10.5 wt%), AIBN (0.17 mmol, 1 wt%) divinylbenzene (6.9 mmol, 32.5 wt%), toluene (4.3 mmol, 14.5 wt%) and 1-dodecanol (6.2 mmol, 41.5 wt%) was prepared under nitrogen atmosphere. The mixture was transferred into a sealed vial and heated into an oil bath at 70 °C for 24 hours. After reaction time the polymer was removed from the vessel and crushed into a mortar. The fine powder obtained was suspended in methanol (15 mL) and stirred for 10 minutes at rt. The solid was then isolated by filtration and washed methanol (15 mL) and dichloromethane (15 mL). The solid was recovered and dried under high vacuum at 40 °C for 3 hours.
The loading of catalyst **P1** (0.5 mmol/g) was determined by the stoichiometry of reagents in the polymerization mixture. The polymerization occurred with a full conversion as any trace of monomer **3** was recovered from the organic layer used to wash the solid (toluene and 1-dodecanol were fully recovered).

FT-IR (KBr pellet) ν_{max} 3020, 2927, 2869, 1695, 1605, 1512, 1448, 1245, 905, 830, 798, 710 cm^{-1};
BET Surface area: 485 $m^2\ g^{-1}$.

*Synthesis of monolithic reactor **M1***

Monolith **M1** was prepared following the same procedure used for the preparation of catalyst **P1**. The mixture of reagents was poured into a stainless steel HPLC column (*i.d.* = 0.4 cm, *l* = 12.5 cm) sealed at the bottom end, paying attention to fill completely the available volume. The top end was sealed and the column was weighed in order to determine the exact amount of the feed mixture. The column was then placed vertically into an oil batch and heated at 70 °C for 24 hours. After cooling to rt the seals were replaced by metal frits and the soluble components were removed by flushing the column with THF (150 mL) using a syringe pump (0.3 mL/min).
The loading of monolithic reactor **M1** (0.5 mmol/g) was determined by the stoichiometry of reagents in the polymerization mixture. The polymerization occurred with a full conversion as any trace of monomer **3** was recovered from the organic layer used to wash the solid (toluene and 1-dodecanol were fully recovered).

Characterization

The supported catalyst **P1** was characterized by performing HRMAS NMR (High Resolution Magic Angle Spinning Nuclear Magnetic Resonance) experiments in order to obtain evidence for the presence of the organic moieties anchored on the polymeric backbone and confirm catalysts structure. The polymer was swelled in DMF-*d7*.

P1

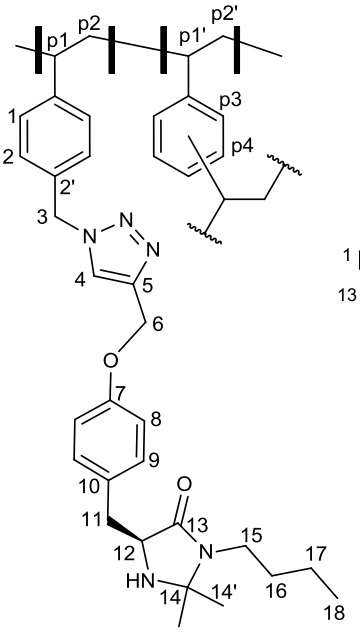

	1	2	2'	3	4	5	6	7	8	9	10	11
^{1}**H**	7.1	7.4		3.5			3.9		7.1	7.4		2.9
^{13}**C**	112	128	137	59.4	124	143	62	157.6	114.9	130.7	124	40

	12	13	14	14'	15	16	17	18	9	10	11
^{1}**H**	3.2			1.5	3.4;3.2 [a]	1.6	1.4	1.4	7.4		2.9
^{13}**C**	59.4	173.8	76.1	28	37.4	31.7	20.3	13.7	130.7	124	40

[a] Sistema AB

Polymer Backbone

p1/ p1'	p2/p2'
1.5	1.1
15.5	15.5

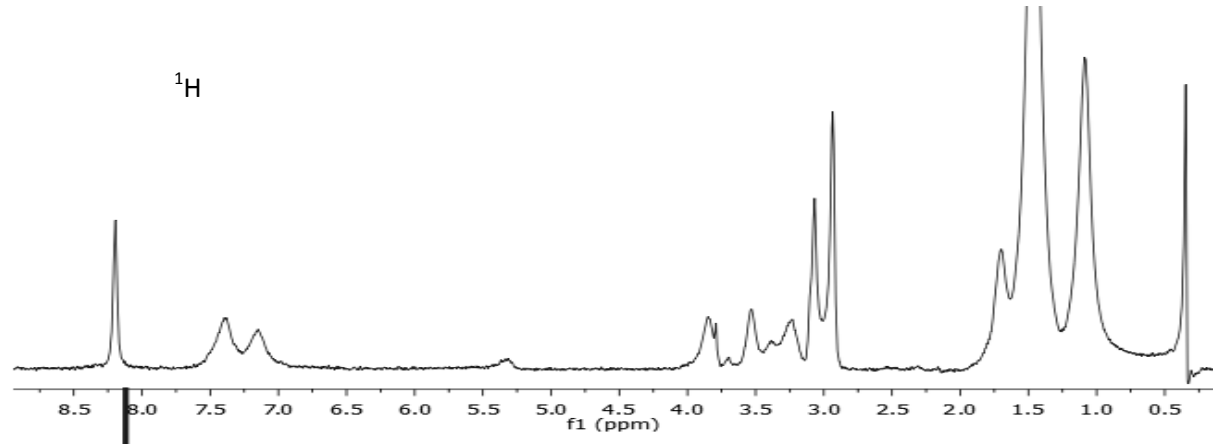

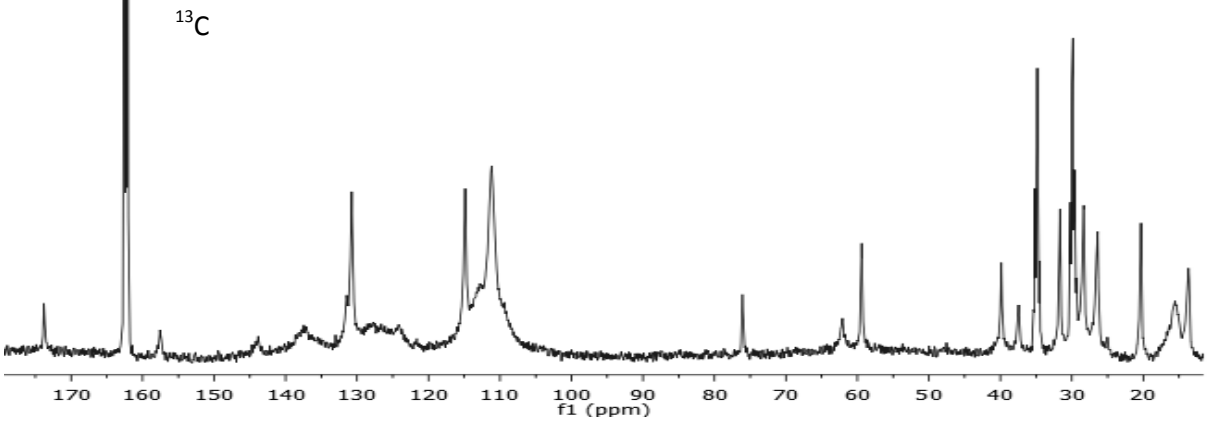

Stereoselective Diels-Alder cycloadditions

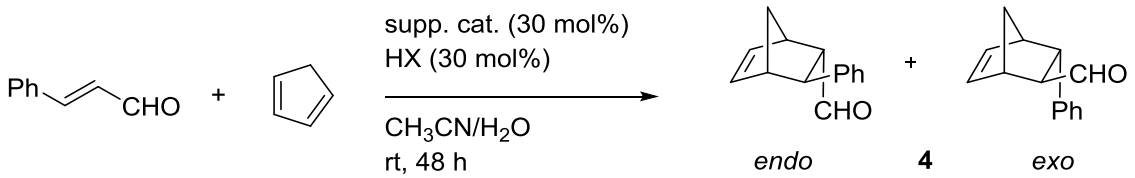

General procedure for batch reaction

The supported catalyst (0.1 mmol) was placed into a vial and suspended in acetonitrile/water 95:5 mixture (2 mL). HX (TFA or HBF_4, 0.1 mmol) was added and the mixture was stirred for 5 minutes at rt. Then *trans*-cinnamaldehyde (0.3 mmol) and freshly distilled cyclopentadiene (1.5 mmol) were added and the mixture was stirred at rt for 48 hours. After reaction time the solid was filtered, washed with ethyl acetate (3 mL) and concentrated *in vacuo*. The residue was purified by column chromatography on silica gel. The enantiomeric excess of the product was determined by HPLC on chiral stationary phase after conversion to the corresponding alcohol (reduction with $NaBH_4$, 3 equiv., in MeOH 0.1 M for 30 min at rt).

General procedure for continuous flow reaction

Preparation of packed-bed reactors

A stainless steel HPLC column (*i.d.* = 0.4 cm, *l* = 12.5 cm) was filled with silica-supported catalysts (**S1**-**S5**) or polymer-supported catalyst **P1** (approx. 1.0 g) and it was sealed at both ends with metal frits. The reactor was washed with 5 mL of HX (TFA or HBF_4) solution (0.2 M in CH_3CN/H_2O 95:5 mixture) using a syringe pump (flow rate = 0.3 mL/h). Afterwards the reactor was washed with 2 mL of CH_3CN/H_2O 95:5 mixture to remove acid excess (flow rate = 0.3 mL/h).

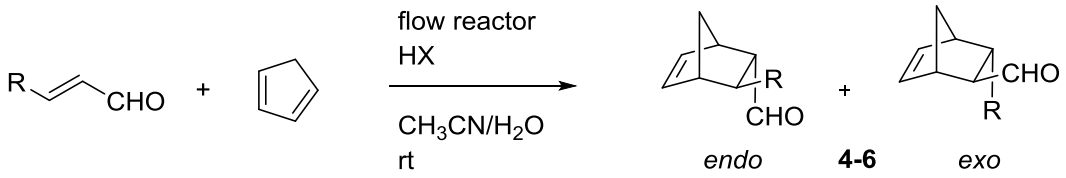

A mixture of *trans*-cinnamaldehyde (0.2 M in CH_3CN/H_2O 95:5 mixture) and freshly distilled cyclopentadiene (1.0 M in CH_3CN/H_2O 95:5 mixture) was prepared and it was pumped into the reactor (packed-bed or monolithic) with a syringe pump at the indicated flow rate at rt. The outcome of the reactor was collected at predefined intervals of time. The crude was concentrated *in vacuo* and the residue was purified by column chromatography. The enantiomeric excess of the product was determined by HPLC on chiral stationary phase after conversion to the corresponding alcohol (reduction with $NaBH_4$, 3 equiv., in MeOH 0.1 M for 30 min at rt).

3-phenylbicyclo[2.2.1]hept-5-ene-2-carbaldehyde 4

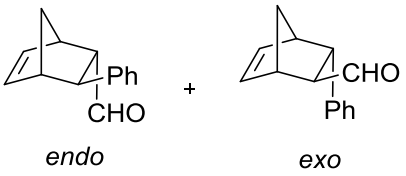

endo *exo*

Prepared according to the general procedure. The crude mixture was purified by column chromatography on silica gel eluting with hexane/ethyl acetate 9:1 to afford the title product as colorless oil. All analytical data are in agreement with literature.[i]

^{1}H-NMR (300 MHz, $CDCl_3$) *endo* δ_H 9.61 (d, 1H), 7.14-7.34 (m, 5H), 6.43 (dd, 1H), 6.18 (dd, 1H), 3.34 (m, 1H), 3.14 (bs, 1H), 3.10 (d, 1H), 2.99 (dd, 1H), 1.82 (d, 1H), 1.61-1.64 (m, 1H) ppm; **^{13}C-NMR** (75 MHz, $CDCl_3$) *endo* δ_C 203.5, 143.5, 139.2, 133.7,128.5, 127.3, 126.3, 60.8, 48.3, 47.1, 45.6, 45.1 ppm;

^{1}H-NMR (300 MHz, $CDCl_3$) *exo* δ_H 9.93 (d, 1H), 7.14-7.34 (m, 5H), 6.34 (dd, 1H), 6.08 (dd, 1H), 3.73 (m, 1H), 3.23 (m, 2H), 2.60 (d, 1H), 1.61-1.64 (dd, 2H) ppm; **^{13}C-NMR** (75 MHz, $CDCl_3$) *exo* δ_C 202.7, 142.5, 136.5, 136.2, 128.1, 127.8, 126.1, 59.4, 48.4, 47.5, 45.4, 45.3 ppm.

The enantiomeric excess was determined after reduction to the corresponding alcohol by HPLC on chiral stationary phase with Daicel Chiralcel OJ-H column: eluent hexane/*i*PrOH = 7/3, flow rate 0.8 mL/min, λ=210 nm, $\tau_{minor,endo}$ = 11.4 min, $\tau_{major,endo}$ = 23.4 min, $\tau_{minor,exo}$ = 30.7 min, $\tau_{major,exo}$ = 40.8 min.

3-(2-nitrophenyl)bicyclo[2.2.1]hept-5-ene-2-carbaldehyde 5

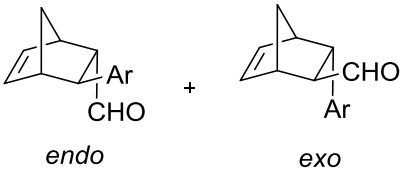

endo *exo*

Ar = *o*-NO_2-Ph

Prepared according to the general procedure. The crude mixture was purified by column chromatography on silica gel eluting with pentane/diethyl ether 9:1 to afford the title product as a yellowish oil. All analytical data are in agreement with literature.[i]

^{1}H-NMR (300 MHz, $CDCl_3$) *endo* δ_H 9.78 (d, 1H), 7.69 (d, 1H), 7.50-7.57 (m, 1H), 7.24-7.43 (m, 1H), 7.14-7.16 (d, 1H), 6.44-6.48 (dd, 1H), 5.99 (dd, 1H), 4.06 (m, 1H), 3.54 (m, 1H), 3.26 (d, 1H), 2.59 (m, 1H), 1.63-1.65 (d, 1H), 1.55 (m, 1H) ppm;

^{1}H-NMR (300 MHz, $CDCl_3$) *exo* δ_H 9.37 (d, 1H), 7.79 (d, 1H), 7.50-7.57 (m, 1H), 7.24-7.43 (m, 2H), 6.44-6.48 (m, 1H), 6.19 (dd, 1H), 3.41 (d, 1H), 3.30 (m, 1H), 3.10 (d, 1H), 2.93 (m, 1H), 1.81 (m, 1H), 1.63 (m, 1H) ppm;

The enantiomeric excess was determined after reduction to the corresponding alcohol by HPLC on chiral stationary phase with Daicel Chiralcel AD column: eluent hexane/*i*PrOH = 95/5, flow rate 0.8 mL/min, λ=254 nm, $\tau_{minor,endo}$ = 14.9 min, $\tau_{major,endo}$ = 17.6 min, $\tau_{minor,exo}$ = 18.9 min, $\tau_{major,exo}$ = 22.1 min.

3-methylbicyclo[2.2.1]hept-5-ene-2-carbaldehyde 6

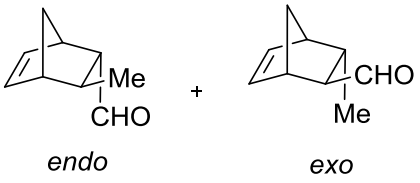

endo *exo*

Prepared according to the general procedure. The crude mixture was purified by column chromatography on silica gel eluting with pentane/diethyl ether 9:1 to afford the title product as a colorless oil. All analytical data are in agreement with literature.[i]

^{1}H-NMR (300 MHz, $CDCl_3$) *endo* δ_H 9.37 (d, 1H), 6.29 (dd, 1H), 6.05 (dd, 1H), 3.13 (bs, 1H), 2.56 (bs, 1H), 2.33 (dd, 1H), 1.82 (m, 1H), 1.57 (m, 1H), 1.48 (m, 1H), 1.17 (d, 3H) ppm;

^{1}H-NMR (300 MHz, $CDCl_3$) *exo* δ_H 9.78 (d, 1H), 6.24 (dd, 1H), 6.16 (dd, 1H), 3.01 (bs, 1H), 2.79 (bs, 1H), 2.40-2.50 (dd, 1H), 1.75-1.80 (m, 1H), 1.40-1.50 (m, 2H), 0.90 (d, 3H) ppm.

The enantiomeric excess was determined on the aldehyde by GC on chiral stationary phase with 20% permethylated β-cyclodextrine column: oven temperature = 75°C, He flow = 2 mL/min, pressure = 2 bar, $\tau_{major,exo}$ = 67.1 min, $\tau_{minor,exo}$ = 68.4 min, $\tau_{minor,endo}$ = 72.1 min, $\tau_{major,endo}$ = 78.7 min.

Stereoselective α-alkylation of aldehydes

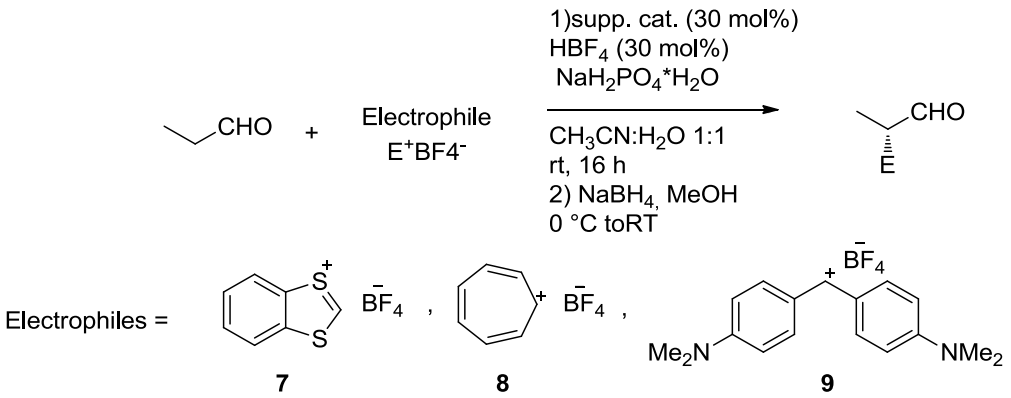

General procedure for batch reaction

The supported catalyst (0.04 mmol) was placed into a vial and suspended in CH_3CN/H_2O 1:1 mixture (2 mL). HBF_4 (0.4 mmol) was added and the mixture was stirred for 5 minutes at rt. Then electrophile (0.12 mmol), $NaH_2PO_4*H_2O$ (0.12 mmol) and freshly distilled propanal (0.36 mmol) were added and the mixture was stirred at rt for 16 hours. After reaction time the crude mixture was diluted with Et_2O (3 mL), the supported catalyst was filtered and washed with Et_2O (2 mL). The organic layer was separated and the aqueous phase was extracted twice with Et_2O (1 mL). The combined organic layers were dried with Na_2SO_4 and diluted with MeOH (3 mL). Then $NaBH_4$ (0.6 mmol) was slowly added at 0 °C and the mixture was stirred at 0 °C for 1 hour. The reaction was quenched with H_2O (3 mL) and AcOEt (5 mL) was added. The organic layer was separated and the aqueous phase was extracted twice with AcOEt (5 mL). The organic layers were recovered, washed with brine and dried with Na_2SO_4 and concentrated *in vacuo*. The residue was purified by flash column chromatography on silica gel. The enantiomeric excess of the product was determined by HPLC on chiral stationary phase.

General procedure for continuous flow reaction

Preparation of packed-bed reactors

A stainless steel HPLC column (*i.d.* = 0.4 cm, *l* = 6 cm) was filled with **S1** (0.37 g, 0.15 mmol) or **P1** (0.22 g, 0.11 mmol) and it was sealed at both ends with metal frits. The reactor was washed with 2 mL of CH_3CN/H_2O 7:3 mixture using a syringe pump (flow rate = 0.2 mL/h).

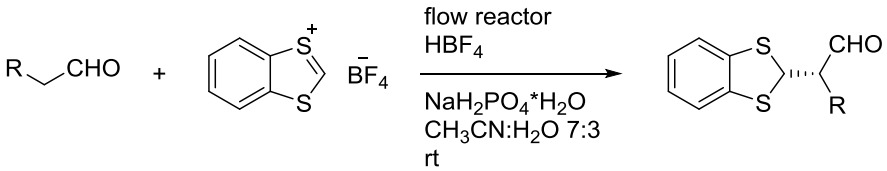

1,3-benzodithiolylium tetrafluoroborate (0.3 mmol when **S1** was used, 0.22 mmol when **P1** was used), aldehyde (3 equiv.) and $NaH_2PO_4*H_2O$ (1 equiv.) were dissolved in CH_3CN/H_2O 95:5 mixture (2 mL) and the mixture was pumped into the reactor with a syringe pump at the indicated flow rate at rt. Subsequently the flow reactor was washed with CH_3CN/H_2O 95:5 mixture (2 mL). The output of the reactor was collected at 0 °C in an ice bath and was diluted with Et_2O (3 mL), the supported catalyst was filtered and washed with Et_2O (2 mL). The organic layer was separated and the aqueous phase was extracted twice with Et_2O (1 mL). The combined organic layers were dried with Na_2SO_4 and diluted with MeOH (3 mL). Then $NaBH_4$ (0.6 mmol) was slowly added at 0 °C and the mixture was stirred at 0 °C for 1 hour. The reaction was quenched with H_2O (3 mL) and AcOEt (5 mL) was added. The organic layer was separated and the aqueous phase was extracted twice with AcOEt (5 mL). The organic layers were recovered, washed with brine and dried with Na_2SO_4 and concentrated *in vacuo*. The residue was purified by flash column chromatography on silica gel. The enantiomeric excess of the product was determined by HPLC on chiral stationary phase.

(*S*)-2-(benzo[d][1,3]dithiol-2-yl)propanal 10

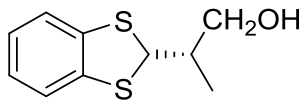

Prepared according to the general procedure. The crude mixture was purified by column chromatography on silica gel eluting with hexane/ethyl acetate 9:1 to afford the title product as a colorless oil. All analytical data are in agreement with literature.[iv]

^{1}H-NMR (300 MHz, $CDCl_3$) δ_H 7.21 (dd, 2H), 7.02 (dd, 2H), 5.13 (d, 1H), 3.70 (d, 2H), 2.17-2.09 (m, 1H), 1.06 (d, 3H) ppm; **^{13}C-NMR** (75 MHz, $CDCl_3$) δ_C 137.7 (2C), 125.4 (2C), 122.0, 121.9, 64.8, 56.5, 43.6, 13.2 ppm.

The enantiomeric excess was determined by HPLC on chiral stationary phase with Daicel Chiralcel OD-H column: eluent hexane/*i*PrOH = 9/1, flow rate 0.8 mL/min, λ=230 nm, τ_{minor} = 8.9 min, τ_{major} = 10.5 min.

[iv] A. Gualandi, E. Emer,M. G. Capdevila, P. G. Cozzi, A*ngew. Chem. Int. Ed.* **2011**, *50*, 7842.

(*R*)-2-(cyclohepta-2,4,6-trien-1-yl)propan-1-ol 11

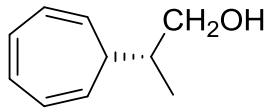

Prepared according to the general procedure. The crude mixture was purified by column chromatography on silica gel eluting with exane/ethyl acetate 8:2 to afford the title product as a colorless oil. All analytical data are in agreement with literature.[iv]

^{1}H-NMR (300 MHz, $CDCl_3$) δ_H 6.69 (m, 2H), 6.25 (m, 2H), 5.33 (m, 2H), 3.81 (dd, 2H), 3.64 (dd, 2H), 2.05 (m, 1H), 1.55 (m, 2H), 1.41 (bs, 1H), 1.11 (d, 3H) ppm; **^{13}C-NMR** (75 MHz, $CDCl_3$) δ_C 130.8 (2C), 125.0, 124.9, 124.0, 123.2, 66.5, 41.4, 37.3, 14.5 ppm.

The enantiomeric excess was determined by HPLC on chiral stationary phase with Daicel Chiralcel OJ-H column: eluent hexane/*i*PrOH = 95/5, flow rate 0.8 mL/min, λ=254 nm, τ_{minor} = 9.8 min, τ_{major} = 11.0 min.

(*R*)-3,3-bis(4-(dimethylamino)phenyl)-2-methylpropan-1-ol 12

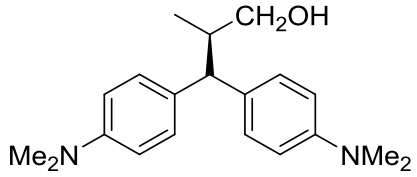

Prepared according to the general procedure. The crude mixture was purified by column chromatography on silica gel eluting with dichloromethane/methanol 98:2 to afford the title product as a colorless oil. All analytical data are in agreement with literature.[iv]

^{1}H-NMR (300 MHz, $CDCl_3$) δ_H 7.18 (m, 4H), 6.69 (m, 4H), 3.92 (d, 1H), 3.61 (dd, 1H), 3.58 (d, 1H), 3.51 (dd, 1H), 2.91 (s, 6H), 2.90 (s, 6H), 2.48 (m, 1H) 0.97 (d, 3H) ppm; **^{13}C-NMR** (75 MHz, $CDCl_3$) δ_C 149.0, 149.9 133.0 (2C), 128.6 (2C), 128.3 (2C), 113.1 (2C), 113.0 (2C), 67.2, 53.7, 40.8 (4C), 39.6, 16.4 ppm.

The enantiomeric excess was determined by HPLC on chiral stationary phase with Daicel Chiralcel OD-H column: eluent hexane/*i*PrOH = 9/1, flow rate 0.8 mL/min, λ=254 nm, τ_{major} = 18.4 min, τ_{minor} = 31.7 min.

(*S*)-2-(benzo[d][1,3]dithiol-2-yl)octan-1-ol 13

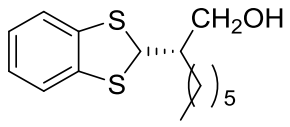

Prepared according to the general procedure. The crude mixture was purified by column chromatography on silica gel eluting with exane/ethyl acetate 9:1 to afford the title product as a colorless oil. All analytical data are in agreement with literature.[iv]

^{1}H-NMR (300 MHz, $CDCl_3$) δ_H 7.23 (dd, 2H), 7.02 (dd, 2H), 5.20 (d, 1H), 3.85 (dd, 1H), 3.79 (dd, 2H), 1.94 (m, 1H), 1.30 (m, 10H), 0.89 (t, 3H) ppm; **^{13}C-NMR** (75 MHz, $CDCl_3$) δ_C 137.7, 137.6, 125.4, 125.3, 122.0 (2C), 62.4, 56.6, 47.6, 31.6, 29.3, 28.1, 27.1, 22.5, 14.0 ppm.

The enantiomeric excess was determined by HPLC on chiral stationary phase with Daicel Chiralcel OD-H column: eluent hexane/*i*PrOH = 95/5, flow rate 0.8 mL/min, λ=230 nm, τ_{minor} = 10.7 min, τ_{major} = 15.1 min.

(*S*)-2-(benzo[d][1,3]dithiol-2-yl)-2-phenylethan-1-ol 14

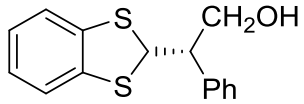

Prepared according to the general procedure. The crude mixture was purified by column chromatography on silica gel eluting with exane/ethyl acetate 9:1 to afford the title product as a colorless oil. All analytical data are in agreement with literature.[iv]

^{1}H-NMR (300 MHz, $CDCl_3$) δ_H 7.34-7.27 (m, 5H), 7.20 (m, 1H), 7.13 (m, 1H), 7.02 (m, 2H), 5.34 (d, 1H), 4.05 (m, 2H), 3.37-3.30 (m, 1H) ppm; **^{13}C-NMR** (75 MHz, $CDCl_3$) δ_C 139.1, 137.2, 128.8 (2C), 128.6, 128.4, 127.7 (2C), 125.6, 125.4, 122.3, 122.2, 64.4, 56.2, 54.9 ppm.

The enantiomeric excess was determined by HPLC on chiral stationary phase with Daicel Chiralcel OD-H column: eluent hexane/*i*PrOH = 9/1, flow rate 0.8 mL/min, λ=230 nm, τ_{minor} = 19.0 min, τ_{major} = 23.5 min.

4.1.2 Chiral Primary Amines derived from Cinchona Alkaloids

Polymer-supported cinchona primary amine

*Synthesis of compound **16***

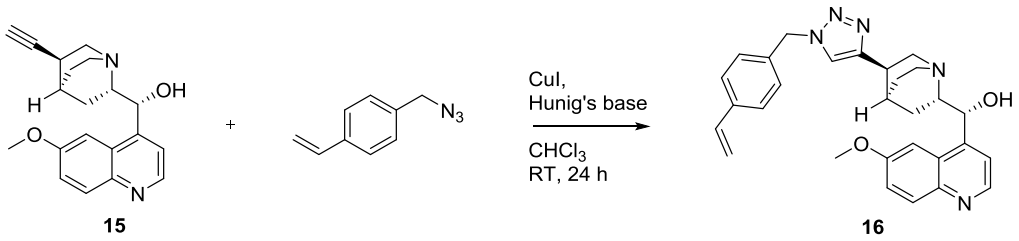

15 16

Compound **15**[v] (1.87 mmol, 0.6 g) was dissolved in dry $CHCl_3$ (15 mL) under nitrogen atmpsphere, then copper (I) iodide (0.09 mmol) and Hunig's base (9.4 mmol) were added. The solution was stirred for 15 minutes, then a solution of 4-azidomethylstyrene (2.43 mmol) in dry $CHCl_3$ (3 mL) was slowly added. The mixture was stirred for 24 hours at rt then NH_4OH (5 ml, 33 wt% solution) was added. The organic layer was washed twice NH_4OH (5 ml, 33 wt% solution), once with brine (8 mL), dried with sodium sulfate and concentrated *in vacuo* yielding to a brownish oil. The residue was purified by column chromatography on silica gel eluting with dichloromethane/methanol 9:1 to 7:3 to afford **16** as withe-off solid (1.76 mmol, 94% yield).

^{1}H-NMR (300 MHz, $CDCl_3$) δ_H 8.66 (d, J=4.3 Hz, 1H), 7.95 (d, 1H), 7.53 (d, 1H), 7.33 (d, J=7.8 Hz, 2H), 7.30 (dd, J=9.1 Hz, 1H), 7.23 (d, J=0.89 Hz, 1H), 7.11 (d, 2H), 7.09 (d, 1H), 6.70 (dd, 1H), 5.79 (d, J=17.6 Hz, 1H), 5.73 (b, 1H), 5.37 (s, 2H), 5.32 (d, J=10.9 Hz, 1H), 3.87 (s, 3H), 3.68 (m, 1H), 3.39 (m, 2H), 3.06 (m, 1H), 2.79 (m, 1H), 2.11 (bs, 1H), 1.89 (m, 1H), 1.79 (m, 1H), 1.66 (m, 1H), 1.39 (m, 1H) ppm; **^{13}C-NMR** (75 MHz, $CDCl_3$) δ_C 157.9, 150.4, 147.4, 146.7, 144.2, 138.1, 135.9, 133.9, 131.5, 128.2, 126.8, 126.5, 121.7, 120.3, 118.5, 114.9, 101.2, 70.8, 59.71, 55.9, 53.8, 43.4, 32.9, 27.8, 26.8, 21.5 ppm; **HRMS** (ESI+) m/z calculated for $C_{29}H_{32}N_5O_2$(+1): 482.2551; found 482.2549; **$[\alpha_D]^{23}$** = -92 (c: 0.30 $CHCl_3$).

[v] K.M. Kacprzak, W. Lindner, N.M. Maier, *Chirality* **2008**, *20*, 441.

*Synthesis of monomer **17***

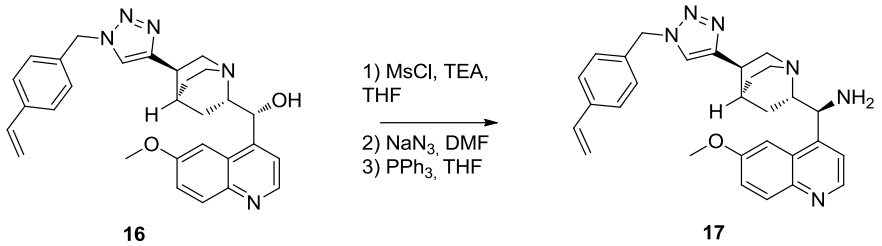

16 **17**

Compound **16** (1.76 mmol) was dissolved in dry THF (17mL) under nitrogen atmosphere, then dry triethylamine (8.8 mmol) was added. The solution was cooled to 0 °C with an ice-water bath and after 10 minutes of stirring, methanesulfonyl chloride (5.3 mmol) was added drop wise. After 5 minutes the mixture was warmed to room temperature and it was stirred for 5 hours. The reaction was monitored by TLC (R_f = 0.56, CH_2Cl_2/MeOH = 9/1). After reaction time $NaHCO_3$ (5 ml, s.s.) was added. The organic layer was separated, and then the aqueous phase was extracted three times with dichloromethane (12 mL). The combined organic layers were dried with anhydrous Na_2SO_4, concentrated *in vacuo* and used without further purification. The pale yellow solid obtained was dissolved in DMF (15 mL) and then NaN_3 (2.8 mmol) was added. The mixture was stirred at 70 °C for 18 hours; the reaction was monitored by TLC (R_f = 0.48, CH_2Cl_2/MeOH = 9/1). After reaction time the solvent was removed under vacuum. The crude product was dissolved in dichloromethane (15 ml) and water was added (8 ml). The organic layer was separated and the aqueous phase was extracted twice with dichloromethane (8ml). The combined organic layers were dried with anhydrous Na_2SO_4 and concentrated *in vacuo* affording a brownish solid that was used without further purification. It was dissolved in dry THF (12 ml) under nitrogen atmosphere and heated to 50 °C. A solution of triphenylphosphine (2.1 mmol) in dry THF (3 ml) was slowly added and the mixture was stirred at 50 °C for 4 hours. After reaction time the mixture was cooled to room temperature and distilled water (1 ml) was added. After 15 hours of stirring, the solvent was removed *in vacuo*, the crude product was diluted in dichloromethane (12 ml) and HCl (3 mL, 10 % wt solution) was added up to pH 2. The organic layer was washed twice with dichloromethane (8 ml) then NH_4OH (3 ml, 33 %wt solution) was added up to pH 8. The organic phase was extracetd three times with dichloromethane (15 ml), then the combined organic layers were washed with brine, dried with anhydrous Na_2SO_4 and concentrated *in vacuo* affording a yellowish solid. The residue was purified by column chromatography on silica gel eluting with CH_2Cl_2/MeOH/NH_4OH 98:2:1 to 95:5.1 yielding to **17** as a white-off solid (1.12 mmol, 64% yield).

^{1}H-NMR (300 MHz, $CDCl_3$): δ_H 8.71 (d, J=4.6 Hz, 1H), 8.02 (d, 1H), 7.64 (b, 1H), 7.41 (d, 1H), 7.40 (d, 2H), 7.38 (d, J=9.2 Hz, 1H), 7.18 (d, J=8.6 Hz, 2H), 7.17 (s, 1H), 6.72 (dd, 1H), 5.82 (d, J=17.6 Hz, 1H), 5.46 (s, 2H), 5.33 (d, J=11.4 Hz, 1H), 4.62 (bs, 1H), 3.99 (s, 3H), 3.54 (dd, 1H), 3.49 (dd, 1H), 3.32 (m, 1H), 3.30 (m, 1H), 3.08 (m, 1H), 2.93 (m, 1H), 1.92 (bs, 1H), 1.67 (m, 2H), 1.32 (m, 1H), 0.76 (m, 1H) ppm; **^{13}C-NMR** (75 MHz, $CDCl_3$): δ_C 157.7, 151.3, 147.9, 146.8, 144.7, 138.1, 135.9, 134.1, 131.8, 128.8, 128.2, 126.8, 121.2, 120.2, 119.9, 115.0, 102.0, 61.6, 55.8, 55.6, 53.8, 41.1, 33.2, 27.9, 27.7, 26.0 ppm; **HRMS** (ESI+) m/z calculated for $C_{29}H_{33}N_6O_1$(+1): 481.2710; found 481.2715; **$[\alpha_D]^{23}$** = +129 (c: 0.22 $CHCl_3$).

*Synthesis of catalysts **P2-P4***

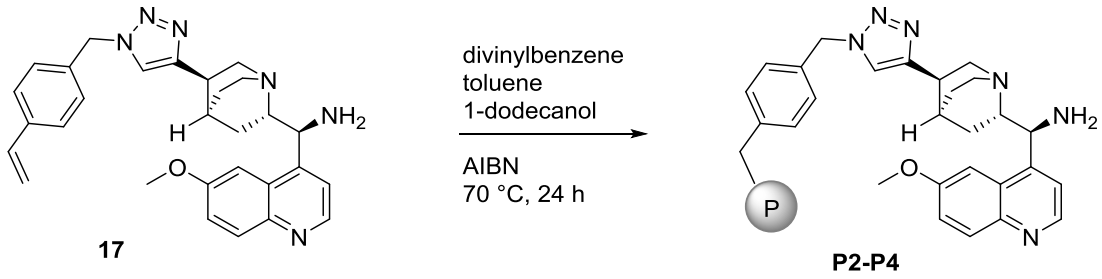

17 **P2-P4**

A mixture of monomer **17**, AIBN, divinylbenzene, toluene and 1-dodecanol was prepared under nitrogen atmosphere (see below for the composition of polymerization mixtures). The mixture was transferred into a sealed vial and heated into an oil bath at 70 °C for 24 hours. After reaction time the polymer was removed from the vessel and crushed into a mortar. The fine powder obtained was suspended in methanol (10 mL) and stirred for 10 minutes at rt. The solid was then isolated by filtration and washed methanol (10 mL) and dichloromethane (10 mL). The solid was recovered and dried under high vacuum at 40 °C for 3 hours.
Catalysts loadings (mmol/g) were determined by the stoichiometry of reagents in the polymerization mixture. The polymerization occurred with a full conversion as any trace of **17** was recovered from the organic layer used to wash the solid (toluene and 1-dodecanol were fully recovered).

P2: loading = 0.5 mmol/g.
Prepared using monomer **17** (0.4 mmol, 11 wt%), divinylbenzene (4.47 mmol, 32 wt%), toluene (2.77 mmol, 14 wt%), 1-dodecanol (4.16 mmol, 42 wt%) and AIBN (0.11 mmol, 1 wt%);

P3: loading = 0.3 mmol/g.
Prepared using monomer **17** (0.08 mmol, 6 wt%), styrene (0.56 mmol, 9 wt%, as co-monomer), divinylbenzene (1.35 mmol, 27 wt%), toluene (2.23 mmol, 32 wt%), 1-dodecanol (0.88 mmol, 25 wt%) and AIBN (0.04 mmol, 1 wt%);

P4: loading = 0.7 mmol/g.
Prepared using monomer **17** (0.68 mmol, 11 wt%), divinylbenzene (5.00 mmol, 22 wt%), toluene (10.28 mmol, 32 wt%), 1-dodecanol (5.38 mmol, 34 wt%) and AIBN (0.17 mmol, 1 wt%);

*Synthesis of catalysts **P5***

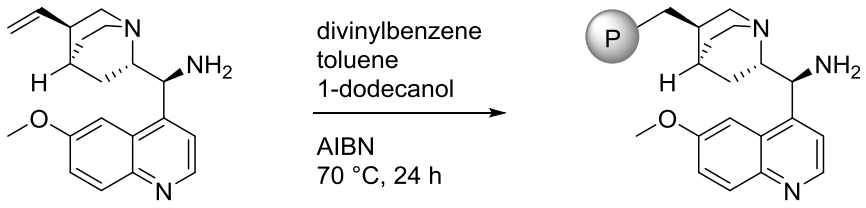

18 **P5**

Catalyst **P4** was prepared starting from **18** according to the procedure described above for the synthesis of catalysts **P2-P4**.

P5: loading = 0.8 mmol/g.
Prepared using monomer 9-amino-*epi*-quinine[vi] **18** (0.78 mmol, 11 wt%), divinylbenzene (3.88 mmol, 22 wt%), toluene (7.97 mmol, 32 wt%), 1-dodecanol (4.19 mmol, 34 wt%) and AIBN (0.14 mmol, 1 wt%);
0.26 mmol of monomer **18** recovered from the organic phase.

[vi] H. Brunner, J. Bugler, B. Nuber, *Tetrahedron: Asymmetry* **1995**, *6*, 1699.

Characterization

P4 was studied by ^{13}C- CP and DP MAS NMR. As a consequence of the high cross-linking degree, both techniques gave spectra with broad signals, as expected on the basis of literature[16] data showing that in the polymer the line-width is proportional to the degree of cross-linking. Moreover, the presence of several aromatic rings could give rise to a tight packing of the polymer chains, favoured by Ar-Ar interactions, leading to a very rigid system with difficult relaxation modes.[17] The ^{13}C- DPMAS NMR experiments afforded spectra resolved enough, with sharper signals, but unfortunately it was impossible to eliminate the side bands, working both on rotation rate and temperature.[18] On the contrary, the ^{13}C- CPMAS NMR spectra showed broader signals but no side bands; nevertheless, by comparing the results arising from both techniques and by comparison with the solution spectra of the monomer, it was possible to elucidate the structure and confirm the incorporation of the quinine moiety into the poly(styrene) backbone.

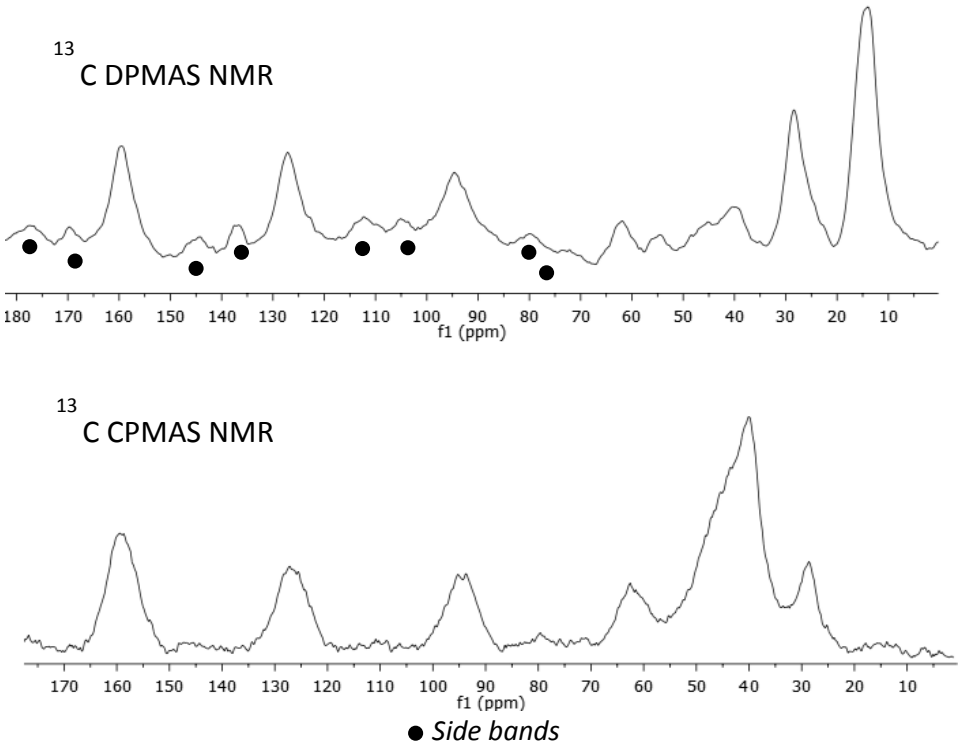

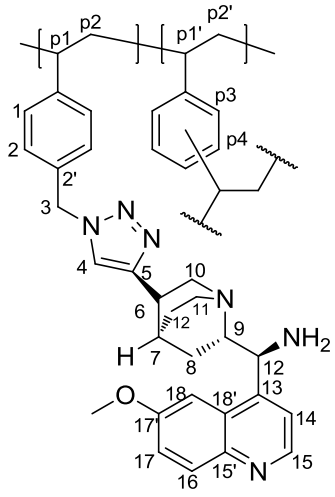

P4

^{13}C CPMAS

14-15 ppm:	**p1/p1'**
28-29 ppm :	C-8, C-7, C-12
40-45 ppm:	**weak signal**
58-60 ppm:	**weak signal**
95-100 ppm:	C-18, C-17
120-127 ppm:	C-14, C-16, C-4 , p2/p2'(?)
155-159 ppm:	C-5, C-15, C-15', C-17'

^{13}C DPMAS

14-15 ppm:	not present
28-29 ppm :	C-8, C-7, C-12
40-45 ppm:	C-3, C-6, C-11, OMe
58-60 ppm:	C-9, C-10, C-12
95-100 ppm:	C-18, C-17
120-127 ppm:	C-14, C-16, C-4 , p2/p2'(?)
155-159 ppm:	C-5, C-15, C-15', C-17'

PEG-supported cinchona primary amine

*Synthesis of catalyst **G1***

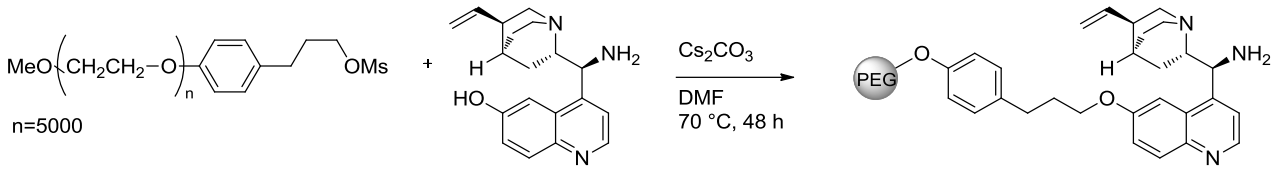

Compound **19**[vii] (1 mmol, 5.0 g) was dried under high vacuum at 80° C for 1 hour and then it was dissolved in dry DMF (10 mL). After that a solution of **20**[viii] (4 mmol) and Cs_2CO_3 (8 mmol) in dry DMF (30 mL) was added. After 48 hours stirring at 70° C, the mixture was cooled at room temperature, the solvent was evaporated under vacuum, the residue was dissolved in CH_2Cl_2 (10 mL) and the solution was filtered on a short pad of celite. The mixture was concentrated *in vacuo* and the resulting oil was poured dropwise in cold Et_2O (250 mL). The precipitated was filtered, washed with Et_2O (5 mL), and dried under vacuum to give **G1** as brownish solid (0.95 mmol, 95% yield). Excess of **20** was recovered from the ether solution after treatment with trifluoroacetic acid (4 mmol). The organic layer was concentrated *in vacuo* and the residue was purified by flash column chromatography on silica-gel eluting with AcOEt/MeOH 1:1 with 1% Et_3N.

^{1}H-NMR (300 MHz, $CDCl_3$) δ_H 8.74 (d, J=4.5 Hz, 1H), 8.02 (d, J=9.2 Hz, 1H), 7.63 (bs, 1H), 7.45 (d, 1H), 7.39 (dd, 1H), 7.13 (d, J=8 Hz, 2H), 6.85 (d, 2H), 5.80 (ddd, J=7.4 Hz, 1H), 5.00 (d, 1H), 4.96 (d, 1H), 4.56 (d, J=10.7 Hz, 1H), 4.15 (2H), 3.6 (dd, 2H), 3.38 (s, 3H), 3.32 (m, 1H), 2.75 (m, 2H), 2.3 (bs, 2H), 2.16 (m, 2H), 1.61 (m, 1H), 1.5 (m, 2H), 1.48 (1H), 1.4 (m, 2H), 0.75 (dd, J=7.8 Hz, 1H) ppm; **^{13}C-NMR** (75 MHz, $CDCl_3$) δ_C 157, 156.5, 147.5, 147, 145.1, 142.2, 133.4, 132.0, 129.8, 128.5, 121.8, 119.3, 114.4, 114.6, 102.6, 66.3, 59.3, 56.2, 50.4, 41.6, 39.3, 31.2, 31.3, 28.8, 27.2, 26.7 ppm.

[vii] M. Benaglia, G. Celentano, M. Cinquini, A. Puglisi, F. Cozzi, *Adv. Synth. Catal.* **2002**, *344*, 149

[viii] W. Chen, W. Du, Y.Z. Duan, Y. Wu, S.Y. Yang, Y.C. Chen, *Angew. Chem. Int. Ed.* **2007**, *46*, 7667.

Silica-supported cinchona primary amine

*Synthesis of compound **21***

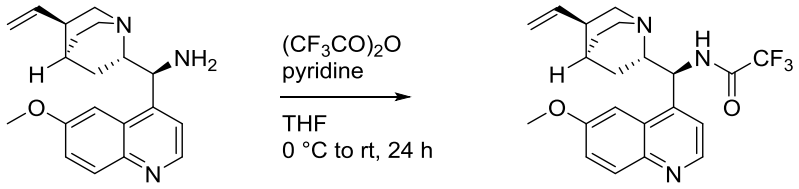

18 **21**

9-amino-*epi*-quinine **18** (0.45 g, 1.39 mmol) was dissolved in dry THF (11 mL) under nitrogen atmosphere then pyridine (2.78 mmol) was added. The solution was cooled to 0 °C with an ice-water bath and after 10 minutes of stirring, freshly distilled trifluoroacetic anhydride (1.39 mmol) was added drop wise. After 10 minutes the mixture was warmed to room temperature and it was stirred for 24 hours. After reaction time $NaHCO_3$ (3 mL, s.s.) and CH_2Cl_2 (15 mL) were added. The organic layer was separated, and then the aqueous phase was extracted twice with CH_2Cl_2 (9 mL). The combined organic layers were dried with anhydrous Na_2SO_4 and concentrated *in vacuo* and the residue was purified by flash column chromatography on silica gel eluting with CH_2Cl_2/ MeOH 98:2 to 95:5 affording **21** as a white-off solid (1.04 mmol, 75% yield).

^{1}H-NMR (300 MHz, $CDCl_3$) δ_H 8.77 (d, J=4.5 Hz 1H), 8.07 (d, J=9.2 Hz 1H), 7.5 (d, J=2.6 Hz, 1H), 7.43 (dd, 1H), 7.35 (d, 1H), 5.72 (ddd, J=17.14 Hz, J=10.3 Hz, J=7.3 Hz 1H), 5.24 (b, 1H), 5.02 (dt, J=1.4 Hz, 1H), 4.98 (ddd, 1H), 3.95 (s, 3H), 3.18 (m, 1H), 3.05 (m, 1H), 2.82 (m, 1H), 2.78 (dd, J=5 Hz, J=2.4 Hz 1H), 2.36 (m, 1H), 1.74 (m, 1H), 1.66 (m, 2H), 1.52 (m, 1H), 1.02 (dd, J= 13.7 Hz, J=6.8 Hz, 1H) ppm; **^{13}C-NMR** (75 MHz, $CDCl_3$) δ_C 158.1, 157 (q), 147.5, 144.9, 142.4, 140.8, 132.1, 127.8, 121.9, 121.7-110.0 (q), 117.6, 115.0, 101.3, 59.5, 55.8, 55.6, 40.8, 39.3, 27.7, 27.2, 26.1 ppm; **^{19}F-NMR** (281 MHz, $CDCl_3$) δ -76.09 ppm.

*Synthesis of compound **22***

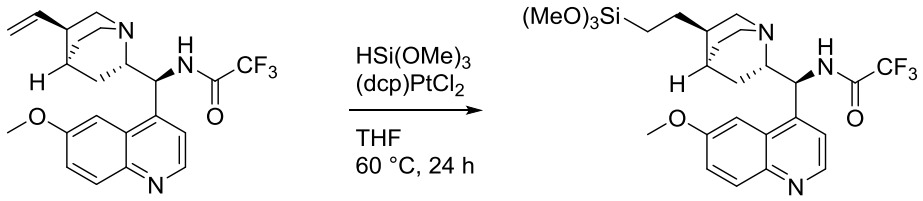

21 **22**

Compound **21** (0.54 g, 1.3 mmol) and (dcp)$PtCl_2$ (0.06 mmol) were dissolved in dry THF (13 mL) under nitrogen atmosphere and trimethoxy silane (3.89 mmol) was slowly added. The mixture was stirred at 60 °C for 24 hours. After reaction time the solvent was evaporated *in vacuo* and compound **22** was obtained as brownish oil (1.3 mmol, 99% yield). It was used in the following step without any further purification.

^{1}H-NMR (300 MHz, $CDCl_3$) δ_H 8.71 (d, 1H), 7.99 (d, 1H), 7.65 (bs, 1H), 7.42 8d, 1H), 7.34-7.38 (dd, 1H), 5.21 (bs, 1H), 3.96 (s, 3H), 3.61 (s, 3H), 3.52 (s, 6H), 3.26-3.34 (m, 2H), 3.06 (bs, 1H), 2.80 (bs, 1H), 2.48 (bs, 1H), 1.86 (m, 2H), 1.59-1.72 (m, 3H), 1.35 (m, 2H), 0.98 (bs, 1H), 0.52 (m, 2H) ppm; **^{13}C-NMR** (75 MHz, $CDCl_3$) δ_C 158.1, 157.7-156.2 (q), 147.3, 144.7, 142.6, 131.7, 127.9, 122.0, 119.8, 121.5-109.9 (q), 101.3, 67.8, 59.1, 57.4, 55.4, 51.1, 50.4, 40.9, 37.9, 28.11, 27.0, 25.7, 24.9, 24.8, 6.8 ppm; **^{19}F-NMR** (281 MHz, $CDCl_3$) δ_F -76.0.

*Synthesis of compound **S6***

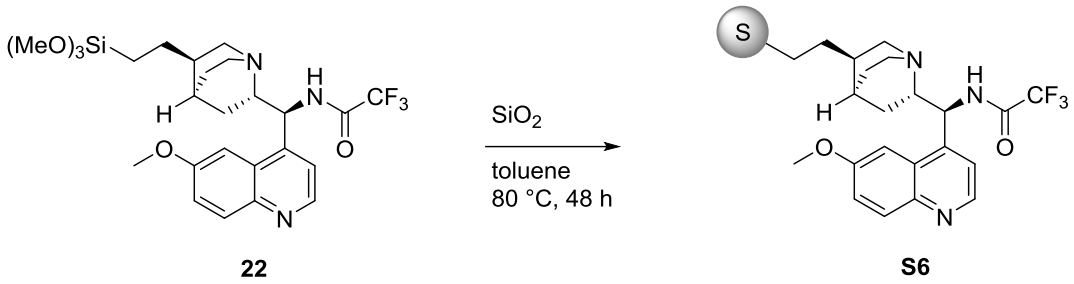

Compound **22** (0.70 g, 1.3 mmol) was dissolved in dry toluene (13 mL) under nitrogen atmosphere then Apex Prepsil Silica Media 8 µm (1.00 g) was added. The mixture was stirred at 80 °C for 48 hours then it was filtered, the solid was washed with dichloromethane (10 mL) and methanol (10 mL), and it was recovered and dried under high vacuum for 3 hours. The organic phase was concentrated under vacuum and unreacted compound **22** was recovered. **S6** was obtained as a yellowish solid; the loading was determined by weight difference (1.26 g, 0.5 mmol/g).

*Synthesis of catalyst **S7***

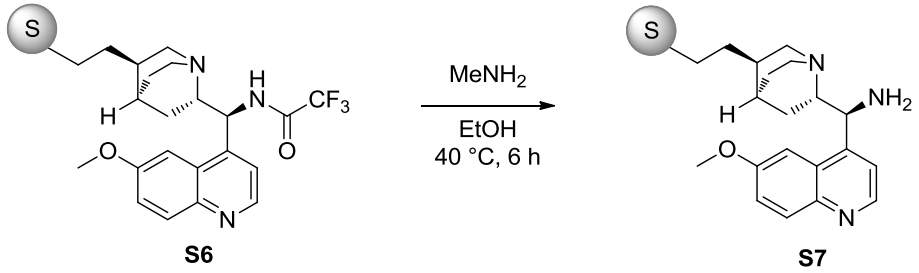

S6 (300 mg) was suspended in EtOH (3 mL) under nitrogen atmosphere and then methylamine was added (3 mL, 33% wt EtOH solution). The mixture was stirred at 40 °C for 6 hours then the solid was filtered, washed with methanol (10 mL) and dichloromethane (10 mL) and dried under high vacuum for 3 hours; catalyst **S7** was obtained as a yellowish solid (280 mg, 0.5 mmol/g).

*Synthesis of compound **S8***

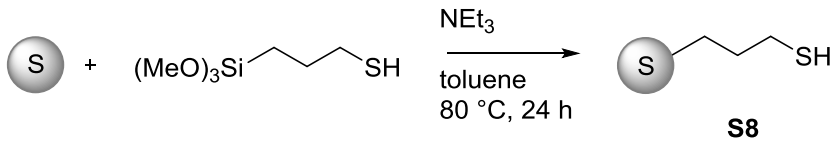

S8

Apex Prepsil Silica Media 8 µm silica (1.9 g) was dried under high vacuum at 100 °C for 1 hour. Dry toluene (19 mL) and dry triethylamine (0.57 mmol) were then added under hydrogen atmosphere. After 5 minutes mercaptopropyltrimethoxysilane (MPTMS) (5.7 mmol) was added dropwise. The mixture was stirred at 80 °C for 24 hours. After reaction time the solid was filtered and washed with methanol (10 mL) and dichloromethane (10 mL) and then dried under high vacuum for 3 hours. The organic layer was concentrated *in vacuo* and unreacted MPTMS was recovered (3.8 mmol). **S8** was obtained as a white solid (1.85 g, 1.0 mmol/g); the loading was determined by the amount of MPTMS recovered after the reaction.

*Synthesis of catalyst **S9***

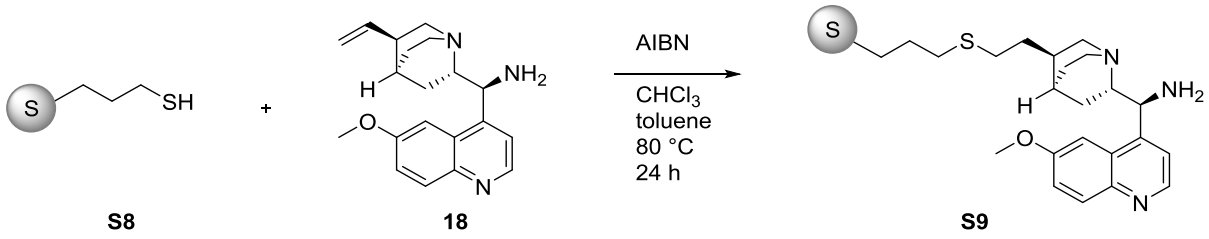

S8 **18** **S9**

S8 (620 mg) was suspended in dry toluene (10 mL) under nitrogen atmosphere and then a solution of **18** (0.56 mmol, g) and AIBN (0.56 mmol) in dry chloroform (3 mL) was slowly added. The mixture was stirred at 80 °C for 24 hours under nitrogen atmosphere. After reaction time the solid was filtered and washed with CH_2Cl_2 (10 mL) and methanol (10 mL) and then dried under high vacuum for 3 hours. The organic layer was concentrated *in vacuo* and unreacted compound **5** was recovered (0.26 mmol).

Catalyst **S9** was obtained as a yellowish solid (600 mg, 0.5 mmol/g); the loading was determined by the amount of unreacted compound **18** recovered from the organic layer.

Characterization

*Catalyst **S7***

Solid state ^{13}C and ^{29}Si DP MAS NMR spectra were used for structural elucidation of amide **10**. Then, the same technique allowed us to monitor hydrolysis of amide **S6** to catalyst **S7**. ^{13}C CPMAS NMR experiments confirmed that the trifluoroacetyl moiety was lost upon hydrolysis of the material. The ^{13}C spectra of amide **S6** (a) and the corresponding amine **S7** (b) are reported in Figure 1; the comparison of two spectra revealed the disappearance of the **C**F_3 quartet at 114, 116, 118, 120 ppm in the amine, and the decreased intensity, nearly to a half, of the signal at 160 ppm (ascribed to the aromatic carbon **C**-OCH_3 and the **C**=O amidic carbon).

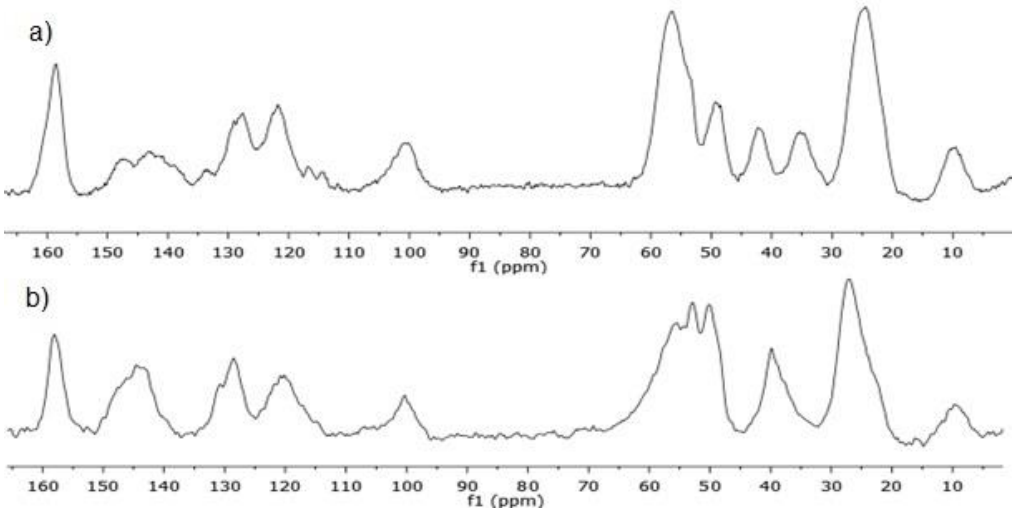

Figure 1. ^{13}C DPMAS NMR of compound **S6** (a) and **S7** (b).

^{29}Si DPMAS NMR spectra, reported in Figure 2, showed significant changes passing from amide **S6** to amine **S7**. After deconvolution of the silicon signals it was possible to calculate the values of Q_n (silicon atoms which do not bear organic functionality), T_n (silicon atoms carrying organic residues), SC (surface coverage, determined as $(T_1+T_2+T_3)/ (Q_2+Q_3+T_1+T_2+T_3)$ and MC (molecular concentration, mmol/g).[19] In particular, the silicon signals of T_1 species decreased significantly passing from 14.7% to 2.6%. Moreover, the surface coverage SC and the loading of the molecule decreased from 46.4% to 34.4% and from 2.14 to 1.88 mmol/g respectively (Table 1). These results revealed that an evident partial loss of the organic moiety from the material is occurring upon hydrolysis. This may account for the results in the catalytic tests (see below).

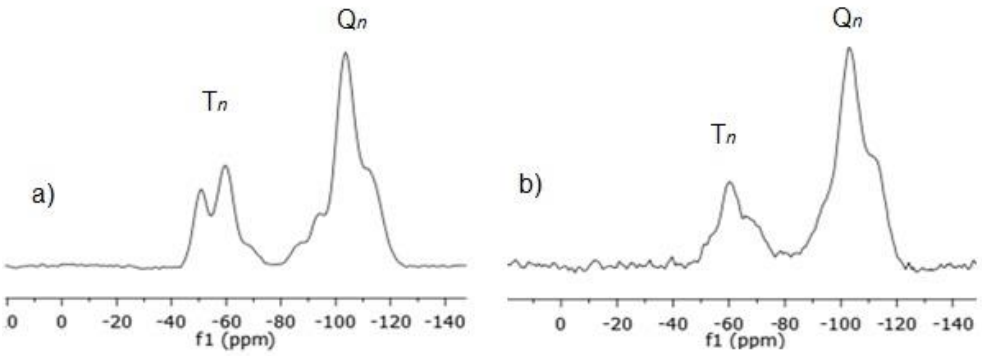

Figure 2. ^{29}Si DPMAS NMR of compound **S6**(a) and **S7** (b).

Table 49. T_n, Q_n, SC and MC values of compounds **S6**, **S7** and **S9** obtained by ^{29}Si DPMAS NMR after spectra deconvolution.

Cat	T_1 % -53 ppm	T_2 % -60 ppm	T_3 % -68 ppm	Q_2 % -96 ppm	Q_3 % -103 ppm	Q_4 % -113 ppm	SC %	MC (mmol/g)
S6	14.7	19.7	3.6	9.1	34.8	18.1	46.4	2.14
S7	2.6	18.7	7.3	4.4	50.2	16.8	34.4	1.88
S9	5.5	25.1	9.6	4.6	34.7	20.5	50.6	1.87

*Catalyst **S9***

Solid state ^{13}C and ^{29}Si MAS NMR allowed us to confirm the structure of the catalyst **S9**. This showed a ^{13}C spectrum very similar to that of **S7**; also in this case it was possible to confirm the incorporation of the quinine moiety into the silica network by comparison of **S9** ^{13}C spectrum with the solution spectrum of compound **18**. Moreover the linking of the quinuclidine ring with the $SiOCH_2CH_2SCH_2CH_2$ group was revealed by the ^{13}C resonances at 50.2, 26.6 and 11.2 ppm ascribed to the methylene carbons of this chain.

The ^{29}Si DPMAS NMR spectrum displayed, after deconvolution, a 3:2 ratio between Q_n and T_n species with the percentage for each specie reported in Table 1. With respect to **S7**, we have a greater surface coverage SC (50.6 % *vs* 34.4%) and a very similar molar concentration MC (1.87 mmol/g).

Stereoselective Michael additions

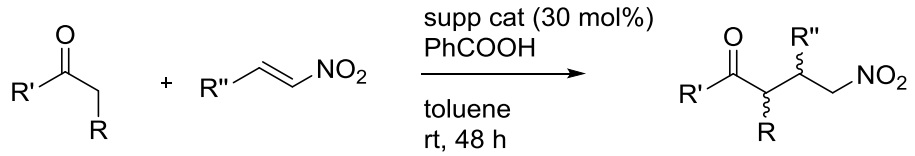

General procedure for batch reaction

The supported catalyst (0.04 mmol), nitroalkene (0.12 mmol) and benzoic acid (0.04 mmol) were placed into a vial and carbonyl compound (0.6 mmol) and dry toluene (1 mL) was added under nitrogen atmosphere. The vial was sealed and the mixture was stirred at rt for 48 hours. After reaction time the solid was filtered, washed with ethyl acetate (3 mL), recovered and dried under high vacuum. The organic layer was concentrated *in vacuo* and the residue was purified by column chromatography on silica gel. The enantiomeric excess of the product was determined by HPLC on chiral stationary phase.

General procedure for continuous flow reaction

Preparation of packed-bed reactor

A stainless steel HPLC column (*i.d.* = 0.4 cm, *l* = 6 cm) was filled with **P2** (0.31 g, 0.22 mmol) and it was sealed at both ends with metal frits. The reactor was washed with PhCOOH solution (0.3 M in toluene, 2 mL) using a syringe pump (flow rate = 0.5 mL/h). Afterwards the reactor was washed with toluene (2 mL) to remove acid excess (flow rate = 0.5 mL/h).

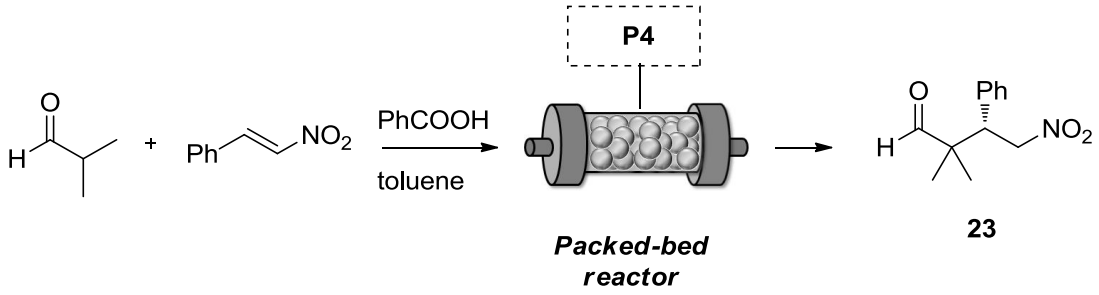

A mixture of *trans*-β-nitrostyrene (0.4 M in toluene) and freshly distilled *i*-butyraldehyde (2.0 Mtoluene) was prepared and it was pumped into the packed-bed reactor with a syringe pump at the indicated flow rate at rt. The outcome of the reactor was collected at predefined intervals of time. The crude was concentrated *in vacuo* and the residue was purified by column chromatography. The enantiomeric excess of the product was determined by HPLC on chiral stationary phase

(*S*)-2,2-dimethyl-4-nitro-3-phenylbutanal 23

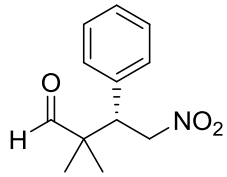

Prepared according to the general procedure. The crude mixture was purified by column chromatography on silica gel eluting with hexane/ethyl acetate 9:1 afford the title product as a colorless oil. All analytical data are in agreement with literature.[ix]

^{1}H-NMR (300 MHz, $CDCl_3$) δ_H 9.55 (s, 1H), 7.33 (m, 3H), 7.22 (d, 2H), 4.83-4.92 (dd, 1H), 4.68-4.74 (dd, 1H), 3.81 (dd, 1H), 1.15 (s, 3H), 1.03 (s, 3H) ppm; **^{13}C-NMR** (75 MHz, $CDCl_3$) δ_C 204.2, 135.1, 128.9, 128.5, 127.9, 76.1, 48.1, 21.4, 18.5 ppm.

The enantiomeric excess was determined by HPLC on chiral stationary phase with Daicel Chiralcel OD-H column: eluent hexane/*i*PrOH = 8/2, flow rate 0.8 mL/min, λ=210 nm, τ_{minor} = 16.1 min, τ_{major} = 22.1 min.

(*S*)-3-(4-chlorophenyl)-2,2-dimethyl-4-nitrobutanal 24

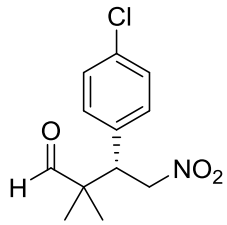

Prepared according to the general procedure. The crude mixture was purified by column chromatography on silica gel eluting with hexane/ethyl acetate 8:2 afford the title product as a colorless oil. All analytical data are in agreement with literature.[x]

^{1}H-NMR (300 MHz, $CDCl_3$) δ_H 9.52 (s, 1H), 7.32 (d, 2H), 7.15 (d, 2H), 4.80-4.88 (dd, 1H), 4.68-4.74 (dd, 1H), 3.76 (dd, 1H), 1.15 (s, 3H), 1.04 (s, 3H) ppm; **^{13}C-NMR** (75 MHz, $CDCl_3$) δ_C 203.8, 133.9, 133.8, 130.2, 128.7, 75.9, 48.0, 47.5, 21.4, 18.5 ppm.

The enantiomeric excess was determined by HPLC on chiral stationary phase with Daicel Chiralcel OD-H column: eluent hexane/*i*PrOH = 8/2, flow rate 0.8 mL/min, λ=210 nm, τ_{minor} = 16.8 min, τ_{major} = 26.1 min.

(*S*)-3-(4-trifluoromethylphenyl)-2,2-dimethyl-4-nitrobutanal 25

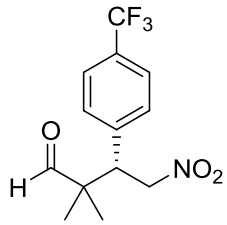

Prepared according to the general procedure. The crude mixture was purified by column chromatography on silica gel eluting with hexane/ethyl acetate 85:15 afford the title product as a colorless oil. All analytical data are in agreement with literature.[xi]

^{1}H-NMR (300 MHz, $CDCl_3$) δ_H 9.53 (s, 1H), 7.61 (d, 2H), 7.36 (d, 2H), 4.87-4.95 (dd, 1H), 4.73-4.79 (dd, 1H), 3.86 (dd, 1H), 1.17 (s, 3H), 1.05 (s, 3H) ppm; **^{13}C-NMR** (75 MHz, $CDCl_3$)

[ix] S.H. McCooey, S.J. Connon, *Org Lett*. **2007**, *9,* 599.

[x] C. Chang, S-H. Li, R. J. Reddy, K. Chen, *Adv. Synth. Catal.* **2009**, *351*, 1273.

[xi] J-R. Chen, Y-Q, Zou, L. Fu, F. Ren, F. Tan, W-J. Xiao, *Tetrahedron* **2010**, *66*, 5367.

δ_C 203.5, 139.7, 130.4, 130.1, 129.7, 129.5, 125.6, 75.8, 48.1, 48.0, 21.7, 18.8 ppm; **^{19}F-NMR** (221 MHz, $CDCl_3$) δ_F -63.4 ppm.

The enantiomeric excess was determined by HPLC on chiral stationary phase with Daicel Chiralcel OD-H column: eluent hexane/*i*PrOH = 8/2, flow rate 0.8 mL/min, λ=210 nm, τ_{minor} = 14.5 min, τ_{major} = 23.4 min.

(*S*)-2,2,5-trimethyl-3-(nitromethyl)hexanal 26

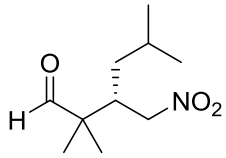

Prepared according to the general procedure. The crude mixture was purified by column chromatography on silica gel eluting with hexane/ethyl acetate 9:1 afford the title product as a colorless oil. All analytical data are in agreement with literature.[ix]

^{1}H-NMR (300 MHz, $CDCl_3$) δ_H 9.48 (s, 1H), 4.43-4.50 (dd, 1H), 4.22-4.28 (dd, 1H), 2.68 (m, 1H), 1.56 (m, 1H), 1.19-1.28 (m, 2H), 1.10 (s, 3H), 1.09 (s, 3H), 0.94 (d, 3H), 0.92 (d, 3H) ppm; **^{13}C-NMR** (75 MHz, $CDCl_3$) δ_C 203.7, 74.3, 48.3, 39.0, 38.2, 25.5, 23.1, 21.0, 19.3, 17.9 ppm.

The enantiomeric excess was determined by HPLC on chiral stationary phase with Daicel Chiralcel OD-H column: eluent hexane/*i*PrOH = 9/1, flow rate 0.8 mL/min, λ=210 nm, τ_{minor} = 7.4 min, τ_{major} = 8.9 min.

(*2R,3S*)-2-methyl-4-nitro-2,3-diphenylbutanal 27

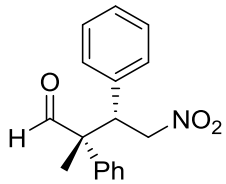

Prepared according to the general procedure. The crude mixture was purified by column chromatography on silica gel eluting with hexane/ethyl acetate 9:1 afford the title product as a colorless oil. All analytical data are in agreement with literature.[ix]

^{1}H-NMR (300 MHz, $CDCl_3$) δ_H 9.59 (s, 1H), 7.17-7.40 (m, 3H), 7.15 (m, 3H), 7.07 (dd, 2H), 6.96 (dd, 2H), 5.01-5.09 (dd, 1H), 4.85-4.90 (dd, 2H), 4.20-4.25 (dd, 1H), 1.55 (s, 3H) ppm; **^{13}C-NMR** (75 MHz, $CDCl_3$) δ_C 201.0, 137.2, 135.3, 129.2, 128.9, 128.9, 128.1, 128.0, 127.6, 127.2, 76.1, 56.6, 49.5, 16.6 ppm.

The enantiomeric excess was determined by HPLC on chiral stationary phase with Daicel Chiralcel OD-H column: eluent hexane/*i*PrOH = 95/5, flow rate 0.6 mL/min, λ=210 nm, τ_{major} = 39.3 min, τ_{minor} = 60.3 min.

(*2S,3S*)-2-ethyl-2-methyl-4-nitro-3-phenylbutanal 28

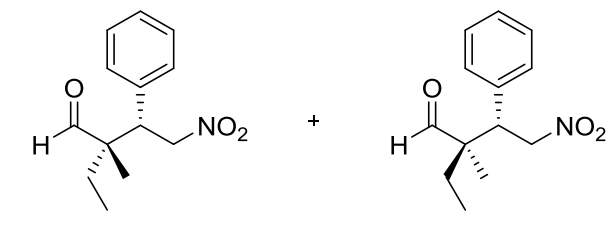

major diastereosomer minor diastereosomer

Prepared according to the general procedure. The crude mixture was purified by column chromatography on silica gel eluting with hexane/ethyl acetate 9:1 afford the title product as a colorless oil (2/1 mixture of diastereoisomers). All analytical data are in

agreement with literature.[ix]

^{1}H-NMR (300 MHz, $CDCl_3$) major diastereoisomer δ_H 9.56 (s, 1H), 7.17-7.36 (m, 5H), 4.81-4.86 (dd, 1H), 4.61-4.67 (dd, 1H), 3.79-3.84 (dd, 1H) 1.56-1.64 (m, 1H), 1.29-1.34 (m, 1H), 1.12 (s, 3H), 0.84 (t, 3H) ppm; **^{13}C-NMR** (75 MHz, $CDCl_3$) major diastereoisomer δ_C 205.4, 135.3, 129.2, 128.7, 128.2, 76.7, 51.8, 47.4, 28.1, 15.3, 8.1 ppm;
^{1}H-NMR (300 MHz, $CDCl_3$) minor diastereoisomer δ_H 9.46 (s, 1H), 7.17-7.36 (m, 5H), 4.79-4.87 (dd, 1H), 4.75-4.91 (dd, 1H), 3.76-3.81 (dd, 1H), 1.67-1.79 (m, 1H), 1.58-1.62 (m, 1H), 1.13 (s, 3H), 0.91 (t, 3H) ppm; **^{13}C-NMR** (75 MHz, $CDCl_3$) minor diastereoisomer δ_C 205.1, 135.3, 129.1, 128.3, 127.5, 76.4, 51.2, 49.2, 27.0, 16.8, 8.6 ppm.
The enantiomeric excess was determined by HPLC on chiral stationary phase with Daicel Chiralcel OD-H column: eluent hexane/*i*PrOH = 95/5, flow rate 0.8 mL/min, λ=210 nm, *major diastereosiomer* τ_{minor} = 28.6 min, τ_{major} = 43.5 min, *minor diastereosiomer* τ_{minor} = 24.1 min, τ_{major} = 30.7 min.

(*R*)-2-((*S*)-2-nitro-1-phenylethyl)cyclohexan-1-one 29

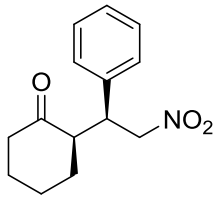

Prepared according to the general procedure. The crude mixture was purified by column chromatography on silica gel eluting with hexane/ethyl acetate 9:1 afford the title product as a white solid. All analytical data are in agreement with literature.[ix]

^{1}H-NMR (300 MHz, $CDCl_3$) δ_H 7.28-7.35 (m, 3H), 7.18-7.20 (d, 2H), 4.93-4.98 (dd, 1H), 4.62-4.71 (dd, 1H), 3.74-3.82 (dt, 1H), 2.71 (m, 1H), 2.49 (m, 2H), 2.11 (m, 3H), 1.68-1.84 (m, 5H), 1.24-1.36 (m, 1H) ppm; **^{13}C-NMR** (75 MHz, $CDCl_3$) δ_C 211.9, 137.7, 128.9, 128.1, 127.7, 78.9, 52.5, 43.9, 42.7, 33.2, 29.7, 28.5, 25.0.
The enantiomeric excess was determined by HPLC on chiral stationary phase with Daicel Chiralcel OD-H column: eluent hexane/EtOH = 98/2, flow rate 0.1 mL/min, λ=210 nm, τ_{major} = 119.1 min, τ_{minor} = 126.9 min.

(*4R,5S*)-4-methyl-6-nitro-5-phenylhexan-3-one 30

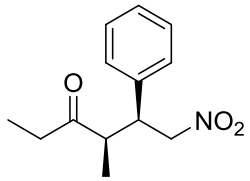

Prepared according to the general procedure with a reaction time of 120 h. The crude mixture was purified by column chromatography on silica gel eluting with hexane/ethyl acetate 9:1 afford the title product as a colorless oil. All analytical data are in agreement with literature.[ix]

^{1}H-NMR (300 MHz, $CDCl_3$) δ_H 7.31-7.36 (m, 3H), 7.17-7.20 (m, 2H), 4.59-4.74 (m, 2H), 3.69-3.76, (dt, 2H), 2.97-3.07 (m, 1H), 2.57-2.70 (dq, 1H), 2.37-2.50 (dq, 1H), 1.10 (t, 3H), 0.99 (d, 3H) ppm; **^{13}C-NMR** (75 MHz, $CDCl_3$) δ_C 213.6, 137.6, 129.0, 128.9, 127.9, 127.8, 78.3, 48.3, 46.0, 35.4, 16.3, 7.6 ppm.
The enantiomeric excess was determined by HPLC on chiral stationary phase with Daicel Chiralcel OD-H column: eluent hexane/*i*PrOH = 98/2, flow rate 0.8 mL/min, λ=210 nm, τ_{minor} = 32.9 min, τ_{major} = 42.8 min.

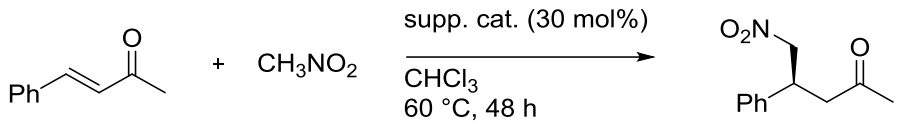

31

General procedure for batch reaction:

The supported catalyst (0.05 mmol) and benzalacetone (0.15 mmol) were placed into a vial and nitromethane (1 mmol) and dry chloroform (1 mL) were added under nitrogen atmosphere. The vial was sealed and the mixture was stirred at 60 °C for 48 hours. After reaction time the solid was filtered, washed with ethyl acetate (3 mL), recovered and dried under high vacuum. The organic layer was concentrated *in vacuo* and the residue was purified by column chromatography on silica gel. The enantiomeric excess of the product was determined by HPLC on chiral stationary phase.

(*S*)-5-nitro-4-phenylpentan-2-one 31

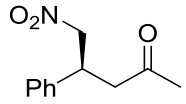

Prepared according to the general procedure. The crude mixture was purified by column chromatography on silica gel eluting with hexane/ethyl acetate 8:2 afford the title product as a white solid. All analytical data are in agreement with literature.[xii]

^{1}H-NMR (300 MHz, $CDCl_3$) δ_H 7.20-7.33 (m, 5H), 4.57-4.70 (m, 2H), 3.98-4.03 (m, 1H), 2.92 (d, 2H), 2.12 (s, 3H) ppm; **^{13}C-NMR** (75 MHz, $CDCl_3$) δ_C 205.4, 138.8, 129.1, 127.9, 127.4, 79.4, 46.1, 39.0, 30.4 ppm.

The enantiomeric excess was determined by HPLC on chiral stationary phase with Daicel Chiralpack AS column: eluent hexane/*i*PrOH = 8/2, flow rate 0.8 mL/min, λ=210 nm, τ_{major} = 21.0 min, τ_{minor} = 29.1 min.

[xii] W. Liu, D. Mei, W. Wang, D. Duan, *Tetrahedron Letters* **2013**, *24*, 3791.

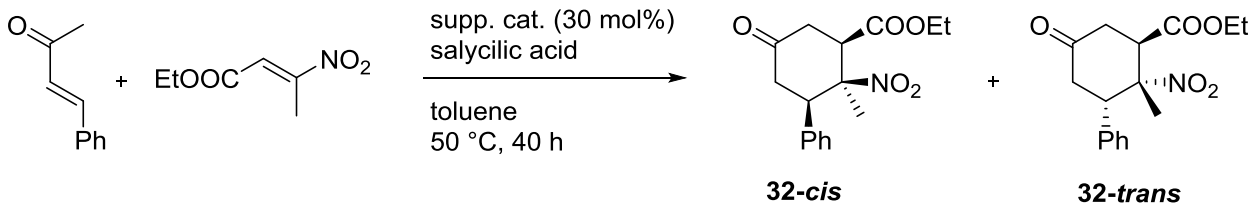

General procedure for batch reaction

The supported catalyst (0.05 mmol), benzalacetone (0.3 mmol), salycilic acid (0.06 mmol) and *trans*-ethyl-3-nitrobut-2-enoate (0.15 mmol) were placed into a vial and toluene (1 mL) was added under nitrogen atmosphere. The vial was sealed and the mixture was stirred at 50 °C for 48 h. After reaction time the solid was filtered, washed with AcOEt (3 mL), recovered and dried under vacuum. The organic layer was concentrated and the residue purified by column chromatography on silica gel. The enantiomeric excess was determined by HPLC on chiral stationary phase.

Ethyl (*1R,2S,3R*)-2-methyl-2-nitro-5-oxo-3-phenylcyclohexane-1-carboxylate 32

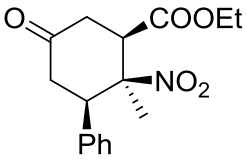

Prepared according to the general procedure. The crude mixture was purified by column chromatography on silica gel eluting with hexane/ethyl acetate 9:1 afford the title product as a white solid. All analytical data are in agreement with literature.[xiii]

^{1}H-NMR (300 MHz, $CDCl_3$) δ_H 7.36-7.33 (m, 3H), 7.09-7.06 (m, 2H), 4.28-4.13 (m, 2H), 3.56-3.41 (m, 1H+1H), 3.28-3.15 (m, 1H+1H), 2.82 (ddd, J=15.6, 5.6, 1.7 Hz, 1H), 2.57 (ddd, J=15.5, 4.5, 1.8 Hz, 1H), 1.58 (s, 3H), 1.27 (t, J=7.1 Hz, 3H) ppm; **^{13}C-NMR** (75 MHz, CDCl3) δ_C 205.9, 169.2, 135.7, 129.0, 128.8, 128.2, 86.8, 61.9, 51.6, 51.4, 43.1, 40.7, 23.3, 13.95 ppm.
The enantiomeric excess was determined by HPLC on chiral stationary phase with Daicel Chiralcel OD-H column: eluent hexane/*i*PrOH = 8/2, flow rate 0.8 mL/min, λ=210 nm, τ_{minor} = 20.4 min, τ_{major} = 34.8 min.

Ethyl (*1R,2R,3S*)-2-methyl-2-nitro-5-oxo-3-phenylcyclohexane-1-carboxylate 32

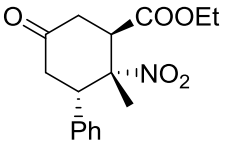

Prepared according to the general procedure. The crude mixture was purified by column chromatography on silica gel eluting with hexane/ethyl acetate 9:1 afford the title product as a white solid. All analytical data are in agreement with literature.

^{1}H-NMR (300 MHz, $CDCl_3$) δ_H 7.36-7.33 (m, 3H), 7.12-7.08 (m, 2H), 4.21 (qd, J=7.1, 1.6 Hz, 2H), 3.87 (dd, J=9.5, 5.5 Hz, 1H), 3.65 (dd, J=9.8, 5.2 Hz, 1H), 3.24 (dd, J =16.7, 9.8 Hz, 1H), 3.09 (dd, J=17.1, 5.4 Hz, 1H), 2.75 (dd, J=16.8, 5.2 Hz, 1H), 2.65 (dd, J=17.1, 9.5 Hz, 1H), 1.83 (s, 3H), 1.28 (t, J = 7.1 Hz, 3H) ppm; **^{13}C-NMR** (75 MHz, $CDCl_3$) δ_C 206.0, 170.5, 136.4, 128.9, 128.6, 128.5, 90.0, 61.8, 49.1, 46.4, 42.4, 39.5, 21.3, 14.0 ppm.

[xiii] E. Massolo, M. Benaglia, D. Parravicini, D. Brenna, R. Annunziata, *Tetrahedron Letters* **2014**, *55*, 6639.

The enantiomeric excess was determined by HPLC on chiral stationary phase with Daicel Chiralpack AD column: eluent hexane/*i*PrOH = 9/1, flow rate 0.8 mL/min, λ=210 nm, τ_{major} = 17.2 min, τ_{minor} = 20.3 min.

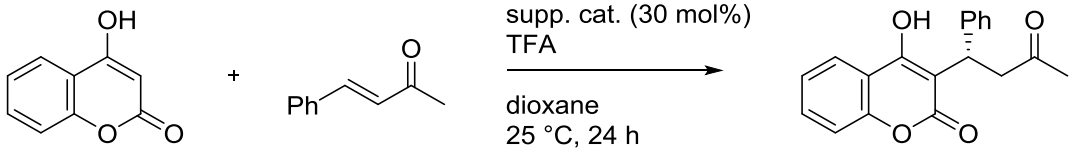

33

The supported catalyst (0.05 mmol), benzalacetone (0.3 mmol) and 4-hydroxycoumarin (0.15 mmol) were placed into a vial and trifluoroacetic acid (0.06 mmol) and dry dioxane (1 mL) were added under nitrogen atmosphere. The vial was sealed and the mixture was stirred at 50 °C for 48 hours. After reaction time the solid was filtered, washed with ethyl acetate (3 mL), recovered and dried under high vacuum. The organic layer was concentrated *in vacuo* and the residue was purified by column chromatography on silica gel. The enantiomeric excess of the product was determined by HPLC on chiral stationary phase.

(*S*)-4-hydroxy-3-(3-oxo-1-phenylbutyl)-2H-chromen-2-one 33

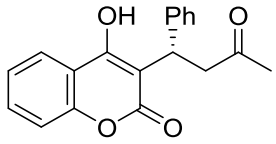

Prepared according to the general procedure. The crude mixture was purified by column chromatography on silica gel eluting with hexane/ethyl acetate 7:3 afford the title product as a white solid. All analytical data are in agreement with literature.[xiv]

The title compound was found to exist in rapid equilibrium with a pseudo- diastereomeric hemiketal form in solution. However, the equilibrium is very rapid and therefore no pseudo-diastereomers were observed during HPLC analysis using the mixture of hexane/*i*PrOH containing 0.1% TFA as the eluent.

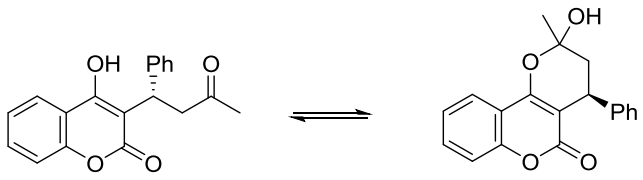

^{1}H-NMR (300 MHz, $CDCl_3$) δ_H 7.98 (dd, 1H), 7.93 (dd, 2.38H), 7.85 (dd, 3.15H), 7.58-7.50 (m, 7.83H), 7.22-7.4 (m, 54.13H), 4.73 (dd, 1.24H), 4.32 (dd, J = 3.6 , 2.87H), 4.12-4.18 (m, 5.53H), 3.9 (dd, 1.55H), 3.35 (dd, 1.8H), 3.2 (bs, 2.76H), 2.6-2.4 (m, 10.6H), 2.09-2.00 (dd, 5H), 1.76 (s, 12H), 1.71 (s, 10H) ppm; **^{13}C-NMR** (75 MHz, $CDCl_3$) δ_C 212.4, 161.6, 159.8, 152.8, 152.7, 143.3, 141.6, 131.9, 131.4, 129.0, 128.5, 128.1, 127.9, 127.0, 126.6, 126.3, 123.9, 123.8, 123.5, 123.0, 122.7, 116.5, 116.3, 116.1, 115.8, 103.9, 101.2, 100.6, 99.1, 45.1, 42.6, 40.1, 35.2, 34.8, 34.4, 30.0, 29.6, 27.8, 27.3 ppm.

The enantiomeric excess was determined by HPLC on chiral stationary phase with Daicel Chiralpack AD column: eluent hexane/*i*PrOH = 8/2 0.1 TFA, flow rate 0.8 mL/min, λ=280 nm, τ_{minor} = 7.82, τ_{major} = 19.5 min min.

[xiv] J.W. Xie, L. Yue, W. Chen, W. Du, J. Zhu, J.G. Deng, Y.C. Chen**,** *Org. Lett.* **2007**, *9,* 413.

4.1.3 Chiral Picolinamides

Silica-supported picolinamide

*Synthesis of compound **35***

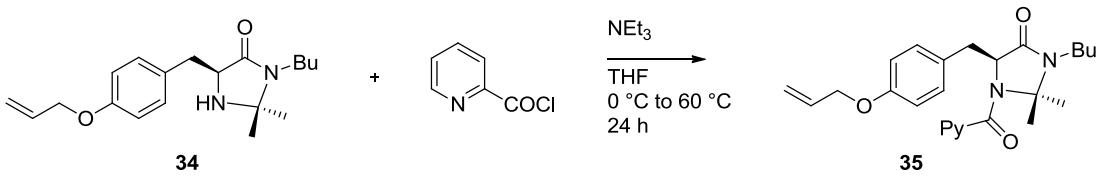

34 **35**

A mixture of compound **34**[xv] (0.94 mmol) and triethylamine (4.7 mmol) in dry THF (6 mL) was cooled to 0 °C. Then a solution of picolynoil chloride[xvi] (2.82 mmol) in dry THF (6 mL) was slowly added under nitrogen atmosphere. The mixture warmed at rt and then stirred at 60 °C for 24 hours. After reaction time distilled H_2O (5 mL) was added ant the aqueous phase was extracted 4 times with AcOEt (12 mL). The combined organic layers were dried with Na_2SO_4, concentrated *in vacuo*, and the residue was purified by column chromatography on silica gel eluting with hexane/ethyl acetate 4:6 to 2:8 afford **35** as brownish solid (0.55 mmol, 59% yield).

^{1}H-NMR (300 MHz, $CDCl_3$) δ_H 8.61-8.63 (d, J = 4.6 Hz, 1H), 7.87-7.94 (m, 2H), 7.42-7.46 (t, J = 6.9 Hz, 1H), 6.87-6.90 (d, J = 8.6 Hz, 2H), 6.75-6.78 (d, J = 8.6 Hz, 2H), 5.97-6.10 (m, 1H), 5.63-5.66 (dd, J = 2.7, 5.5 Hz, 1H), 5.36-5.41 (dd, J = 1.3, 17.3 Hz, 1H), 5.26-5.29 (d, J = 1.2, 10.5 Hz, 1H), 4.88-4.50 (d, J = 5.3 Hz, 2H), 3.13-3.25 (m, 1H), 2.99-3.09 (m, 2H), 2.06-2.13 (m, 1H), 1.73 (s, 3H), 1.60-1.68 (m, 1H), 1.39-1.52 (m, 1H), 1.23-1.34 (m, 2H), 0.95 (s, 3H), 0.93-0.98 (t, J = 6.8 Hz, 3H) ppm; **^{13}C-NMR** (300 MHz, $CDCl_3$) δ_C 168.3, 166.3, 157.6, 154.4, 148.2, 137.4, 133.1, 131.2 (2C), 127.8, 125.4 124.0, 117.6, 114.6 (2C), 80.6, 68.7, 60.8, 60.4, 39.8, 36.2, 30.8, 24.5, 24.0, 20.5, 13.7 ppm; **MS** (ESI+) m/z for $C_{25}H_{32}N_3O_3^+$: 422.1 **$[\alpha_D]^{23}$** = +200.1 (c: 0.46 $CHCl_3$).

*Synthesis of compound **36***

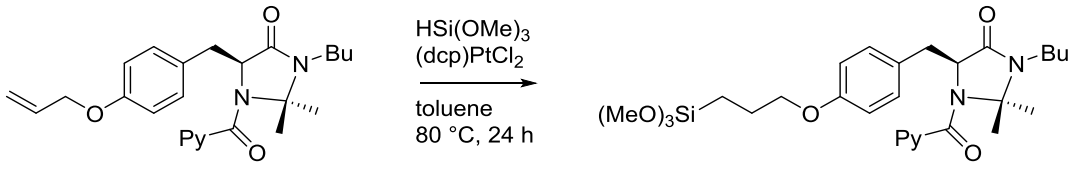

35 **36**

Compound **35** (0.55 mmol) and $(dcp)PtCl_2$ (0.03 mmol) were dissolved in dry toluene (10 mL) under nitrogen atmosphere and trimethoxy silane (1.65 mmol) was slowly added. The mixture was stirred at 80 °C for 24 hours. After reaction time the solvent was evaporated *in vacuo* and compound **36** was obtained as brownish oil (0.55 mmol, 99% yield). It was used in the following step without any further purification.

[xv] A. Puglisi, M. Benaglia, R. Annunziata, V. Chiroli, R. Porta, A. Gervasini, *J. Org. Chem.* **2013**, *78*, 11326.
[xvi] S. Guizzetti, M. Benaglia, S. Rossi, *Org. Lett.* **2009**, *11*, 2928.

^{1}H-NMR (300 MHz, $CDCl_3$) δ_H 8.61-8.63 (d, J = 4.6 Hz, 1H), 7.86-7.94 (m, 2H), 7.41-7.46 (m, 1H), 6.86-6.89 (d, J = 8.6 Hz, 2H), 6.72-6.75 (d, J = 8.6 Hz, 2H), 5.63-5.66 (m, 1H), 3.85-3.91 (m, 2H), 3.60-3.63 (3s, 9H), 3.14-3.24 (m, 1H), 3.01-3.07 (m, 2H), 2.08-2.15 (m, 1H), 1.78-1.92 (m, 2H), 1.74 (s, 3H), 1.60 (m, 2H), 1.45-1.52 (m, 2H), 1.28-1.37 (m, 2H), 0.96-1.05 (m, 6H) ppm; **^{13}C-NMR** (300 MHz, $CDCl_3$) δ_C 168.4, 165.4, 158.3, 154.5, 148.2, 137.3, 131.4 (2C), 127.5, 125.3, 124.0, 119.1, 114.4 (2C), 80.7, 69.7 (3C), 60.8, 50.5, 39.8, 36.3, 30.8, 24.6, 24.1, 22.5, 20.5, 13.7, ppm;

*Synthesis of catalysts **S10***

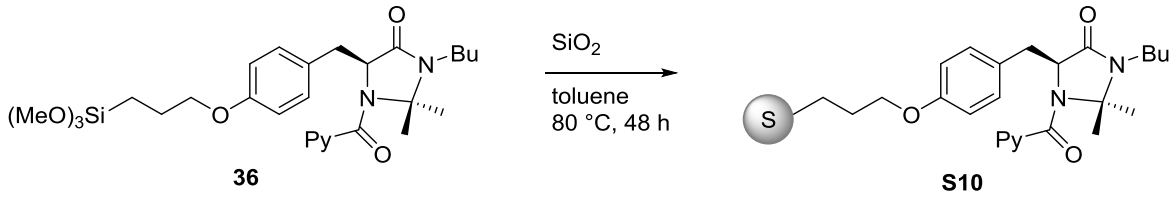

Compound **36** (0.55 mmol) was dissolved in dry toluene (13 mL) under nitrogen atmosphere then Apex Prepsil Silica Media 8 µm (0.55 g) was added. The mixture was stirred at 80 °C for 48 hours then it was filtered, the solid was washed with dichloromethane (10 mL) and methanol (10 mL), and it was recovered and dried under high vacuum for 3 hours. The organic phase was concentrated under vacuum and unreacted compound **36** was recovered. **S10** was obtained as a yellowish solid; the loading was determined by weight difference (0.57 g, 0.25 mmol/g).

*Synthesis of compound **37***

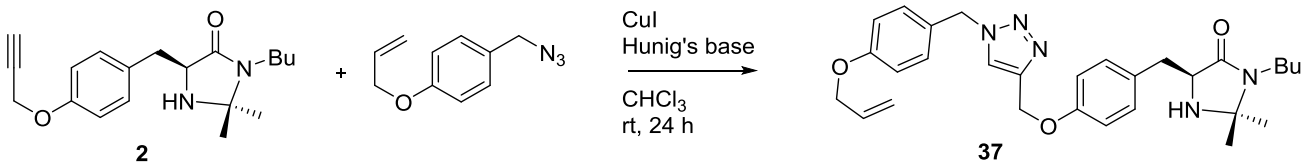

Compound **2** (0.73 mmol) was dissolved in dry chloroform (10 mL) under nitrogen atmosphere then CuI (0.04 mmol) and Hunig's base (3.7 mmol) were added. The mixture was stirred at rt for 15 minutes, then a solution of benzyl azide derivative (0.95 mmol) in dry chloroform (3 mL) was slowly added. The mixture was stirred for 24 hours at rt then NH_4OH (5 ml, 33 wt% solution) was added. The organic layer was washed twice NH_4OH (5 ml, 33 wt% solution), once with brine (8 mL), dried with sodium sulfate and concentrated *in vacuo* yielding to a brownish oil. The residue was purified by column chromatography on silica gel eluting with CH_2Cl_2:MeOH 98:2 to afford **37** as yellowish oil (0.52 mmol, 0.61 g, 71% yield).

^{1}H-NMR (300 MHz, $CDCl_3$) δ_H 7.48 (s, 1H), 7.20-7.23 (d, J = 8.8 Hz, 2H), 7.12-7.15 (d, J = 8.7 Hz, 2H), 6.89-6.92 (d, J = 6.4 Hz, 2H), 6.87-6.89 (d, J = 6.4 Hz, 2H), 5.97-6.09 (m, 1H), 5.44 (s, 2H), 5.37-5.42 (d, J = 17.3 Hz, 1H), 5.26-5.30 (d, J = 10.5 Hz, 1H), 5.12 (s, 2H), 4.51-4.54 (m, 2H), 3.69-3.72 (t, J = 5.3 Hz, 1H), 3.24-3.33 (m, 1H), 3.01-3.03 (m, 2H), 2.85-2.94 (m, 1H), 1.69 (bs, 1H), 1.41-1.52 (m, 2H), 1.26-1.30 (m, 2H), 1.25 (s, 3H), 1.14 (s, 3H), 0.89-0.93 (t, J = 7.4 Hz, 3H) ppm; **^{13}C-NMR** (300 MHz, $CDCl_3$) δ_C 173.8, 158.9, 157.2, 144.3, 132.9, 130.7 (2C), 129.6, 129.5 (2C), 126.6, 122.5, 117.8, 115.2 (2C), 114.8 (2C), 76.0, 68.8, 62.0, 58.8, 53.7, 40.2, 36.0, 31.4, 28.1, 26.5, 20.3, 13.8 ppm; **MS** (ESI+) m/z for $C_{29}H_{37}N_5O_3Na^+$: 526.2; **$[\alpha_D]^{23}$** = -37.0 (c: 0.36 $CHCl_3$).

*Synthesis of compound **38***

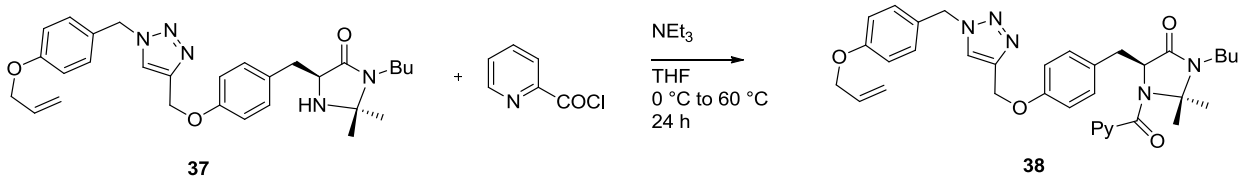

37 38

A mixture of compound X (0.48 mmol) and triethylamine (2.9 mmol) in dry THF (6 mL) was cooled to 0 °C. Then a solution of picolynoil chloride (1.4 mmol) in dry THF (3 mL) was slowly added under nitrogen atmosphere. The mixture warmed at rt and then stirred at 60 °C for 24 hours. After reaction time distilled H_2O (5mL) was added ant the aqueous phase was extracted 4 times with AcOEt (10 mL). The combined organic layers were dried with Na_2SO_4, concentrated *in vacuo*, and the residue was purified by column chromatography on silica gel eluting with hexane/ethyl acetate 2:8 afford **38** as brownish solid (0.33 mmol, 69% yield)

^{1}H-NMR (300 MHz, $CDCl_3$) δ_H 8.60-8.63 (m, 1H), 7.86-7.94 (m, 2H), 7.48 (s, 1H), 7.42-7.46 (m, 1H), 7.23-7.26 (d, J = 8.8 Hz, 2H), 6.92-6.94 (d, J = 8.7 Hz, 2H), 6.87-6.90 (d, J = 6.4 Hz, 2H), 6.80-6.82 (d, J = 6.4 Hz, 2H), 5.99-6.12 (m, 1H), 5.63-5.66 (m, 1H), 5.47 (s, 2H), 5.34-5.46 (d, J = 17.3 Hz, 1H), 5.30-5.34 (d, J = 10.5 Hz, 1H), 5.11 (s, 2H), 4.54-4.57 (m, 2H), 3.20-3.23 (m, 1H), 2.99-3.07 (m, 2H), 2.07-2.14 (m, 1H), 1.73 (s, 3H), 1.59-1.73 (m, 2H), 1.39-1.51 (m, 2H), 1.28-1.37 (m, 3H), 0.93-0.98 (t, J = 7.4 Hz, 3H), 0.92 (s, 3H), ppm; **^{13}C-NMR** (300 MHz, $CDCl_3$) δ_C 168.3, 166.3, 159.0, 157.4, 154.4, 148.2, 144.3, 137.4, 132.9, 131.3 (2C), 129.7(2C), 128.4, 126.5, 125.4, 124.1, 122.3, 117.9, 115.3 (2C), 114.6 (2C), 80.6, 68.9, 62.0, 60.8, 53.8, 39.8, 36.3, 30.8, 24.6, 24.1, 20.5, 13.7 ppm; **MS** (ESI+) m/z for $C_{35}H_{40}N_6O_4Na^+$: 631.4 **$[\alpha_D]^{23}$** = +206.6 (c: 0.28 $CHCl_3$).

*Synthesis of compound **39***

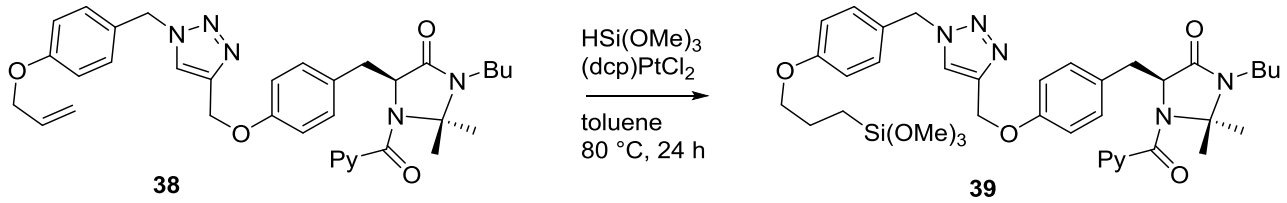

38 39

Compound **38** (0.33 mmol) and (dcp)$PtCl_2$ (0.016 mmol) were dissolved in dry THF (8 mL) under nitrogen atmosphere and trimethoxy silane (1.0 mmol) was slowly added. The mixture was stirred at 80 °C for 24 hours. After reaction time the solvent was evaporated *in vacuo* and compound **39** was obtained as brownish oil (0.33 mmol, 99% yield). It was used in the following step without any further purification.

^{1}H-NMR (300 MHz, $CDCl_3$) δ_H 8.61-8.62 (m, 1H), 7.85-7.89 (m, 2H), 7.49 (s, 1H), 7.43-7.47 (m, 1H), 7.22-7.25 (d, J = 8.8 Hz, 2H), 6.79-6.92 (m, 6H), 5.61-5.64 (m, 1H), 5.46 (s, 2H), 5.10 (s, 2H), 3.90-3.95 (m, 2H), 3.61 (s, 9H), 3.08-3.21 (m, 1H), 2.99-3.04 (m, 2H), 2.09-2.17 (m, 1H), 1.78-1.98 (m, 2H), 1.73 (s, 3H), 1.64 (m, 2H), 1.43-1.52 (m, 2H), 1.27-1.34 (m, 2H), 0.92-1.07 (m, 6H) ppm.

*Synthesis of catalysts **S11***

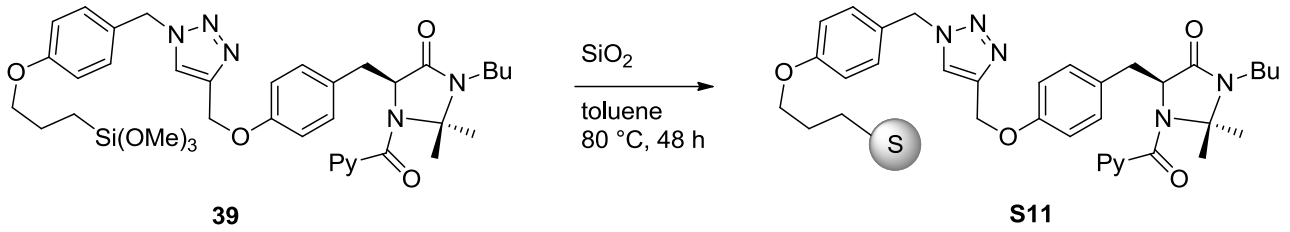

39 **S11**

Compound **39** (0.33 mmol) was dissolved in dry toluene (10 mL) under nitrogen atmosphere then Apex Prepsil Silica Media 8 µm (0.33 g) was added. The mixture was stirred at 80 °C for 48 hours then it was filtered, the solid was washed with dichloromethane (10 mL) and methanol (10 mL), and it was recovered and dried under high vacuum for 3 hours. The organic phase was concentrated under vacuum and unreacted compound **39** was recovered. **S11** was obtained as a yellowish solid; the loading was determined by weight difference (0.35 g, 0.3 mmol/g).

*Synthesis of compound **40***

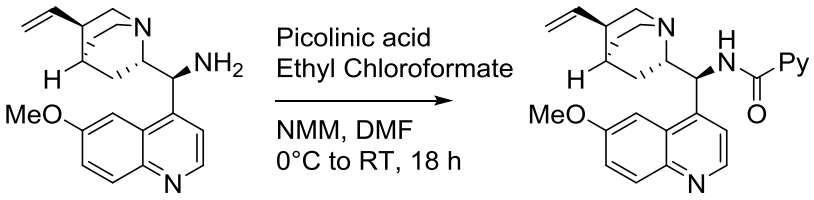

18 **40**

Picolinic acid (1.5 mmol) was placed into a two necked flask and dissolved in dry THF (12 mL) under nitrogen atmosphere. Triethylamine (2.2 mmol) was added and the mixture was cooled to 0 °C. Ethyl chloroformate (1.5 mmol) was added dropwise and the mixture was stirred for 15 minutes at the same temperature, then 2 h at room temperature. After reaction time a solution of **18** (1.5 mmol) in dry THF (8 mL), was added slowly. The reaction was stirred at room temperature for 3 hours. After reaction time H_2O (3 mL) was added and the crude was concentrated in vacuum, diluted with AcOEt and then washed with H_2O. Collected organic phases were dried with Na_2SO_4, concentrated in vacuum, and the residue was purified by column chromatography on silica gel eluting with CH_2Cl_2:MeOH 95:5. Compound **40** was obtained as brownish oil (1.04 mmol, 77% yield).

^{1}H-NMR (300 MHz, $CDCl_3$) δ_H 8.88 (br s, 1H), 8.70 (d, J = 4 Hz, 1H), 8.46 (d, J = 4 Hz, 1H), 8.03-7.96 (m, 2H), 7.75 (d, J = 3 Hz, 1H), 7.71-7.66 (m, 1H), 7.42 (d, J = 4 Hz, 1H), 7.34-7.26 (m, 2H), 5.80-5.69 (m, 1H), 5.62 (br s, 1H), 5.01-4.91 (m, 2H), 3.94 (s, 3H), 3.44-3.36 (m, 1H), 3.33-3.23 (m, 2H), 2.81-2.68 (m, 2H), 2.27 (br, 1H), 1.66-1.48 (m, 4H), 0.96-0.88 (m, 1H).

*Synthesis of compound **41***

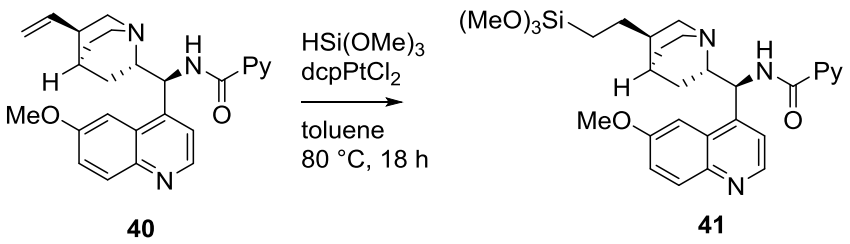

40 **41**

Compound **40** (0.5 mmol) and (dcp)$PtCl_2$ (0.02 mmol) were dissolved in dry THF (8 mL) under nitrogen atmosphere and trimethoxy silane (1.5 mmol) was slowly added. The mixture was stirred at 60 °C for 24 hours. After reaction time the solvent was evaporated *in vacuo* and compound **41** was obtained as brownish oil (0.5 mmol, 99% yield). It was used in the following step without any further purification.

^{1}H-NMR (300 MHz, $CDCl_3$) δ_H8.94 (bs, 1H), 8.71 (d, 1H), 8.52 (bs, 1H), 7.97-8.05 (m, 2H), 7.74 (bs, 2H), 7.43 (s, 1H), 7.33 (d, 2H), 6.61 (bs, 1H), 3.96 (s, 3H), 3.59 (s, 9H), 3.26-3.34 (m, 2H), 3.06 (bs, 1H), 2.80 (bs, 1H), 2.48 (bs, 1H), 1.86 (m, 2H), 1.59-1.72 (m, 3H), 1.35 (m, 2H), 0.98 (bs, 1H), 0.52 (m, 2H) ppm;

*Synthesis of catalysts **S12***

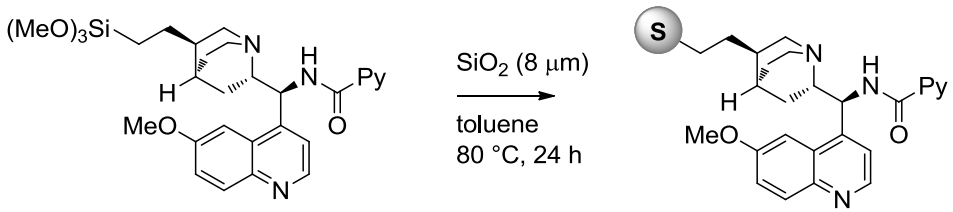

41 **S12**

Compound **41** (0.5 mmol) was dissolved in dry toluene (10 mL) under nitrogen atmosphere and then Apex Prepsil Silica Media 8 µm (0.5 g) was added. The mixture was stirred at 80 °C for 48 hours after which it was then filtered. The solid was washed with dichloromethane (10 mL) and methanol (10 mL), and it was recovered and dried under high vacuum for 3 hours. The organic layer was concentrated under vacuum and unreacted compound **41** was recovered. **S12** was obtained as a yellowish solid; the loading was determined by weight difference (0.52 g, 0.5 mmol/g).

*Synthesis of compound **43***

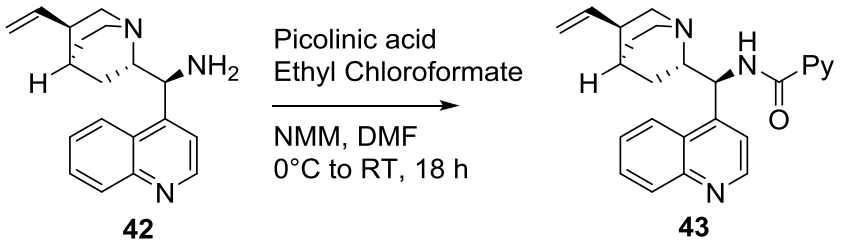

Picolinic acid (1.5 mmol) was placed into a two necked flask and dissolved in dry THF (12 mL) under nitrogen atmosphere. Triethylamine (2.2 mmol) was added and the mixture was cooled to 0 °C. Ethyl chloroformate (1.5 mmol) was added dropwise and the mixture was stirred for 15 minutes at the same temperature, then 2 h at room temperature. After reaction time a solution of **42** (1.5 mmol) in dry THF (8 mL), was added slowly. The reaction was stirred at room temperature for 3 hours. After reaction time H_2O (3 mL) was added and the crude was concentrated in vacuum, diluted with AcOEt and then washed with H_2O. Collected organic phases were dried with Na_2SO_4, concentrated in vacuum, and the residue was purified by column chromatography on silica gel eluting with CH_2Cl_2:MeOH 95:5. Compound **43** was obtained as brownish oil (1.04 mmol, 77% yield).

^{1}H-NMR (300 MHz, $CDCl_3$) δ_H 8.98 (br s, 1H), 8.89 (d, J = 4 Hz, 1H), 8.48-8.43 (m, 2H), 8.13 (d, J = 7 Hz, 1H), 8.03 (d, J = 2 Hz, 1H), 7.75-7.69 (m, 1H), 7.65-7.60 (m, 1H), 7.50- 7.49 (d, J = 4 Hz, 1H), 7.37 (dd, J = 2 Hz, 5 Hz, 1H), 5.80-5.69 (m, 1H), 5.64 (br s, 1H), 5.03-4.94 (m, 2H), 3.42-3.18 (m, 3H), 2.88-2.73 (m, 2H), 2.31 (br s, 1H), 1.71-1.53 (m, 3H), 1.50-1.42 (m, 1H), 0.99-0.92 (m, 2H).

*Synthesis of compound **44***

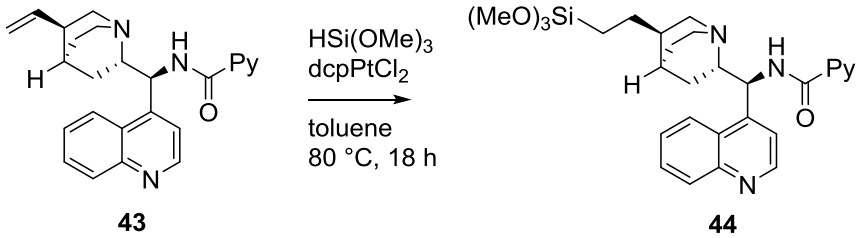

Compound **43** (0.5 mmol) and (dcp)$PtCl_2$ (0.02 mmol) were dissolved in dry THF (8 mL) under nitrogen atmosphere and trimethoxy silane (1.5 mmol) was slowly added. The mixture was stirred at 60 °C for 24 hours. After reaction time the solvent was evaporated *in vacuo* and compound **44** was obtained as brownish oil (0.5 mmol, 99% yield). It was used in the following step without any further purification.

^{1}H-NMR (300 MHz, $CDCl_3$) δ_H8.94 (bs, 1H), 8.71 (d, 1H), 8.52 (bs, 1H), 7.97-8.05 (m, 2H), 7.74 (bs, 2H), 7.43 (s, 1H), 7.33 (d, 2H), 6.61 (bs, 1H), 3.96 (s, 3H), 3.59 (s, 9H), 3.26-3.34 (m, 2H), 3.06 (bs, 1H), 2.80 (bs, 1H), 2.48 (bs, 1H), 1.86 (m, 2H), 1.59-1.72 (m, 3H), 1.35 (m, 2H), 0.98 (bs, 1H), 0.52 (m, 2H) ppm;

*Synthesis of catalysts **S13***

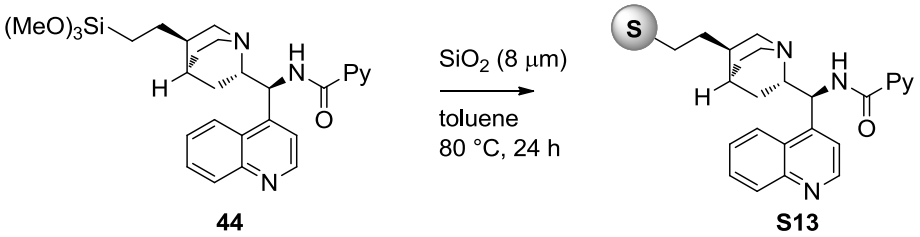

44 **S13**

Compound **44** (0.5 mmol) was dissolved in dry toluene (10 mL) under nitrogen atmosphere and then Apex Prepsil Silica Media 8 µm (0.5 g) was added. The mixture was stirred at 80 °C for 48 hours after which it was then filtered. The solid was washed with dichloromethane (10 mL) and methanol (10 mL), and it was recovered and dried under high vacuum for 3 hours. The organic layer was concentrated under vacuum and unreacted compound **44** was recovered. **S13** was obtained as a yellowish solid; the loading was determined by weight difference (0.52 g, 0.4 mmol/g).

Polymer-supported picolinamides

*Synthesis of compound **45***

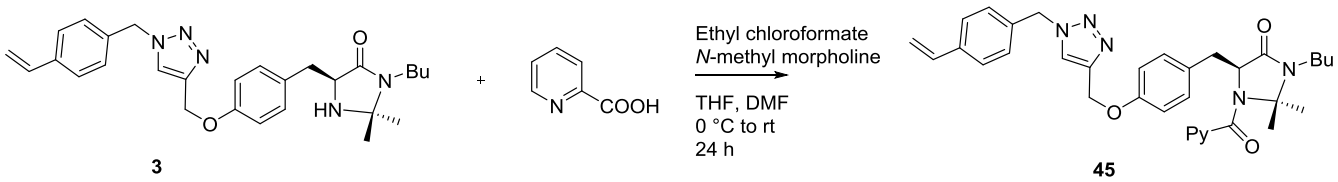

Picolinic acid (1.58 mmol) was placed into a two necked flask dissolved in dry THF (12 mL) under nitrogen atmosphere. N-methyl-morpholine (2.38 mmol) was added and the mixture was cooled at 0 °C. Ethyl chloroformate (1.58 mmol) was added dropwise and the mixture was stirred for 15 minutes at same temperature, then 2 h at room temperature. After reaction time a solution of **3** (1.58 mmol) in dry DMF (8 mL), was added slowly with a dropping funnel. The reaction was stirred at room temperature overnight. After reaction time the solvent was evaporated under vacuum and the crude product was dissolved in AcOEt then washed with H_2O. Collected organic phases were dried with Na_2SO_4, concentrated *in vacuo*, and the residue was purified by column chromatography on silica gel eluting with ethyl acetate afford **45** as brownish solid (1.04 mmol, 66% yield).

^{1}H-NMR (300 MHz, $CDCl_3$) δ_H 8.60-8.61 (d, 1H), 7.86-7.92 (m, 2H), 7.51 (s, 1H), 7.41-7.44 (m, 3H), 7.24-7.27 (d, J = 8.8 Hz, 2H), 6.87-6.90 (d, J = 8.7 Hz, 2H), 6.79-6.82 (d, J = 6.4 Hz, 2H), 6.67-6.76 (m, 1H), 5.74-5.80 (d, J = 17.3 Hz, 1H), 5.62-5.65 (m, 1H), 5.52 (s, 2H), 5.29-5.32 (d, J = 17.3 Hz, 1H), 5.12 (s, 2H), 3.13-3.22 (m, 1H), 3.00-3.09 (m, 2H), 2.10-2.18 (m, 1H), 1.72 (s, 3H), 1.57-1.65 (m, 2H), 1.39-1.52 (m, 2H), 1.36-1.39 (m, 3H), 0.87-0.97 (m, 3H), 0.95 (s, 3H), ppm; **^{13}C-NMR** (300 MHz, $CDCl_3$) δ_C 168.3, 166.3, 157.4, 154.5, 148.2, 144.4, 138.2, 137.4, 135.9, 133.8, 131.3 (2C), 128.4 (2C), 126.9 (2C), 125.3, 124.0, 122.5, 115.0, 114.6 (2C), 80.6, 62.0, 60.8, 54.0, 39.8, 36.3, 30.8, 29.7, 24.6, 24.1, 20.5, 13.7 ppm; **HRMS** (EI): calculated for $C_{34}H_{38}O_3N_6Na_1$(+1): 601.2897; found 601.2892. **$[\alpha_D]^{23}$** = + 175.7 (c: 0.5 $CHCl_3$).

*Synthesis of catalysts **P6***

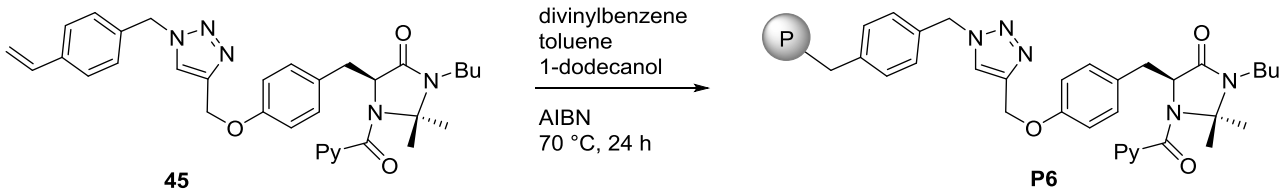

A mixture of compound **45** (1.05 g, 11 wt%), AIBN (95 mg, 1 wt%) divinylbenzene (6.9 mmol, 22 wt%), toluene (3.5 mL, 32 wt%) and 1-dodecanol (3.25 g, 34 wt%) was prepared under nitrogen atmosphere. The mixture was transferred into a sealed vial and heated into an oil bath at 70 °C for 24 hours. After reaction time the polymer was removed from the vessel and crushed into a mortar. The fine powder obtained was suspended in methanol (15 mL) and stirred for 10 minutes at rt. The solid was then isolated by filtration and washed methanol (15 mL) and dichloromethane (15 mL). The solid was recovered and dried under high vacuum at 40 °C for 3 hours.

The loading of catalyst **P6** (0.57 mmol/g) was determined by the stoichiometry of reagents in the polymerization mixture. The polymerization occurred with a full conversion as any trace of monomer **45** was recovered from the organic layer used to wash the solid (toluene and 1-dodecanol were fully recovered).

*Synthesis of catalyst **P9***

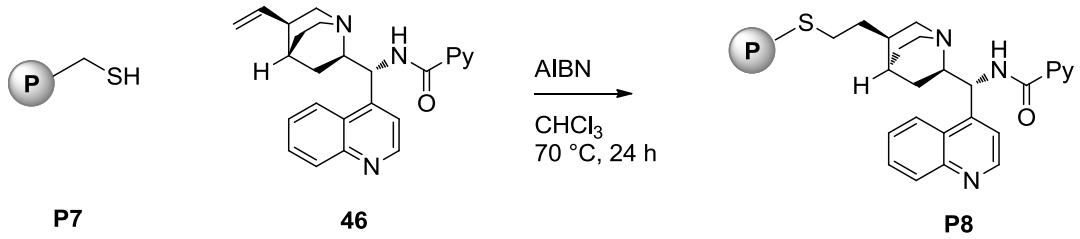

P7 **46** **P8**

P7[xvii] (0.63 g, 1.0 mmol/g) was suspended in dry toluene (10 mL) under nitrogen atmosphere and then a solution of **46** (1.0 mmol, g) and AIBN (1.0 mmol) in dry chloroform (3 mL) was slowly added. The mixture was stirred at 80 °C for 24 hours under nitrogen atmosphere. After this reaction time the solid was filtered and washed with CH_2Cl_2 (10 mL) and methanol (10 mL) and then dried under high vacuum for 3 hours. The organic layer was concentrated in vacuum and unreacted compound **46** was recovered and purified by column chromatography. The loading of **P8** was determined by weight difference (0.65 g, 0.3 mmol/g).

*Synthesis of catalyst **P10***

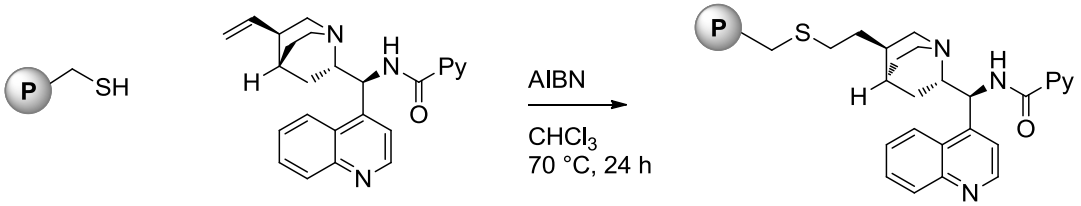

P7 **43** **P9**

P7 (0.63 g, 1.0 mmol/g) was suspended in dry toluene (10 mL) under nitrogen atmosphere and then a solution of **43** (1.0 mmol, g) and AIBN (1.0 mmol) in dry chloroform (3 mL) was slowly added. The mixture was stirred at 80 °C for 24 hours under nitrogen atmosphere. After this reaction time the solid was filtered and washed with CH_2Cl_2 (10 mL) and methanol (10 mL) and then dried under high vacuum for 3 hours. The organic layer was concentrated in vacuum and unreacted compound **43** was recovered and purified by column chromatography. The loading of **P9** was determined by weight difference (0.65 g, 0.2 mmol/g).

[xvii] Braslau, R.; Rivera, F.; Tansakul, C. *Reactive and Functional Polymers* **2013**, *73*, 624.

*Synthesis of non-supported catalyst **45N***

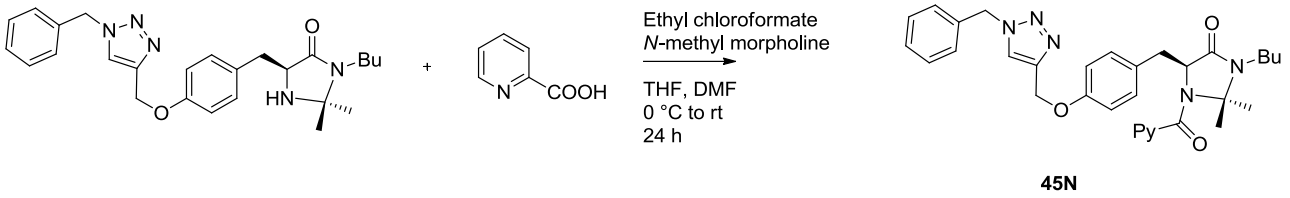

45N

Picolinic acid (1.6 mmol) was dissolved in dry THF (12 mL) under nitrogen atmosphere. N-methyl-morpholine (2.4 mmol) was added and the mixture was cooled at 0 °C. Ethyl chloroformate (1.6 mmol) was added dropwise and the mixture was stirred for 15 minutes at same temperature, then 2 h at room temperature. After reaction time a solution of imidazolidinone (1.6 mmol) in dry DMF (8 mL), was slowly added. The reaction was stirred at room temperature overnight. After reaction time the solvent was evaporated under vacuum and the crude product was dissolved in AcOEt then washed with H_2O. Collected organic layers were dried with Na_2SO_4, concentrated *in vacuo*, and the residue was purified by column chromatography on silica gel (eluent: Hex/AcOEt=2/8) to afford **45N** as a brownish oil (1.24 mmol, 78% yield).

^{1}H-NMR (300 MHz, $CDCl_3$): δ 8.60-8.61 (d, 1H), 7.87-7.90 (m, 2H), 7.52 (s, 1H), 7.41-7.37 (m, 3H), 7.30-7.27 (m, 2H), 6.87 (d, 2H), 6.80 (d, 2H), 5.62-5.65 (m, 1H), 5.53 (s, 2H), 5.11 (s, 2H), 4.13 (q, 1H), 3.12-3.18 (m, 1H), 3.00-3.08 (m, 2H), 2.05-2.13 (m, 1H), 1.57-1.63 (m, 2H), 1.39-1.52 (m, 2H), 1.36-1.39 (m, 3H), 0.87-0.97 (m, 3H), 0.95 (s, 3H) ppm; **^{13}C-NMR** (300 MHz, $CDCl_3$): δ 168.3, 165.3, 157.4, 154.4, 148.2, 144.4, 138.2, 137.4, 134.5, 131.3, 129.1 (2C), 128.7, 128.3, 128.1 (2C), 125.4, 124.0, 122.7, 114.6 (2C), 80.6, 61.9, 60.7, 54.2, 39.8, 36.3, 30.8, 24.6, 24.1, 20.5, 13.7 ppm; **HRMS** (ESI+) m/z calculated for $C_{32}H_{36}O_3N_6Na_1$(+1): 575.2741; found 575.2748; **$[\alpha_D]^{23}$** = + 201.3 (c: 0.65 $CHCl_3$).

General procedure for batch reaction

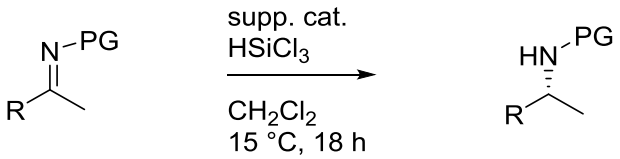

Supported catalyst (0.02 mmol) and imine (0.1 mmol) were introduced into a vial and dissolved in dry CH_2Cl_2 (1 mL) under inert atmosphere. $HSiCl_3$ (1 M solution in CH_2Cl_2, 5 equiv.) was added at 0° C and then the reaction was stirred at room temperature for 18 hours. After this reaction time the supported catalyst was removed by filtration and washed with dichloromethane. The organic layer was treated with NaOH 10% aq. until basic pH = 9. The organic layer was collected, dried with Na_2SO_4 and concentrated under vacuum. The residue was purified by column chromatography on silica gel. The enantiomeric excess was determined by HPLC on chiral stationary phase.

General procedure for continuous flow reaction

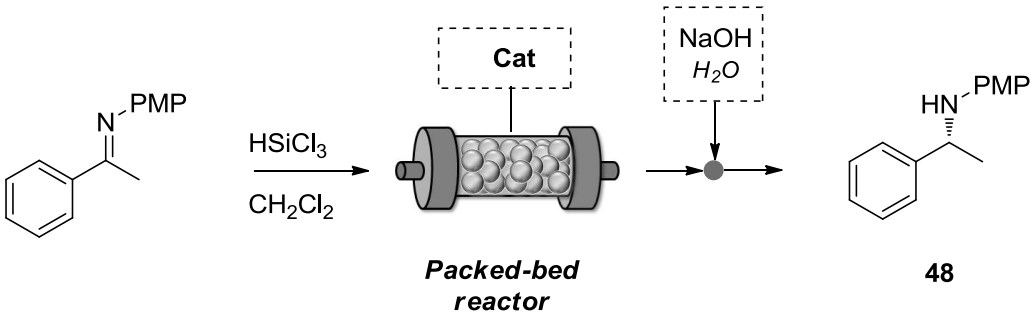

A 0.05 M mixture of imine (0.1 mmol) and $HSiCl_3$ (5 equiv.) in dry CH_2Cl_2 (2 mL) was charged into a 2.5 mL SGE gas tight syringe and fixed on a syringe pump. The syringe was connected to the packed bed reactor and flushed at the indicated flow rate. The reactor was then washed with pure CH_2Cl_2 at the same flow rate. The outcome of the reactor was collected into a flask containing NaOH 10% solution. After phase separation and concentration the product was isolated. At predetermined intervals of time the product was collected and analyzed. The yield was determined by chromatography and the ee was determined on HPLC on chiral stationary phase.

(*R*)-*N*-(1-phenylethyl)aniline 47

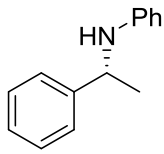

Prepared according to the general procedure. The crude mixture was purified by column chromatography on silica gel eluting with hexane/ethyl acetate 95:5 afford the title product as a yellowish solid. All analytical data are in agreement with literature.[xviii]

^{1}H-NMR (300 MHz, $CDCl_3$) δ_H 7.23-7.19 (m, 7H), 6.61-6.49 (m, 3H), 4.48 (q, 1H), 1.53 (d, 3H) ppm.

The enantiomeric excess was determined by HPLC on chiral stationary phase with Daicel Chiralcel OD-H column: eluent Hexane/*i*PrOH = 99/1, flow rate 0.8 mL/min, λ=254 nm, τ_{minor} = 13.2 min, τ_{major} = 15.9 min.

(*R*)-4-methoxy-*N*-(1-phenylethyl)aniline 48

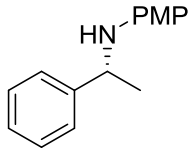

Prepared according to the general procedure. The crude mixture was purified by column chromatography on silica gel eluting with hexane/ethyl acetate 95:5 afford the title product as a yellowish solid. All analytical data are in agreement with literature.[xviii]

^{1}H-NMR (300 MHz, $CDCl_3$) δ_H 7.43-7.26 (m, 5H), 6.73 (d, 2H), 6.58 (d, 2H), 4.46 (q,1H), 3.74 (s, 3H), 1.58 (d, 3H) ppm.

The enantiomeric excess was determined by HPLC on chiral stationary phase with Daicel Chiralcel OD-H column: eluent Hexane/*i*PrOH = 99/1, flow rate 0.8 mL/min, λ=254 nm, τ_{major}=17.9 min, τ_{minor}=21.0 min.

(*R*)-4-methoxy-*N*-(1-(4-methoxyphenyl)ethyl)aniline 49

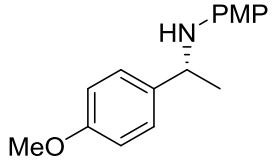

Prepared according to the general procedure. The crude mixture was purified by column chromatography on silica gel eluting with hexane/ethyl acetate 95:5 afford the title product as a yellowish solid. All analytical data are in agreement with literature.[xviii]

^{1}H-NMR (300 MHz, $CDCl_3$) δ_H 7.30 (d, 2H), 6.87 (d, 2H), 6.71 (d, 2H), 6.49 (d, 2H), 4.40 (q, 1H), 3.80 (s, 3H), 3.72 (s, 3H), 1.49 (d, 3H) ppm.

The enantiomeric excess was determined by HPLC on chiral stationary phase with Daicel Chiralcel OD-H column: eluent Hexane/*i*PrOH = 9/1, flow rate 0.8 mL/min, λ=254 nm, τ_{major}=11.5 min, τ_{minor} = 12.9 min.

[xviii] A. V. Malkov, M. Figlus, S. Stoncius, P. Kocovsky, *J. Org. Chem.* **2006**, *72*, 1315.

(*R*)-4-methoxy-*N*-(1-(p-tolyl)ethyl)aniline 50

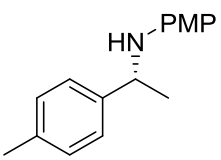

Prepared according to the general procedure. The crude mixture was purified by column chromatography on silica gel eluting with hexane/ethyl acetate 95:5 afford the title product as a yellowish solid. All analytical data are in agreement with literature.[xix]

^{1}H-NMR (300 MHz, $CDCl_3$) δ_H 7.29-7.26 (d, 2H), 7.16-7.14 (d, 2H), 6.73-6.70 (d, 2H), 6.54-6.52 (d, 2H), 4.45-4.38 (q, 1H), 3.72 (s, 3H), 2.35 (s, 3H), 1.53(d, 3H) ppm.

The enantiomeric excess was determined by HPLC on chiral stationary phase with Daicel Chiralcel OD-H column: eluent Hexane/*i*PrOH = 98/2, flow rate 0.8 mL/min, λ=254 nm, τ_{major}=12.4 min, τ_{minor}=14.5 min.

(*R*)-*N*-(1-(4-chlorophenyl)ethyl)-4-methoxyaniline 51

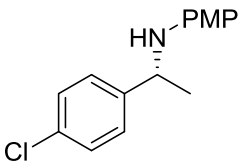

Prepared according to the general procedure. The crude mixture was purified by column chromatography on silica gel eluting with hexane/ethyl acetate 95:5 afford the title product as a yellowish solid. All analytical data are in agreement with literature.[xx]

^{1}H-NMR (300 MHz, $CDCl_3$) δ: 7.31-7.25 (m, 4H), 6.70-6.67 (d, 2H), 6.44-6.42 (d, 2H), 4.40 (q, 1H), 3.72 (s, 3H), 1.48 (d, 3H).

The enantiomeric excess was determined by HPLC on chiral stationary phase with Daicel Chiralcel OD-H column: eluent Hexane/*i*PrOH = 98/2, flow rate 0.5 mL/min, λ=254 nm, τ_{major} = 33.4 min, τ_{minor}= 37.7 min.

(*R*)-4-methoxy-*N*-(1-(4-nitrophenyl)ethyl)aniline 52

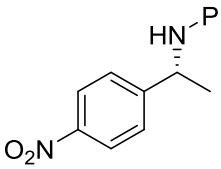

Prepared according to the general procedure. The crude mixture was purified by column chromatography on silica gel eluting with hexane/ethyl acetate 95:5 afford the title product as a yellowish solid. All analytical data are in agreement with literature.[xix]

^{1}H-NMR (300 MHz, $CDCl_3$) δ_H 8.18 (m, 2H), 7.55 (d, 2H), 6.70 (m, 2H), 6.40(m, 2H), 4.50 (q, 1H), 3.86 (bs, 1H), 3.69 (s, 3H), 1.52(d, 3H) ppm.

The enantiomeric excess was determined by HPLC on chiral stationary phase with Daicel Chiralcel OD-H column: eluent Hexane/*i*PrOH = 99:1, flow rate 0.8 mL/min, λ=254 nm, τ_{major} = 37.5 min, τ_{minor} =44.5

[xix] S. Hoffmann, A. M. Seajad, B. List, *Angew. Chem. Int. Ed.* **2005**, *44*, 7424.

[xx] R. I. Storer, D. E. Carrera, Y. Ni, D. W. C. MacMillan, *J. Am. Chem. Soc.* **2005**, *128*, 84.

(*R*)-*N*-(1-(4-fluorophenyl)ethyl)-4-methoxyaniline 53

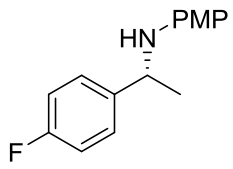

Prepared according to the general procedure. The crude mixture was purified by column chromatography on silica gel eluting with hexane/ethyl acetate 95:5 afford the title product as a yellowish solid. All analytical data are in agreement with literature.[xx]

^{1}H-NMR (300 MHz, $CDCl_3$) δ_H 7.28-7.33 (m, 2H), 6.95-7.00 (m, 2H), 6.68 (d, 2H), 6.43 (d, 2H), 4.37 (q, 1H), 3.68 (s, 3H), 1.45 (d, 3H)ppm.

The enantiomeric excess was determined by HPLC on chiral stationary phase with Daicel Chiralcel OD-H column: eluent Hexane/*i*PrOH = 98/2, flow rate 0.8 mL/min, λ=254 nm, τ_{major}=19.6 min, τ_{minor} = 22.9 min.

(*R*)-4-methoxy-*N*-(1-(4-(trifluoromethyl)phenyl)ethyl)aniline 54

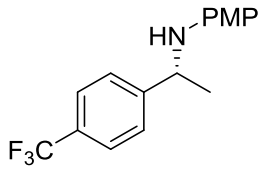

Prepared according to the general procedure. The crude mixture was purified by column chromatography on silica gel eluting with hexane/ethyl acetate 95:5 afford the title product as a yellowish solid. All analytical data are in agreement with literature.[xviii]

^{1}H-NMR (300 MHz, $CDCl_3$) δ_H 7.56 (d, 2H), 7.47 (d, 2H), 6.69 (d, 2H), 6.42 (d, 2H), 4.44 (q, 1H), 3.81 (bs, 1H), 3.68 (s, 3H), 1.48 (d, 3H) ppm.

The enantiomeric excess was determined by HPLC on chiral stationary phase with Daicel Chiralcel OD column: eluent Hexane/*i*PrOH = 98/2, flow rate 0.8 mL/min, λ=254 nm, τ_{major} = 22.2 min, τ_{minor} = 29.3 min.

(*R*)-*N*-(1-(3-bromophenyl)ethyl)-4-methoxyaniline 55

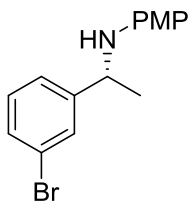

Prepared according to the general procedure. The crude mixture was purified by column chromatography on silica gel eluting with hexane/ethyl acetate 95:5 afford the title product as a yellowish solid. All analytical data are in agreement with literature.[xxi]

^{1}H-NMR (300 MHz, $CDCl_3$) δ_H 7.52-7.50 (m, 1H), 7.36-7.25 (m, 2H), 7.20-7.15 (m, 1H), 6.71-6.67 (d, 2H), 6.47-6.42 (d, 2H), 4.36 (q, 1H), 3.69 (s, 3H), 1.48 (d, 3H) ppm.

The enantiomeric excess was determined by HPLC on chiral stationary phase with Daicel Chiralcel OD-H column: eluent Hexane/*i*PrOH = 98/2, flow rate 0.8 mL/min, λ=230 nm, τ_{major}=22.7 min, τ_{minor}=28.3 min.

[xxi] M. Rueping, E. Sugiono, C. Azap, T. Theissmann, M. Bolte, *Org. Lett.* **2005**, *7*, 3781.

(*R*)-4-methoxy-*N*-(1-(naphthalen-2-yl)ethyl)aniline 56

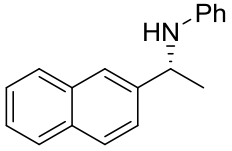

Prepared according to the general procedure. The crude mixture was purified by column chromatography on silica gel eluting with hexane/ethyl acetate 95:5 afford the title product as a yellowish solid. All analytical data are in agreement with literature.[xviii]

^{1}H-NMR (300 MHz, $CDCl_3$) δ_H 7.78-7.82 (m, 5H), 7.41-7.51 (m, 3H), 6.65-6.69 (m, 2H), 6.48-6.52 (m, 2H), 4.55 (q, 1H), 3.88 (br, 1H), 1.56 (d, 3H) ppm.

The enantiomeric excess was determined on the free amine by HPLC on chiral stationary phase with Daicel Chiralcel OD-H column: eluent Hexane/*i*PrOH = 99/1, flow rate 1.0 mL/min, λ=254 nm, τ_{major} = 21.6 min, τ_{minor} = 22.86 min.

***(R)-N*-(1-(3-(benzyloxy)phenyl)ethyl)-4-methoxyaniline 57**

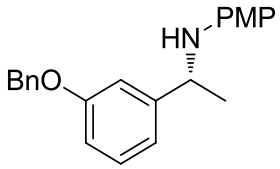

Prepared according to the general procedure. The crude mixture was purified by column chromatography on silica gel eluting with hexane/ethyl acetate 95:5 afford the title product as a yellowish solid. All analytical data are in agreement with literature.[xxii]

^{1}H-NMR (300 MHz, $CDCl_3$) δ_H 7.5-7.0 (m, 9H), 6.72 (d, 2H), 6.51 (d, 2H), 5.06 (s, 2H), 4.40 (q, 1H) 3.73 (s, 3H), 1.52 (d, 3H). **MS** (ESI+) m/z for $C_{22}H_{23}NO_2$(+1): 333.8; **$[\alpha_D]^{23}$** = + 4.2 (c: 0.9 $CHCl_3$).

The enantiomeric excess was determined by HPLC on chiral stationary phase with Daicel Chiralcel OD-H column: eluent Hexane/*i*PrOH = 98/2, flow rate 1.0 mL/min, λ=254 nm, τ_{major} = 31.8 min, τ_{minor} = 46.7 min.

***(R)-N*-(4-methoxyphenyl)-2,3-dihydro-1H-inden-1-amine 58**

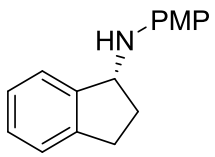

Prepared according to the general procedure. The crude mixture was purified by column chromatography on silica gel eluting with hexane/ethyl acetate 97:3 afford the title product as a yellowish solid. All analytical data are in agreement with literature.[xxiii]

^{1}H-NMR (300 MHz, $CDCl_3$) δ_H 7.41 (d, 1H), 7.28 (m, 3H), 6.83 (d, 2H), 6.73 (d, 2H), 4.98 (t, 1H), 3.79 (s, 3H), 3.02 (m, 1H), 2.93 (sest, 1H), 2.60 (m, 1H), 1.94 (m, 1H).

The enantiomeric excess was determined by chiral HPLC with Daicel Chiralcel IB column, eluent: 99:1 Hex/IPA; 0.75 mL/min flow rate, detection: 230 nm, t_{major} 14.7 min, t_{minor} 15.7 min.

[xxii] A. Genoni, M. Benaglia, E. Mattiolo, S. Rossi, L. Raimondi, P. C. Barrulas, A. J. Burke *Tetrahedron. Lett.*, **2015**, *42*, 5752.

[xxiii] S. L. Buchwald, M. C. Hansen, *Org. Lett.* **2000**, *2*, 713.

(*R*)-4-methoxy-*N*-(2,2,2-trifluoro-1-phenylethyl)aniline 59

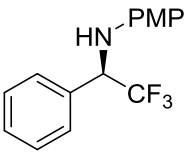

Prepared according to the general procedure. The crude mixture was purified by column chromatography on silica gel eluting with hexane/ethyl acetate 95:5 afford the title product as a yellowish solid. All analytical data are in agreement with literature.[xxiv]

^{1}H-NMR (300 MHz, $CDCl_3$) δ_H 7.44-7.46 (m, 2H), 7.36-7.42 (m, 3H), 6.72-6.76 (m, 2H), 6.59-6.63 (m, 2H), 4.81 (q, 1H), 3.72 (s, 3H) ppm; **^{19}F-NMR** (281 MHz, $CDCl_3$) δ_F -74.5 ppm.

The enantiomeric excess was determined by HPLC on chiral stationary phase with Daicel Chiralcel OD-H column: eluent Hexane/*i*PrOH = 95/5, flow rate 0.8 mL/min, λ=254 nm, τ_{minor}=13.2 min, τ_{major}=20.7 min.

(*R*)-4-methoxy-*N*-(1,1,1-trifluorobutan-2-yl)aniline 60

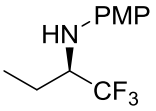

Prepared according to the general procedure. The crude mixture was purified by column chromatography on silica gel eluting with hexane/ethyl acetate 95:5 afford the title product as a yellowish solid. All analytical data are in agreement with literature.[xxiv]

^{1}H-NMR (300 MHz, $CDCl_3$) δ_H 6.78 (d, 2H), 6.64 (d, 2H), 3.75 (s, 3H), 3.71-3.59 (m, 1H), 3.27 (bs, 1H), 1.86-2.00 (m, 1H), 1.49-1.64 (m, 1H), 1.05 (t, 3H) ppm; **^{19}F-NMR** (281 MHz, $CDCl_3$) δ_F -76.3 ppm.

The enantiomeric excess was determined by HPLC on chiral stationary phase with Daicel Chiralcel OD-H column: eluent Hexane/*i*PrOH = 99/1, flow rate 0.8 mL/min, λ=254 nm, τ_{miajor}=10.1 min, τ_{minor}=12.1 min.

Methyl (*S*)-2-((4-methoxyphenyl)amino)-2-phenylacetate 61

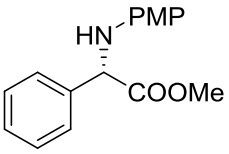

Prepared according to the general procedure. The crude mixture was purified by column chromatography on silica gel eluting with hexane/ethyl acetate 8:2 afford the title product as a yellowish solid. All analytical data are in agreement with literature.[xxv]

^{1}H-NMR (300 MHz, $CDCl_3$) δ_H 7.53-7.51 (m, 2H), 7.39-7.36 (m, 3H), 6.75 (d, 2H), 6.56 (d, 2H), 5.03 (s, 1H), 4.70 (br s, 1H), 3.73 (s, 3H), 3.71 (s, 3H). ppm.

The enantiomeric excess was determined by HPLC on chiral stationary phase with Daicel Chiralcel OJ-H column: eluent Hexane/*i*PrOH = 7/3, flow rate 0.8 mL/min, λ=210 nm, τ_{minor} = 50.3 min, τ_{major} = 54.2 min.

[xxiv] A. Genoni, M. Benaglia, E. Massolo, S. Rossi, *Chem. Commun.* **2013**, *49*, 8365.
[xxv] M. Bonsignore, M. Benaglia, R. Annunziata, G. Celentano, *Synlett*, **2011**, *8*, 1085.

Methyl (*R*)-3-((4-methoxyphenyl)amino)-3-phenylpropanoate 62

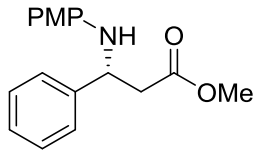

Prepared according to the general procedure. The crude mixture was purified by column chromatography on silica gel eluting with hexane/ethyl acetate 95:5 afford the title product as a yellowish solid. All analytical data are in agreement with literature. [xxv]

^{1}H-NMR (300 MHz, $CDCl_3$) δ_H 7.32-7.20 (m, 5H), 6.70 (d, 2H), 6.50 (d, 2H), 4.78 (m, 1H), 3.70 (s, 3H), 3.60 (s, 3H), 2.75 (d, 2H) ppm.

The enantiomeric excess was determined by HPLC on chiral stationary phase with Chiralcel cellulose 1 3 micron column: eluent Hexane/*i*PrOH = 95/5, flow rate 0.8 mL/min, λ=210 nm, τ_{major} = 22.7 min, τ_{minor} = 31.0 min.

Methyl (*R*)-3-((4-methoxyphenyl)amino)-3-(4-(trifluoromethyl)phenyl)propanoate 63

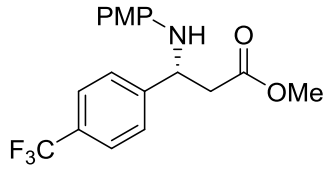

Prepared according to the general procedure. The crude mixture was purified by column chromatography on silica gel eluting with hexane/ethyl acetate 9:1 afford the title product as a yellowish solid. All analytical data are in agreement with literature.[xxv]

^{1}H-NMR (300 MHz, $CDCl_3$) δ_H 7.61 (d, 2H), 7.52 (d, 2H), 6.74 (d, 2H), 6.53 (d, 2H), 4.84 (t, 1H), 3.72 (s, 3H), 3.69 (s, 3H), 2.82 (d, 2H) ppm.

The enantiomeric excess was determined by HPLC on chiral stationary phase with Daicel Chiralcel OD column: eluent Hexane/*i*PrOH = 9/1, flow rate 0.8 mL/min, λ=254 nm, τ_{minor} = 14.5 min, τ_{major} =1 6.5 min.

Ethyl (*R*)-3-((4-methoxyphenyl)amino)-3-(4-nitrophenyl)propanoate 64

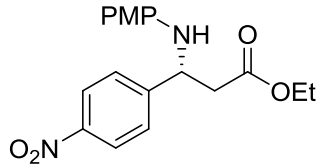

Prepared according to the general procedure. The crude mixture was purified by column chromatography on silica gel eluting with hexane/ethyl acetate 9:1 afford the title product as a yellowish solid. All analytical data are in agreement with literature.[xxv]

^{1}H-NMR (300 MHz, $CDCl_3$) δ_H 8.19 (d, 2H), 7.58 (d, 2H), 6.72 (d, 2H), 6.49 (d, 2H), 4.86 (t, 1H), 4.48 (bs, 1H), 4.14 (q, 2H), 3.71 (s, 3H), 2.84 (dd, 1H), 2.81 (dd, 1H), 1.22 (t, 3H), ppm.

The enantiomeric excess was determined by HPLC on chiral stationary phase with Daicel Chiralcel AD column: eluent hexane/*i*PrOH = 9/1, flow rate 0.8 mL/min, λ=230 nm, τ_{major} = 42.7 min, τ_{minor} = 46.7 min.

General Set-Up of Continuous Flow Reactions with Solid Supported Organocatalysts

4.2 Microreactor Tehnology

4.2.1 Stereoselective Flow Synthesis of APIs Intermediates

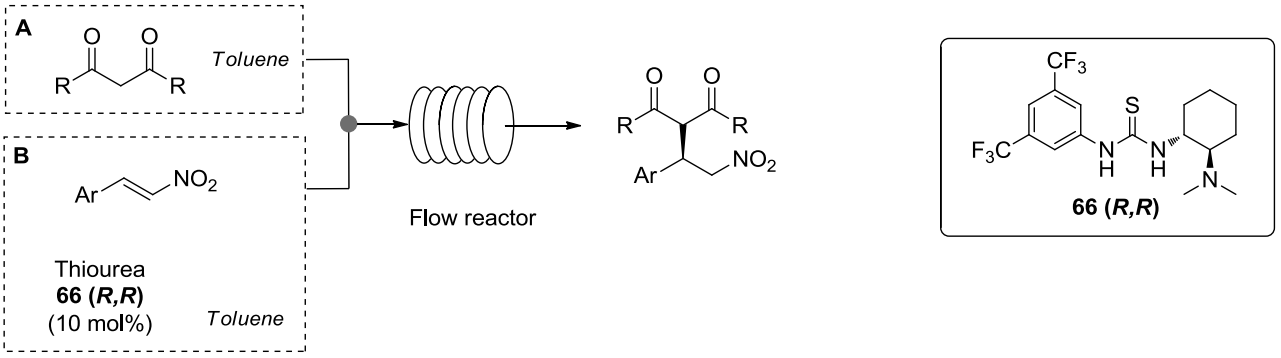

General procedure for continuous flow reaction

Syringe A was filled with a solution of *trans*-β-nitrostyrene (2 mmol) and phenantrene (1 mmol, internal standard) in dry toluene (1 mL). Syringe B was loaded with a solution of chiral thiourea **66**[xxvi] (0.2 mmol) and acetylacetone (4 mmol) in dry toluene (0.6 mL). Syringes A and B were connected to a syringe pump and the reagents were pumped into the microreactor at the indicated flow rate (mL/min) and temperature. Three reactor volumes were discarded before starting sample collection in order to achieve steady-state conditions. Reaction outcome was collected into a vial at room temperature and analyzed through ^{1}H-NMR spectroscopy and HPLC in order to determine conversion and enantiomeric excess.

Diethyl (*R*)-2-(2-nitro-1-phenylethyl)malonate 65

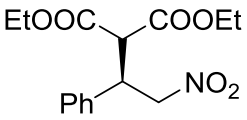

Prepared according to the general procedure. The crude mixture was purified by column chromatography on silica gel eluting with hexane/ethyl acetate 8:2 to afford the title product as colorless oil. All analytical data are in agreement with literature.[xxvi]

^{1}H-NMR (300 MHz, $CDCl_3$): δ_H 1.95 (s, 3H), 2.29 (s, 3H), 4.25-4.29 (m, 1H), 4.38 (d, J = 10.7 Hz, 1H), 4.60-4.69 (m, 2H), 7.09-7.21 (m, 2H), 7.21-7.39 (m, 3H).

The enantiomeric excess was determined by HPLC on chiral stationary phase with Daicel Chiralcel OD-H column: eluent hexane/*i*PrOH = 98/2, flow rate 0.8 mL/min, λ=280 nm, τ_{minor} = 7.9 min, τ_{major} = 10.8 min.

[xxvi] T. Okino, T. Hoashi, T. Furukawa, X. Xu, Y. Takemoto, *J. Am. Chem. Soc.* **2005**, *127*, 119.

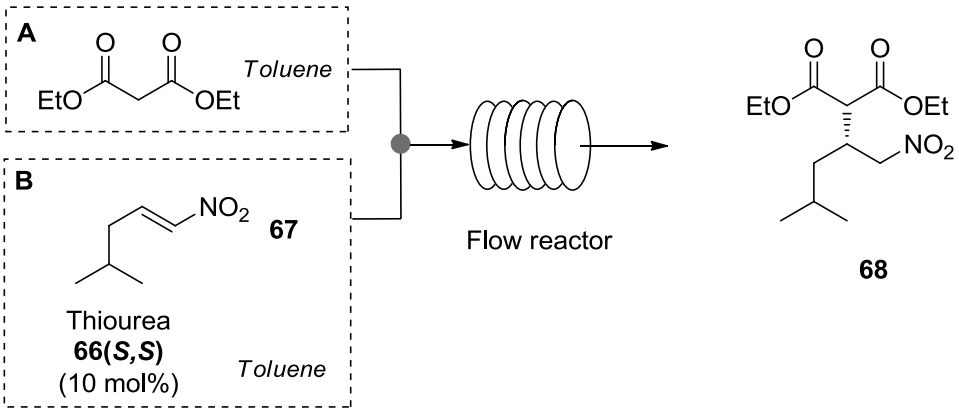

General procedure for continuous flow reaction

Syringe A was filled with a solution of nitroalkene **67** (2 mmol) and phenantrene (1 mmol, internal standard) in dry toluene (1 mL). Syringe B was loaded with a solution of chiral thiourea **66** (0.2 mmol) and diethylmalonate (6.6 mmol). Syringes A and B were connected to a syringe pump and the reagents were pumped into the microreactor at the indicated flow rate (μL/min) and temperature. Three reactor volumes were discarded before starting sample collection in order to achieve steady-state conditions. Reaction outcome was collected into a vial at room temperature and analyzed through ^{1}H-NMR spectroscopy and HPLC in order to determine conversion and enantiomeric excess.

Diethyl (*S*)-2-(4-methyl-1-nitropentan-2-yl)malonate 68

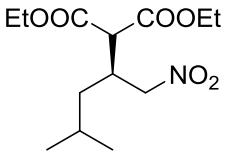

Prepared according to the general procedure. The crude mixture was purified by column chromatography on silica gel eluting with hexane/ethyl acetate 8:2 afford the title product as colorless oil. All analytical data are in agreement with literature.[xxvi]

^{1}H-NMR (300 MHz, $CDCl_3$): δ_H 4.70 (dd, J = 13, 5 Hz, 1H), 4.51 (dd, J = 13, 6 Hz, 1H), 4.28-4.20 (m, 4H), 3.62 (d, J = 5 Hz, 1H), 3.00-2.95 (m, 1H), 1.72-1.66 (m, 1H), 1.38-1.28 (m, 8H), 0.96-0.92 (m, 6H).

The enantiomeric excess was determined by HPLC on chiral stationary phase with Daicel Chiralcel OD-H column: eluent hexane/*i*PrOH = 98/2, flow rate 0.8 mL/min, λ = 280 nm, τ_{minor} = 7.9 min, τ_{major}= 10.8 min.

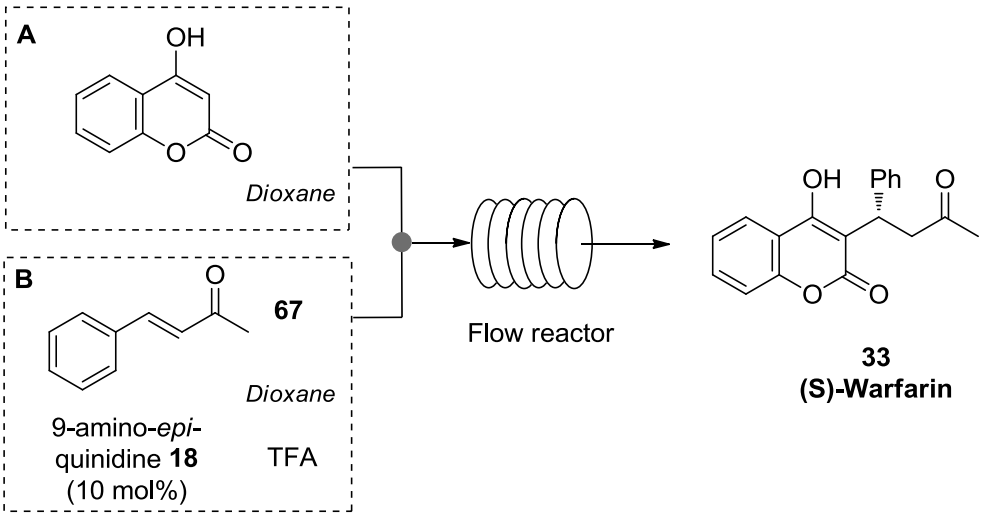

General procedure for continuous flow reaction

Syringe A was filled with a solution of 4-hydroxy-coumarin (0.2 mmol) in dry dioxane (1 mL). Syringe B was loaded with a solution of chiral primary amine **18** (0.02 mmol), trifluoroacetic acid (0.03 mmol) and benzalacetone (0.4 mmol) in dry dioxane (1 mL). Syringes A and B were connected to a syringe pump and the reagents were pumped into the microreactor at the indicated flow rate (μL/min) and temperature. Three reactor volumes were discarded before starting sample collection in order to achieve steady-state conditions. Reaction outcome was collected into a vial at room temperature and analyzed through ^{1}H-NMR spectroscopy and HPLC in order to determine conversion and enantiomeric excess.

4.2.2 Continuous Flow Reduction of Nitro Compounds

General procedure for continuous flow reaction

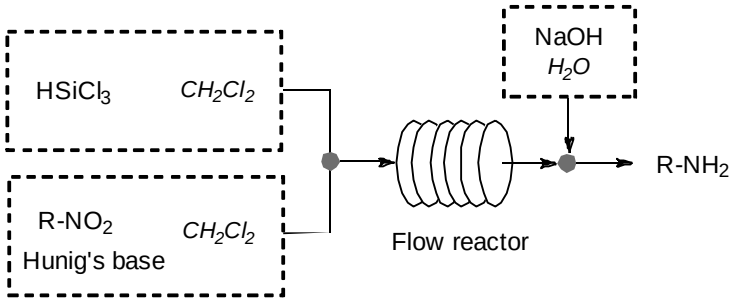

Syringe A was filled with a solution of $HSiCl_3$ (2.4 mmol) in dry CH_2Cl_2 (1.5 mL). Syringe B was loaded with a solution of nitro compound (0.6 mmol) and Hunig's base (3.6 mmol) in dry CH_2Cl_2 (1.5 mL). Syringes A and B were connected to a syringe pump and the reagents were pumped into the microreactor at the indicated flow rate (mL/min) at room temperature. The outcome of the reactor was collected containing 10% NaOH solution. Five reactor volumes were collected. CH_2Cl_2 was removed *in vacuo* and aqueous layer was extracted three times with ethyl acetate. The combined organic layers were washed with brine, dried with Na_2SO_4 and concentrated *in vacuo*. ^{1}H-NMR of the crude gave reaction conversion; in case of a full conversion of the starting material no further purification was required.

4-amino benzophenone 69

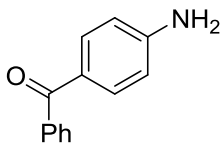

Prepared according to the general procedure. **2a** was obtained as yellowish solid (95 mg, 96 % yield). **^{1}H-NMR** (300 MHz, $CDCl_3$) δ_H 7.72 (m, 4H), 7.54 (t, *J* = 7.4 Hz, 1H), 7.46 (t, *J* = 7.4 Hz, 2H), 6.68 (d, *J* = 8.4 Hz, 2H), 4.10 (bs, 2H, NH).

***p*-toluidine 70**

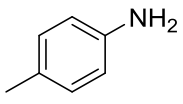

Prepared according to the general procedure. **2b** was obtained as yellowish solid (51 mg, 96% yield). **^{1}H-NMR** (300 MHz, $CDCl_3$) δ_H 7.01 (d, *J* = 8.6 Hz, 2H), 6.66 (d, *J* = 8.6 Hz, 2H), 3.31 (bs, 2H), 2.27 (bs, 2H, NH).

4-bromoaniline 71

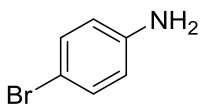

Prepared according to the general procedure. **2c** was obtained as white solid (78 mg, 92% yield). **^{1}H-NMR** (300 MHz, $CDCl_3$) δ_H 7.28 (d, *J* = 8.6 Hz, 2H), 6.58 (d, *J* = 8.6 Hz, 2H), 3.68 (bs, 2H, NH).

2,4-dichloroaniline 72

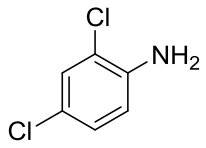

Prepared according to the general procedure. **2d** was obtained as yellowish solid (75 mg, 92% yield). **^{1}H-NMR** (300 MHz, $CDCl_3$) δ_H 7.26 (d, *J* = 2,2 Hz, 1H), 7.06 (dd, *J* = 8,6 Hz, J = 2,2 Hz, 1H), 6.70 (d, *J* = 8,6 Hz, 1H), 3.96 (bs, 1H).

4-fluoroaniline 73

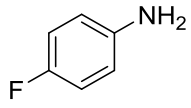

Prepared according to the general procedure. **2e** was obtained as yellowish solid (50 mg, 90% yield). **^{1}H-NMR** (300 MHz, $CDCl_3$) δ_H 6.82-6.88 (m, 2H), 6.59-6.64 (m, 2H), 3.49 (bs, 2H, NH).

Methyl 4-aminobenzoate 74

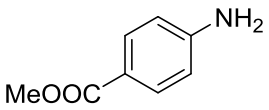

Prepared according to the general procedure. **2f** was obtained as yellowish solid (72 mg, 95% yield). **^{1}H-NMR** (300 MHz, $CDCl_3$) δ_H 7.84 (d, 2H), 6.64 (d, 2H), 4.04 (bs, 2H, NH), 3.85 (s, 3H).

2-phenylethanamine 75

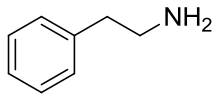

Prepared according to the general procedure. **2g** was obtained as yellowish oil (55 mg, 91% yield). **^{1}H-NMR** (300 MHz, $CDCl_3$) δ_H 7.1-7.4 (m, 5H), 2.98 (dd, *J* = 7.4 Hz, 2H), 2.83 (dd, *J* = 7.4 Hz, 2H), 1.62 (bs, 1H).

(*S*)-2-(2-nitroethyl)-1,4-dioxaspiro[4.5]decane 76

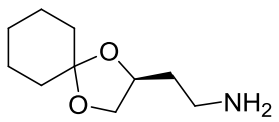

Prepared according to the general procedure. **2h** was obtained as yellowish oil (86 mg, 93% yield). **^{1}H-NMR** (300 MHz, $CDCl_3$) δ_H 4,36 (m, J=5,6 Hz, 1H), 4,16 (dd, *J* = 8,7 Hz, J=5,6 Mz, 1H), 3,79 (dd, J = 8,7 Hz, J=5,6 Hz, 1H), 2.62 (m, 2H), 1.66 (m, 2H), 1,63 (m, 2H), 1,57-1,59 (m, 6H), 1,41 (bs, 2H); **$[\alpha_D]^{25}$** = +29.2 (c: 0.36 $CHCl_3$).

4'-chloro-[1,1'-biphenyl]-2-amine 77

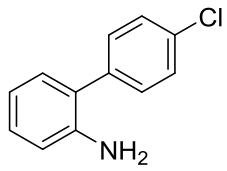

Prepared according to the general procedure. All analytical data are in agreement with literature.[xxvii] **77** was obtained as yellowish solid (100 mg, 98% yield). **^{1}H-NMR** (300 MHz, $CDCl_3$) δ_H 7.38-7.44 (m, 4H), 7.08-7.19 (m, 2H), 6.75-6.85 (m, 2H), 3.71 (bs, 2H).

(3*S*,4*R*)-ethyl 4-(4-chlorophenyl)-2-oxopyrrolidine-3-carboxylate 78

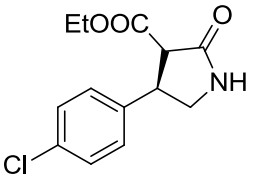

Prepared according to the general procedure. The crude mixture was purified by column chromatography on silica gel eluting with dichloromethane/methanol 95:5 afford the title product as a white solid (64 mg, 48% yield). All analytical data are in agreement with literature.[xxviii] **^{1}H NMR** (300 MHz, $CDCl_3$) δ_H 7.31-7.324 (m, 2H), 7.18-7.21 (m, 2H), 5.83 (bs, 1H), 4.20-4.26 (q, 2H), 4.05-4.13 (m, 1H), 3.78-3.84 (t, 1H), 3.47-3.50 (d, 1H), 3.36-3.42 (t, 1H), 1.28 (t, 3H); **$[\alpha_D]^{25}$** = +88.3 (c: 0.96 $CHCl_3$).

[xxvii] Z. Liang, L. Ju, Y. Xie, L. Huang, Y. Zhang, *Chem. Eur. J.* **2012**, *18*, 15816.
[xxviii] T. Okino, Y. Hoashi, T. Furukawa, X. Xu, Y. Takemoto, *J. Am. Chem. Soc.* **2005**, *127*, 119.

General Set-Up of Continuous Flow Reactions with Microreactors

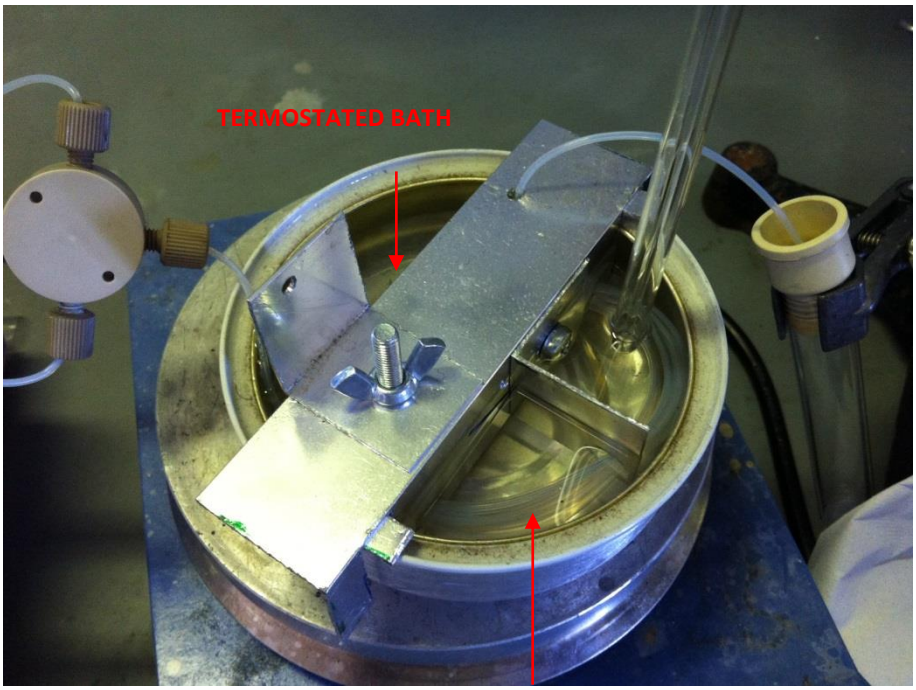

4.2.3 Synthesis of Chiral 1,2-Amino Alcohols using 3D-printed Reactors

Synthesis of compound 80

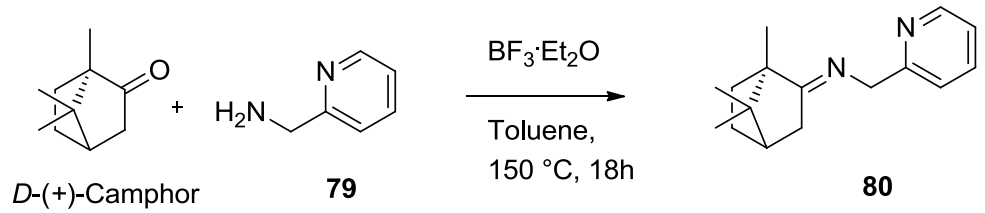

D-(+)-Camphor **79** **80**

In a two-necked flask, with addition of Dean-Stark and dropping funnel, *D*-(*+*)-Camphor (6.6 mmol), was placed under N_2 atmosphere then amine **79** (6.6 mmol) and BF_3Et_2O (0.4 mmol) were added and dissolved in toluene (16 mL). Reaction mixture was heated at 150 °C with a Dean Stark apparatus and stirred for 24 hours. After reaction time the crude was cooled to room temperature, diluted with ethyl acetate and washed with $NaHCO_3$ s.s.; the organic phase was extracted three times with AcOEt, dried over Na_2SO_4 and concentrated under vacuum. Imine **80** was obtained as dark yellow oil and was used in the following step without any further purification. Full conversion was demonstrated by NMR analysis of the crude.

^{1}H-NMR (300 MHz, $CDCl_3$) δ_H 8.50 (d, J = 4.82 Hz, 1H), 7.65 (dt, J = 7.70, 1.86 Hz, 1H), 7.48 (d, J = 7.83 Hz, 1H), 7.13 (m, 1H), 4.63 (d, J = 16.46 Hz, 1H), 4.55 (d, J = 16.3 Hz, 1H), 2.45 (m, 1H), 1.98 (m, 1H), 1.85 (m, 1H), 1.73 (m, 1H), 1.44 (m, 2H), 1.26 (m, 1H), 1.07 (s, 3H), 0.96 (s, 3H), 0.78 (s, 3H) ppm.

Synthesis of chiral aminopyridine 81

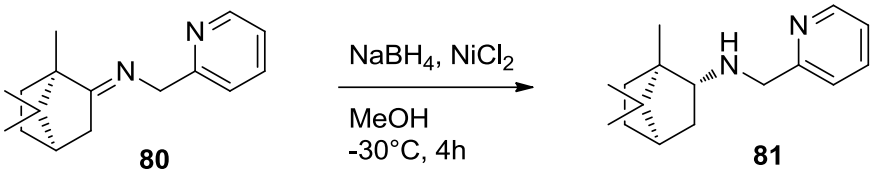

80 **81**

In a two-necked flask a solution of **80** (5.9 mmol) in methanol (60 mL) was prepared under N_2 atmosphere and cooled to -30 °C. $NiCl_2$ (11.8 mmol) was added and then $NaBH_4$ (5.9 mmol) was slowly introduced under stirring. Reaction progress was monitored by thin layer chromatography. After 24 hours no more starting material was detected; reaction mixture was concentrated, diluted with dichloromethane washed with an aqueous solution of NH_4Cl and extracted with dichloromethane; combined organic phases were dried over Na_2SO_4 and concentrated under vacuum. The crude mixture was purified by column chromatography on silica gel eluting with ethyl acetate affording **81** as a yellowish oil with (3.5 mmol, 60% yield).

^{1}H-NMR (300 MHz, $CDCl_3$) δ_H 8.55 (d, J = 4.39 Hz, 1H), 7.66 (dt, J = 7.66, 0.76 Hz, 1H), 7.37 (d, J = 6.79 Hz, 1H), 7.17 (m, 1H), 3.95 (d, J = 14.2 Hz, 1H), 3.88 (d, J = 14.18 Hz, 1H), 2.68 (m, 1H), 1.72-1.51 (m, 6H), 1.28 (m, 1H), 1.12 (s, 3H), 0.99 (s, 3H), 0.85 (s, 3H) ppm.

Synthesis of compound 82

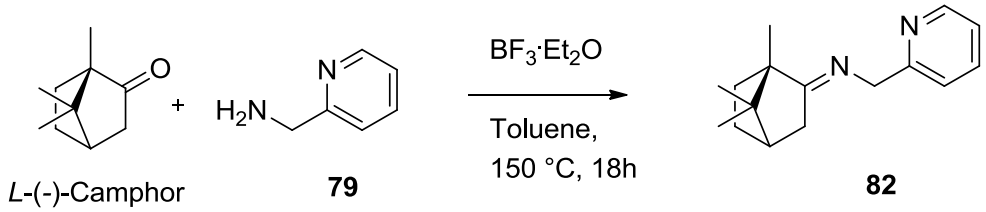

L-(-)-Camphor **79** **82**

In a two-necked flask, with addition of Dean-Stark and dropping funnel, *L*-(-)-Camphor (6.6 mmol), was placed under N_2 atmosphere then amine **79** (6.6 mmol) and BF_3Et_2O (0.4 mmol) were added and dissolved in toluene (16 mL). Reaction mixture was heated at 150 °C with a Dean Stark apparatus and stirred for 24 hours. After reaction time the crude was cooled to room temperature, diluted with ethyl acetate and washed with $NaHCO_3$ s.s.; the organic phase was extracted three times with AcOEt, dried over Na_2SO_4 and concentrated under vacuum. Imine **82** was obtained as dark yellow oil and was used in the following step without any further purification. Full conversion was demonstrated by NMR analysis of the crude.

^{1}H-NMR (300 MHz, $CDCl_3$) δ_H 8.50 (d, J = 4.82 Hz, 1H), 7.65 (dt, J = 7.70, 1.86 Hz, 1H), 7.48 (d, J = 7.83 Hz, 1H), 7.13 (m, 1H), 4.63 (d, J = 16.46 Hz, 1H), 4.55 (d, J = 16.3 Hz, 1H), 2.45 (m, 1H), 1.98 (m, 1H), 1.85 (m, 1H), 1.73 (m, 1H), 1.44 (m, 2H), 1.26 (m, 1H), 1.07 (s, 3H), 0.96 (s, 3H), 0.78 (s, 3H) ppm.

Synthesis of chiral aminopyridine 83

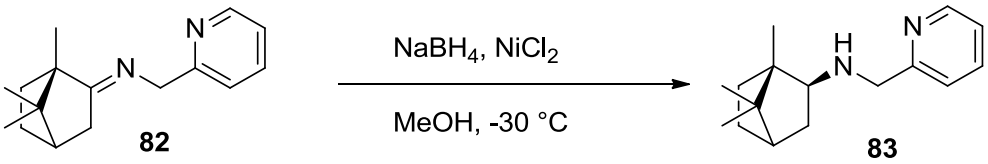

82 **83**

In a two-necked flask a solution of **80** (5.9 mmol) in methanol (60 mL) was prepared under N_2 atmosphere and cooled to -30 °C. $NiCl_2$ (11.8 mmol) was added and then $NaBH_4$ (5.9 mmol) was slowly introduced under stirring. Reaction progress was monitored by thin layer chromatography. After 24 hours no more starting material was detected; reaction mixture was concentrated, diluted with dichloromethane washed with an aqueous solution of NH_4Cl and extracted with dichloromethane; combined organic phases were dried over Na_2SO_4 and concentrated under vacuum. The crude mixture was purified by column chromatography on silica gel eluting with ethyl acetate affording **83** as a yellowish oil with (3.5 mmol, 60% yield).

^{1}H-NMR (300 MHz, $CDCl_3$) δ_H 8.55 (d, J = 4.39 Hz, 1H), 7.66 (dt, J = 7.66, 0.76 Hz, 1H), 7.37 (d, J = 6.79 Hz, 1H), 7.17 (m, 1H), 3.95 (d, J = 14.2 Hz, 1H), 3.88 (d, J = 14.18 Hz, 1H), 2.68 (m, 1H), 1.72-1.51 (m, 6H), 1.28 (m, 1H), 1.12 (s, 3H), 0.99 (s, 3H), 0.85 (s, 3H) ppm. **^{13}C-NMR** (75 MHz, $CDCl_3$): 160.85, 149.04, 136.19, 122.19, 121.60, 66.52, 54.22, 48.46, 46.72, 45.28, 38.74, 36.84, 27.33, 20.59, 12.17 ppm. **MS (ESI)**: 245.3.

General procedure for stereoselective Henry reaction

Batch reaction

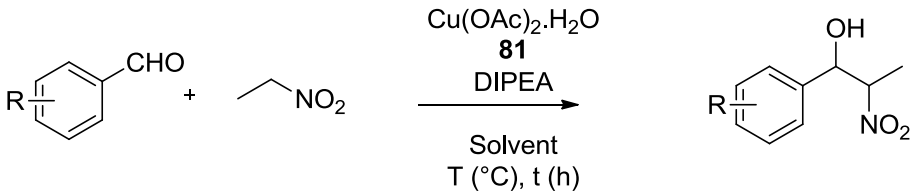

In a round-bottom flask, chiral aminopyridine **81** (or **83**) (15 mg, 0.0625 mmol) and $Cu(OAc)_2$ (10 mg, 0.05 mmol) were dissolved in the indicated solvent (1.75 mL) and the solution was stirred for 10 minutes; then aldehyde (0.25 mmol, 25 µL) was added and mixture was stirred for 30 minutes. After this period the mixture was cooled to the desired temperature and nitroethane (2.5 mmol, 179 µL) and DIPEA (0.25 mmol, 44 µL) were added. The mixture was stirred at the same temperature for the indicated temperature. After reaction time the crude mixture was diluted with ethyl acetate (5 mL), quenched with HCl 10% (1 mL) and rapidly extracted with ethyl acetate (3x5 mL); the combined organic layers were then washed with brine, dried over Na_2SO_4 and concentrated under vacuum conditions. The crude product was purified by column chromatography on silica gel.

Flow reaction

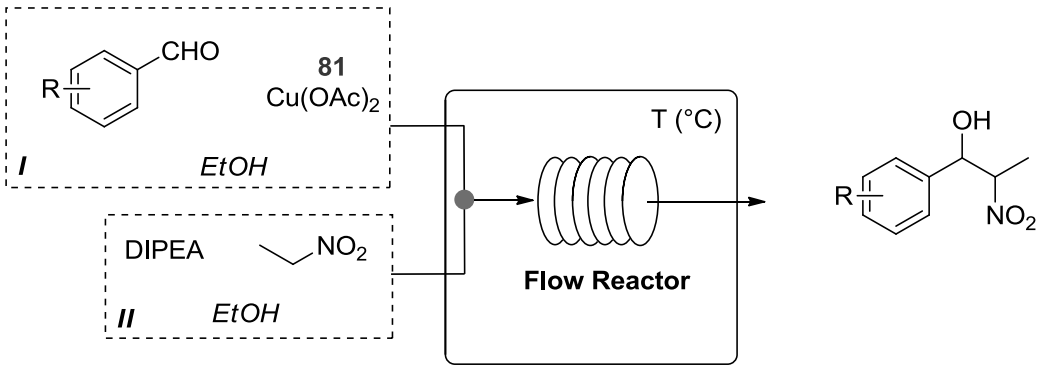

In a round-bottom flask, ligand **81** (or **83**) (0.0625 mmol) and $Cu(OAc)_2$ (0.0625 mmol) were dissolved in ethanol (1.75 mL) and the solution was stirred for 10 minutes; aldehyde (0.25 mmol) was, then, added and mixture was again stirred for 30 minutes; in another flask, nitroethane (2.5 mmol) and DIPEA (0.25 mmol) were added in ethanol. The solutions were charged into two different syringes, placed on a syringe-pump and injected into the indicate flow reactor at the indicated flow rate and temperature. The outcome of the reactor was collected at -78 °C. After reaction time the crude mixture was diluted with ethyl acetate (5 mL), quenched with HCl 10% (1 mL) and rapidly extracted with ethyl acetate three times (5 mL); the combined organic layers were then washed with brine, dried over Na_2SO_4 and concentrated under vacuum conditions. The crude mixture was purified by column chromatography on silica gel.

1-(3-(benzyloxy)phenyl)-2-nitropropan-1-ol 84

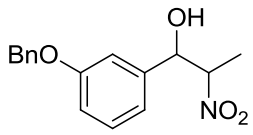

Prepared according to the general procedure. The crude mixture was purified by column chromatography on silica gel eluting with hexane/ethyl acetate 9:1. The title product was obtained as a yellowish oil. All analytical data are in agreement with literature.

^{1}H-NMR (300 MHz, $CDCl_3$) anti δ_H 7.48-6.93 (m, 9H), 5.38 (d, J = 3.03 Hz, 1H), 5.08 (s, 2H), 4.73-4.63 (m, 1H), 1.48 (d, J = 6.83 Hz, 3H); syn δ_H 7.48-6.93 (m, 9H), 5.13 (s, 2H), 4.98 (d, J = 8.86 Hz, 1H), 4.76 (m, 1H), 1.31 (d, J = 6.83 Hz, 3H) ppm. **^{13}C-NMR** (75 MHz, $CDCl_3$): 159.05, 140.24, 139.94, 136.72, 129.87, 128.64, 128.09, 127.55, 119.50, 118.45, 115.61, 114.85, 113.44, 112.67, 88.38, 87.36, 76.18, 73.73, 70.09, 16.43, 11.95 ppm; **MS** (ESI): 287.1.

The enantiomeric excess was determined by HPLC on chiral stationary phase with Phenomenex Lux Cellulose-1 column: eluent Hexane/*i*PrOH = 90/10, flow rate 0.8 mL/min, λ=210 nm, anti τ_{1S2R} = 39.3 min, anti τ_{1R2S} = 21.2 min, syn τ_{1S2S} = 32.9 min, syn τ_{1R2R} = 24.6 min.

2-nitro-1-phenylpropan-1-ol 85

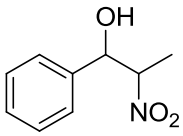

Prepared according to the general procedure. The crude mixture was purified by column chromatography on silica gel eluting with hexane/ethyl acetate 9:1. The title product was obtained as a yellowish oil.. All analytical data are in agreement with literature. [xxix]

^{1}H-NMR (300 MHz, $CDCl_3$) anti: δ_H 7.41-7.38 (m, 5H), 5.43 (d, J = 3.52 Hz, 1H), 4.74-4.70 (m, 1H), 1.53 (d, J = 6.82 Hz, 3H); syn: 7.41-7.38 (m, 5H), 5.05 (d, J = 9.01 Hz, 1H), 4.83-4.79 (m, 1H), 1.34 (d, J = 6.8 Hz, 3H) ppm.

The enantiomeric excess was determined by HPLC on chiral stationary phase with Phenomenex Lux Cellulose-1 column: eluent Hexane/*i*PrOH = 95/5, flow rate 0.8 mL/min, λ=230 nm, anti τ_{1S2R} = 25.9 min, anti τ_{1R2S} = 16.9 min, syn τ_{1S2S} = 24.3 min, syn τ_{1R2R} = 18.9 min

[xxix] D. Uraguchi, S. Sakaki, T. Ooi, *J. Am. Chem. Soc.* **2007** , *129*, 12392.

1-(2,5-dimethoxyphenyl)-2-nitropropan-1-ol 86

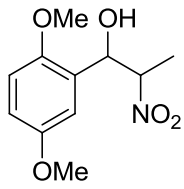

Prepared according to the general procedure. The crude mixture was purified by column chromatography on silica gel eluting with hexane/ethyl acetate 9:1. The title product was obtained as a yellowish oil. All analytical data are in agreement with literature. [xxx]

^{1}H-NMR (300 MHz, $CDCl_3$) anti δ_H 7.02 (s, 1H), 6.82 (d, J = 1.54 Hz, 2H), 5.51 (d, J = 2 Hz, 1H), 4.90 (m, 1 H), 3.83 (s, 3H), 3.78 (s, 3H), 1.49 (d, J = 6.89 Hz, 3H); syn δ_H 6.85 (m, 3H), 5.11 (d, J = 8.9 Hz, 1H), 4.96 (m, 1H), 3.85 (s, 3H), 3.78 (s, 3H), 1.36 (d, J = 6.77 Hz, 3H) ppm.

The enantiomeric excess was determined by HPLC on chiral stationary phase with Daicel Chiralcel AD column: eluent Hexane/*i*PrOH = 9/1, flow rate 0.8 mL/min, λ=210 nm, anti $\tau_{1S,2R}$ = 14.8 min, anti $\tau_{1R,2S}$ = 17.0 min, syn $\tau_{1S,2S}$ = 20.7 min, syn $\tau_{1R,2R}$ = 34.7 min

1-(3,4-bis(benzyloxy)phenyl)-2-nitropropan-1-ol 87

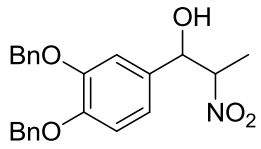

Prepared according to the general procedure. The crude mixture was purified by column chromatography on silica gel eluting with hexane/ethyl acetate 9:1. The title product was obtained as a yellowish oil.

^{1}H-NMR (300 MHz, $CDCl_3$) anti δ_H 7.48-6.85 (m, 13H), 5.26 (d, J = 3.78 Hz, 1H), 5.17 (s, 4H), 4.59 (m, 1H), 1.43 (d, J = 6.81 Hz, 3H); syn δ_H 7.48-6.85 (m, 13H), 5.18 (s, 4H), 4.90 (d, J = 9.13 Hz, 1H), 4.66 (m, 1H), 1.22 (d, J = 6.80 Hz, 3H) ppm. **^{13}C-NMR** (75 MHz, $CDCl_3$): 149.5, 148.9, 137.0, 136.9, 131.9, 131.6, 128.5, 128.0, 127.5, 127.3, 120.3, 119.2, 114.8, 113.7, 113.1, 88.5, 87.5, 76.0, 73.7 71.3, 71.2, 16.3, 12.2

The enantiomeric excess was determined by HPLC on chiral stationary phase with Phenomenex Amylose-2 column: eluent Hexane/*i*PrOH/EtOH = 70/25/5, flow rate 0.9 mL/min, λ=210 nm, anti $\tau_{1S,2R}$ = 11.6 min, anti $\tau_{1R,2S}$ = 10.1 min, syn $\tau_{1S,2S}$ = 20.2 min, syn $\tau_{1R,2R}$ = 12.8 min

[xxx] K. Lang, J. Park, S. Hong, Angew. Chem. Int. Ed., **2012** , *51*, 1620.

General procedure for continuous flow hydrogenation

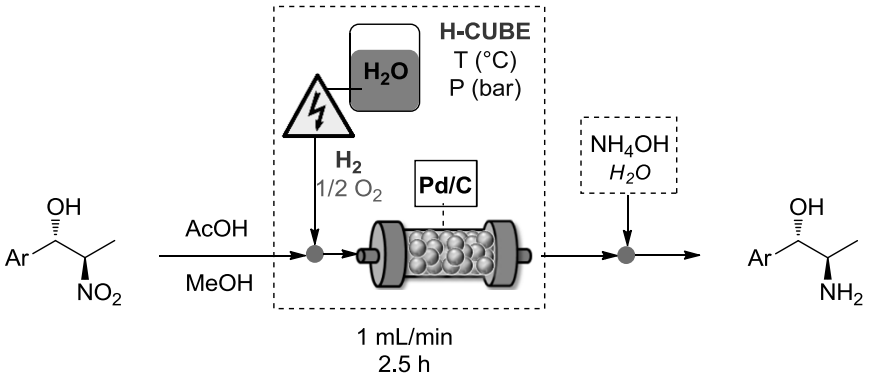

Nitroalcohol **84-87** (1 mmol) was placed into a beaker and dissolved in methanol (10 mL) and AcOH was added (30 mmol, 500 µL). The reaction mixture was pumped into H-Cube Mini containing a cartridge of Pd/C (l = 3.5 cm) at the indicated pressure of H_2 and temperature. Reaction progress was monitored by TLC. After 2.5 hours no more starting material was detected. The crude was concentrated under vacuum.

1-(3-(benzyloxy)phenyl)-2-nitropropan-1-ol 88

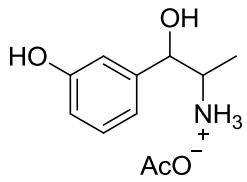

Prepared according to the general procedure at 50 bar and 50 °C. The crude mixture was concentrated and dried under vacuum. The product was obtained in the form of acetate salt as withe solid. All analytical data are in agreement with literature.

^{1}H-NMR (300 MHz, CD_3OD) anti δ_H 7.23-6.73 (m, 4H), 4.90 (d, J = 3.03 Hz, 1H), 3.49 (m, 1H), 1.96 (s, 3H), 1.11 (d, J = 6.63 Hz, 3H); syn δ_H 7.23-6.73 (m, 4H), 4.42 (d, J = 8.53 Hz, 1H), 3.34 (m, 1H), 1.96 (s, 3H), 1.12 (d, J = 6.65 Hz, 3H) ppm.

The enantiomeric excess was determined by HPLC on chiral stationary phase (reverse phase).

2-nitro-1-phenylpropan-1-ol 89

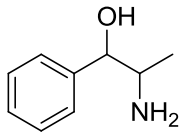

Prepared according to the general procedure procedure at 15 bar and 30 °C. The crude mixture was purified by treatment with NH_4OH (33% wt.) and extraction with AcOEt (5 times). The title product was obtained as a yellowish solid. All analytical data are in agreement with literature. [xxxi]

^{1}H-NMR (300 MHz, $CDCl_3$) anti δ_H 7.34-7.25 (m, 5H), 4.45 (d, J = 5.47 Hz, 1H), 3.06-2.97 (m, 1H), 1.03 (d, J = 6.54 Hz, 3H); syn δ_H 7.34-7.25 (m, 5H), 4.23 (d, J = 6.52 Hz, 1H), 3.06-2.97 (m, 1H), 0.88 (d, J = 6.56 Hz, 3H) ppm.

[xxxi] G. K. Lalwani, A. Sudalai, *Tetrahedron Letters*, **2015** , *56*,6488.

1-(2,5-dimethoxyphenyl)-2-nitropropan-1-ol 90

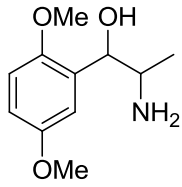

Prepared according to the general procedure at 20 bar and 30 °C. The crude mixture was purified by treatment with NH_4OH (33% wt.) and extraction with AcOEt (5 times). The title product was obtained as a yellowish solid. All analytical data are in agreement with literature. [xxxii]

^{1}H-NMR (300 MHz, $CDCl_3$) anti δ_H 7.01-6.74 (m, 3H), 4.77 (d, J = 4.63 Hz, 1H), 3.78 (s, 6H), 3.30 (m, 1H), 1.00 (d, J = 6.52 Hz, 3H); syn δ_H 7.01-6.74 (m, 3H), 4.56 (d, J = 5.83 Hz, 1H), 3.14 (m, 1H), 1.06 (d, J = 6.49 Hz, 3H) ppm.

General procedure for derivatization of aminoalcohols

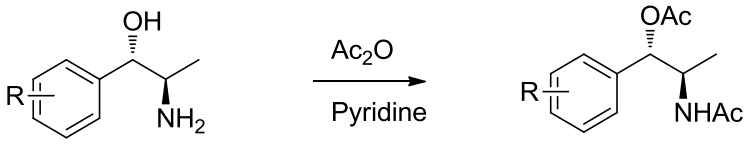

1,2-Amino alcohol was dissolved in pyridine and Ac_2O was slowly added. The reaction was stirred at rt for 24 hours. After reaction time a small portion of ice was added and the the crude was trated with HCl 37%. The aqueous layer was extracted with dichloromethane. The combined organic phases were treated with NaOH 10%, washed with brine, dried with Na_2SO_4 and concentrated under vacuum. The crude product was purified by column chromatography on silica gel.

2-acetamido-1-phenylpropyl acetate 91

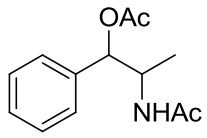

Prepared according to the general procedure. The crude mixture was purified by column chromatography on silica gel eluting with Dichloromethane/ Methanol 98:2. The title product was obtained as a yellowish oil. All analytical data are in agreement with literature. [xxxiii]

^{1}H-NMR (300 MHz, $CDCl_3$) anti δ_H 7.34-7.26 (m, 5H), 5.83 (d, J = 3.81 Hz, 1H), 4.45 (m, 1H), 2.13 (s, 3H), 1.92 (s, 3H), 1.05 (d, J = 6.84 Hz, 3H); syn δ_H 7.34-7.26 (m, 5H), 5.70 (d, J = 6.92 Hz, 1H), 4.42 (m, 1H), 2.09 (s, 3H), 1.91 (s, 3H), 1.03 (d, J = 6.56 Hz, 3H) ppm.
The enantiomeric excess was determined by HPLC on chiral stationary phase with Daicel Chiralcel AD column: eluent Hexane/*i*PrOH = 90/10, flow rate 0.8 mL/min, λ=210 nm, anti τ_{1S2R} = 10.6 min, anti τ_{1R2S} = 13.2 min.

[xxxii] K. Lang, J. Park, S. Hong, Angew. Chem. Int. Ed., **2012** , *51*, 1620.
[xxxiii] R. A. Feick *et al. J. Med. Chem*., **2005** , *48*, 1229.

2-acetamido-1-(2,5-dimethoxyphenyl)propyl acetate 92

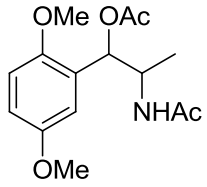

Prepared according to the general procedure. The crude mixture was purified by column chromatography on silica gel eluting with Dichloromethane/ Methanol 98:2. The title product was obtained as a yellowish oil. All analytical data are in agreement with literature. [xxxiv]

^{1}H-NMR (300 MHz, $CDCl_3$) anti: δ_H 6.85-6.78 (m, 3H), 6.10 (d, J = 4.91 Hz, 1H), 4.42 (m, 1H), 3.82 (s, 3H), 3.76 (s, 3H), 2.13 (s, 3H), 1.90 (s, 3H), 1.08 (d, J = 6.76 Hz, 3H); syn δ_H 6.85-6.76 (m, 3H), 6.12 (d, J = 5.69 Hz, 1H), 4.42 (m, 1H), 3.80 (s, 3H), 3.76 (s, 3H), 2.11 (s, 3H), 1.88 (s, 3H), 1.09 (d, J = 6.77 Hz, 3H) ppm. **^{13}C-NMR** (75 MHz, $CDCl_3$): 189.5, 170.2, 169.1, 153.6, 150.4, 127.2, 113.4, 112.8, 111.6, 72.3, 56.2, 56.1, 55.7, 48.1, 23.4, 21.1, 16.0 ppm.

The enantiomeric excess was determined by HPLC on chiral stationary phase with Phenomenex Lux Cellulose-1 3u column: eluent Hexane/*i*PrOH = 9/1, flow rate 0.8 mL/min, λ=210 nm, anti τ_{1R2S} = 18.2 min, anti τ_{1S2R} = 19.7 min.

[xxxiv] B. Baltzy, *J. Am. Chem. Soc.*, **1942**, *64,* 3040.

Multi-step flow synthesis

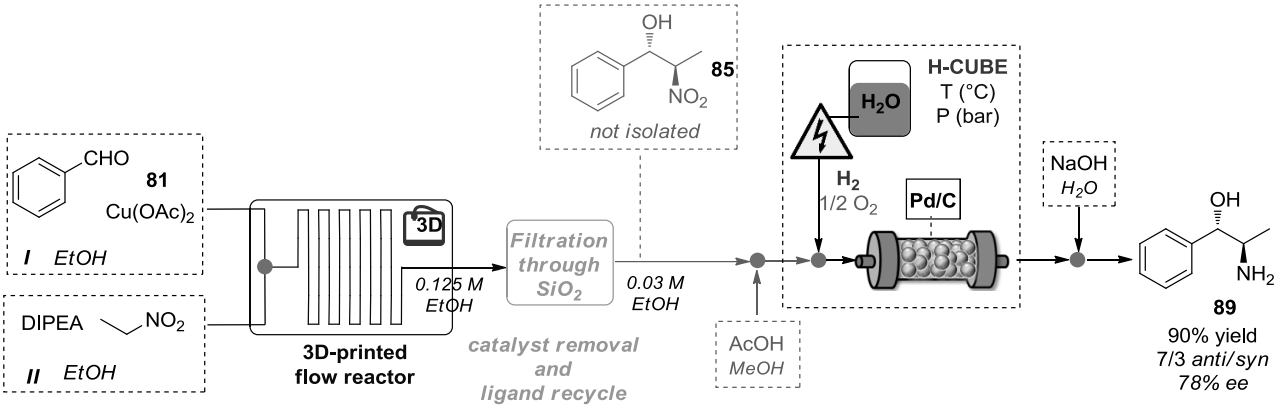

Two syringes of 2.5 mL were taken: ***I*** was charged with a preformed mixture (after 30 min of stirring) of benzaldehyde (0.375 mmol), **81** (0.375mmol) and $Cu(OAc)_2$ (0.075 mmol) in EtOH (1.46 mL, 0.250 M). Syringe ***II*** was charged with nitroethane (0.270 mL, 3.75 mmol), DIPEA (65 µL, 0.375 mmol) and EtOH (1.26 mL). The two syringes were connected to a syringe pump and the reagents directed to the flow reactor at -20 °C for a residence time of 30 minutes. The collected mixture (dark blue solution, 3 mL) was filtered over a short pad of silica (*h*: 1 cm, *d*: 2 cm) and eluted with EtOH (6 mL). To the crude product (light yellow) 500 µL (30 eq) of AcOH were added and it was subjected to continuous flow hydrogenation with H CUBE (T: 30 °C, P: 1 bar, flow rate 0.1 mL/min). Reaction was followed using TLC and after recirculation for 2.5 hours the solvent was evaporated, treated with NH_4OH 33% wt. and extracted five times with AcOEt. Amino alcohol **89** was obtained in 90% yield (over 2 steps), 7/3 *dr* and 78% ee as pure with solid, with no need for further purification. (*dr* and ee were determined after derivatization of **89** into the corresponding bis-acetylate)**.**

3D-Printed flow reactors

The 3D-printed flow reactors were designed by using a 3D CAD software package (Autodesk123D®), which is freely distributed and produces a .stl file. A further optimization of the geometry was performed using Netfabb basic 5.2 free software (Autodesk®) in order to optimize and validate the final design.
Cura 15.02 software was used in order to set-up all the parameters related to the material used for the 3D printing process and to slice the model into thin layers. The final .gcode file generated can be directly read by the Sharebot NG 3D-printer and use for print the device.
This 3D printer heats a 1.75 mm thermopolymer filament through the extruder, depositing the material in a layer-by-layer fashion, converting the design into the desired 3D reactionware.
The thermoplastics employed to fabricate the devices presented herein are:

- PLA: Polylactic acid purchased from 3D filo supply (http://www.3dfilo.it)
- HIPS: High Impact Polystyrene purchased form Reprapper supply (http://www.reprappertech.com)
- NYLON: Nylon taulman 645 - TAU-002 (Nylon 6,6) purchased from 3Dprima supply (www.3dprima.com)

Generally, the shape of the 3D-printed reactionware devices was chosen in order to combine a short design and print time with the robustness required for a flow system. Details about the different geometry devices and 3d-printing parameters are reported below.

1 mL (squared channel: 1.41 x 1.41mm)

VIRTUAL DESIGN

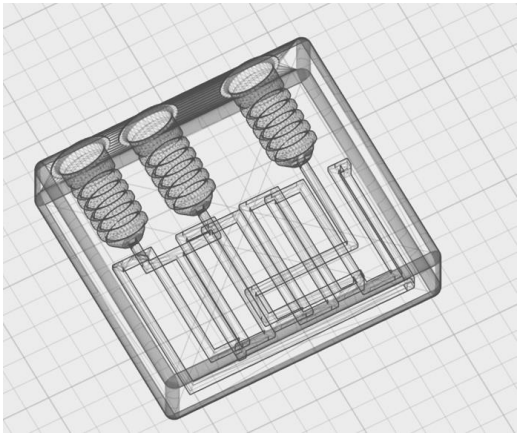

FINAL REALIZATION - (HIPS version)

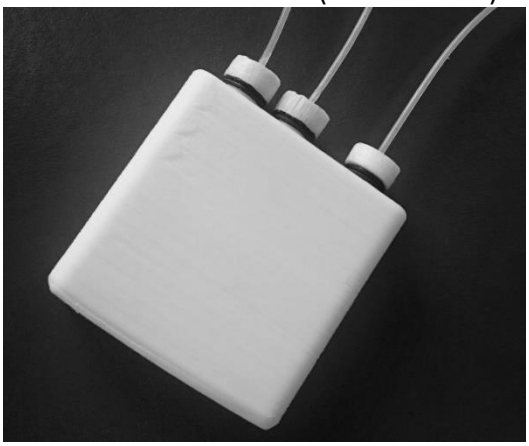

Schematic representation of the 1 ml reactionware device employed in this work showing the internal channels (virtual design) and the final 3D printed reactors with connections. This reactor present two inputs (A and B) and one output (C).
Total reactor size: 56 x 60 x 16 mm (HxLxW)
Squared section channel: 1.41 x 1.41 x 500 mm
Section area: 2 mm^2
Total volume (calculated): 1 mL

HIPS parameters

Print time: 20 hours 11 minutes

Filament used: 22.68 m 67.0g

QUALITY	
Layer height (mm)	0.05
Shell thickness (mm)	1.6
Initial layer thickness (mm)	0.2
Initial layer width (%)	150
Cut off object bottom (mm)	0
Dual extrusion overlap (mm)	0.15
RETRACTION	
Enable retraction	YES
Retraction speed (mm/s)	50
Retraction distance (mm)	2
Minimun travel (mm)	1.5
Enable combing	ALL
Minimal extrusion before retracting (mm)	0.02
Z hop when retracting (mm)	0
SKIRT	
Line count (n°)	1
Start distance (mm)	3.0
Minimal lenght (mm)	150.0
FILL	
Bottom/top thickness (mm)	1.6
Fill density (%)	100
INFILL	
solid infill top	YES
solid infill bottom	YES
infill overlap (%)	15
SPEED AND TEMPERATURE	
Print speed (mm/s)	40
Travel speed (mm)	150
Bottom layer speed (mm/s)	20
Infill speed (mm/s)	0
Top/bottom speed (mm/s)	20
Outer shell speed (mm/s)	0
Innes shell speed (mm/s)	0
Printing temperature (°C)	240
Bed temperature (°C)	85

FILAMENT	
Diameter (mm)	1.75
Flow (%)	100
COOL	
Minimal layer time (s)	10
Enable cooling fan	YES
Fan full on at height (mm)	0.5
Fan speed min (%)	0
Fan speed max (%)	0
Minimun speed (mm/s)	15
Cool head lift	NO
SUPPORT	
Support type (grid / line)	LINES
Overhang angle for support (deg)	0
Fill amount (%)	30
Distance X/Y (mm)	0.7
Distance Z (mm)	0.15
Platform adhesion type	Brim
Brim line amount	25
RAFT	
Extra margin (mm)	20
Line spacing (mm)	3.0
Base thickness (mm)	0.3
Base line width (mm)	1.0
Interface thickness (mm)	0.27
Interface line width (mm)	0.4
Airgap	0
First layer airgap	0.22
Surface layers	0
Surface layers thickness (mm)	0.27
Surface layer line width (mm)	0.4
FIX ORRIBLE	
Combine everything (Type-A)	NO
Combine everything (Type-B)	NO
Keep open faces	NO
Extensive stiching	NO

PLA parameters

Print time: 18 hours 9 minutes

Filament used: 22.68m 67.0g

QUALITY	
Layer height (mm)	0.1
Shell thickness (mm)	1.4
Initial layer thickness (mm)	0.2
Initial layer width (%)	150
Cut off object bottom (mm)	0
Dual extrusion overlap (mm)	0.1
5	
RETRACTION	
Enable retraction	YES
Retraction speed (mm/s)	50
Retraction distance (mm)	2
Minimun travel (mm)	1
Enable combing	ALL
Minimal extrusion before retracting (mm)	0.0
2	
Z hop when retracting (mm)	0
SKIRT	
Line count (n°)	5
Start distance (mm)	5.0
Minimal lenght (mm)	150
.0	
FILL	
Bottom/top thickness (mm)	1.8
Fill density (%)	100
INFILL	
solid infill top	YES
solid infill bottom	YES
infill overlap (%)	35
SPEED AND TEMPERATURE	
Print speed (mm/s)	20
Travel speed (mm)	150
Bottom layer speed (mm/s)	20
Infill speed (mm/s)	0
Top/bottom speed (mm/s)	20
Outer shell speed (mm/s)	0
Innes shell speed (mm/s)	0
Printing temperature (°C)	220
Bed temperature (°C)	40
FILAMENT	
Diameter (mm)	1.75
Flow (%)	100
COOL	
Minimal layer time (s)	10
Enable cooling fan	YES
Fan full on at height (mm)	0.4
Fan speed min (%)	0
Fan speed max (%)	0
Minimun speed (mm/s)	10
Cool head lift	NO
SUPPORT	
Support type (grid / line)	GRI
D	
Overhang angle for support (deg)	60
Fill amount (%)	15
Distance X/Y (mm)	1
Distance Z (mm)	0.1
Platform adhesion type	NO
NE	
Brim line amount	15
RAFT	
Extra margin (mm)	5.0
Line spacing (mm)	3.0
Base thickness (mm)	0.3
Base line width (mm)	1.0
Interface thickness (mm)	0.2
7	
Interface line width (mm)	0.4
Airgap	0
First layer airgap	0.2
2	
Surface layers	2
Surface layers thickness (mm)	0.2
7	
Surface layer line width (mm)	0.4
FIX ORRIBLE	
Combine everything (Type-A)	YES
Combine everything (Type-B)	NO
Keep open faces	NO
Extensive stiching	NO

NYLON parameters

Print time: 17 hours 33 minutes

Filament used: 22.661m 67.0g

QUALITY	
Layer height (mm)	0.1
Shell thickness (mm)	1.4
Initial layer thickness (mm)	0.26
Initial layer width (%)	150
Cut off object bottom (mm)	0
Dual extrusion overlap (mm)	0.15
RETRACTION	
Enable retraction	YES
Retraction speed (mm/s)	40
Retraction distance (mm)	2
Minimun travel (mm)	5.0
Enable combing	ALL
Minimal extrusion before retracting (mm)	0.02
Z hop when retracting (mm)	0.075
SKIRT	
Line count (n°)	1
Start distance (mm)	3.0
Minimal lenght (mm)	150.0
FILL	
Bottom/top thickness (mm)	3.2
Fill density (%)	50
INFILL	
solid infill top	YES
solid infill bottom	YES
infill overlap (%)	15
SPEED AND TEMPERATURE	
Print speed (mm/s)	40
Travel speed (mm)	150
Bottom layer speed (mm/s)	35
Infill speed (mm/s)	0
Top/bottom speed (mm/s)	0
Outer shell speed (mm/s)	0
Innes shell speed (mm/s)	0
Printing temperature (°C)	240
Bed temperature (°C)	60

FILAMENT	
Diameter (mm)	1.75
Flow (%)	100
COOL	
Minimal layer time (s)	10
Enable cooling fan	YES
Fan full on at height (mm)	0.5
Fan speed min (%)	0
Fan speed max (%)	0
Minimun speed (mm/s)	10
Cool head lift	NO
SUPPORT	
Support type (grid / line)	GRID
Overhang angle for support (deg)	90
Fill amount (%)	20
Distance X/Y (mm)	0.8
Distance Z (mm)	0.15
Platform adhesion type	Brim
Brim line amount	25
RAFT	
Extra margin (mm)	20
Line spacing (mm)	3.0
Base thickness (mm)	0.3
Base line width (mm)	1.0
Interface thickness (mm)	0.27
Interface line width (mm)	0.4
Airgap	0
First layer airgap	0.22
Surface layers	0
Surface layers thickness (mm)	0.27
Surface layer line width (mm)	0.4
FIX ORRIBLE	
Combine everything (Type-A)	NO
Combine everything (Type-B)	NO
Keep open faces	NO
Extensive stiching	NO

1 ml (circular channel: 1.0 x 1.0 mm)

VIRTUAL DESIGN

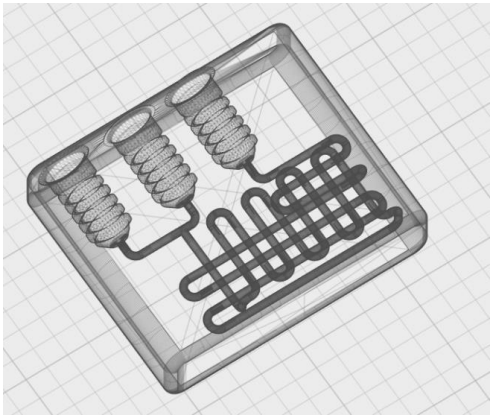

FINAL REALIZATION

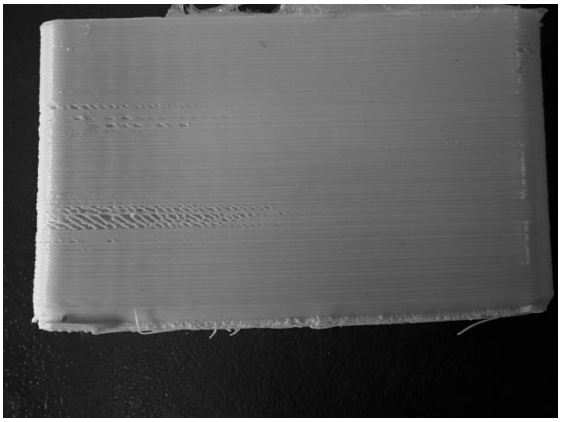

Schematic representation of the 1 ml reactionware device employed in this work showing the internal channels (virtual design) and the final 3D printed reactors with connections. This reactor present two inputs (A and B) and one output (C).

Total reactor size: 53 x 63 x 16 mm (HxLxW)
Circular section channel: 1.59 mm diameter
Section area: 2 mm^2
Total volume (calculated): 1 mL

PLA parameters
Print time: 18 hours 41 minutes
Filament used: 21.502m 64.0g

QUALITY

Layer height (mm)	0.1
Shell thickness (mm)	1.4
Initial layer thickness (mm)	0.2
Initial layer width (%)	150
Cut off object bottom (mm)	0
Dual extrusion overlap (mm)	0.1
5	

RETRACTION

Enable retraction	YES
Retraction speed (mm/s)	50
Retraction distance (mm)	2
Minimun travel (mm)	1
Enable combing	ALL
Minimal extrusion before retracting (mm)	0.0
2	
Z hop when retracting (mm)	0

SKIRT

Line count (n°)	5
Start distance (mm)	5.0
Minimal lenght (mm)	150
.0	

FILL

Bottom/top thickness (mm)	1.8
Fill density (%)	100

INFILL

solid infill top	YES
solid infill bottom	YES
infill overlap (%)	35

SPEED AND TEMPERATURE

Print speed (mm/s)	20
Travel speed (mm)	150
Bottom layer speed (mm/s)	20
Infill speed (mm/s)	0
Top/bottom speed (mm/s)	20
Outer shell speed (mm/s)	0
Innes shell speed (mm/s)	0
Printing temperature (°C)	220
Bed temperature (°C)	40

FILAMENT

Diameter (mm)	1.75
Flow (%)	100

COOL

Minimal layer time (s)	10
Enable cooling fan	YES
Fan full on at height (mm)	0.4
Fan speed min (%)	0
Fan speed max (%)	0
Minimun speed (mm/s)	10
Cool head lift	NO

SUPPORT

Support type (grid / line)	GRI
D	
Overhang angle for support (deg)	60
Fill amount (%)	15
Distance X/Y (mm)	1
Distance Z (mm)	0.1
Platform adhesion type	NO
NE	
Brim line amount	15

RAFT

Extra margin (mm)	5.0
Line spacing (mm)	3.0
Base thickness (mm)	0.3
Base line width (mm)	1.0
Interface thickness (mm)	0.2
7	
Interface line width (mm)	0.4
Airgap	0
First layer airgap	0.2
2	
Surface layers	2
Surface layers thickness (mm)	0.2
7	
Surface layer line width (mm)	0.4

FIX ORRIBLE

Combine everything (Type-A)	YES
Combine everything (Type-B)	NO
Keep open faces	NO
Extensive stiching	NO

1 ml (squared channel: 1.0 x 1.0 mm)

VIRTUAL DESIGN

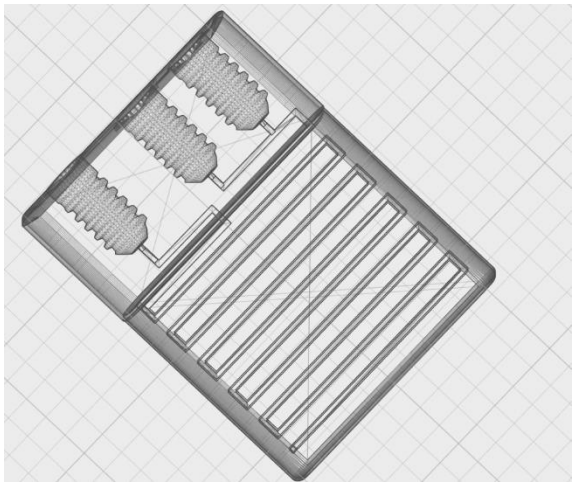

FINAL REALIZATION - (PLA version)

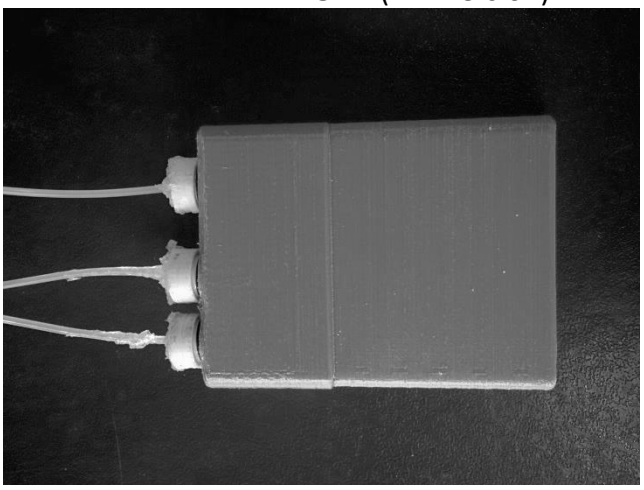

Schematic representation of the 1 ml reactionware device employed in this work showing the internal channels (virtual design) and the final 3D printed reactors with connections. This reactor present two inputs (A and B) and one output (C).

Total reactor size: 72 x 55 x 16 mm (HxLxW)
Circular section channel: 1.00 x 1.00 x 1000 mm
Section area: 1 mm^2
Total volume (calculated): 1 mL

PLA parameters
Print time: 34 hours 30 minutes
Filament used: 16.956m 50.0g

QUALITY	
Layer height (mm)	0.1
Shell thickness (mm)	1.4
Initial layer thickness (mm)	0.2
Initial layer width (%)	150
Cut off object bottom (mm)	0
Dual extrusion overlap (mm)	0.15
RETRACTION	
Enable retraction	YES
Retraction speed (mm/s)	50
Retraction distance (mm)	2
Minimun travel (mm)	1
Enable combing	ALL
Minimal extrusion before retracting (mm)	0.02
Z hop when retracting (mm)	0
SKIRT	
Line count (n°)	5
Start distance (mm)	5.0
Minimal lenght (mm)	150.0
FILL	
Bottom/top thickness (mm)	1.8
Fill density (%)	100
INFILL	
solid infill top	YES
solid infill bottom	YES
infill overlap (%)	35
SPEED AND TEMPERATURE	
Print speed (mm/s)	20
Travel speed (mm)	150
Bottom layer speed (mm/s)	20
Infill speed (mm/s)	0
Top/bottom speed (mm/s)	20
Outer shell speed (mm/s)	0
Innes shell speed (mm/s)	0
Printing temperature (°C)	220
Bed temperature (°C)	40

FILAMENT	
Diameter (mm)	1.75
Flow (%)	100
COOL	
Minimal layer time (s)	10
Enable cooling fan	YES
Fan full on at height (mm)	0.5
Fan speed min (%)	100
Fan speed max (%)	100
Minimun speed (mm/s)	10
Cool head lift	NO
SUPPORT	
Support type (grid / line)	GRID
Overhang angle for support (deg)	60
Fill amount (%)	15
Distance X/Y (mm)	1
Distance Z (mm)	0.1
Platform adhesion type	None
Brim line amount	15
RAFT	
Extra margin (mm)	5.0
Line spacing (mm)	3.0
Base thickness (mm)	0.3
Base line width (mm)	1.0
Interface thickness (mm)	0.27
Interface line width (mm)	0.4
Airgap	0
First layer airgap	0.22
Surface layers	2
Surface layers thickness (mm)	0.27
Surface layer line width (mm)	0.4
FIX ORRIBLE	
Combine everything (Type-A)	YES
Combine everything (Type-B)	NO
Keep open faces	NO
Extensive stiching	NO

10 ml (squared channel: 2.65 x 2.65 mm)

VIRTUAL DESIGN

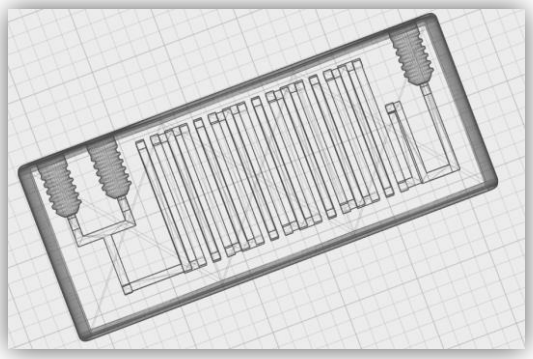

FINAL REALIZATION - (HIPS version)

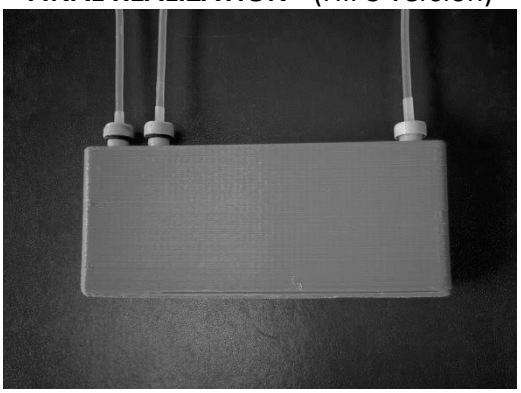

Schematic representation of the 10 ml reactionware device employed in this work showing the internal channels (virtual design) and the final 3D printed reactors with connections. This reactor present two inputs (A and B) and one output (C).

Total reactor size: 145 x 60 x 19 mm (HxLxW)
Circular section channel: 2.65 x 2.65 x 1424 mm
Section area: 7 mm^2
Total volume (calculated): 10 mL

PLA parameters
Print time: 26 hours 42 minutes
Filament used: 66.215 m 197.0 g

QUALITY

Layer height (mm)	0.1
Shell thickness (mm)	1.4
Initial layer thickness (mm)	0.2
Initial layer width (%)	150
Cut off object bottom (mm)	0
Dual extrusion overlap (mm)	0.1
5	

RETRACTION

Enable retraction	YES
Retraction speed (mm/s)	50
Retraction distance (mm)	2
Minimun travel (mm)	1
Enable combing	ALL
Minimal extrusion before retracting (mm)	0.0
2	
Z hop when retracting (mm)	0

SKIRT

Line count (n°)	5
Start distance (mm)	5.0
Minimal lenght (mm)	150
.0	

FILL

Bottom/top thickness (mm)	1.8
Fill density (%)	100

INFILL

solid infill top	YES
solid infill bottom	YES
infill overlap (%)	35

SPEED AND TEMPERATURE

Print speed (mm/s)	20
Travel speed (mm)	150
Bottom layer speed (mm/s)	20
Infill speed (mm/s)	0
Top/bottom speed (mm/s)	20
Outer shell speed (mm/s)	0
Innes shell speed (mm/s)	0
Printing temperature (°C)	220
Bed temperature (°C)	40

FILAMENT

Diameter (mm)	1.75
Flow (%)	100

COOL

Minimal layer time (s)	10
Enable cooling fan	YES
Fan full on at height (mm)	0.4
Fan speed min (%)	0
Fan speed max (%)	0
Minimun speed (mm/s)	10
Cool head lift	NO

SUPPORT

Support type (grid / line)	GRI
D	
Overhang angle for support (deg)	60
Fill amount (%)	15
Distance X/Y (mm)	1
Distance Z (mm)	0.1
Platform adhesion type	NO
NE	
Brim line amount	15

RAFT

Extra margin (mm)	5.0
Line spacing (mm)	3.0
Base thickness (mm)	0.3
Base line width (mm)	1.0
Interface thickness (mm)	0.2
7	
Interface line width (mm)	0.4
Airgap	0
First layer airgap	0.2
2	
Surface layers	2
Surface layers thickness (mm)	0.2
7	
Surface layer line width (mm)	0.4

FIX ORRIBLE

Combine everything (Type-A)	YES
Combine everything (Type-B)	NO
Keep open faces	NO
Extensive stiching	NO

General Set-Up of Continuous Flow Reactions with 3D Printed Reactors

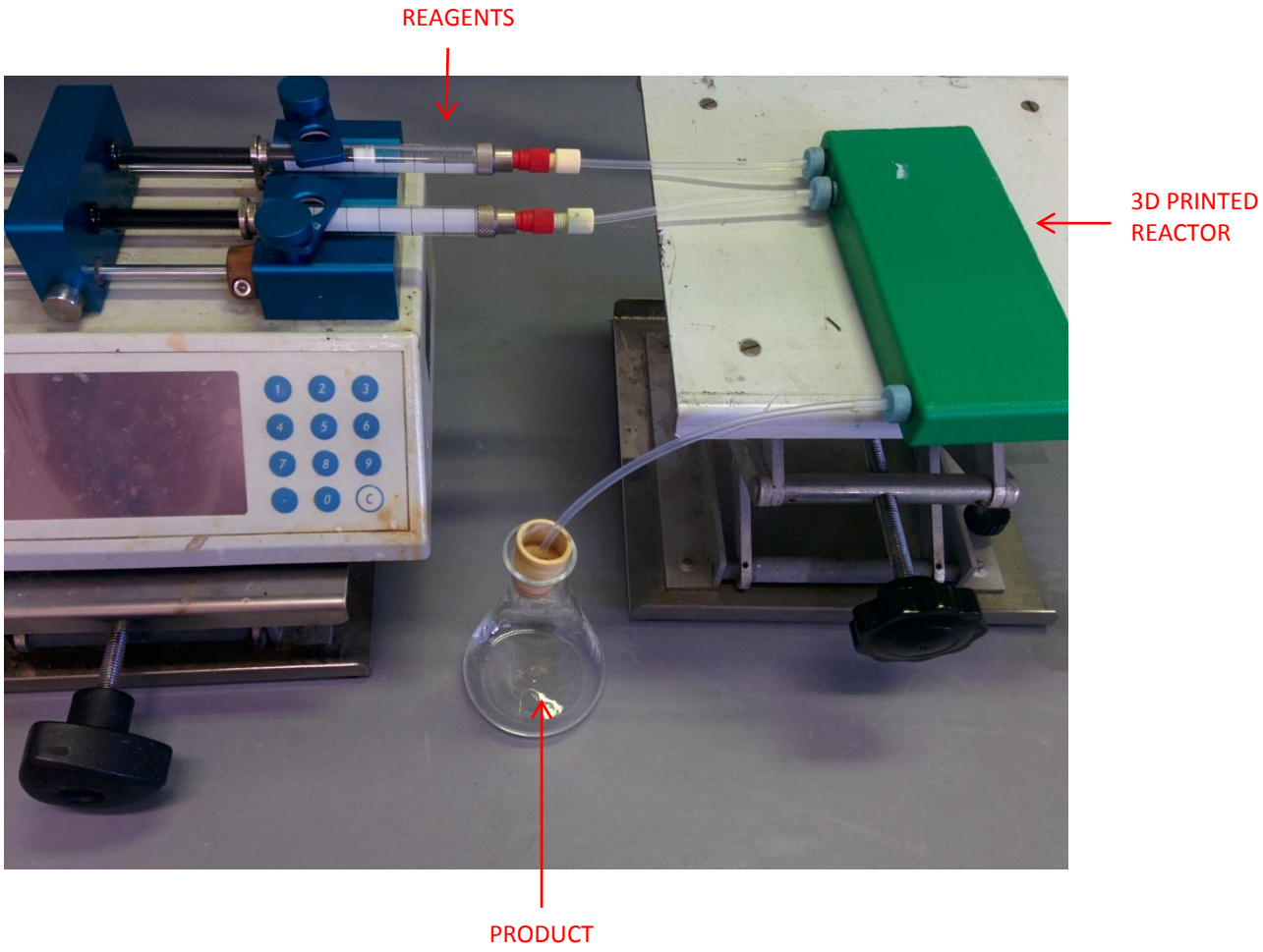

4.3 Photoredox Catalysis

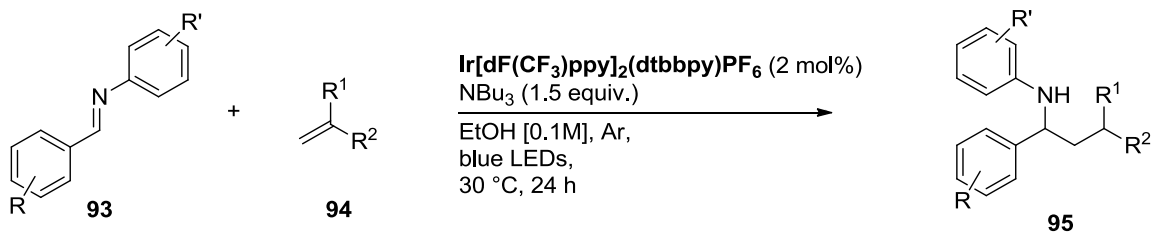

General procedure for the reductive coupling of imines with olefins

In an oven-dried test tube equipped with magnetic stir bar were placed $Ir[F(CF_3)ppy]_2(bpy)PF_6$ (3.9 mg, 0.004 mmol, 0.02 equiv.), the imine **93** (0.2 mmol, 1.0 equiv.) and the olefin **94** (1.0 mmol, 5.0 equiv., if solid). The tube was closed with a septum and purged three times with a sequence vacuum/argon before addition of degassed ethanol (2.0 mL), NBu_3 (71 μL, 0.3 mmol, 1.5 equiv.), and the corresponding olefin **3** (1.0 mmol, 5.0 equiv., if liquid). The tube was placed in a beaker wrapped with 11W blue LEDs stripes and irradiated for 24 hours. After complete conversion, the reaction mixture was concentrated *in vacuo*, and the residue was purified by column chromatography on silica gel (see below for eluent used). In some cases, residual amounts of tributylamine were observed in the purified material, and were removed by co-evaporation *in vacuo* with isopropanol or water followed by toluene.

Methyl 4-phenyl-4-(phenylamino)butanoate 95aa

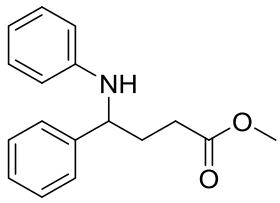

Prepared according to the general procedure with 3.0 equivalents of olefin. The crude mixture was purified by column chromatography on silica gel eluting with pentane/ethyl acetate 9:1 to afford the title product as a off white solid.

^{1}H-NMR (600 MHz, $CDCl_3$) δ_H 7.31-7.36 (m, 4H), 7.24-7.26 (m, 1H), 7.07-7.10 (t, J = 7.4 Hz, 2H), 6.63-6.65 (t, J = 7.3 Hz, 1H), 6.52-6.53 (d, J = 7.7 Hz, 2H), 4.37-4.39 (t, J = 7.6 Hz, 1H), 4.27 (bs, 1H), 3.67 (s, 3H), 2.42-2.44 (t, J = 7.2 Hz, 2H), 2.09-2.18 (m, 2H) ppm; **^{13}C-NMR** (151 MHz, $CDCl_3$) δ_C 174.0, 147.1, 143.1 129.1, 128.7, 127.2, 126.4, 117.3, 113.3, 57.7, 51.7, 33.2, 31.0 ppm; **HRMS** (EI): calc. for $[C_{17}H_{19}NO_2]$ 269.1410, measured 269.1410; **FT-IR** ν_{max}(ATR) 3398, 2944, 1721, 1598, 1499, 1194 cm^{-1}; **m.p.** 95-98 °C.

4-phenyl-4-(phenylamino)butanenitrile 95ab

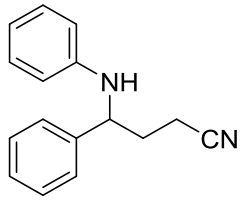

Prepared according to the general procedure. The crude mixture was purified by column chromatography on silica gel eluting with pentane/ethyl acetate 9:1 to 8:2 to afford the title product as a off white solid.

^{1}H-NMR (600 MHz, $CDCl_3$) δ_H 7.34-7.37 (m, 4H), 7.27-7.29 (m, 1H), 7.11-7.14 (t, J = 7.3 Hz, 2H), 6.69-6.71 (t, J = 7.3 Hz, 1H), 6.58-6.60 (d, J = 7.2 Hz, 2H), 4.50-4.52 (t, J = 7.0 Hz, 1H), 4.04 (bs, 1H), 2.43-2.48 (m, 1H), 2.33-2.39 (m, 1H), 2.17-2.21 (m, 1H), 2.10-2.13 (m, 1H) ppm; **^{13}C-NMR** (151 MHz, $CDCl_3$) δ_C 146.6, 141.6, 129.3, 129.0, 127.8, 126.3, 119.3, 118.1, 113.6, 56.9, 33.6, 14.5 ppm; **HRMS** (EI): calc. for $[C_{17}H_{19}NO_2]$ 236.1308, measured 236.1307; **FT-IR** ν_{max}(ATR) 3386, 3027, 2936, 2246, 1737, 1600, 1497, 1312 cm^{-1}; **m.p.** 63-65 °C.

***N,N*-dimethyl-4-phenyl-4-(phenylamino)butanamide 95ac**

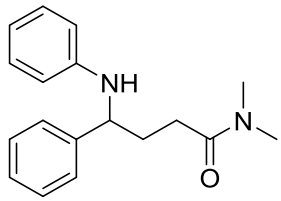

Prepared according to the general procedure with 3.0 equivalents of olefin. The crude mixture was purified by column chromatography on silica gel eluting with pentane/ethyl acetate 6:4 to afford the title product as a off white solid.

^{1}H-NMR (600 MHz, $CDCl_3$) δ_H 7.36-7.37 (d, J = 7.3 Hz, 2H), 7.30-7.32 (t, J = 7.8 Hz, 2H), 7.21-7.23 (t, J = 7.3 Hz, 1H), 7.05-7.07 (t, J = 7.3 Hz, 2H), 6.59-6.61 (t, J = 7.4 Hz, 1H), 6.49-6.50 (d, J = 7.2 Hz, 2H), 4.88 (bs, 1H), 4.36-4.38 (dd, J = 5.1, 8.4 Hz, 1H), 2.96 (s, 3H), 2.91 (s, 3H), 2.37-2.46 (m, 2H), 2.18-2.22 (m, 1H), 2.10-2.16 (m, 1H) ppm; **^{13}C-NMR** (151 MHz, $CDCl_3$) δ_C 172.7, 147.5, 143.9, 129.0, 128.6, 126.9, 126.3, 116.8, 113.1, 58.3, 37.1, 35.6, 33.1, 30.3 ppm; **HRMS** (EI): calc. for $[C_{18}H_{22}N_2O]$ 282.1727, measured 282.1727.; **FT-IR** ν_{max}(ATR) 3358, 2928, 1742, 1621, 1493 cm^{-1}; **m.p.** 154-155 °C.

***N*-(1-phenyl-3-(phenylsulfonyl)propyl)aniline 95ad**

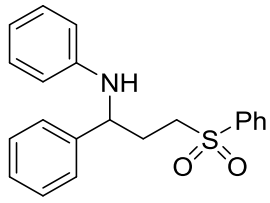

Prepared according to the general procedure with 3.0 equivalents of olefin. The crude mixture was purified by column chromatography on silica gel eluting with pentane/ethyl acetate 9:1 to 8:2 to afford the title product as a yellowish solid.

^{1}H-NMR (600 MHz, $CDCl_3$) δ_H 7.88-7.90 (d, J = 7.4 Hz, 2H), 7.65-7.67 (t, J = 7.4 Hz, 1H), 7.55-7.58 (d, J = 7.5 Hz, 2H), 7.25 (m, 5H), 7.07-7.09 (t, J = 7.4 Hz, 2H), 6.65-6.67 (t, J = 7.3 Hz, 1H), 6.50-6.51 (d, J = 7.3 Hz, 2H), 4.42-4.44 (t, J = 7.4 Hz, 1H), 4.13 (bs, 1H), 3.22-3.27 (m, 1H), 3.13-3.18 (m, 1H), 2.17-2.28 (m, 2H) ppm; **^{13}C-NMR** (151 MHz, $CDCl_3$) δ_C 146.6, 141.8, 139.0, 133.8, 129.4, 129.2, 128.9, 128.0, 127.6, 126.2, 117.9, 113.5, 56.6, 53.4, 30.7 ppm; **HRMS** (EI): calc. for $[C_{21}H_{22}NO_2S]^+$ 352.1366, measured 352.1372; **FT-IR** ν_{max}(ATR) 3391, 2924, 1599, 1304, 1279, 1139, 742, 689 cm^{-1}; **m.p.** 130-132 °C.

Ethyl 4-phenyl-4-(phenylamino)butanoate 95ae

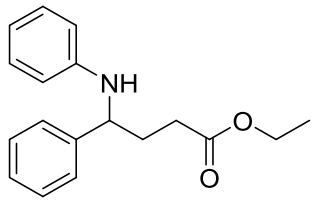

Prepared according to the general procedure. The crude mixture was purified by column chromatography on silica gel eluting with pentane/ethyl acetate 95:5 to 9:1 to afford the title product as a yellowish solid. All analytical data are in agreement with literature.[xxxv]

^{1}H-NMR (600 MHz, $CDCl_3$) δ_H 7.31-7.36 (m, 4H), 7.22-7.26 (m, 1H), 7.08-7.10 (t, J = 7.4 Hz, 2H), 6.63-6.66 (t, J = 7.7 Hz, 1H), 6.52-6.53 (d, J = 7.7 Hz, 2H), 4.38-4.40 (t, J = 7.4 Hz, 1H), 4.30 (bs, 1H), 4.12-4.15 (q, J = 7.2 Hz, 2H), 2.41-2.43 (t, J = 7.3 Hz, 2H), 2.09-2.18 (m, 2H), 1.24-1.26 (t, J = 7.2 Hz, 3H) ppm; **^{13}C-NMR** (151 MHz, $CDCl_3$) δ_C 173.6, 147.2, 143.2, 129.1, 128.7, 127.2, 126.4, 117.3, 113.3, 60.6, 57.8, 33.2, 31.3, 14.2 ppm.

Tert-butyl 4-phenyl-4-(phenylamino)butanoate 95af

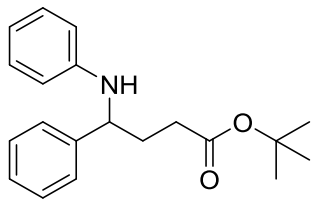

Prepared according to the general procedure. The crude mixture was purified by column chromatography on silica gel eluting with pentane/ethyl acetate 95:5 to afford the title product as a yellowish solid.

^{1}H-NMR (600 MHz, $CDCl_3$) δ_H 7.31-7.36 (m, 4H), 7.21-7.24 (m, 1H), 7.06-7.08 (t, J = 7.4 Hz, 2H), 6.61-6.63 (t, J = 7.3 Hz, 1H), 6.49-6.50 (d, J = 7.3 Hz, 2H), 4.34-4.36 (t, J = 6.9 Hz, 2H), 2.31-2.34 (td, J = 2.6, 7.2 Hz, 2H), 2.11-2.17 (m, 1H), 2.04-2.09 (m, 1H), 1.44 (s, 9H) ppm; **^{13}C-NMR** (151 MHz, $CDCl_3$) δ_C 173.0, 147.2, 143.4, 129.1, 128.6, 127.1, 126.3, 117.1, 113.2, 80.6, 57.9, 33.3, 32.5, 28.1 ppm; **HRMS** (EI): calc. for $[C_{20}H_{26}NO_2]^+$ 312.1958, measured 312.1956; **FT-IR** ν_{max}(ATR) 3402, 2974, 2075, 1711, 1601, 1511, 1147, 747 cm^{-1}; **m.p.** 76-77 °C.

2,2,3,3,3-pentafluoropropyl 4-phenyl-4-(phenylamino) butanoate 95ag

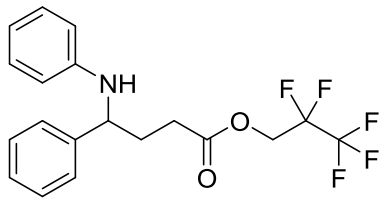

Prepared according to the general procedure. The crude mixture was purified by column chromatography on silica gel eluting with pentane/ethyl acetate 95:5 to 9:1 to afford the title product as a colourless oil.

^{1}H-NMR (600 MHz, $CDCl_3$) δ_H 7.29-7.32 (m, 4H), 7.21-7.26 (m, 1H), 7.05-7.09 (t, J = 7.4 Hz, 2H), 6.62-6.66 (t, J = 7.3 Hz, 1H), 6.50-6.52 (d, J = 7.4 Hz, 2H), 4.50-4.53 (t, J = 13.0 Hz, 2H), 4.37-4.41 (t, J = 7.2 Hz, 1H), 4.12 (bs, 1H), 2.49-2.53 (t, 2H), 2.09-2.22 (m, 2H). ppm; **^{13}C-NMR** (151 MHz, $CDCl_3$, fluorine-decoupled) δ_C 171.8, 146.9, 142.6, 129.1, 128.8, 127.4, 126.3, 118.4, 117.6, 113.4, 112.0, 59.1, 57.4, 32.8, 30.6 ppm; **HRMS** (EI): calc. for $[C_{19}H_{19}NO_2\ F_5]^+$ 388.1331, measured 388.1337; **FT-IR** ν_{max}(ATR)3378, 2944, 1742, 1368, 1197, 749 cm^{-1}.

[xxxv] C.-H. Yeh, R. P. Korivi, C.-H. Cheng, *Angew. Chem. Int. Ed.* **2008**, *47*, 4892

2-hydroxyethyl 4-phenyl-4-(phenylamino)butanoate 95ah

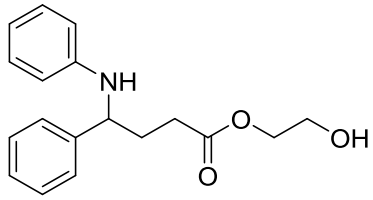

Prepared according to the general procedure. The crude mixture was purified by column chromatography on silica gel eluting with pentane/ethyl acetate 95:5 to 9:1 to afford the title product as a yellowish solid.

^{1}H-NMR (600 MHz, $CDCl_3$) δ_H 7.31-7.35 (m, 4H), 7.22-7.26 (m, 1H), 7.08-7.10 (t, J = 7.4 Hz, 2H), 6.63-6.65 (t, J = 7.3 Hz, 1H), 6.52-6.53 (d, J = 7.4 Hz, 2H), 4.38-4.41 (t, J = 7.0 Hz, 1H), 4.24 (bs, 1H), 4.19-4.21 (t, J = 4.7 Hz, 2H), 3.79-3.80 (t, J = 4.3 Hz, 2H), 2.46-2.48 (t, J = 7.2 Hz, 2H), 2.09-2.21 (m, 2H), 1.86 (bs, 1H) ppm; **^{13}C-NMR** (151 MHz, $CDCl_3$) δ_C 173.9, 147.1, 143.0, 129.1, 128.7, 127.2, 126.3, 117.4, 113.3, 66.2, 61.1, 57.7, 33.1, 31.2 ppm; **HRMS** (EI): calc. for [$C_{18}H_{21}NO_3$] 299.1516; measured 299.1515, **FT-IR** ν_{max}(ATR) 3383, 2942, 1719, 1597, 1496, 1188 cm^{-1}; **m.p.** 61-63 °C.

2-(dimethylamino)ethyl 4-phenyl-4-(phenylamino)butanoate 95ai

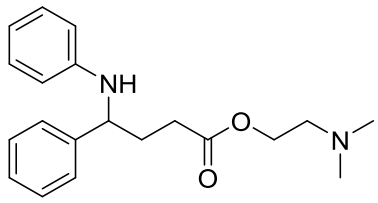

Prepared according to the general procedure. The crude mixture was purified by column chromatography on silica gel eluting with dichloromethane/methanol/triethylamine 98:1:1 to afford the title product as a brownish solid.

^{1}H-NMR (600 MHz, $CDCl_3$) δ_H 7.30-7.34 (m, 4H), 7.21-7.23 (t, J = 7.1 Hz, 1H), 7.06-7.09 (t, J = 7.4 Hz, 2H), 6.61-6.64 (t, J = 7.4 Hz, 1H), 6.50-6.52 (d, J = 7.5 Hz, 2H), 4.37-4.39 (t, J = 7.2 Hz, 1H), 4.16-4.18 (t, J = 5.7 Hz, 2H), 2.54-2.56 (t, J = 5.7 Hz, 2H), 2.44-2.46 (t, J = 7.3 Hz, 2H), 2.27 (s, 6H), 2.08-2.17 (m, 2H). ppm; **^{13}C-NMR** (151 MHz, $CDCl_3$) δ_C 173.6, 147.1, 143.1, 129.1, 128.7, 127.2, 126.3, 117.3, 113.2, 62.1, 57.7, 45.6, 33.2, 32.1 ppm; **HRMS** (EI): calc. for [$C_{20}H_{26}N_2O_2$] 327.2067, measured 327.2067; **FT-IR** ν_{max}(ATR) 3302, 2958, 2782, 1731, 1599, 1315, 1171, 751 cm^{-1}; **m.p.** 54-56 °C.

Methyl 2-methyl-4-phenyl-4-(phenylamino)butanoate 95aj

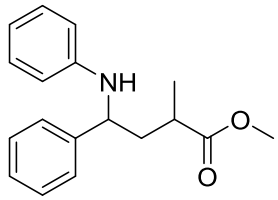

Prepared according to the general procedure. The crude mixture was purified by column chromatography on silica gel eluting with pentane/ethyl acetate 95:5 to 9:1 to afford the title product as a yellowish solid. The *dr* was determined by ^{1}H-NMR of the crude mixture. The relative configuration was assigned by comparison with literature[2] after cyclization to the corresponding γ-lactam.

^{1}H-NMR (600 MHz, $CDCl_3$) δ_H 7.30-7.36 (m, 4H), 7.21-7.24 (m, 1H), 7.07-7.09 (t, J = 7.4 Hz, 2H), 6.62-6.65 (t, J = 7.3 Hz, 1H), 6.50-6.51 (d, J = 7.7 Hz, 2H), 4.41-4.43 (dd, J = 2.5, 5.6 Hz, 1H), 4.16 (bs, 1H), 3.63 (s, 3H), 2.56-2.65 (m, 1H), 2.22-2.26 (m, 1H), 1.85-1.90 (m, 1H), 1.23-1.24 (d, J = 7.2 Hz, 3H) ppm; **^{13}C-NMR** (151 MHz, $CDCl_3$) δ_C 176.8, 129.1, 128.6, 127.1, 126.3, 117.3, 113.3, 113.1, 56.1, 51.8, 42.1, 36.5, 17.7 ppm; **HRMS** (EI): calc. for [$C_{18}H_{21}NO_2$] 283.1567; measured 283.1566; **FT-IR** ν_{max}(ATR) 3402, 2949, 1718, 1603, 1484, 1176 cm^{-1}; **m.p.** 86-88 °C.

Benzyl 2-methyl-4-phenyl-4-(phenylamino)butanoate 95 ak

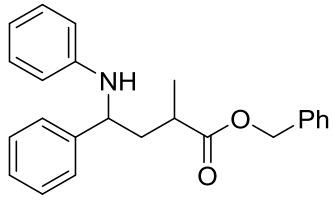

Prepared according to the general procedure. The crude mixture was purified by column chromatography on silica gel eluting with pentane/ethyl acetate 95:5 to afford the title product as a brownish solid. The *dr* was determined by ^{1}H-NMR of the crude mixture. The relative configuration was assigned by comparison.

^{1}H-NMR (600 MHz, $CDCl_3$) δ_H 7.27-7.35 (m, 9H), 7.20-7.22 (m, 1H), 7.05-7.08 (t, J = 7.4 Hz, 2H), 6.62-6.65 (t, J = 7.3 Hz, 1H), 6.44-6.46 (d, J = 7.7 Hz, 2H), 5.09 (s, 2H), 4.40-4.42 (dd, J = 3.2, 5.2 Hz, 1H), 4.41 (bs, 1H), 2.68-2.71 (m, 1H), 2.22-2.27 (m, 1H), 1.85-1.89 (m, 1H), 1.24-1.25 (d, J = 7.1 Hz, 3H) ppm; **^{13}C-NMR** (151 MHz, $CDCl_3$) δ_C 176.1, 147.1, 143.3, 135.9, 129.1, 128.6 (2C), 128.6, 126.2, 117.3, 113.3 (2C), 113.2, 66.3, 56.0, 42.3, 36.6, 17.8 ppm; **HRMS** (EI): calc. for $[C_{24}H_{25}NO_2]$ 359.1880; measured 359.1894; **FT-IR** ν_{max}(ATR) 3405, 2951, 1720, 1599, 1489, 1145 cm^{-1}; **m.p.** 101-104 °C.

2-bromoethyl 2-methyl-4-phenyl-4-(phenylamino)butanoate 95al

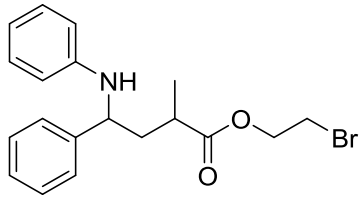

Prepared according to the general procedure. The crude mixture was purified by column chromatography on silica gel eluting with pentane/ethyl acetate 95:5 to afford the title product as a colorless oil. The *dr* was determined by ^{1}H-NMR of the crude mixture. The relative configuration was assigned by comparison.

^{1}H-NMR (600 MHz, $CDCl_3$) δ_H 7.30-7.36 (m, 4H), 7.21-7.24 (m, 1H), 7.07-7.09 (t, J = 7.4 Hz, 2H), 6.63-6.65 (t, J = 7.3 Hz, 1H), 6.51-6.53 (d, J = 7.7 Hz, 2H), 4.46-4.48 (t, J = 5.7 Hz, 1H), 4.33-4.35 (t, J = 6.0 Hz, 2H), 4.14 (bs, 1H), 3.43-3.46 (td, J = 1.8, 5.9 Hz, 2H), 2.67-2.70 (m, 1H), 2.23-2.28 (m, 1H), 1.88-1.93 (m, 1H), 1.26-1.27 (d, J = 7.2 Hz, 3H) ppm; **^{13}C-NMR** (151 MHz, $CDCl_3$) δ_C 175.8, 147.1, 143.2, 129.1, 128.7, 127.1, 126.3, 117.4, 113.4, 63.8, 56.0, 42.0, 36.5, 28.8, 17.7 ppm; **HRMS** (EI): calc. for $[C_{19}H_{23}NO_2Br]^+$ 376.0907, measured 376.0907; **FT-IR** ν_{max}(ATR) 3403, 2970, 1729, 1600, 1502, 1164, 750 cm^{-1}.

Methyl 2-acetamido-4-phenyl-4-(phenylamino)butanoate 95am

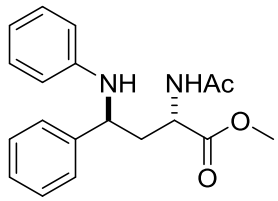

Prepared according to the general procedure. The crude mixture was purified by column chromatography on silica gel eluting with pentane/ethyl acetate 1:1 to 4:6 to afford the title product as yeloowish solid. Diastereoisomers were isolated separately as white solids. The *dr* was determined by ^{1}H-NMR of the crude mixture and confirmed after products isolation. The relative configuration was assigned by NOESY experiment after cyclization to the corresponding γ-lactam.

^{1}H-NMR (600 MHz, $CDCl_3$) δ_H 7.29-7.34 (m, 4H), 7.21-7.24 (m, 1H), 7.08-7.10 (t, J = 7.4 Hz, 2H), 6.63-6.66 (t, J = 7.3 Hz, 1H), 6.54-6.55 (d, J = 7.6 Hz, 2H), 6.28-6.30 (d, J = 6.7 Hz, 1H), 4.89 (bs, 1H), 4.68-4.71 (m, 1H), 4.50-4.52 (dd, J = 4.6, 9.6 Hz, 1H), 3.80 (s, 3H), 2.29-2.33 (m, 1H), 2.16-2.21 (m,

1H), 1.99 (s, 3H) ppm; **^{13}C-NMR** (151 MHz, $CDCl_3$) δ_C 172.6, 169.9, 147.1, 143.0, 129.1, 128.8, 127.3, 126.1, 117.4, 113.3, 55.3, 52.8, 50.5, 41.6, 23.1 ppm; **HRMS** (EI): calc. for [$C_{19}H_{22}N_2O_3$ Na] 349.1523, measured 349.1521 ; **FT-IR** ν_{max}(ATR) 3315, 3036, 2950, 1739, 1655, 1506, 1213, 747, 696 cm^{-1}; **m.p.** 146-148 °C.

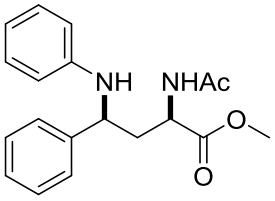

^{1}H-NMR (600 MHz, $CDCl_3$) δ_H 7.30-7.32 (m, 4H), 7.22-7.24 (m, 1H), 7.08-7.11 (t, J = 7.4 Hz, 2H), 6.66-6.68 (t, J = 7.3 Hz, 1H), 6.54-6.55 (d, J = 7.6 Hz, 2H), 6.20-6.21 (d, J = 7.6 Hz, 1H), 4.74-4.77 (m, 1H), 4.48-4.50 (dd, J = 4.8, 8.5 Hz, 1H), 4.18 (bs, 1H), 3.67 (s, 3H), 2.32-2.37 (m, 1H), 2.21-2.25 (m, 1H), 1.96 (s, 3H) ppm; **^{13}C-NMR** (151 MHz, $CDCl_3$) δ_C 172.6, 169.8, 146.6, 142.6, 129.2, 128.8, 127.4, 126.3, 118.0, 113.9, 55.5, 52.6, 50.7, 40.3, 23.1 ppm; **HRMS** (EI): calc. for [$C_{19}H_{22}N_2O_3$ Na] 349.1523, measured 349.1521; **FT-IR** ν_{max}(ATR) 3406, 3248, 2947, 1734, 1643, 1532, 1208, 845cm^{-1}; **m.p.** 145-148 °C.

Dimethyl 2-(2-phenyl-2-(phenylamino)ethyl)succinate 95an

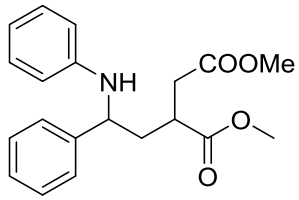

Prepared according to the general procedure. The crude mixture was purified by column chromatography on silica gel eluting with pentane/ethyl acetate 95:5 to 9:1 to afford the title product as a white solid. The *dr* was determined by ^{1}H-NMR of the crude mixture. The relative configuration was assigned by NOESY experiment after cyclization to the corresponding γ-lactam.

^{1}H-NMR (600 MHz, $CDCl_3$) δ_H 7.29-7.36 (m, 4H), 7.20-7.23 (m, 1H), 7.07-7.10 (t, J = 7.4 Hz, 2H), 6.62-6.65 (t, J = 7.3 Hz, 1H), 6.51-6.53 (d, J = 7.7 Hz, 2H), 4.41-4.47 (m, 2H), 3.70 (s, 3H), 3.67 (s, 3H), 3.09-3.13 (m, 1H), 2.77-2.81 (m, 1H), 2.50-2.54 (m, 1H), 2.22-2.27 (m, 1H), 1.86-1.91 (m, 1H) ppm; **^{13}C-NMR** (151 MHz, $CDCl_3$) δ_C 174.8, 172.3, 147.1, 143.3, 129.1, 128.7, 127.1, 126.1, 117.3, 113.3, 56.2, 52.1, 52.0, 40.3, 38.3, 36.9 ppm; **HRMS** (EI): calc. for [$C_{20}H_{23}NO_4$] 364.1519, measured 364.1515; **FT-IR** ν_{max}(ATR) 3413, 2950, 1732, 1600, 1437, 1196, 744 cm^{-1}; **m.p.** 72-74 °C.

Methyl (E)-4-methyl-6-phenyl-6-(phenylamino)hex-3-enoate 95ao

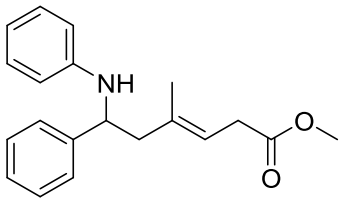

Prepared according to the general procedure. The crude mixture was purified by column chromatography on silica gel eluting with pentane/ethyl acetate 98:2 to afford the title product as a colourless oil.

^{1}H-NMR ($CDCl_3$, 600 MHz) δ_H 7.38-7.39 (d, J = 7.4 Hz, 2H), 7.30-7.33 (t, J = 7.4 Hz, 2H), 7.21-7.24 (t, J = 7.4 Hz, 1H), 7.05-7.07 (t, J = 7.5 Hz, 2H), 6.62-6.64 (t, J = 7.3 Hz, 1H), 6.48-6.49 (d, J = 7.8 Hz, 2H), 5.49-5.52 (t, J = 7.0 Hz, 1H), 4.36-4.38 (dd, J = 4.5, 10.2 Hz, 1H), 3.71 (s, 3H), 3.12-3.16 (dd, J = 7.6, 17.0 Hz, 1H), 3.06-3.10 (dd, J = 6.8, 17.2 Hz, 1H), 2.53-2.56 (dd, J = 3.9, 13.8 Hz, 1H), 2.36-2.40 (dd, J = 10.3, 13.8 Hz, 1H), 1.66 (s, 3H) ppm; **^{13}C-NMR** ($CDCl_3$, 151 MHz) δ_C 172.4, 147.6, 144.3, 136.1, 128.9, 128.6, 126.9, 126.1, 120.1, 117.3, 113.5, 55.5, 51.9, 49.7, 33.4, 15.8 ppm; **HRMS** (EI): calc. for [$C_{20}H_{24}NO_2$] 310.1802, measured 310.1796; **FT-IR** ν_{max}(ATR) 3393, 3024, 2984, 1732, 1600, 1502, 1160, 749, 696 cm^{-1}.

Methyl 4-(*p*-methoxyphenyl)-4-(phenylamino)butanoate 95ba

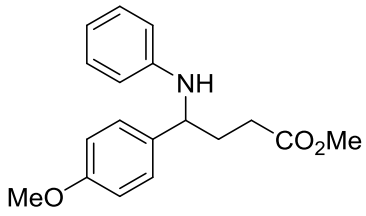

Prepared according to the general procedure with 3.0 equivalents of olefin. The crude mixture was purified by column chromatography on silica gel eluting with pentane/ethyl acetate 10:1 to afford the title product as a colourless solid.

^{1}H-NMR ($CDCl_3$, 600 MHz) δ_H 7.27 (d, J = 8.6 Hz, 2H), 7.00 (t, J = 7.9 Hz, 2H), 6.87 (d, J = 8.6 Hz, 2H), 6.65 (t, J = 7.3 Hz, 1H), 6.54 (d, J = 7.9 Hz, 2H), 4.35 (t, J = 6.7 Hz, 1H), 4.23 (bs, 1H), 3.79 (s, 3H), 3.68 (s, 3H), 2.42 (t, J = 7.2 Hz, 2H), 2.14-2.20 (m, 1H), 2.05-2.11 (m, 1H) ppm; **^{13}C-NMR** ($CDCl_3$, 151 MHz) δ_C 174.1, 158.8, 147.3, 135.1, 129.2, 127.5, 117.4, 114.2, 113.4, 57.2, 55.3, 51.8, 33.3, 31.1 ppm; **HRMS** (EI): calc. for [$C_{18}H_{21}NO_3$] 299.1516, measured 299.1517; **FT-IR** ν_{max}(ATR) 3376, 2954, 1714, 1599, 1506, 1442, 1241, 1172, 1029, 816, 746, 690 cm^{-1}; **m.p.** 49-51 °C.

Methyl 4-(*o*-methoxyphenyl)-4-(phenylamino)butanoate 95ca

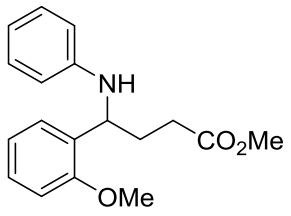

Prepared according to the general procedure with 3.0 equivalents of olefin. The crude mixture was purified by column chromatography on silica gel eluting with pentane/ethyl acetate 95:5 to afford the title product as a yellowish oil.

^{1}H-NMR ($CDCl_3$, 600 MHz) δ_H 7.25-7.26 (dd, J = 1.6, 7.6 Hz, 1H), 7.18-7.21 (td, J = 1.7, 7.0 Hz, 1H), 7.06-7.09 (t, J = 7.4 Hz, 2H), 6.86-6.89 (m, 2H), 6.60-6.62 (t, J = 7.3 Hz, 1H), 6.51-6.53 (d, J = 7.6 Hz, 2H), 4.72-4.74 (t, J = 6.3 Hz, 1H), 4.39 (bs, 1H), 3.88 (s, 3H), 3.65 (s, 3H), 2.37-2.47 (m, 2H), 2.09-2.17 (m, 2H). ppm; **^{13}C-NMR** ($CDCl_3$, 151 MHz) δ_C 174.3, 156.9, 147.3, 130.5, 129.0, 128.0, 127.2, 120.8, 117.1, 113.2, 110.5, 55.3, 52.6, 51.6, 31.4, 31.2 ppm; **HRMS** (EI): calc. for [$C_{18}H_{21}NO_3$] 299.15160, measured 299.15173; **FT-IR** ν_{max}(ATR) 3403, 2949, 1730, 1599, 1499, 1236, 748 cm^{-1}.

Methyl 4-(*p*-tolyl)-4-(phenylamino)butanoate 95da

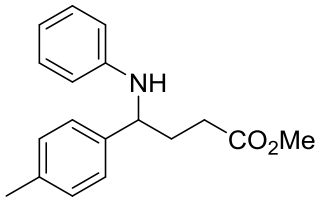

Prepared according to the general procedure with 3.0 equivalents of olefin. The crude mixture was purified by column chromatography on silica gel eluting with pentane/ethyl acetate 10:1 to afford the title product as a yellow oil.

^{1}H-NMR ($CDCl_3$, 600 MHz) δ_H 7.23 (d, J = 8.0 Hz, 2H), 7.13 (d, J = 7.9 Hz, 2H), 7.09 (dd, J = 7.4, 8.4 Hz, 2H), 6.64 (t, J = 7.3 Hz, 1H), 6.53 (d, J = 7.7 Hz, 2H), 4.35 (t, J = 6.9 Hz, 1H), 4.23 (bs, 1H), 3.67 (s, 3H), 2.42 (t, J = 7.2 Hz, 2H), 2.32 (s, 3H), 2.13-2.19 (m, 1H), 2.05-2.11 (m, 1H) ppm; **^{13}C-NMR** ($CDCl_3$, 151 MHz) δ_C 174.2, 147.3, 140.1, 136.9, 129.5, 129.2, 126.4, 117.4, 113.4, 57.5, 51.8, 33.3, 31.2, 21.2 ppm; **HRMS** (EI): calc. for [$C_{18}H_{21}NO_2$] 283.1567, measured 283.1565; **FT-IR** ν_{max}(ATR) 3392, 2950, 2922, 1716, 1600, 1511, 1434, 1315, 1202, 1170, 810, 740, 690 cm^{-1}.

Methyl 4-(*p*-fluorophenyl)-4-(phenylamino)butanoate 95ea

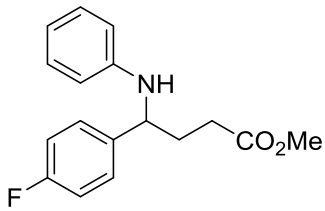

Prepared according to the general procedure using distilled tributylamine with 3.0 equivalents of olefin. The crude mixture was purified by column chromatography on silica gel eluting with pentane/ethyl acetate 10:1 to afford the title product as a colourless solid.

^{1}H-NMR ($CDCl_3$, 400 MHz) δ_H 7.29-7.33 (m, 2H), 7.09 (dd, J = 7.4, 8.5 Hz, 2H), 7.01 (t, J = 8.7 Hz, 2H), 6.66 (t, J = 7.3 Hz 1H), 6.50 (d, J = 7.6 Hz, 2H), 4.37 (t, J = 7.2 Hz, 1H), 4.26 (bs, 1H), 3.68 (s, 3H), 2.42 (t, J = 7.2 Hz, 2H), 2.05-2.19 (m, 2H) ppm; **^{13}C-NMR** ($CDCl_3$, 100 MHz) δ_C 174.0, 162.0 (d, $J_{C\text{-}F}$ 245 Hz), 147.1, 139.0 (d, $J_{C\text{-}F}$ 3.1 Hz), 129.3, 128.0 (d, $J_{C\text{-}F}$ 8.0 Hz), 117.7, 115.7 (d, $J_{C\text{-}F}$ 21.4 Hz), 113.4, 57.3, 51.9, 33.5, 31.1 ppm; **HRMS** (EI): calc. for [$C_{17}H_{18}NO_2F$] 287.1316, measured 287.1315; **FT-IR** ν_{max}(ATR) 3374, 2956, 1716, 1599, 1502, 1197, 828, 747, 691 cm^{-1}; **m.p.** 59-61 °C.

Methyl 4-(*p*-chlorophenyl)-4-(phenylamino)butanoate 95fa

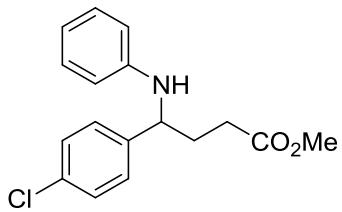

Prepared according to the general procedure with 3.0 equivalents of olefin. The crude mixture was purified by column chromatography on silica gel eluting with pentane/ethyl acetate 10:1 to afford the title product as a yellow oil.

^{1}H-NMR ($CDCl_3$, 600 MHz) δ_H 7.29 (s, 4H) 7.09 (dd, J = 7.4, 8.6 Hz, 2H), 6.66 (t, J = 7.3 Hz, 1H), 6.48 (dd, J = 1.0, 8.6 Hz, 2H), 4.36 (t, J = 6.6 Hz, 1H), 4.29 (bs, 1H), 3.68 (s, 3H), 2.43 (dt, J = 2.3, 7.1 Hz, 2H), 2.05-2.15 (m, 2H) ppm; **^{13}C-NMR** ($CDCl_3$, 151 MHz) δ_C 174.0, 147.0, 141.9, 132.9, 129.3, 129.0, 127.9, 117.7, 113.4, 57.3, 21.9, 33.3, 31.0 ppm; **HRMS** (EI): calc. for [$C_{17}H_{18}NO_2Cl$] 303.1021, measured 303.1024; **FT-IR** ν_{max}(ATR) 3387, 2955, 1714, 1599, 1489, 1195, 1088, 818, 747, 691 cm^{-1}.

Methyl 4-(*p*-bromophenyl)-4-(phenylamino)butanoate 95ga

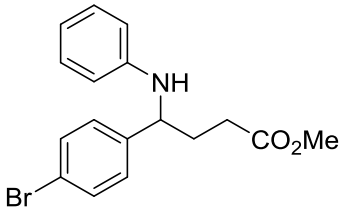

Prepared according to the general procedure with 3.0 equivalents of olefin. The crude mixture was purified by column chromatography on silica gel eluting with pentane/ethyl acetate 10:1 to afford the title product as a yellow oil.

^{1}H-NMR ($CDCl_3$, 600 MHz) δ_H 7.44 (d, J = 8.4 Hz, 2H), 7.23 (d, J = 8.4 Hz, 2H), 7.09 (dd, J = 7.4, 8.5 Hz, 2H), 6.66 (t, J = 7.3 Hz, 1H), 6.48 (d, J = 7.7 Hz, 2H), 4.35 (dd, J = 6.0, 7.6 Hz, 1H), 4.28 (bs, 1H), 3.68 (s, 3H), 2.43 (dt, J = 3.5, 7.1 Hz, 2H), 2.05-2.15 (m, 2H) ppm; **^{13}C-NMR** ($CDCl_3$, 151 MHz) δ_C 174.4, 14.9, 142.4, 131.9, 129.3, 128.3, 121.0, 117.7, 113.4, 57.4, 52.0, 33.3, 31.0 ppm; **HRMS** (EI): calc. for [$C_{17}H_{18}NO_2Br$] 347.0515, measured 347.0515; **FT-IR** ν_{max}(ATR) 3392, 2945, 1722, 1600, 1495, 1189, 1009, 815, 750, 693 cm^{-1}.

Methyl 4-phenyl-4-[(*p*-fluorophenyl)amino]butanoate 95ha

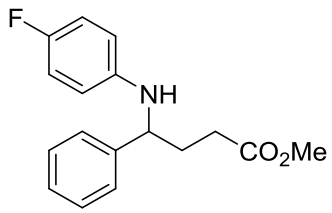

Prepared according to the general procedure using distilled tributylamine with 3.0 equivalents of olefin. The crude mixture was purified by column chromatography on silica gel eluting with pentane/ethyl acetate 10:1 to afford the title product as a colorless solid.

^{1}H-NMR ($CDCl_3$, 400 MHz) δ_H 7.30-7.33 (m, 4H), 7.23-7.25 (m, 1H), 6.79 (t, J = 8.8 Hz, 2H), 6.44 (dd, J = 4.4, 9.0 Hz, 2H), 4.31 (t, J = 7.2 Hz, 1H), 4.17 (bs, 1H), 3.67 (s, 3H), 2.42 (t, J = 7.2 Hz, 2H), 2.06-2.20 (m, 2H) ppm; **^{13}C-NMR** ($CDCl_3$, 100 MHz) δ_C 174.1, 155.8 (d, $J_{C\text{-}F}$ 235 Hz), 143.6 (d, $J_{C\text{-}F}$ 1.1 Hz), 143.0, 128.9, 127.4, 126.5, 115.6 (d, $J_{C\text{-}F}$ 22.3 Hz), 114.23 (d, $J_{C\text{-}F}$ 7.4 Hz), 58.5, 51.9, 33.3, 31.1 ppm; **HRMS** (EI): calc. for [$C_{17}H_{18}NO_2F$] 287.1316, measured 287.1318; **FT-IR** ν_{max}(ATR) 2950, 1729, 1509, 1211, 1169, 821, 459, 700 cm^{-1}; **m.p.** 64-66 °C.

Methyl 4-phenyl-4-[(*p*-chlorophenyl)amino]butanoate 95ia

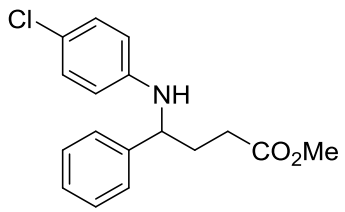

Prepared according to the general procedure using distilled tributylamine with 3.0 equivalents of olefin. The crude mixture was purified by column chromatography on silica gel eluting with pentane/ethyl acetate 10:1 to afford the title product as a colourless solid.

^{1}H-NMR ($CDCl_3$, 400 MHz) δ_H 7.29-7.35 (m, 4H), 7.22-7.26 (m, 1H), 7.02 (d, J = 8.9 Hz, 2H), 6.43 (d, J = 8.9 Hz, 2H), 4.32-4.35 (m, 2H), 3.67 (s, 3H), 2.42 (t, J = 7.3 Hz, 2H), 2.06-2.20 (m, 2H) ppm; **^{13}C-NMR** ($CDCl_3$, 100 MHz) δ_C 174.1, 145.8, 142.7, 129.0, 128.9, 127.5, 126.4, 122.0, 114.5, 58.0, 51.9, 33.2, 31.1 ppm; **HRMS** (EI): calc. for [$C_{17}H_{18}NO_2Cl$] 303.1021, measured 303.1024; **FT-IR** ν_{max}(ATR) 2947, 1722, 1597, 1497, 1443, 1272, 1168, 817, 697 cm^{-1}; **m.p.** 64-66 °C.

Methyl 4-phenyl-4-[(*p*-phenoxyphenyl)amino]butanoate 95ja

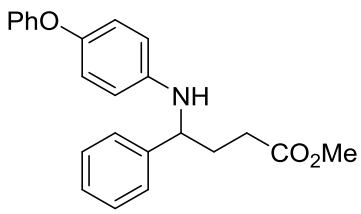

Prepared according to the general procedure with 3.0 equivalents of olefin. The crude mixture was purified by column chromatography on silica gel eluting with pentane/ethyl acetate 10:1 to afford the title product as a colourless oil.

^{1}H-NMR ($CDCl_3$, 600 MHz) δ_H 7.34-7.37 (m, 4H), 7.25-7.28 (m, 3H), 7.00 (t, J = 7.4 Hz, 1H), 6.90 (dd, J = 1.0, 8.7 Hz, 2H), 6.82 (d, J = 8.9 Hz, 2H), 6.52 (d, J = 8.9 Hz, 2H), 4.36 (dd, J = 6.3, 7.5 Hz, 1H), 4.20 (bs, 1H), 3.69 (s, 3H), 2.44 (t, J = 7.2 Hz, 2H), 2.16-2.22 (m, 1H), 2.09-2.15 (m, 1H) ppm; **^{13}C-NMR** ($CDCl_3$, 151 MHz) δ_C 174.1, 159.1, 147.7, 143.9, 143.2, 129.6, 128.9, 127.4, 126.5, 122.0, 121.1, 117.3, 114.4, 58.4, 51.9, 33.4, 31.1 ppm; **HRMS** (EI): calc. for [$C_{23}H_{23}NO_3$] 362.1751, measured 362.1753; **FT-IR** ν_{max}(ATR) 2941, 1725, 1490, 1215, 832, 747 cm^{-1}.

Methyl 4-phenyl-4-[(*p*-methoxyphenyl)amino]butanoate 95ka

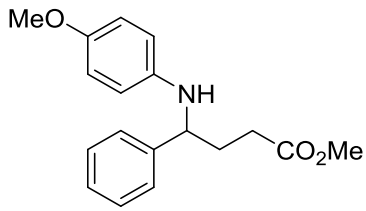

Prepared according to the general procedure. The crude mixture was purified by column chromatography on silica gel eluting with pentane/ethyl acetate 98:2 to 9:1 afford the title product as a yellowish oil. All analytical data are in agreement with literature[xxxv]

^{1}H-NMR (600 MHz, $CDCl_3$) δ_H 7.30-7.33 (m, 4H), 7.22-7.24 (m, 1H), 6.67-6.69 (d, J = 8.4 Hz, 2H), 6.47-6.48 (d, J = 7.7 Hz, 2H), 4.29-4.31 (t, J = 7.2 Hz, 1H), 3.96 (bs, 1H), 3.68 (s, 3H), 3.66 (s, 3H), 2.40-2.42 (t, J = 7.2 Hz, 2H), 2.06-2.16 (m, 2H) ppm; **^{13}C-NMR** (151 MHz, $CDCl_3$) δ_C 174.0, 151.9, 143.3, 141.3, 128.6, 127.2, 126.4, 114.7, 114.5, 58.5, 55.7, 51.7, 33.0 31.0 ppm.

Ethyl 2-methylene-4-phenyl-4-(phenylamino)butanoate 95b

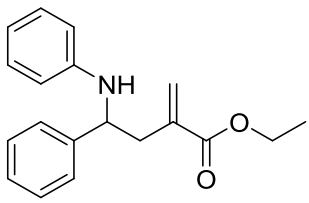

Prepared according to the general procedure. The crude mixture was purified by column chromatography on silica gel eluting with pentane/ethyl acetate 98:2 to afford the title product as a white solid.

^{1}H-NMR (600 MHz, $CDCl_3$) δ_H 7.37-7.39 (d, J = 7.3 Hz, 2H), 7.31-7.34 (t, J = 6.8 Hz, 2H), 7.22-7.26 (m, 1H), 7.06-7.08 (t, J = 7.4 Hz, 2H), 6.62-6.64 (t, J = 7.4 Hz, 1H), 6.49-6.50 (d, J = 7.8 Hz, 2H), 6.49-6.50 (d, J = 1.0 Hz, 1H), 6.23 (d, J = 1.0 Hz, 1H), 4.51-4.53 (m, 2H), 4.21-4.25 (q, 2H), 2.73-2.81 (m, 2H), 1.31-1.33 (t, 3H). ppm; **^{13}C-NMR** (151 MHz, $CDCl_3$) δ_C 167.4, 147.2, 143.4, 137.5, 129.0, 128.6, 127.8, 127.1, 126.3, 117.2, 113.3, 61.1, 58.1, 41.3, 14.2 ppm; **HRMS** (EI): calc. for $[C_{19}H_{22}NO_2]^+$ 296.16451, measured 296.16507; **FT-IR** ν_{max}(ATR) 3401, 2978, 1697, 1600, 1509, 1321, 1149 ,694 cm^{-1}; **m.p.** 64-65 °C.

N-(3-(4-(tert-butyl)phenyl)-1-phenylbut-3-en-1-yl)aniline 95c

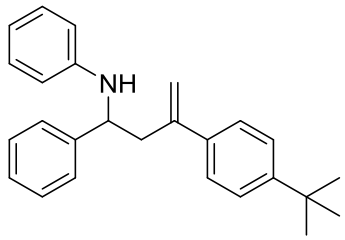

Prepared according to the general procedure. The crude mixture was purified by column chromatography on silica gel eluting with pentane/ethyl acetate 98:2 to afford the title product as white solid.

^{1}H-NMR (600 MHz, $CDCl_3$) δ_H 7.37-7.41 (m, 6H), 7.30-7.33 (m, 1H), 7.22-7.24 (t, J = 7.2 Hz, 2H), 7.00-7.03 (t, J = 7.3 Hz, 2H), 6.59-6.61 (t, J = 7.4 Hz, 1H), 6.38-6.40 (d, J = 7.8 Hz, 2H), 5.38 (s, 1H), 5.10 (s, 1H), 4.33-4.35 (dd, J = 4.7, 9.5 Hz, 1H), 4.17 (bs, 1H), 3.03-3.07 (dd, J = 4.6, 14.6 Hz, 1H), 2.78-2.82 (dd, J = 9.5, 14.6 Hz, 1H), 1.33 (s, 9H) ppm; **^{13}C-NMR** (151 MHz, $CDCl_3$) δ_C 150.8, 147.4, 144.9, 144.2, 137.0, 128.9, 128.6, 126.9, 126.2, 125.9, 125.4, 117.3, 114.9, 113.6, 56.5, 45.5, 34.5, 31.3 ppm; **HRMS** (EI): calc. for $[C_{26}H_{30}N]^+$ 356.23728, measured 356.23785; **FT-IR** ν_{max}(ATR) 3408, 2960, 1601, 1502, 748, 695 cm^{-1}; **m.p.** 68-71 °C.

Synthesis of γ-lactams

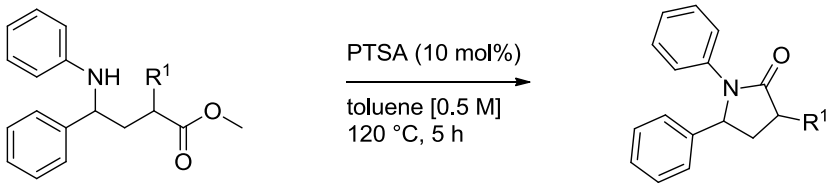

95 **96**

General procedure

In an oven-dried test tube equipped with magnetic stir bar and a reflux condenser were placed **95** (1.0 equiv.) and *p*-toluensulfonic acid PTSA (0.1 equiv.). Toluene was added and the mixture was stirred at 120 °C for 5 hours. After complete conversion, the reaction mixture was concentrated *in vacuo*, and the residue was purified by column chromatography on silica gel (see below for eluent used).

1,5-diphenylpyrrolidin-2-one 96aa

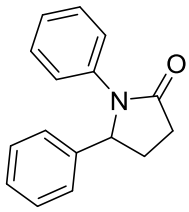

Prepared according to the general procedure. The crude mixture was purified by column chromatography on silica gel eluting with pentane/ethyl acetate 6:4 to afford the title product as a white solid. All analytical data are in agreement with literature.[xxxv]

^{1}H-NMR (600 MHz, $CDCl_3$) δ_H 7.34-7.35 (d, J = 7.8 Hz, 2H), 7.21-7.22 (m, 2H), 7.12-7.16 (m, 5H), 6.95-6.97 (t, J = 7.2 Hz, 1H), 5.15-5.17 (dd, J = 4.5, 7.5 Hz, 1H), 2.64-2.68 (m, 1H), 2.48-2.56 (m, 2H), 1.89-1.93 (m, 1H) ppm; **^{13}C-NMR** (151 MHz, $CDCl_3$) δ_C 174.8, 141.2, 138.1, 128.9, 128.6, 127.6, 125.8, 124.8, 122.0, 63.8, 31.1, 29.1 ppm.

3-methyl-1,5-diphenylpyrrolidin-2-one 96aj

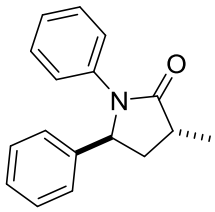

Prepared according to the general procedure. The crude mixture was purified by column chromatography on silica gel eluting with pentane/ethyl acetate 9:1 to 8:2. Diastereoisomers were isolated separately as brownish solids. The relative configuration was assigned by comparison with literature.[xxxv]

^{1}H-NMR (600 MHz, $CDCl_3$) δ_H 7.51-7.53 (d, J = 7.7 Hz, 2H), 7.29-7.32 (m, 2H), 7.19-7.25 (m, 5H), 7.02-7.06 (t, J = 7.4 Hz, 1H), 5.17-5.19 (dd, J = 3.4, 7.2 Hz, 1H), 2.76-2.84 (m, 1H), 2.21-2.26 (m, 2H), 1.28-1.29 (d, J = 7.0 Hz, 3H) ppm; **^{13}C-NMR** (151 MHz, $CDCl_3$) δ_C 177.2, 141.2, 138.7, 128.9, 128.7, 127.6, 125.6, 124.4, 121.0, 61.5, 37.9, 35.8, 15.8 ppm; **HRMS** (EI): calc. for [$C_{17}H_{17}NO$] 252.1383, measured 252.1383 **FT-IR** ν_{max}(ATR) 3357, 2970, 1682, 1494, 1389, 1284, 1027, 753 cm^{-1}; **m.p.** 95-98 °C.

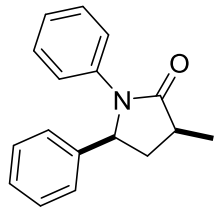

^{1}H-NMR (600 MHz, $CDCl_3$) δ_H 7.29-7.32 (d, J = 7.6 Hz, 2H), 7.16-7.24 (m, 2H), 6.99-7.03 (m, 5H), 7.02-7.06 (t, J = 7.3 Hz, 1H), 5.13-5.16 (dd, J = 6.7, 8.9 Hz, 1H), 2.69-2.83 (m, 2H), 1.62-1.67 (m, 1H), 1.34-1.36 (d, J = 6.8 Hz, 3H) ppm; **^{13}C-NMR** (151 MHz, $CDCl_3$) δ_C 177.2, 141.3, 137.9, 128.7, 128.4, 127.6, 126.4, 124.8, 123.0, 61.8, 39.0, 37.6, 16.5 ppm; **HRMS** (EI): calc. for [$C_{17}H_{17}NO$] 252.1383, measured 252.1383; **FT-IR** ν_{max}(ATR) 3373, 2963, 1673, 1495, 1385, 1259, 1021, 799 cm^{-1}; **m.p.** 99-101 °C

***trans*-N-(2-oxo-1,5-diphenylpyrrolidin-3-yl)acetamide 96am**

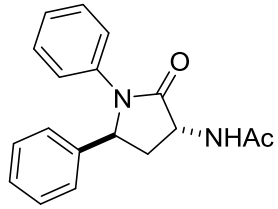

Prepared according to the general procedure. The crude mixture was purified by column chromatography on silica gel eluting with ethyl acetate to afford the title product as a brownish oil. The relative configuration was assigned by NOESY experiment.

^{1}H-NMR (600 MHz, $CDCl_3$) δ_H 7.52-7.54 (d, J = 7.7 Hz, 2H), 7.25-7.34 (m, 5H), 7.17-7.18 (d, 2H), 7.09-7.12 (t, J = 7.4 Hz, 1H), 6.12 (bs, 1H), 5.24-5.27 (d, J = 8.5 Hz, 1H), 4.63-4.69 (m, 1H), 2.76-2.82 (dd, J = 8.9, 12.3 Hz, 1H), 2.37-2.45 (dd, J = 8.8, 12.3 Hz, 1H), 2.04 (s, 3H) ppm; **^{13}C-NMR** (151 MHz, $CDCl_3$) δ_C 171.8, 170.3, 139.0, 136.5, 128.4, 128.2, 127.6, 126.3 125.3, 122.9, 60.4, 52.1, 38.5, 22.6 ppm; **HRMS** (EI): calc. for [$C_{18}H_{18}N_2O_2Na$] 317.1261, measured 317.1265; **FT-IR** ν_{max}(ATR) 3274, 3065, 2924, 1700, 1646, 1389, 1299, 754 cm^{-1}.

***cis*-N-(2-oxo-1,5-diphenylpyrrolidin-3-yl)acetamide**

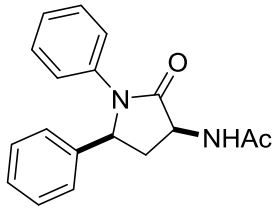

Prepared according to the general procedure. The crude mixture was purified by column chromatography on silica gel eluting with ethyl acetate to afford the title product as a brownish oil. The relative configuration was assigned by NOESY experiment.

^{1}H-NMR (600 MHz, $CDCl_3$) δ_H 7.17-7.30 (m, 9H), 7.05-7.08 (t, J = 7.3 Hz, 1H), 6.45 (bs, 1H), 5.16-5.18 (dd, J = 6.3, 9.8 Hz, 1H), 4.59-4.63 (m, 1H), 3.23-3.27 (m, 1H), 2.07 (s, 3H), 1.88-1.93 (dd, J = 8.9, 12.8 Hz, 1H) ppm; **^{13}C-NMR** (151 MHz, $CDCl_3$) δ_C 172.2, 170.8, 139.5, 137.0, 128.8, 128.6, 128.0, 126.8, 125.7, 123.3, 60.8, 52.5, 38.9, 23.1 ppm; **HRMS** (EI): calc. for [$C_{18}H_{18}N_2O_2Na$] 317.1261, measured 317.1266; **FT-IR** ν_{max}(ATR) 3292, 3066, 2926, 1702, 1659, 1374, 762 cm^{-1}.

Methyl 2-oxo-1,5-diphenylpyrrolidine-3-carboxylateone 96an

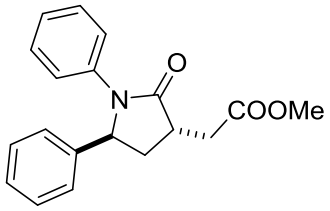

Prepared from **4an** according to the general procedure. The crude mixture was purified by column chromatography on silica gel eluting with ethyl acetate to afford the title product (*trans* diastereoisomer) as a brownish oil. The relative configuration was assigned by NOESY experiment.

^{1}H-NMR (600 MHz, $CDCl_3$) δ_H 7.52-7.53 (d, J = 7.8 Hz, 2H), 7.32-7.34 (t, J = 7.3 Hz, 2H), 7.21-7.28 (m, 5H), 7.06-7.08 (t, J = 7.3 Hz, 1H), 5.23-5.25 (d, J = 7.3 Hz, 1H), 3.69 (s, 3H), 3.17-3.23 (m, 1H), 2.97-3.00 (dd, J = 4.3, 16.7 Hz, 1H), 2.54-2.58 (dd, J = 8.8, 16.7 Hz, 1H), 2.38-2.43 (m, 1H), 2.32-2.36 (m,1H) ppm; **^{13}C-NMR** (151 MHz, $CDCl_3$) δ_C 179.4, 172.3, 140.9, 138.5, 129.1, 128.8, 127.7, 125.6, 124.8, 121.1, 61.7, 51.9, 37.7, 35.5, 35.2 ppm; **HRMS** (EI): calc. for [$C_{19}H_{19}NO_3Na$] 332.1257, measured 332.1256; **FT-IR** ν_{max}(ATR) 3031, 2950, 1734, 1695, 1495, 1384, 1172, 765 cm^{-1}.

Flow photoredox experiments

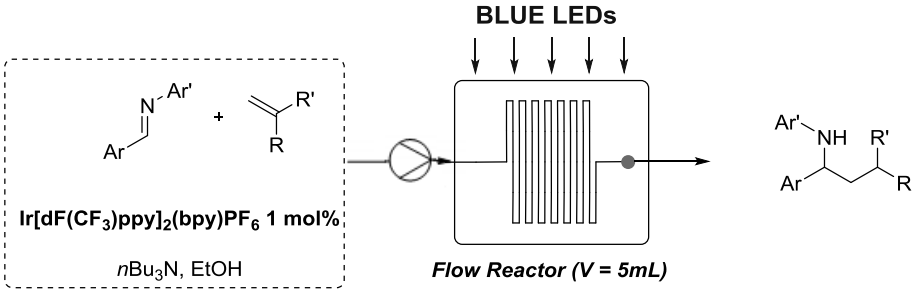

A PTFE tubing (*id* = 0.8 mm, *l* = 10 m, V_i = 5 mL) was wrapped around a glass beaker (*id* = 9 cm, *h* = 5 cm) and placed into a dewar flask where 2 rows of 11W blue LEDs strips were previously fixed. One end of the tubing was connected to a steel needle and the other placed into a receiving flask.

In an oven-dried test tube equipped with magnetic stir bar were placed $Ir[F(CF_3)ppy]_2(bpy)PF_6$ (0.02 equiv.) and the imine (1.0 equiv.). The tube was closed with a septum and purged three times with a sequence vacuum/argon before addition of degassed ethanol, NBu_3 (1.5 equiv.), and olefin (3.0 equiv.). The mixture was stirred for 5 minutes until a homogeneous solution was obtained.

Continuous-flow method:

The mixture was loaded into a 5 mL plastic syringe, pumped into the flow reactor through a syringe pump at the indicated flow rate and irradiated with blue light. Afterwards the reactor was washed with 5 mL of degased EtOH at the same flow rate under continuous light irradiation. The output of the reactor was collected into a round bottom flask, concentrated *in vacuo*, and the residue was purified by column chromatography on silica gel.

Stop-flow method:

The reactor was filled with reagents mixture and irradiated with blue LEDs for 4 hours. After reaction time the the reactor was washed with 5 mL of degased EtOH and the crude was recovered and concentrated in vacuo, and the residue was purified by column chromatography on silica gel.

General procedure for inline monitoring of reaction progress

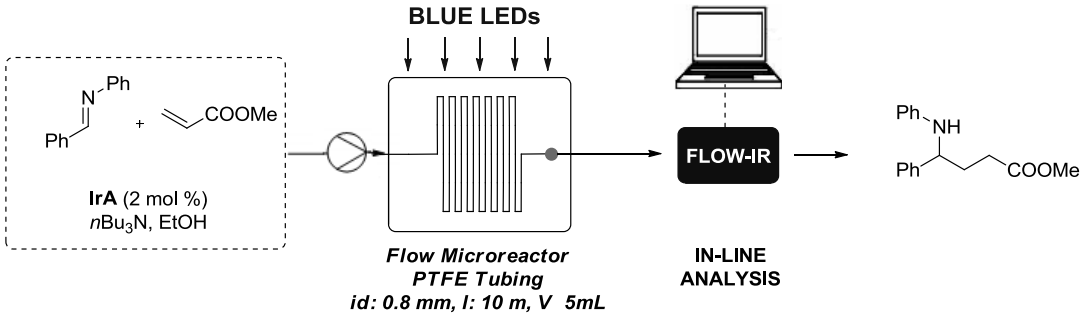

In an oven-dried test tube equipped with magnetic stir bar were placed Ir[F(CF_3)ppy]$_2$(bpy)PF_6 **IrA** (7.8 mg, 0.004 mmol, 0.02 equiv.) and *N*-benzylideneaniline **93a** (0.4 mmol, 1.0 equiv.). The tube was closed with a septum and purged three times with a sequence vacuum/argon before addition of degassed ethanol (4.0 mL), NBu_3 (142 μL, 0.6 mmol, 1.5 equiv.), and methyl acrylate **94a** (108 μL, 1.2 mmol, 3.0 equiv.). The flow reactor was set-up the same as described above and the way out was connected to a Mettler-Toledo FlowIR instrument. The flow reactor was then filled with the crude reaction mixture and irradiated with blue LEDs (stop-flow method). At predefined intervals of time, by injecting 0.3 mL of EtOH in the reactor, an aliquot of the crude mixture was directed to the flowIR and absorbance spectra were recorded. For inline analysis we identified signals at ν = 1633 cm^{-1} and ν = 1607 cm^{-1} corresponding to starting imine **93a** and product **95aa**, respectively. Raw data were analysed with iC-IR analysis software.

Figure 33 shows real time IR spectra of the reaction mixtures in the spectral region of 1640 and 1595 cm^{-1}. It can be easily observed **93a** consumption and **95aa** formation at different retention times.

Figure34 shows the real-time plot of the peak intensity versus retention time for the 1607 cm^{-1} absorption band of **95aa**. Plotted data are normalized to the isolated yield of **95aa** obtained for a residence time corresponding to 4 hours (80% yields).

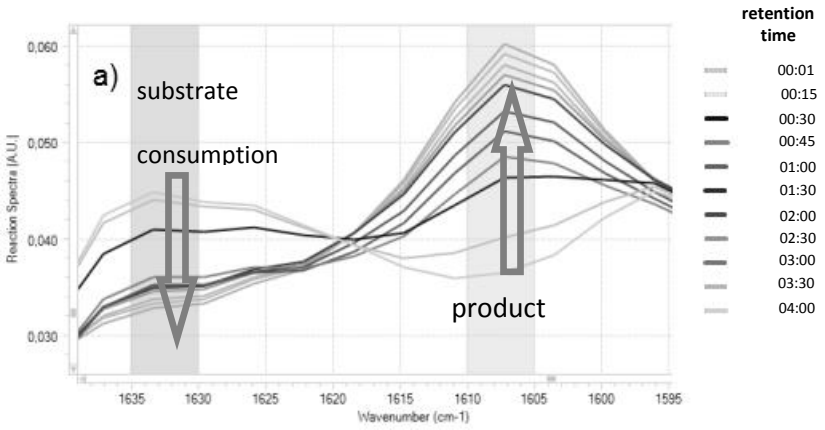

Figure 33. Inline FlowIR analysis: reaction IR spectra showing the consumption of substrate and the formation of product at different reaction times.

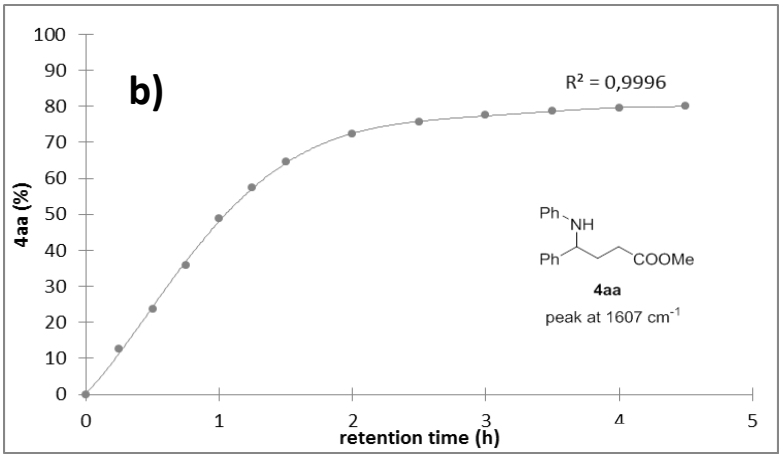

Figure 34. Inline FlowIR analysis: trend-curve of product formation at different retention times.

General Set-Up of Continuous Flow Reactions with Microreactors

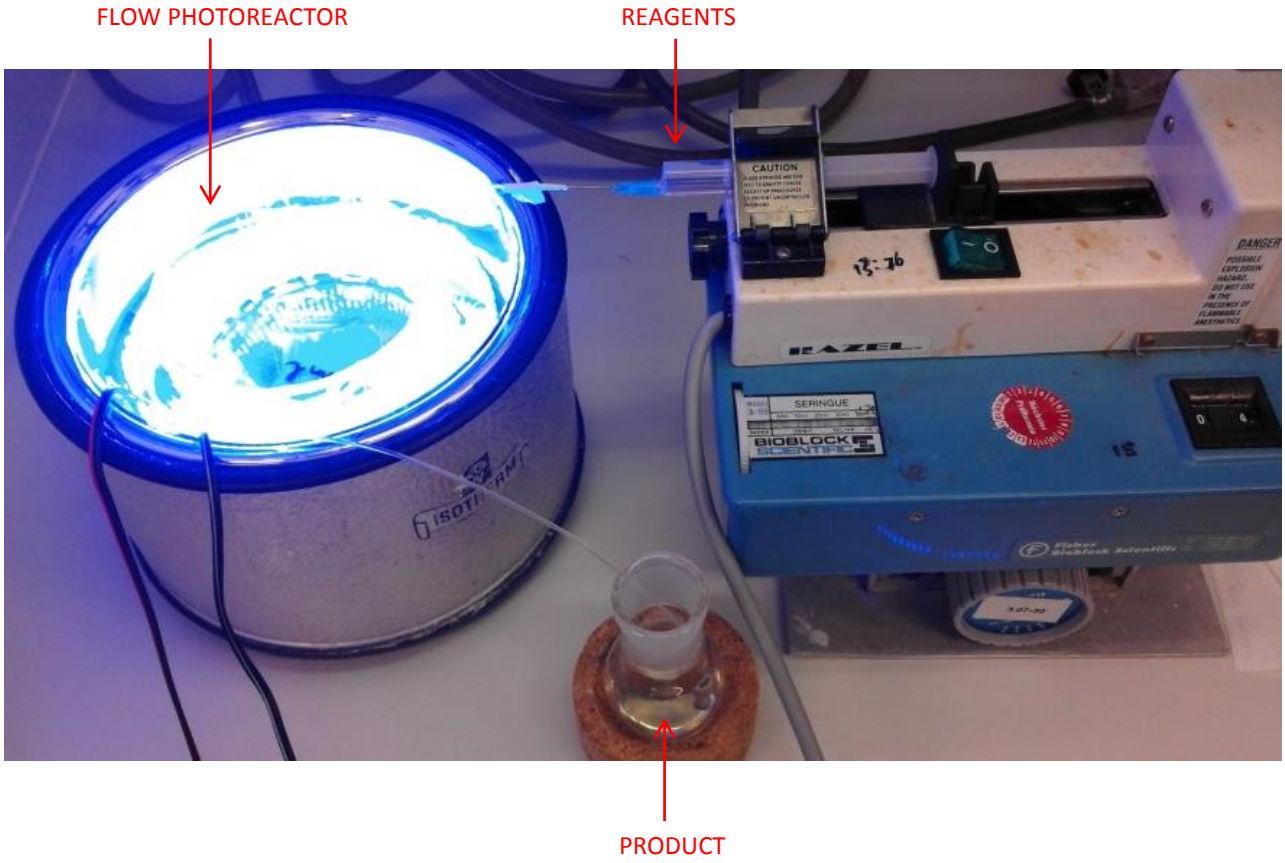

REFERENCES

[1] B. J. Reizman, K. F. Jensen, *Acc. Chem. Res.* **2016**, *49*, 1786.

[2] C. J. Mallia, I. R. Baxendale, *Org. process. Res. Dev.* **2016**, *20*, 327.

[3] a) B. L. Trout *et al. Angew. Chem. Int. Ed.***2013**, *52*, 12359; b) K. F. Jensen *et al., Org. Process Res. Dev.* **2014**, *18*, 402.

[4] A. Adamo, T. F. Jamison, F. F. Jensen *et al. Science* **2016**, 352, 61.

[5] P. T. Anastas, *Green Chemistry Textbook*; Oxford University Press: New York, **2004**.

[6] a) V. Hessel *et al. ChemSusChem***2013**, *6*, 746; b) J. Wegner, S. Ceylan, A. Kirschning, *Adv. Synth. Catal.* **2012**, *354*, 17.

[7] P. T. Anastas, J. C. Warner, *Green Chemistry: Theory and Practice*, Oxford University Press: New York, **1998.**

[8] M. Benaglia, Recoverable and Recyclable Catalysts, Wiley-VCH, Weinheim, **2009**.

[9] R. Munirathinam, J. Huskens, W. Verboom, *Adv. Synth. Catal.* **2015**, *357*, 1093.

[10] For some reviews about continuous flow stereoselective catalytic processes see: a) T. Tsubogo, T. Ishiwata, S. Kobayashi, *Angew. Chem. Int. Ed.* **2013**, *52*, 6590; b) D. Zhao, K. Ding, *ACS Catal.* **2013**, *3*, 928*;* c) X. Y. Mak, P. Laurino, P. H. Seeberger, *Beilstein J. Org. Chem.* **2009**, *5*, DOI:10.3762/bjoc.5.19.

[11] T. Tsubogo, H. Oyamada, S. Kobayashi, *Nature*, **2015**, *520*, 329.

[12] a) T. Okhuma, R. Noyori, *Comprehensive Asymmetric Catalysis*;b) E. N. Jacobsen, A. Pfaltz, H. Yamamoto, Eds.; Springer: New York, NY, USA, **2004**.

[13] a) C. Rodríguez-Escrich, M. A. Pericàs, *Eur. J. Org. Chem*. **2015**, *6*, 1173; b) A. Puglisi, M. Benaglia, V. Chiroli, *Green Chem.* **2013**, *15*, 1790.

[14] a) D. Cantillo, C. O. Kappe, *ChemCatChem* **2014**, *6*, 3286; b) I. V. Gursel, T. Noel, Q. Wang, V. Hessel, *Green Chem.* **2015**, *17*, 2012-2026.

[15] a) S.A. Selkälä, J. Tois, P.M. Pihko, A.M.P. Koskinen, *Adv. Synth. Catal.* **2002**, *344*, 941; b) Y. Zhang, L. Zhao, S. S. Lee, J. Y. Ying, *Adv. Synth. Catal.* **2006**, *348*, 2027; c) N. Haraguchi et al., *Tetrahedron Letters* **2010**, *51*, 1205-1208; d) H. Hagiwara, T. Kuroda, T. Hoshi, T. Suzuki, *Adv. Synth. Catal.* **2010**, *352*, 909; e) J. Y. Shi, C. A. Wang, Z. J. Li, Q. Wang, Y. Zhang, W. Wang, *Chem. Eur. J.* **2011**, *17*, 6206; f) M. Benaglia, G. Celentano, M. Cinquini, A. PUglisi, F. Cozzi, *Adv. Synth. Catal.* **2002**, *344*, 149-152; g) A. Puglisi, M. Benaglia, M. Cinquini, F. Cozzi, G. Celentano, *Eur. J. Org. Chem.* **2004**, 567-573; h) S. Guizzetti, M. Benaglia, J. S. Siegel, *Chem. Commun.* **2012**, 48, 3188-3190; i) Riente, P.; Yadav, J.; Pericas, M. A. *Org. Lett*. **2012**, *14*, 3668.

[16] a) R. E. Dolle, *J. Org. Chem*. **1985**, *50*, 1440; b) G. S. Besra, D. E. Minnikin, P. R. Wheeler, C. Ratledge, *Chem. Phys. Lipids* **1993**, *66*, 23; c) T. Wakabayashi, K. Mori, S. Kobayashi, *J. Am. Chem. Soc.* **2001**, *123*, 1372; d) A. Fürstner, M. Bonnekessel, J. T. Blank, K. Radkowski, G. Seidel, F. Lacombe, B. Gabor, R. Mynott, *Chem. Eur. J.* **2007**, *13*, 8762.

[17] a) P. G. Cozzi, F. Benfatti, L. Zoli, *Angew. Chem. Int. Ed.* **2009**, *48*, 1313; b) F. Benfatti, E. Benedetto, P. G. Cozzi, *Chem. Asian J.* **2010**, *5*, 2047.

[18] For the batch reaction see: A. Salvo, F. Giacalone, R. Noto, M. Gruttadauria, *ChemPlusChem,* **2014**, *79*, 857.

[19] H. Brunner, J. Bugler, B. Nuber, *Tetrahedron: Asymmetry* **1995**, *6*, 1699.

[20] C. E. Song, *Cinchona Alkaloids in Synthesis and Catalysis*, Wiley-VCH, Weinheim, **2009.**

[21] For seminal works see: a) J.-W. Xie, W. Chen, R. Li, M. Zeng, W. Du, L. Yue, Y.-C. Chen, Y.Wu, J. Zhu, J.-G. Deng, *Angew. Chem. Int. Ed.* **2007**, *46*, 389-392; b) G. Bartoli, M. Bosco, A. Carlone, F. Pesciaioli, L. Sambri, P. Melchiorre, *Org. Lett.* **2007**, *9*, 1403-1405; c) S. H. McCooey, S. J. Connon, *Org. Lett.* **2007**, *9*, 599-602.

[22] a) A. Marcelli, H. Hiemstra, *Synthesis* **2010**, 1229 – 1279; b) P. Melchiorre, *Angew. Chem.Int. Ed*. **2012**, *51*, 9748 - 9770; c) J. Duan, P. Li, *Catal. Sci. Technol*. **2014**, *4*, 311-320.

[23] For some example on solid supported cinchona derived primary amines see: a) J. Zhou, J. Wan, X. Ma, W. Wang, *Org. Biomol. Chem*., **2012**, *10*, 4179-4185; b) W. Wang, X. Ma, J. Wan, J. Cao, T. Tang, *Dalton Trans*., **2012**, *41*, 5715–5726.; For a very recent example concerning the application in flow processes see: Izquierdo, J.; Ayats, C.; Henseler, A. H.; Pericàs, M. A. *Org. Biomol. Chem.* **2015**, *13,* 4204.

[24] K.M. Kacprzak, W. Lindner, N.M. Maier, *Chirality* **2008**, *20*, 441.

[25] M. Benaglia, G. Celentano, M. Cinquini, A. Puglisi, F. Cozzi, *Adv. Synth. Catal*. **2002**, *344*, 533-542.

[26] S.H. McCooey, S.J. Connon, *Org Lett*. **2007**, *9,* 599.

[27] W. Liu, D. Mei, W. Wang, D. Duan, *Tetrahedron Letters* **2013**, *24*, 3791.

[28] E. Massolo, M. Benaglia, D. Parravicini, D. Brenna, R. Annunziata, *Tetrahedron Letters* **2014**, *55*, 6639.

[29] J.W. Xie, L. Yue, W. Chen, W. Du, J. Zhu, J.G. Deng, Y.C. Chen**,** *Org. Lett.* **2007**, *9,* 413.

[30] Chiral Amine Synthesis: Methods, Developments and Applications (Ed.: T. C. Nugent), Wiley-VCH, Weinheim, **2010**.

[31] a) M. Benaglia, A. Genoni, M. Bonsignore, M. **2012** ed. Ramon Rios Torres, Wiley; b) S. Rossi, M. Benaglia, E. Massolo, L. Raimondi, *Catal. Sci. Technol.* **2014**, *9*, 2708; c) S. Guizzetti, M. Benaglia, *Eur. J. Org. Chem.* **2010**, 5529.

[32] a) S. Guizzetti, M. Benaglia, R. Annunziata, F. Cozzi, *Tetrahedron* **2009**, *65*, 6354-6363; b) S. Guizzetti, M. Benaglia, M. Bonsignore, L. Raimondi, *Org. Biomol. Chem*. **2011**, *9*, 739-743; c) S. Guizzetti, M. Benaglia, F. Cozzi, S. Rossi, G. Celentano, *Chirality* **2009**, *21*, 233-238; d) M. Bonsignore, M. Benaglia, L. Raimondi, M. Orlandi, G. Celentano, *Beilstein J. Org. Chem.* **2013,** *9,* 633-640.

[33] D. Brenna, R. Porta, E. Massolo, L. Raimondi, M. Benaglia *Submitted for publication.*

[34] A. Puglisi, M. Benaglia, R. Annunziata, V. Chiroli, R. Porta, A. Gervasini, *J. Org. Chem.* **2013**, *78*, 11326.

[35] R. Braslau, F. Rivera, C. Tansakul, C. *Reactive and Functional Polymers*, **2013**, *73*, 624.

[36] C. Wiles, P. Watts, *Eur. J. Org. Chem.* **2008**, 1655.

[37] K. S. Elvira, X. Solvas, R. C. R. Wooton, A. deMello, *Nat. Chem.* **2014**, DOI: 10.1038/NCHEM.1753.

[38] J. Wegner, S. Ceylan, A. Kirschning, *Chem. Commun.* **2011**, *47*, 4583.

[39] Gutmann, B.; Cantillo, D.; Kappe, C. O. *Angew. Chem. Int. Ed*. **2015**, *54*, 6688.

[40] A. Puglisi, M. Benaglia, R. Porta, F. Coccia, *Current Organocatalysis* **2015**, *2*, 79.

[41] S. Rossi, M. Benaglia A. Puglisi C. De Filippo M. Maggini, *J. Flow. Chem*. **2014**, *5*, 17.

[42] O. Bassas, J. Huuskonen, K. Rissanen, A. M. P. Koskinen, *Eur. J. Org. Chem.***2009**, *9*, 1340-1351.

[43]Liu, J.-M.L.; Wang, X.; Ge, Z.-M.; Sun, Q.; Cheng, T.-M.; Li, R.-T. *Tetrahedron* **2011**, *67*, 636-640.

[44] N. Halland, T. Hansen, K. A. Jorgensen, *Angew. Chem. Int. Ed.* **2003**, *42*, 4955–4957.

[45] H. Kim, C. Yen, P. Preston, J. Chin, *Org. Lett.* **2006**, *8*, 5239-5242.

[46] J. Xie, L. Yue, W. Chen, W. Du, J. Zhu, J. Deng, Y. Chen, *Org. Lett.* **2007**, *9*, 413–415.

[47] M. Orlandi, D. Brenna, R. Harms, S. Jost, M. Benaglia *Org. Process Res. Dev.* **2016**, DOI: 10.1021/acs.oprd.6b00205.

[48] M. Orlandi, F. Tosi, M. Bonsignore, M. Benaglia *Org. Lett.* **2015**, *17*, 3941. The methodology is described in a patent: International Patent Application: M. Bonsignore, M. Benaglia, PCT/EP/**2013**/0683 (Università degli Studi di Milano, Milano, Italy), now owned by DexLeChem GmbH (Berlin, Germany).

[49] M. Orlandi, M. Benaglia, F. Tosi, R. Annunziata, F. Cozzi *J. Org. Chem.* **2016**, *81*, 3037-3041.

[50] Review on continuous flow hydrogenation: a) P. J. Cossar, L. Hizartzidis, M. I. Simone, A. McCluskey, C. P. Gordon *Org. Biomol. Chem.* **2015**, *13*, 7119-7130; for some examples of continuous flow multistep synthesis involving a nitro reduction step see: b) J. Hartwig, S. Ceylan, L. Kupracz, L. Coutable, A. Kirschning *Angew. Chem. Int. Ed.* **2013**, *52*, 9813; c) T. Tsubogo, H. Oyamada, S. Kobayashi *Nature* **2015**, *520*, 329.

[51] R. V. Jones, L. Godorhazy, N. Varga, D. Szalay, L. Urge, F. Darvas, *J. Comb. Chem.* **2006**, *8*, 110-116.
[52] D. Cantillo, M. Baghbanzadeh, C. O. Kappe *Angew. Chem. Int. Ed.* **2012**, *51*, 10190-10193.
[53] D. Cantillo, M. M. Moghaddam, C. O. Kappe *J. Org. Chem.* **2013**, *78*, 4530.
[54] R. L. Hartman, J. P. McMullen, K. F. Jensen *Angew. Chem. Int. Ed.* **2011**, *50*, 7502.
[55] T. Okino, Y. Hoashi, T. Furukawa, X. Xu, Y. Takemoto, *J. Am. Chem. Soc.* **2005**, *127*, 119-125.
[56] For a recent example see: K. Hashimoto, N. Kumagai, M. Shibasaki *Org. Lett.* **2014**, *16*, 3496.
[57] R. V. Jones, L. Godorhazy, N. Varga, D. Szalay, L. Urge, F. Darvas, *J. Comb. Chem.* **2006**, *8*, 110-116.
[58] Patent US5121329 A.
[59] Jones D, (writing as Daedalus) *Ariadne column. New Sci* **1974.**
[60] US Patent 4041476.
[61] *U.S. Patent* 4,575,330.
[62] B. Wittbrodt, A. G. Glover J. Laureto, G. C. Anzalone, D. Oppliger, J. L. Irwin, J. M. Pearce, *Mechatronics*, **2013**, *23*, 713-726.
[63] J. M. Pearce, *Science* **2012**, *337*, 1303-1304.
[64] C. Zhang, N. C. Anzalone, R. P. Faria, J. M. Pearce, *Plos One* **2013**, *8*, 59840.
[65] Halford, B. (2014). *"3D Models, without the kit", Chem. Eng. News* **92**, 32–33.
[66] B. Wijnen, E. J. Hunt, G. C. Anzalone, J. M. Pearce, *Plos One* **2014**, *9*, 107216.
[67] a) P. J. Kitson, M. D. Symes, V. Dragone, L. Cronin, *Chem Sci* **2013**, *4*, 3099; b) M. D. Symes, P. J. Kitson, J. Yan, C. J. Richmond, G. J. Cooper, R. W. Bowman, T. Vilbrandt, L. Cronin, *Nat Chem* **2012**, *4*, 349-354.
[68] J. S. Mathieson, M. H. Rosnes, V. Sans, P. J. Kitson, L. Cronin, *Beilstein journal of nanotechnology* **2013**, *4*, 285-291.
[69] G. Chisholm, P. J. Kitson, N. D. Kirkaldy, L. G. Bloor, L. Cronin, *Energ Environ Sci* **2014**, *7*, 3026-3032.
[70] V. Dragone, V. Sans, M. H. Rosnes, P. J. Kitson, L. Cronin, *Beilstein journal of organic chemistry* **2013**, *9*, 951-959.
[71] a) J. L. Erkal, A. Selimovic, B. C. Gross, S. Y. Lockwood, E. L. Walton, S. McNamara, R. S. Martin, D. M. Spence, *Lab on a chip* **2014**, *14*, 2023-2032; b) B. Y. Ahn, E. B. Duoss, M. J. Motala, X. Guo, S. I. Park, Y. Xiong, J. Yoon, R. G. Nuzzo, J. A. Rogers, J. A. Lewis, *Science* **2009**, *323*, 1590-1593.
[72] M. Lee, B. Wu, in *Computer-Aided Tissue Engineering, Vol. 868 (Ed.: M. A. K. Liebschner), Humana Press*, **2012**, pp. 257-267.
[73] E. N. Antonov, V. N. Bagratashvili, M. J. Whitaker, J. J. A. Barry, K. M. Shakesheff, A. N. Konovalov, V. K. Popov, S. M. Howdle, *Advanced Materials* **2005**, *17*, 327-330.
[74] C. X. F. Lam, X. M. Mo, S. H. Teoh, D. W. Hutmacher, *Materials Science and Engineering:* C **2002**, *20*, 49-56.
[75] a) S. Bose, S. Vahabzadeh, A. Bandyopadhyay, *Materials Today* **2013**, *16*, 496-504; b) A. Butscher, M. Bohner, S. Hofmann, L. Gauckler, R. Müller, *Acta Biomaterialia* **2011**, *7*, 907-920.
[76] a) J. N. Hanson Shepherd, S. T. Parker, R. F. Shepherd, M. U. Gillette, J. A. Lewis, R. G. Nuzzo, *Advanced Functional Materials* **2011**, *21*, 47-54; b) Y. B. Lee, S. Polio, W. Lee, G. Dai, L. Menon, R. S. Carroll, S. S. Yoo, *Experimental Neurology* **2010**, *223*, 645-652.
[77] a) B. C. Gross, J. L. Erkal, S. Y. Lockwood, C. Chen, D. M. Spence, *Analytical chemistry* **2014**, *86*, 3240-3253; b) A. Waldbaur, H. Rapp, K. Lange, B. E. Rapp, *Analytical Methods* **2011**, *3*, 2681-2716; c) D. Therriault, S. R. White, J. A. Lewis, *Nat Mater* **2003**, *2*, 265-271.
[78] K. B. Anderson, S. Y. Lockwood, R. S. Martin, D. M. Spence, *Analytical chemistry* **2013**, *85*, 5622-5626.
[79] C. Chen, Y. Wang, S. Y. Lockwood, D. M. Spence, *Analyst* **2014**, *139*, 3219-3226.
[80] G. Comina, A. Suska, D. Filippini, *Lab on a chip* **2014**, *14*, 424-430.
[81] L. Henry, *C. R. Acad. Sci. Paris* **1895**, *120*, 1265; b) L. Henry, *Bull. Soc. Chim. Fr.* **1895**, *13*, 999.

[82] H. Sasai, T. Suzuki, S. Arai, T. Arai, M. Shibasaki, *J. Am. Chem. Soc.* **1992**, *114*, 4418.

[83] J. Boruwa, N. Gogoi, P. P. Saikia, N. C. Barua, *Tetrahedron: Asymmetry* **2006**, *17*, 3315; C. Palomo, M. Oiarbide, A. Laso, *Eur. J. org. Chem.* **2007**, 2561.

[84] Y. Alvarez-Casao, E. Marquez-Lopez, R. P. Herrera, *Symmetry* **2011**, *3*, 220.

[85] G. Blay, V. Hernandez-Olmos, J. R. Pedro *Synlett* **2011,** *9*, 1195.

[86] C. Christensen, K. Juhl, K. A. Jørgensen, *Chem. Commun.* **2001**, 2222.

[87] D. A. Evans, D. Seidel, M. Rueping, H. Lam, J. Shaw, C. Downey, *J. Am. Chem. Soc.* **2003**, *125*, 12692.

[88] G. Blay, L. R. Domingo, V. Hernández-Olmos, J. R. Pedro, J. R. *Chem. Eur. J.* **2008**, *14*, 4725.

[89] G. Ciamician, *Science* **1912**, *September 27*, 385.

[90] M. Reckenthlera, A.G. Griesbecka *Adv. Synth. Catal.* **2013**, *355*, 2727-2744.

[91] Y. Su, N. J. W. Straathof, V. Hessel, T. Noel *Chem. Eur. J.* **2014**, *20*, 10562-10589.

[92] a) Y. Zhu, S. L. Buchwald, *J. Am. Chem. Soc.* **2014**, *136*, 4500; b) M. Li, B. Yücel, J. Adrio, A. Bellomo, P. J. Walsh, *Chem. Sci.* **2014**, *5*, 2383; c) M. Matsumoto, M. Harado, Y. Yamashita, S. Kobayashi, *Chem. Commun.* **2014**, *50*, 13041; d) Y. Wu, L. Hu. Z. Li, L. Deng, *Nature* **2015**, *523*, 445.

[93] a) G. Masson, S. Py, Y. Vallée, *Angew. Chem. Int. Ed.* **2002**, *41*, 1772; b) M. Takahashi, G. C. Micalizio, *J. Am. Chem. Soc.* **2007**, *129*, 7514; c) M. Takahashi, G. C. Micalizio, *Chem. Commun.* **2010**, *46*, 3336.

[94] D. K. Root, W. H. Smith, *J. Electrochem. Soc.* **1982**, *129*, 1231.

[95] a) D. Uraguchi, N. Kinoshita, T. Kizu, T. Ooi, *J. Am. Chem. Soc.* **2015**, *137*, 13768; b) D. Hager, D. W. C. MacMillan, *J. Am. Chem. Soc.* **2014**, *136*, 16986; c) J. L. Jeffrey, F. R. Petronijević, D. W. C. MacMillan, *J. Am. Chem. Soc.* **2015**, *137*, 8404;

[96] M. Nakajima, E. Fava, S. Loescher, Z. Jiang, M. Rueping, *Angew. Chem. Int. Ed.* **2015**, *54*, 8828.

[97] For a recent example see: L. Qi, Y. Chen, *Angew. Chem. Int. Ed.* **2016**, *55,* 13312-13315; For reductive coupling of imine derivatives with electron-deficient olefins using metals, see: b) G. Masson, P. Cividino, S. Py, Y. Vallée, *Angew. Chem. Int. Ed.* **2003**, *42*, 2265; c) C.-H. Yeh, R. P. Korivi, C.-H. Cheng, *Angew. Chem. Int. Ed.* **2008**, *47*, 4892.

[98] a) J. D. Nguyen, J. W. Tucker, M. D. Konieczynska, C. R. J. Stephenson, *J. Am. Chem. Soc.* **2011**, *133*, 4163; b) C.-J. Wallentin, J. D. Nguyen, P. Finkbeiner, C. R. J. Stephenson, *J. Am. Chem. Soc.* **2012**, *134*, 8875.

[99] a) C. F. Carter, H. Lange, S. V. Ley, I. R. Baxendale, B. Wittkamp, J. G. Goode, N. L. Gaunt *Org. Process Res. Dev.* **2010**, *14*, 393-404; b) L. Malet-Sanz, J. Madrzak, S.V. Ley, I.R. Baxendale *Org. Biomol. Chem*. **2010**, *8*, 5324-5332; c) H. Lange, C. F. Carter, M. D. Hopkin, S. V. Ley *Chem. Sci.* **2011**, *2*, 765-769; d) D. C. Fabry, E. Sugiono, M. Rueping, *React. Chem. Eng.* **2016**, *1*, 129.